Acetylcholine in Central Cardiorespiratory Regulation in Health and Depression

James Robert Padley

A thesis submitted in fulfilment of the requirements for the degree of
Doctor of Philosophy (Medicine), University of Sydney

February 2007

Declaration of Originality

I certify that the contents of this thesis represent the original experimental and written work of the candidate except where due acknowledgement is made. All work was conducted in the Hypertension and Stroke Research Laboratories under the supervision of Dr Ann K Goodchild and Professor Paul M Pilowsky. This thesis has not been previously submitted for a degree or diploma to any other Institution. Parts of this text have been published, details of which can be found on page ix.

_____ _____

Signature of candidate Date

Acknowledgements

This thesis would not have been possible without the support of numerous colleagues, friends and family.

First and foremost, thank you to my wonderful supervisors, Ann Goodchild and Paul Pilowsky. Ann, you have been a constant source of knowledge, advice and encouragement. Paul, your humour and boundless energy and enthusiasm for research has always kept me buoyed. None of this would have been possible without you both. I feel very lucky to have had the opportunity to work with you and with the simply wonderful group of people you have attracted to the lab, and whom you continue to attract.

Thank you also to Jean-Luc Elghozi, Dominique Laude, Veronique Baudrie and Arlette Girard, of the Faculté de Médecine, Université René Descartes Paris V, for accepting me and making my time in Paris so enjoyable and fruitful. I am also very grateful to the Ramsey Health Care Foundation for providing a Travel Fellowship.

I am very grateful to the Centenary Foundation of Royal North Shore Hospital and the Australian Postgraduate Award scheme for financial support.

Thank you to all the staff at Gore Hill Research Laboratories. I am especially grateful to Giselle Berend and Lal for their work in establishing and maintaining breeding colonies of the Flinders lines. Many thanks to David Overstreet from the University of North Carolina for making this possible.

Thank you to all the wonderful people I've known and worked with in the Postgraduate Research Students' Society of Royal North Shore Hospital (PReSS).

To the many past and present members of HSRL, thank you so much for the joy and fun you brought to my time there. Without you I could not have become addicted to coffee, or survived with my sanity intact. I won't forget you. I hope you find happiness and success in the paths you take. Tash (the Phantom!) thank you for being with me on this crazy journey and making me smile, Maz I will miss you, Tina and Simo you are the most legendary young old people I know (hehe), Pete (the guerrilla gardener) thank you mate your positive energy is truly contagious and Cara and Mel you girls are awesome, good

luck with all your PhDs. Todd, it was great travelling with you mate (and having many a traveller!). Thank you Qun for your wonderful nature and the beautiful work you do, thank you also Deb, Qi-Jian, Felicity, Darryl, Thomas, Kiran, Kuan, Liz, John, Val, Jemima, Natalie, Koji, Max, Diana, Susan, Tara and James.

To my best mates, Graham, Andy, Lea and Richie: thank you so much, for being there, running amok and staying young at heart. Big hugs. Grae, you have been a constant support and true friend. To Amy, my foreign correspondent, thank you for your support and friendship.

To my family, Mum, Ben and Alex, thank you for your love and support, for putting up with me and sharing my hopes and fears. I know they say you can't choose your family, but I could not have chosen better partners for this journey so far. This thesis is dedicated to you Mum. You have been my inspiration.

Sound, sound the clarion, fill the fife,
Throughout the sensual world proclaim,
One crowded hour of glorious life,
Is worth an age without name.

Thomas Osbert Mordaunt

Abstract

Circulation and breathing movements that are essential for life are regulated by neurons in the hypothalamus and lower brainstem. Activity of these neurons is regulated by peripheral afferent and higher order inputs that release a diverse array of amino acids, amines and peptides. In this thesis we investigated the role of the neurotransmitter acetylcholine (ACh) and its receptors in regulation of cardiorespiratory homeostasis. Secondly, we determined whether or not genetic disturbances in regulation of acetylcholine receptor sensitivity affect central control of circulation, body temperature or respiration.

The findings presented in Chapter 3 reveal a novel functional role of ACh and G-protein coupled muscarinic receptor (mAChR) activation in the rostral ventrolateral medulla (RVLM). We showed for the first time that some non-C1 RVLM neurons express mRNA for the M2 or M3 receptor; however, both C1 and enkephalinergic RVLM neurons were closely apposed by cholinergic terminals positive for the vesicular acetylcholine transporter (vAChT). Physiological studies demonstrated that activation of mAChR within the RVLM in anaesthetised rats increases arterial pressure and sympathetic nerve activity and has differential effects on major cardiorespiratory reflexes: RVLM mAChR activation resets the sympathetic baroreflex to higher arterial pressures and increases its gain and, concomitantly, attenuates excitatory reflexes evoked by peripheral chemoreceptor or somatic afferent stimulation. Retrograde tracing from the RVLM combined with vAChT immunoreactivity showed that neurons in the pedunculopontine tegmental nucleus (PPT) are the sole source of cholinergic input to the RVLM. The PPT-RVLM pathway appears to be part of a central command circuit concerned with adjusting circulatory function appropriate to increased muscle activity. These data support the notion that activation of specific neurotransmitter receptors in the RVLM encodes functional specificity in control of sympathetic outflow and reflex function.

The extent to which genetic variations in central mAChR sensitivity influence autonomic function is unknown. Flinders Sensitive Line (FSL) rats were bred from Sprague Dawley (SD) rats for exaggerated behavioural and hypothermic responses to cholinesterase inhibitors and direct-acting mAChR agonists. A control genetic counterpart, the Flinders Resistant Line (FRL), was also bred in parallel for reduced responses to cholinergic agonists. The findings of Chapter 5 showed for the first time that FSL rats exhibit an increase in M2 and reduction in M3 receptor expression in the rostral medulla, suggesting that cholinergic signalling in this region may be altered. However, alterations of mAChR

expression specific to FSL rats were restricted to this area and there were no changes in cerebellar expression of mAChR in any strain. Physiological studies showed that conscious or anaesthetised FSL rats were more sensitive to thermoregulatory responses to central mAChR activation (ie hypothermia and increase in cutaneous blood flow); whereas pressor responses were reduced compared to SD and FRL rats. The increase in sympathetic activity and depression of respiration evoked by central mAChR activation was unchanged and attenuated, respectively, in FSL rats compared to control strains. These findings indicate that mAChR involved in control of different autonomic functions are regulated independently at the genetic and / or post-transcriptional level.

The findings of Chapters 4 and 6 reveal a novel effect of breeding for cholinergic hypersensitivity in FSL rats on control of vagal and sympathetic outflow. Spectral analysis of blood pressure recordings in conscious FSL rats showed a reduction in total and high frequency power of heart rate variability (HRV), an increase in the LF/HF ratio and reduction in baroreflex sensitivity (BRS) compared to controls. These changes reflect a reduction in reflex vagal input and relative predominance of sympathetic input to the sinus node in FSL rats. Under urethane anaesthesia, FSL rats had a higher heart rate and exhibited lower gain of baroreflex control of splanchnic sympathetic nerve activity (SNA). Moreover, FSL rats were more susceptible to ventricular arrhythmias during infusion of the cardiac glycoside ouabain under anaesthesia compared to controls. These data indicate that FSL rats exhibit impaired reflex regulation of vagal and sympathetic outflow that could underlie increased vulnerability to arrhythmia seen in this strain. The precise brain regions and neurotransmitters that underlie autonomic disturbances seen in FSL rats are unclear. As well as muscarinic hypersensitivity, FSL rats also exhibit increased sensitivity to nicotine, serotonin and dopamine. Multiple chemical sensitivities in FSL rats may arise from functional interactions with mAChR or changes in common intracellular regulatory or signalling pathways.

FSL rats exhibit a number of behavioural and somatic abnormalities consistent with clinical depression, including reduced motivated behaviour and sleep and psychomotor disturbances. These symptoms are also alleviated by treatment with antidepressants, suggesting that similar neurochemical abnormalities may underlie behavioural disturbances seen in FSL rats and human depression. Symptoms of depression are an emerging risk factor in the development of cardiovascular disease and are associated with increased risk of dying from a cardiac-related event. A reduction in HRV and BRS in depressed patients

has been widely reported and is considered to be a key substrate predisposing to arrhythmia in this patient group. In this thesis we demonstrate for the first time that FSL rats exhibit similar autonomic abnormalities to those reported in human depression and are more vulnerable to ouabain-induced ventricular arrhythmias. These findings suggest that biological factors predisposing to autonomic dysfunction and arrhythmia in FSL rats could also operate in human depression. This may involve altered neurotransmission in cardiovascular brain regions, or inappropriate regulation of cardiovascular function by arousal or motor control pathways.

Overall, this thesis provides novel insights into cholinergic mechanisms that regulate cardiorespiratory homeostasis. ACh is important in physiological regulation of circulation via activation of G-protein coupled mAChR in the RVLM. Selective breeding for cholinergic hypersensitivity in FSL and FRL rats results in region- and subtype-specific changes in mAChR expression in the lower brainstem and differentially influences muscarinic control of circulation and breathing. Variations in central mAChR sensitivity may contribute to impaired reflex control of vagal and sympathetic outflow and could hence predispose to cardiac complications including arrhythmias. Future studies may aim to further understand the relationship between endogenous sensitivity of metabotropic neurotransmitter receptors in the CNS and cardiovascular disturbances associated with depression.

TABLE OF CONTENTS

Publications arising from this thesis

Padley JR, Kumar NN, Li Q, Nguyen TBV, Pilowsky PM, Goodchild AK (2007) Central command regulation of circulatory function mediated by descending pontine cholinergic inputs to sympathoexcitatory rostral ventrolateral medulla neurons. *Circulation Research* **100**(2):284-291

Padley JR, Overstreet DH, Pilowsky PM, Goodchild AK (2005) Impaired cardiac and sympathetic autonomic control in rats differing in acetylcholine receptor sensitivity. *American Journal of Physiology Heart and Circulatory Physiology* **289**(5):H1985- 92

Padley JR, Kumar NN, Hildreth CM, Pilowsky PM, Goodchild AK (2007) Differential expression of muscarinic receptor subtypes in the ventral medulla and control of temperature, circulation and breathing in rats with inherited cholinergic sensitivity. *Submitted Am J Physiol Regu Integr Comp.*

Hildreth CM, **Padley JR**, Pilowsky PM, Goodchild AK (2007) Impaired 5-HT1A receptor sensitivity in control of cardiac autonomic function in a genetic animal model of depression. *In preparation.*

Other publications arising from the period of candidature

Seyedabadi M, Li Q, **Padley JR**, Pilowsky PM, Goodchild AK (2006) A novel pressor area at the medullo-cervical junction that is not dependent on the RVLM: efferent pathways and chemical mediators. *Journal of Neuroscience* **26**(20):5420-7

Declaration of contribution to Chapters containing published or submitted work

Chapter 3

Candidate performed all physiological experiments and data analysis and immunohistochemical components of the study. Candidate was the major contributor to the manuscript.

Natasha Kumar and Qun Li contributed to the molecular biological aspects of the study (including *in situ* hybridisation) and both contributed to the manuscript.

Chapter 4

Candidate performed all experimental work and data analysis and was the major contributor to the manuscript.

Chapter 5

Candidate performed all physiological experiments under anaesthesia and related data analysis and was the major contributor to the manuscript.

Natasha Kumar contributed to the molecular biological aspects of the study (including PCR) and Cara Hildreth performed radiotelemetry studies in conscious animals and both contributed to the manuscript.

Chapter 6

Candidate performed all experimental procedures under anaesthesia and related data analysis and wrote the manuscript.

Cara Hildreth performed radiotelemetry studies in conscious animals; however, the candidate conducted all analysis and interpretation of data.

Candidate, James Padley

Natasha Kumar

Cara Hildreth

Qun Li

Thomas Nguyen

Paul Pilowsky

Ann Goodchild

List of Figures

Chapter 1

Chapter 3

Chapter 8

List of Tables

Chapter 1

Chapter 2

Chapter 4

Abbreviations

5-HT	5-hydroxytryptamine
AN	aortic nerve
AP	arterial pressure
BRS	baroreflex sensitivity
CHD	coronary heart disease
DLH	D-L-homocysteic acid
DMX	dorsal motor nucleus of the vagus
ECG	electrocardiogram
EMG	electromyogram
FRL	Flinders Resistant Line
FSL	Flinders Sensitive Line
GAPDH	glyceraldehyde-3-phosphate dehydrogenase
HF	high frequency [re: power spectra]
HR	heart rate
HRV	heart rate variability
IML	intermediolateral cell column
LF	low frequency [re: power spectra]
mAChR	muscarinic acetylcholine receptor
mATR	atropine methylnitrate
MI	myocardial infarction
nAChR	nicotinic acetylcholine receptor
NPY	neuropeptide Y
OXO	oxotremorine
PE	phenylephrine
PI	pulse interval
PNA	phrenic nerve activity
PPT	pedunculopontine tegmental nucleus
PVN	paraventricular nucleus of the hypothalamus
RVLM	rostral ventrolateral medulla
SCOP	scopolamine
SD	Sprague Dawley
SDNN	standard deviation of R-R intervals
SNA	sympathetic nerve activity

SNP	sodium nitroprusside
SPN	sympathetic preganglionic neuron
TBF	tail blood flow
TN	tibial nerve
XIIn	hypoglossal nerve

Chapter 1 Literature Review

'When life came out of the ocean, it had to figure out a way to carry around its own bathing ocean and circulate it…I've thought of each of us, you and me, as our own pinched-off, ambulatory seas, ones in which only our hearts keep us buoyed.'

from 'A Man After His Own Heart '
by Charles Siebert

I. Central control of the Circulation

Introduction

Neurons that regulate cardiovascular function are primarily located within the hypothalamus, brainstem and spinal cord. Their activity patterns are responsible for the rhythmic discharge in sympathetic vasoconstrictor nerves that innervate vascular smooth muscle and sympathetic and vagal nerves that supply the heart. A critical function of these central neurons is to match perfusion with the rate of aerobic metabolism and pulmonary gas-exchange in order to maintain acid-base homeostasis. The critical afferent inputs to these neurons originate from specialised peripheral receptors that encode information about arterial blood pressure (AP) and oxygen saturation, and from central neurons that control respiration whose activity is dictated by interstitial H^+ *(Dampney, 1994b; Pilowsky, 1995; Guyenet, 2006)*. Descending inputs from higher brain regions also modulate patterns of cardiorespiratory activity to meet specific behavioural demands, ranging from intense exercise to sleep *(Dampney et al., 2005)*.

Sympathetic Control of the Circulation

Noradrenergic sympathetic fibres innervating the heart and blood vessels originate in pre- or paravertebral ganglia that in turn receive an excitatory cholinergic input from sympathetic preganglionic neurons (SPN). SPN are located in longitudinal cell clusters within the spinal cord. Most SPN are found within the intermediolateral cell column (IML) *(Strack et al., 1988)* where their segmental distribution is topographically correlated with the outflow to different target organs and ganglia (Fig. 1.1.1) *(Oldfield and McLachlan, 1981; Anderson et al., 1989; Pilowsky et al., 1992)*.

The ongoing activity of SPN is necessary for maintaining vasoconstrictor tone and AP. SPN receive ongoing excitatory inputs that are mainly supraspinal in origin, as demonstrated in intracellular recordings from thoracic and lumbar SPN in cat *(Coote and Westbury, 1979; Hirst and McLachlan, 1980; Dembowsky et al., 1985; Pilowsky et al., 1994a)*.

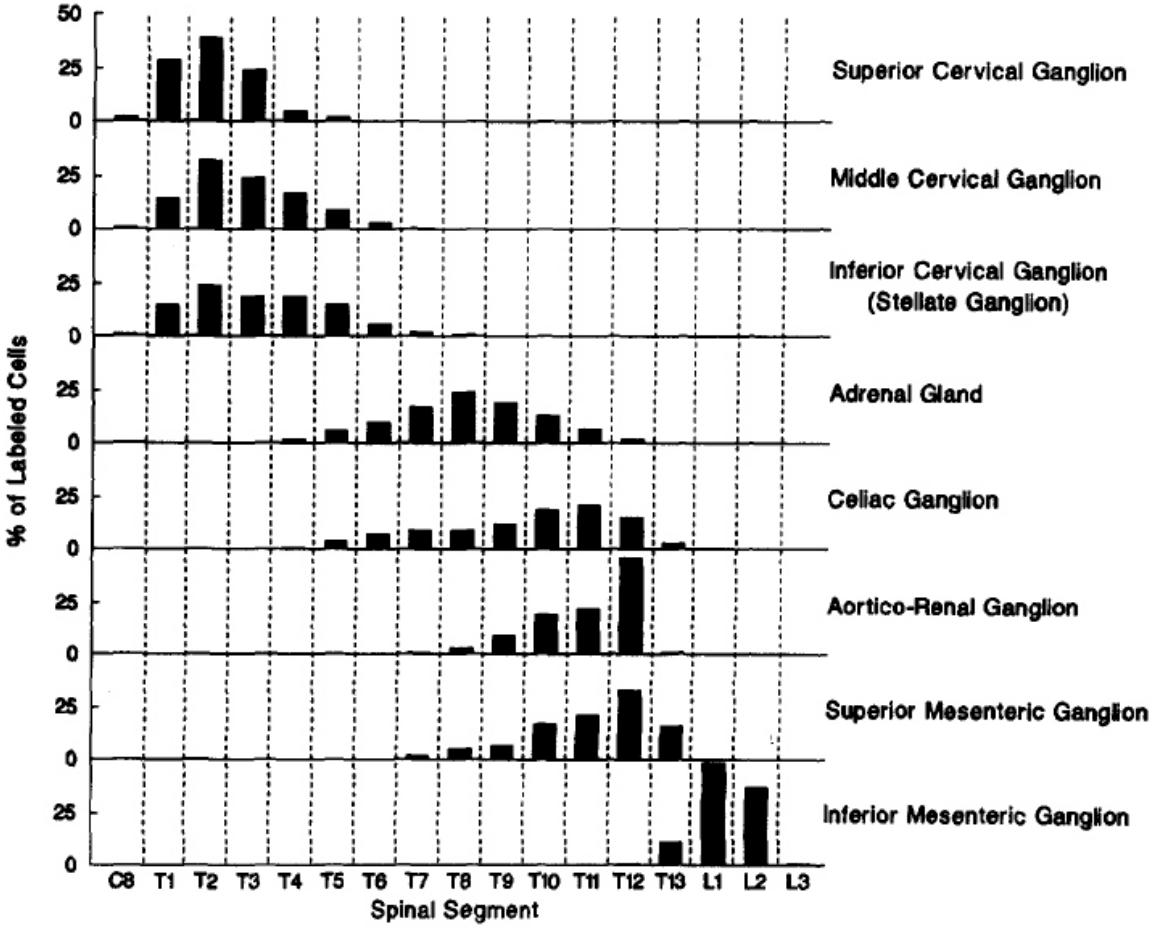

Figure 1.1.1 Topographical distribution of SPN in the rat spinal cord. Histograms are shown illustrating the proportion of SPN labeled following Fluorgold injections into the major sympathetic ganglia and adrenal gland in rats, as indicated on right. The segmental distribution of SPN is topographically correlated with the outflow to different target organs and beds. Adapted from Strack et al. 1988.

Patch-clamp recordings in isolated spinal cord slices from cat and rat show that SPN also receive inhibitory inputs *(Dun et al., 1992)*. GABAergic interneurons located close to the central canal are a potential intraspinal source of ongoing SPN inhibition *(Deuchars et al., 2005)*. Inhibitory neuropeptides including enkephalin also richly innervate SPN and a proportion of these inputs originate from within the spinal cord *(Llewellyn-Smith et al., 2005)*. The functional role of inhibition in control of SPN activity is at present unclear.

Excitatory inputs to SPN originate from several cell groups in the brain *(Loewy et al., 1979; Loewy, 1981; Loewy et al., 1981; Luiten et al., 1985)* as well as neurons in the upper cervical spinal cord *(Jansen and Loewy, 1997; Seyedabadi et al., 2006)*. A key observation by Loewy and colleagues was the restricted distribution of central neurons with inputs to multiple sympathetic beds, demonstrated by transneuronal labeling from the superior cervical (SCG), stellate or celiac ganglia or adrenal medulla *(Strack et al., 1989)*. These *presympathetic* neurons are located in five major cell groups in the medulla, pons and hypothalamus. A cornerstone of research in this field remains an understanding of the central circuitry that determines the coordinated activity of multiple sympathetic outflows and their responses to different afferent signals. In particular, how do single afferent signals generate complex and selective changes in regional sympathetic outflow? In the following sections, the location, connections, neurochemistry and functions of presympathetic cell groups are reviewed with a focus on the role of neurons in the rostral ventrolateral medulla (RVLM).

The Rostral Ventrolateral Medulla (RVLM)

Introduction

The region of the RVLM located immediately caudal to the facial nucleus contains neurons whose activity largely determines ongoing vasomotor and reflex activity in sympathetic efferent pathways *(Reis et al., 1984; Dampney, 1994b, 1994a; Pilowsky and Goodchild, 2002; Guyenet, 2006)*. Its discovery was heralded by Dittmar's experiment in rabbits which found that a knife cut placed at this level caused AP to fall to spinal levels (50 mmHg) and abolished the pressor response to stimulation of a sciatic nerve (Fig. 1.1.2) *(Dittmar, 1873)*. Later studies showed that electrical stimulation within the dorsal or ventral medulla produced large increases in AP *(Wang and Ranson, 1939; Alexander, 1946)*. The work of Feldberg and others in the early 1970s showed that bilateral inhibition of the region of the ventral surface caudal to the trapezoid body and lateral to the pyramids

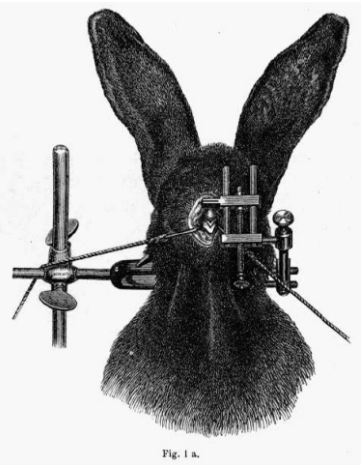

Fig. 1 a.

Versuch A.

Der erste Schnitt geht durch die Fov. anter. und den oberen Rand des Corp. trapez. Der zweite Schnitt liegt etwa 4 mm tiefer, 3 mm über der Spitze des Calamus script. 2mm unter dem unteren Rande des Corp. trapez., 1—1½mm unter dem Tuberc. laterale.

Beide Vagi durchschnitten.

	Dauer der Reizung	Druck steigt oder sinkt von mm	Druck steigt oder sinkt auf mm	in ? Secunden
1. Reizung des Ischiadicus dext. RA 18	4	138	172	6,5
2. Erste Querdurchschneidung.		136	116	
3. Reizung RA 18	12	116	146	8
4. Reizung RA 18	13	122	142	7,5
5. Zweite Querdurchschneidung		126	50	

Weitere Reizungen RA 18 (Dauer 17 Sec.) ferner RA 10 (Dauer 13 und 31 Sec.) sind ohne Effect.

The first cut went through the fovea anterior and the rostral margin of the trapezoid body. The second cut was 4mm lower and 3mm ahead of the calamus scriptorius, 2mm caudal to the caudal margin of the trapezoid body. Both vagi are cut.

	duration of stim. (s)	carotid MAP mmHg before	carotid MAP mmHg after	time lag (s)
1. Stimulation of the nervus ischiadicus (sciatic)	4	138	172	6.5
2. First cut		136	116	
3. Stimulation	12	116	146	8
4. Stimulation	13	122	142	7.5
5. Second cut		126	50	

Further stimulations were without effect.

Figure 1.1.2 Experimental set-up and findings in Dittmar's first stereotaxic experiment in rabbits (1873) (translated from the German by the candidate). Dittmar's study was the first to demonstrate the importance of the rostral medulla in tonic and reflex control of blood pressure. A knife cut through the medulla 2 mm caudal to the trapezoid body (but not more rostral) produced a dramatic fall in carotid AP (to 50 mmHg) and abolished the increase in AP evoked by stimulation of a sciatic nerve.

using pentobarbital, glycine or GABA caused large falls in AP in cats *(Feldberg and Guertzenstein, 1972; Guertzenstein, 1973; Guertzenstein and Silver, 1973; Feldberg and Guertzenstein, 1976)*. Subretrofacial lesions or inhibition of the RVLM in several species causes loss of vasomotor tone and an inability to reflexly restore AP in the short term *(Dampney and Moon, 1980; McAllen et al., 1982; Ross et al., 1984b)*.

Neurons in the RVLM that are exquisitely sensitive to baroreceptor activity project to the spinal cord where they excite, probably monosynaptically, a large number of vasoconstrictor and cardiac SPN *(Brown and Guyenet, 1985; Morrison et al., 1988; Haselton and Guyenet, 1989b; Lipski et al., 1995; Lipski et al., 1996; Oshima et al., 2006)*. The ongoing activity of RVLM neurons is partly dependent upon activation of ionotropic glutamate receptors and metabotropic receptors *(Seyedabadi et al., 2001; Dampney et al., 2003b; Horiuchi et al., 2004)*; their excitability is powerfully restrained by ongoing GABAergic inputs *(Sun and Guyenet, 1985; Li et al., 1991; Lipski et al., 1996)*. An enduring theoretical framework for understanding the regulation of AP is that continuous activity of RVLM neurons and their sensitivity to inhibitory baroreceptor input maintains normal levels of vasomotor tone *(Horiuchi and Dampney, 1998)*. Branching projections from RVLM neurons to hypothalamic and other brainstem regions *(Tucker et al., 1987; Verberne et al., 1999a)* also regulates functions closely linked to control of AP, including control of sodium and water balance. Excitation of cell bodies within the RVLM evokes large increases in AP, adrenal medullary catecholamine and posterior pituitary hormone release *(Goodchild et al., 1982; Ross et al., 1984b)*.

The RVLM is also a key nodal point in several somatic and cardiovascular reflexes where largely convergent afferent inputs modulate the ongoing activity of sympathoexcitatory neurons *(Verberne et al., 1999a)*. Blockade of excitatory or inhibitory amino acid transmission in the RVLM abolishes the sympathetic components of several key homeostatic reflexes, including the arterial baroreflex, peripheral chemoreflex and nociceptive somatosympathetic reflex *(Guertzenstein and Silver, 1973; Feldberg and Guertzenstein, 1976; Miyawaki et al., 1996a; Miyawaki et al., 1996b)*. RVLM neurons also play an important role in sympathetic glucoregulatory responses *(Madden et al., 2006)*.

Several amino acid, amine and peptide inputs modulate the ongoing activity of RVLM neurons or selectively alter their reflex responsiveness *(Dampney et al., 1996; Miyawaki et al., 2001, 2002b; Padley et al., 2003; Saigusa et al., 2003; Makeham et al., 2005)*.

Presumably these inputs arise from regions of the brain concerned with adjusting circulatory function to meet specific behavioural (eg. during sleep/wake or exercise) or adaptive requirements (eg. thirst and satiety), or following injury (eg. haemorrhage or acute pain). However, the precise functional role of many of these inputs in regulation of cardiovascular reflexes or sympathetic tone is unknown.

Much of this work has been performed in anaesthetised animals and the precise role of the RVLM in the waking state is yet to be defined. Recent studies have indicated at least that the magnitude of depressor and pressor effects of amino acids injected into the RVLM is similar in conscious and anaesthetised rats *(Araujo et al., 1999; Campos and McAllen, 1999b; Sakima et al., 2000)*. In the absence of RVLM activity an adaptive central response acts to restore normal levels of AP. For example, normal AP is maintained in rats that have been recovered following bilateral electrolytic lesion of the RVLM under anaesthesia *(Cochrane et al., 1988; Cochrane and Nathan, 1989)*. An enduring paradox is that other presympathetic cell groups do not appear to provide increased excitatory drive to raise the threshold of vasoconstrictor SPN. Rather, AP is restored mainly by increased activity of the renin-angiotensin system and release of vasopressin *(Cochrane and Nathan, 1994)*.

Caudal Medullary Regions Involved in Cardiovascular Regulation

Several regions in the caudal medulla provide input to the RVLM, hypothalamus or spinal cord and modulate sympathetic or neurohumoral functions. Excitation of the region immediately caudal to the RVLM (caudal ventrolateral medulla (CVLM)) evokes depressor responses and inhibition or lesion of this area leads to increases in AP *(Pilowsky et al., 1987)*. GABA-containing interneurons in the CVLM exhibit tonic baroreceptor-related discharge *(Schreihofer and Guyenet, 2003)* and project monosynaptically to inhibit RVLM neurons *(Li et al., 1991; Masuda et al., 1991)*. Activation or withdrawal of this pathway is crucial in the arterial baroreflex *(Ross et al., 1984b; Dampney et al., 1988; Masuda et al., 1991; Horiuchi and Dampney, 1998)*. Injection of the GABA-A receptor antagonist bicuculline bilaterally into the RVLM evokes large increases in AP *(Ross et al., 1984b; Horiuchi and Dampney, 1998; Miyawaki et al., 2003)* and prevents reflex reductions in firing rate of RVLM neurons induced by increases in AP *(Sun and Guyenet, 1985)*. Other inputs to CVLM neurons also contribute to ongoing inhibition of RVLM activity; large increases in AP are evoked by bicuculline injection into the RVLM or

following blockade of excitatory inputs to the CVLM in baro-intact or barodenervated rats *(Sved et al., 2000; Schreihofer and Guyenet, 2002, 2003)*.

Catecholaminergic neurons caudal to the RVLM project to hypothalamic neurosecretory neurons in the paraventricular nucleus and control posterior pituitary hormone release; their stimulation evokes release of vasopressin following baroreceptor activation *(Blessing and Willoughby, 1985; McAllen and Blessing, 1987)*. A caudal pressor area (CPA) is located at a level just caudal to the emergence of the hypoglossal roots *(Gordon and McCann, 1988; Possas et al., 1994; Natarajan and Morrison, 2000; Horiuchi and Dampney, 2002; Sun and Panneton, 2002; Seyedabadi et al., 2006)*. The CPA may directly excite *(Possas et al., 1994)* or inhibit ongoing inhibitory inputs *(Horiuchi and Dampney, 2002)* into the RVLM; for example, inhibition of the CPA leads to falls in AP and pressor responses evoked from the region are blocked by inhibition of the RVLM *(Possas et al., 1994; Seyedabadi et al., 2006)*. Neurons in a recently defined medullo-cervical pressor area (MCPA), located in the caudal most VLM extending into upper cervical segments, appear to provide descending excitatory input to SPN independent of the RVLM *(Seyedabadi et al., 2006)*. A schematic illustration of the major afferent and efferent connections of the RVLM and other medullary regions involved in cardiovascular regulation is shown in Fig 1.1.3.

Location and Neurochemical Phenotype of Sympathoexcitatory Neurons in the RVLM

The VLM extends from the pyramidal decussation caudally to the caudal pole of the facial nucleus rostrally. In rat, the VLM is located within the paragigantocellular reticular nucleus and contains the lateral reticular nucleus *(Paxinos and Watson, 1996)*. The RVLM extends caudally from the facial nucleus and is bordered dorsally by the compact formation of the nucleus ambiguus (NA). In cat the RVLM is synonymous with the subretrofacial nucleus, which accurately describes the location of spinally projecting sympathoexcitatory RVLM neurons *(Dampney and Moon, 1980; McAllen et al., 1994)*. In rat, these neurons are clustered immediately caudal to the facial nucleus extending for approximately 1 mm *(Verberne et al., 1999a; Phillips et al., 2001)*.

The identity of neurons in the RVLM important in AP control was focused originally on catecholamine-containing neurons whose distribution overlaps sites where effective lesion

lowers AP or stimulation alters autonomic and neurosecretory function *(Blessing et al., 1981; Goodchild et al., 1982; Ross et al., 1984b)*. Dahlström and Fuxe described catecholamine-fluorescing neurons throughout the medulla and proposed that some had spinal projections based upon increased fluorescence following spinal transection *(Dahlström and Fuxe, 1965)*. Hökfelt et al. showed that many rostrally-located cells that project to the cord also contained the adrenaline-synthesizing enzyme PNMT *(Hökfelt et al., 1974)*. It is now well established that cells in the VLM differentially express the enzymes required for adrenaline (C1 cell group) or noradrenaline synthesis (A1 cell group) and that they are topographically distributed (Fig. 1.1.3) *(Blessing et al., 1981; Chalmers et al., 1981; Blessing et al., 1986; Minson et al., 1990a; Halliday and McLachlan, 1991b, 1991a; Goodchild et al., 2000; Phillips et al., 2001)*.

Many C1 neurons form part of the descending sympathoexcitatory projection from the RVLM (70 - 80 %) *(Haselton and Guyenet, 1989b; Jeske and McKenna, 1992)*; however, the bulbospinal projection includes both C1 and non-C1 RVLM neurons. Some rostral C1 and non-C1 cells have branching hypothalamic and spinal projections and C1 cells located in the caudal third of the RVLM project exclusively to the hypothalamus *(Tucker et al., 1987; Verberne et al., 1999a)*. This explains why RVLM stimulation leads to increases in AP as well as release of posterior pituitary hormones *(Ross et al., 1984b)*. Almost all bulbospinal RVLM neurons (incl. 80 % of C1 cells) utilise glutamate as a primary transmitter indicated by expression of the type 2 vesicular glutamate transporter (vGLUT2) *(Stornetta et al., 2002)*.

Is the expression of adrenaline-synthetic enzymes in C1 neurons indicative of a functional role for adrenaline in control of SPN activity? Many cell bodies in the VLM are immunoreactive to TH or DβH, which are required for dopamine synthesis and conversion to noradrenaline respectively, in several species including rat, cat, rabbit, guinea pig and sheep *(Blessing et al., 1986; Tillet, 1988; Halliday and McLachlan, 1991a, 1991b; Goodchild et al., 2000; Phillips et al., 2001)*. The number of cell bodies immunoreactive to PNMT, which converts noradrenaline to adrenaline, however, shows considerable species variation ranging from high abundance in rat to very little in cat and virtually none in sheep *(Tillet, 1988; Halliday and McLachlan, 1991b; Phillips et al., 2001)*. Hence, the assumption that 'C1' neurons utilise adrenaline may not be true for all species.

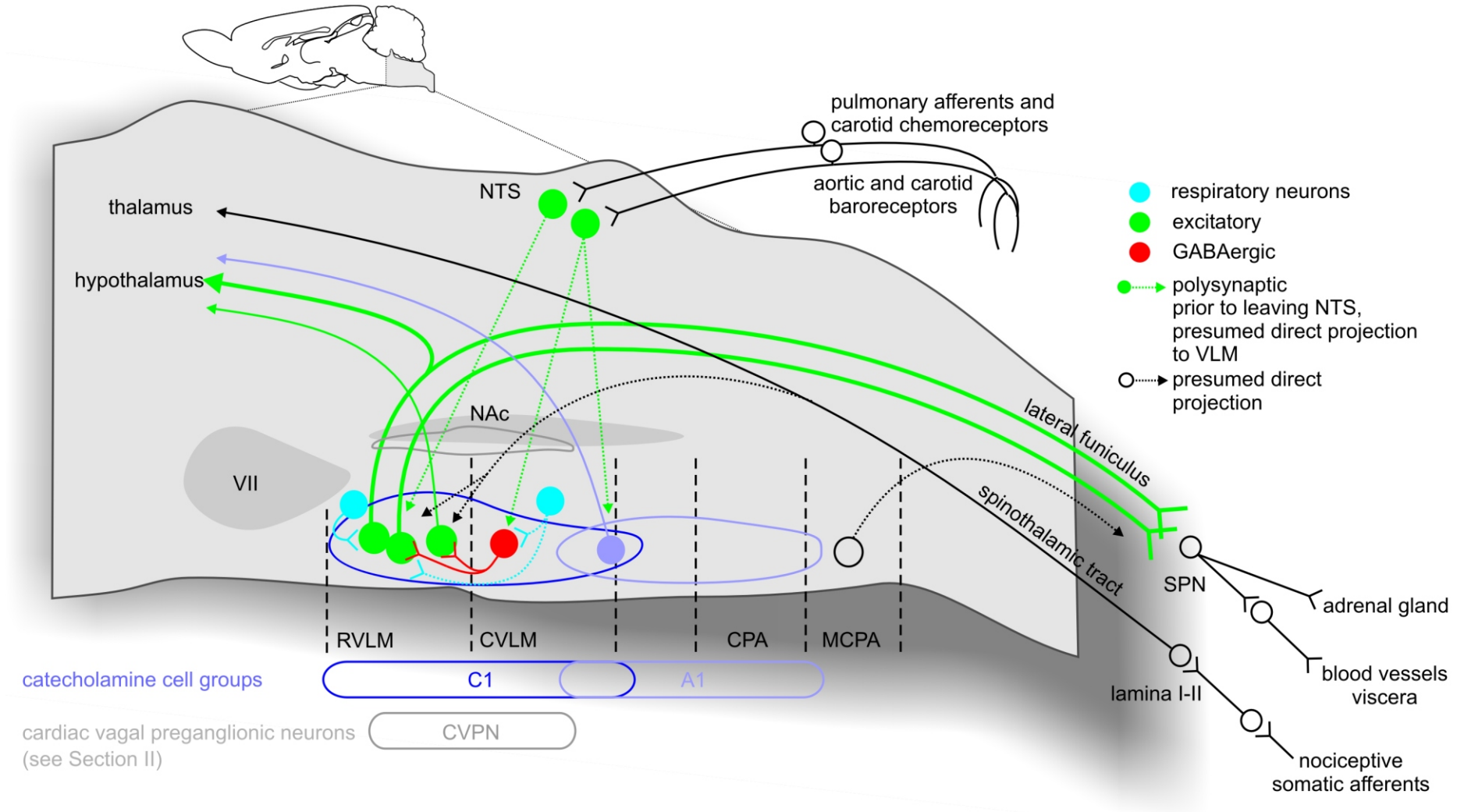

Figure 1.1.3. Major afferent and efferent connections of the RVLM and location of medullary regions important in cardiovascular regulation. Schematic sagittal view of rat brain showing presympathetic neurons in the RVLM (green) that project to the spinal cord where they provide continuous excitatory drive to vasoconstrictor SPN. This excitatory input is crucial to maintaining vasomotor tone and AP. Some RVLM neurons have projections to the hypothalamus that regulate levels of hormones, such as vasopressin, that are vasoactive and promote water resorption in the kidney. RVLM neurons receive cardiopulmonary and somatic afferent inputs that reflexly modulate circulation in order to maintain homeostasis or adapt to real or perceived injury.

Phillips et al. demonstrated that in rat most bulbospinal 'C1' neurons contained all the enzymes required for adrenaline synthesis, although about a quarter had very low or undetectable message for the catecholamine precursor aromatic L-amino acid decarboxylase (AADC) *(Phillips et al., 2001)*. Thus, in this species it appears that a majority of sympathoexcitatory neurons utilise adrenaline as a co-transmitter. This is supported by the modulatory effect of adrenaline on cervical SPN recorded in adult rat *in vivo (Lewis and Coote, 1990)* or in slice preparations from neonatal rat *(Miyazaki et al., 1989)*. Adrenaline can have excitatory or inhibitory effects on SPN depending on the receptor subtype that is activated (α–1 or α–2) *(Shi et al., 1988)*.

Several neuropeptides that modulate activity of SPN in the spinal cord are co-expressed in bulbospinal C1 and non-C1 neurons in the RVLM. The endogenous opiate precursor preproenkephalin (PPE) is expressed in most non-C1 bulbospinal neurons and ~ 20 % of bulbospinal C1 neurons *(Stornetta et al., 2001)*. In contrast, neuropeptide Y is virtually absent in C1 cells projecting only to the thoracic cord but present in 96 % of C1 neurons projecting to the hypothalamus *(Stornetta et al., 1999)*. The substance P precursor preprotachykinin (PPT) is also co-expressed in ~ 20 % of bulbospinal C1 neurons: TH- and substance P-immunoreactivity is colocalised in terminals within the IML in rat *(Li et al., 2005)*. RVLM neurons that project to the cord and hypothalamus are therefore likely to be a rich source of aminergic and peptidergic input into these areas. Other neurochemicals, including cocaine- and amphetamine-related transcript (CART) *(Burman et al., 2004)*, are thought to be expressed in a majority of C1 and non-C1 sympathoexcitatory neurons, although their precise functions are unknown.

Role of C1 Neurons in Tonic and Reflex Functions of the RVLM

The importance of C1 neurons in the RVLM in generating vasomotor tone has been questioned by recent selective lesioning studies using the neurotoxin saporin conjugated to DβH. Following injection into the IML the toxin is taken up selectively by catecholaminergic terminals and transported back to cell bodies, which are then destroyed. Schreihofer and Guyenet showed that delivery of the toxin in this way destroys ~ 80 % of RVLM neurons containing DβH or PNMT, as well as other bulbospinal catecholamine-containing cell groups *(Schreihofer and Guyenet, 2000; Schreihofer et al., 2000)*. Madden and Sved documented up to 99 % loss of C1 neurons in some animals following direct

injection of DβH-saporin into the RVLM *(Madden and Sved, 2003)*. Despite destruction of almost all C1 neurons, AP remains fairly normal *(Schreihofer et al., 2000; Guyenet et al., 2001; Madden and Sved, 2003)*. This could suggest either that only a few remaining C1 cells are sufficient to maintain AP, or that only non-C1 bulbospinal neurons are critical in this regard, or alternatively that AP is maintained by release of vasopressin or angiotensin.

Specific destruction of the C1 cell group by direct injection of DβH-saporin into the RVLM *(Madden et al., 1999; Madden and Sved, 2003; Madden et al., 2006)* or IML *(Schreihofer and Guyenet, 2000)* markedly diminished cardiovascular reflexes: > 80 % loss of C1 neurons markedly attenuated or eliminated reflex sympathoexcitatory responses to baroreceptor unloading, hypoxia or sciatic nerve stimulation and reflex increases in plasma noradrenaline in response to hypotension or hypoglycaemia. The fact that the RVLM is a critical synaptic relay in the expression of cardiovascular reflexes is well established; these data were the first to indicate a specific contribution of the C1 cell group.

Electrophysiological Characteristics of RVLM Neurons

Electrical stimulation of the RVLM elicits early and late discharges in sympathetic nerves that putatively arise from activation of groups of neurons with myelinated vs lightly- or unmyelinated axons *(Morrison et al., 1988)*. In general, RVLM neurons with exclusively bulbospinal projections are fast conducting (2 - 3 m/s); whereas neurons with branching projections to the hypothalamus and thoracic cord are slowly conducting (<1 m/s) *(Haselton and Guyenet, 1989b; Stornetta et al., 1999; Verberne et al., 1999a)*. Neurons with slowly-conducting (lightly- or unmyelinated) axons appear to be C1 cells; whereas the majority of fast-conducting bulbospinal neurons are non-C1 cells *(Schreihofer and Guyenet, 1997)*.

Intracellular recordings from bulbospinal barosensitive RVLM neurons *in vivo* showed that they have an irregular discharge and their membrane excitability is regulated by ongoing excitatory and inhibitory inputs *(Lipski et al., 1996)*. An intriguing observation was that interspike intervals of RVLM neurons become highly regular during depolarization induced by injury or large depolarizing currents *(Lipski et al., 1996)*. In barodenervated cats RVLM neurons exhibit regular rhythmic discharge that is dependent upon activation of excitatory amino acid receptors: presumably inhibitory baroreceptor-related inputs to the RVLM are substantially reduced in barodenervated animals *(Barman and Gebber, 1992; Barman et al., 2005)*. Inhibitory inputs therefore play an important role in regulating

excitability of RVLM neurons and account for their typically *irregular* firing pattern *in vivo*.

Presumed AP-regulating RVLM neurons displayed a regular pacemaker-like discharge in medullary slices isolated from their natural afferents *(Sun et al., 1988b; Kangrga and Loewy, 1995)* or after blockade of excitatory synaptic inputs *in vivo (Sun et al., 1988a)*. Hence, one possibility is that some RVLM neurons have intrinsic bursting characteristics that set the basic rhythm, which is then modulated by synaptic inputs *(Sun et al., 1988a; Sun et al., 1988b; Kangrga and Loewy, 1995)*. Lipski et al. did not find evidence for pacemaker potentials in RVLM neurons in adult rats *in vivo (Lipski et al., 1996)*, supporting a predominant role for antecedent synaptic inputs at least in the anaesthetised animal with major afferents intact. Nevertheless, other evidence suggests that an intrinsic membrane conductance of some neurons within the RVLM may be important. Miyawaki et al. explored the effects of microinjection of various ion channel modulators into the RVLM of anaesthetised rats *(Miyawaki et al., 2003)*. Only nickel (in relatively high amounts) was found to have a profound sympathoinhibitory and hypotensive effect, which the authors suggest resulted from selective inhibition of low voltage-activated 'T-type' calcium channels *(Miyawaki et al., 2003)*. These channels can generate burst firing and pacemaker activity *(Chemin et al., 2002)*.

Origin of Ongoing Synaptic Inputs to RVLM Neurons

The spontaneous activity of RVLM neurons and the characteristic bursting pattern of sympathetic nerve discharge are both absent above ~ 150 mmHg *(Brown and Guyenet, 1985; Morrison et al., 1988; Haselton and Guyenet, 1989b; Lipski et al., 1995)*. RVLM neurons receive ongoing inhibitory baroreceptor-related input evident in strong pulse-synchronous activity characterised by increased firing during the falling phase of the AP wave *(Brown and Guyenet, 1985; Lipski et al., 1996)*. Low frequency stimulation of aortic nerve afferents produced chloride-mediated IPSPs in bulbospinal RVLM neurons recorded intracellularly, providing evidence for direct baromediated inhibition *(Lipski et al., 1996)*.

Many RVLM neurons also exhibit firing patterns related to respiration, the proportion and strength of which is related to central respiratory drive. *In vivo* these are characterised either by an inspiratory depression, inspiratory activation, early inspiratory depression and post-inspiratory activation or no clear modulation *(McAllen, 1987; Haselton and Guyenet, 1989a; Miyawaki et al., 1995)* (see Section III).

Peripheral chemoreceptor- and somatic afferent-related input are important sources of excitatory drive to many RVLM neurons. Short lasting hypoxia induced activation of almost all presympathetic RVLM neurons recorded in rat *(Sun and Spyer, 1991a; Sun and Reis, 1993, 1994)* whereas others found that about half were excited by hypoxia *(Kanjhan et al., 1995)*. Similarly, nociceptive stimulation excites many RVLM neurons *(Sun and Spyer, 1991b; Kanjhan et al., 1995; Verberne et al., 1999a)*. Cardiopulmonary receptor activation with phenylbiguanide also inhibits many baro-inhibited RVLM neurons *(Verberne et al., 1999a)*.

Neurons that are strongly inhibited by baroreceptor and cardiopulmonary inputs but weakly modulated by nociceptive afferents are found within 300 μm caudal to the facial nucleus and project to the hypothalamus or thoracic cord but not both *(Verberne et al., 1999a)*. In contrast, most baroinhibited neurons that are strongly activated by noxious stimuli are located 600-800 μm caudal to facial and project to the hypothalamus *(Verberne et al., 1999a)*. Convergent afferent inputs are integrated via summation of synaptic inputs in RVLM neurons; for example, the degree of cardiac rhythmicity and sensitivity to aortic nerve stimulation of single RVLM units is modulated by periodic inputs from central respiratory neurons *(Miyawaki et al., 1995)*.

McAllen et al. demonstrated using cross-correlation analysis that there is little evidence for synchronicity (unrelated to baroreceptor or respiratory inputs) between pairs of RVLM neurons recorded extracellularly in cat *(McAllen et al., 2001)*. Moreover, there was little evidence for synaptic interconnections between pairs of RVLM neurons *(McAllen et al., 2001)*. Hence, as a group of premotor units driving rhythmic discharge of sympathetic nerves, RVLM neurons do not appear to be part of a synaptically interconnected or oscillator driven network. Rather, they appear to act as independent units that are rhythmically entrained by the arrival of common afferent inputs. A role for descending inputs that release angiotensin or glutamate to tonically excite RVLM neurons has been postulated *(Dampney et al., 2000; Dampney et al., 2005; Stocker et al., 2006)*, although the sources and significance of these inputs in normal physiological states is still unclear.

Afferent and Efferent Connections of the RVLM

Direct spinal projections from the RVLM have been demonstrated using injection of retrograde tracers into various levels of the thoracic cord *(Amendt et al., 1979; Blessing et*

al., 1981; Ross et al., 1981; Caverson et al., 1983; Ross et al., 1984a). RVLM neurons do not appear to have a topographical organisation correlated to spinal outflow level, although C1 neurons located more rostrally appear to target the adrenal medulla *(Jeske and McKenna, 1992; Pyner and Coote, 1998)*. The projection to the cord is bilateral with ipsilateral predominance *(Jeske and McKenna, 1992)*; projections to adrenal SPN have a strong ipsilateral predominance *(Moon et al., 2002)*. Direct synaptic contacts have been demonstrated between RVLM terminals in the cord and SPN retrogradely labeled from the SCG or adrenal medulla *(Zagon and Smith, 1993; Pyner and Coote, 1998; Moon et al., 2002)*.

The RVLM is also reciprocally connected to regions of the rostral and caudal medulla and several higher brain regions *(Blessing and Willoughby, 1987; Haselton and Guyenet, 1990; Yasui et al., 1990; Verberne, 1995; Horiuchi et al., 1999)*. Injections of retrograde tracing agents into the RVLM labels cells predominantly ispilaterally in the medulla (inferior olive, ventromedial and midline medulla, medial nucleus tractus solitarius (NTS), area postrema, dorsal motor nucleus of the vagus (DMX), the CVLM, the NA and a contralateral region just medial to the NA), and pons (periaqueductal grey and adjacent cuneiform nucleus, lateral parabrachial (PBN) / Kölliker-Fuse (K-F) nucleus, laterodorsal and pedunculopontine tegmental nuclei, A5). The RVLM also connects with regions of the hypothalamus (lateral, perifornical, dorsomedial and paraventricular (PVN) subnuclei), basal forebrain (central nucleus of the amygdala) and cortex (insular and medial prefrontal cortex) *(Dampney, 1994b; Verberne and Owens, 1998)*. Projections to the RVLM from these numerous brain regions are important sources of amine, peptide and amino acid inputs.

Innervation of the RVLM by higher brain structures presumably plays an important role in modulation of circulatory function. In most cases, however, the functional significance of input from pontine, hypothalamic or cortical regions is unclear *(Verberne and Owens, 1998)*. In some cases there is more information. For example, a small group of cells in the PVN appears to selectively target the RVLM and IML *(Toth et al., 1999; Pyner and Coote, 2000)*. A glutamatergic projection from the PVN to the RVLM is activated in rats deprived of water *(Stocker et al., 2006)*, suggesting that it may play a role in central sympathoregulatory responses to changes in osmolality and blood volume. Numerous PVN neurons with spinal or RVLM projections express the immediate early gene *c-fos*, a marker of neuronal activation, following non-hypotensive haemorrhage *(Badoer et al., 1993)*,

water deprivation *(Stocker et al., 2006)*, blood volume expansion or right atrial stretch *(Pyner et al., 2002)*.

Other studies have used *c-fos* expression to map patterns of CNS activation following other homeostatic disturbances. RVLM neurons express *c-fos* following hypertension *(Horiuchi et al., 1999)*, hypotension *(Polson et al., 1995)* or hypoxia in conscious rabbits *(Hirooka et al., 1997)* or hypotensive and non-hypotensive blood loss in anaesthetised rats *(Badoer et al., 1993)*. Neurons in the K-F and medial NTS that project to the RVLM are also activated following AP-altering or hypoxic stimuli but neurons in the CVLM are selectively activated by changes in AP *(Polson et al., 1995; Hirooka et al., 1997; Horiuchi et al., 1999)*. Hence, the RVLM is part of an integrated lower brainstem network concerned with homeostasis, although it is probably the final common pathway for modulation of sympathetic outflow. Neurons in the central nucleus of the amygdala and PBN, but not those that project to the RVLM, are also activated following AP-altering stimuli *(Polson et al., 1995; Hirooka et al., 1997; Horiuchi et al., 1999)*. These neurons are presumably involved to some extent in the emotional, arousal or respiratory responses to homeostatic disturbance.

Although immediate early gene expression has been widely used to mark neuronal activation, it has several disadvantages including a long time course of activation (1-2 hrs). A promising alternative may be to utilise the rapid phosphorylation of intracellular proteins as a marker of activated or inhibited neurons following different stimuli. Immunoreactivity to phosphorylated mitogen-activated protein kinase (MAPK) specifically labels neurons in the RVLM, CVLM and other autonomic regions following short-term anaesthesia or hypotension *(Springell et al., 2005)*.

Peptides and Monoamines are Neuromodulators in the RVLM

Diverse aminergic and peptidergic inputs to the RVLM differentially modulate their ongoing activity and or their responses to reflex inputs; these include acetylcholine *(Giuliano et al., 1989; Huangfu et al., 1997)*, serotonin *(Miyawaki et al., 2001)*, opiates *(Stasinopoulos et al., 2000; Miyawaki et al., 2002b)*, cannabinoids *(Padley et al., 2003)*, angiotensin *(Li and Guyenet, 1995; Saigusa et al., 2003)*, substance P *(Makeham et al.,*

2005), orexin *(Machado et al., 2002)* and many others (see *(Pilowsky and Goodchild, 2002)*.

Amino acid transmission in the RVLM is critical to all sympathetic reflexes *(Kiely and Gordon, 1993; Miyawaki et al., 1996a; Miyawaki et al., 1996b)*. Metabotropic receptor activation, on the other hand, appears to selectively modulate inhibitory or excitatory sympathetic reflexes. The selective 5-HT1A receptor agonist 8-OHDPAT *(Miyawaki et al., 2001)* and the δ-opiate receptor agonist DPDPE *(Miyawaki et al., 2002b)* when injected into the RVLM inhibit the somatosympathetic reflex but leave other reflexes unaffected. In contrast, the μ-opiate receptor agonist DAMGO selectively inhibits the baroreflex *(Miyawaki et al., 2002b)*. Activation of neurokinin-1 receptors (NK-1R) does not affect sympathetic reflexes; whereas their antagonism selectively attenuates sympathoexcitation induced by brief hypoxia *(Makeham et al., 2005)*. These effects are thought to be mediated by activation of receptors selectively located presynaptically on either somatic, baroreceptor- or peripheral chemoreceptor-related afferents innervating the RVLM (eg *(Stasinopoulos et al., 2000; Makeham et al., 2001)*. Activation of angiotensin type 1 (AT-1) receptors in the RVLM produces brief sympathoexcitation and has been shown to slightly increase maximum SNA baroreflex responses *(Saigusa et al., 2003)* or have no effect on baroreflex gain *(Head and Mayorov, 2001)*. Many RVLM neurons express AT-1 receptor postsynaptically *(Li and Guyenet, 1995; Hu et al., 2002)*, suggesting that direct excitation of some RVLM neurons by angiotensin may indirectly affect the reflex sympathetic effects of activating or unloading baroreceptors.

The fact that cardiovascular reflexes can be selectively modulated suggests that neurotransmitter inputs may encode specific patterns of autonomic responses appropriate to different behavioural or homeostatic adaptations. For example, serotonergic raphé neurons in the medulla play an important role in patterned autonomic responses to nociceptive stimuli *(Snowball et al., 1997)* and haemorrhage *(Heslop et al., 2002)*. Inputs to the RVLM from the raphé may evoke appropriate parallel cardiovascular adjustments, including sympathoinhibition and a selective inhibition of the nociceptive somatosympathetic reflex, via 5-HT1A receptor activation, *(Miyawaki et al., 2001)*. The neurochemical content and putative physiological roles of various inputs to RVLM neurons are illustrated in Fig 1.1.4.

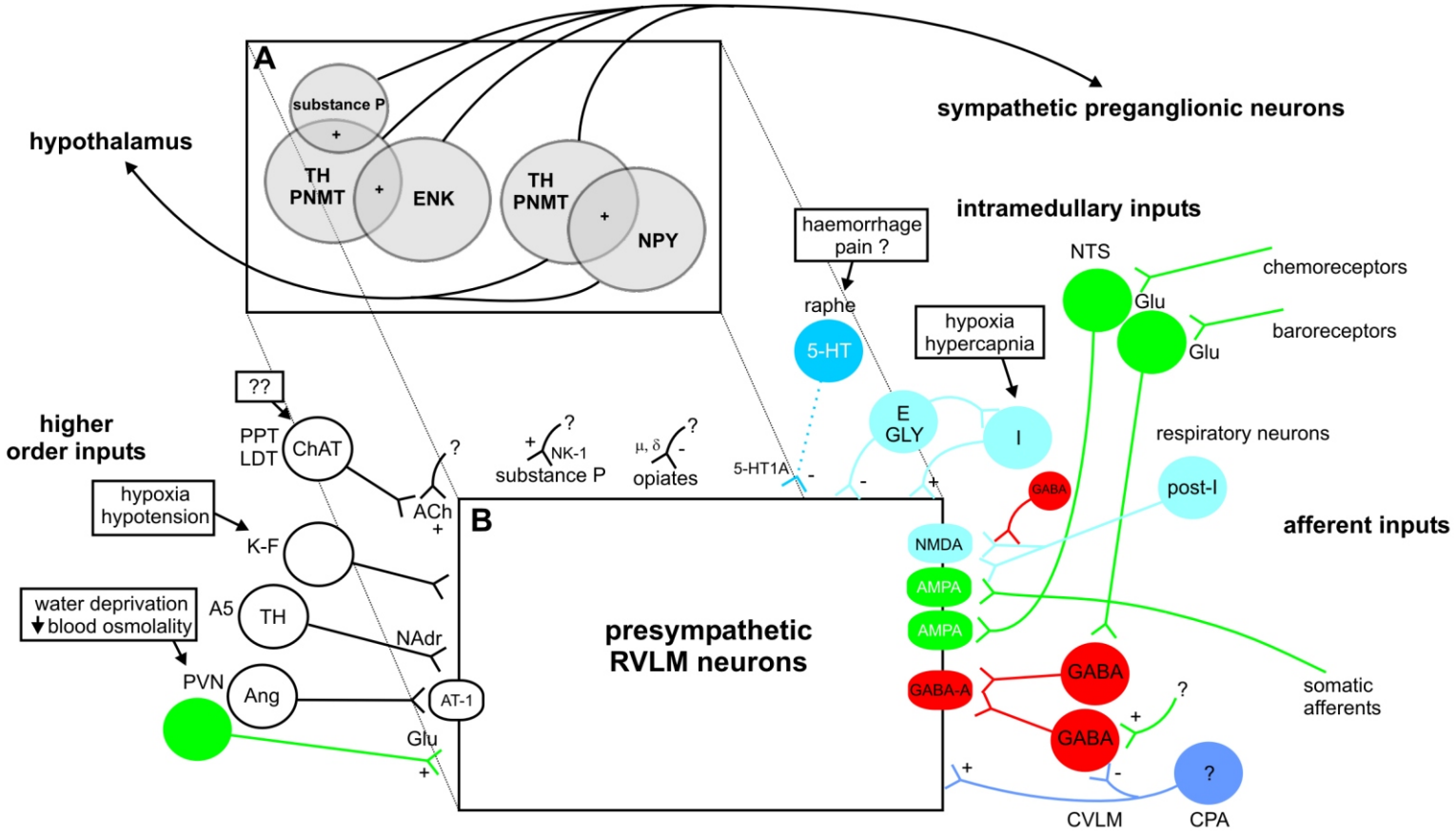

Figure 1.1.4. Diversity of neurochemical content of RVLM neurons with spinal and or hypothalamic projections and inputs to the region.
A: A majority of spinally projecting neurons (50-80 %) contain TH/PNMT (C1 group) and of the non-C1 cells around 80 % contain preproenkephalin mRNA (ENK). 20 % of C1 cells also contain ENK or substance P (+ sign denotes expression of both TH/PNMT and one of these peptides). Virtually all neurons projecting to the hypothalamis, with or without a branching spinal projection, contain NPY.
B: Individual RVLM neurons (shown as a hypothetical black box) receive a wide range of amino acid, peptide and amine inputs that have excitatory (+) or inhibitory (-) effects on their ongoing activity. Amino acid receptor activation is critical to transmission of afferent reflex inputs and inputs from central respiratory neurons (where known, the specific receptor subtype involved is shown on the neuron (postsynaptic)). Some peptides and amines selectively modulate these reflexes, suggesting that their receptors are located presynaptically in the RVLM (for illustration purposes only, and where known, the precise receptor subtype involved is written next to the terminal from which its endogenous ligand is released, although they are probably selectively expressed in the terminals of some reflex inputs to the region (see text). Specific physiological stimuli (indicated in boxes) appear to trigger activation of some of these inputs to make appropriate cardiovascular adjustments; although the functional significance of most intramedullary and higher order inputs to the RVLM is unknown.

Differential Control of Sympathetic Outflow by the RVLM

Several hypotheses have been proposed to explain how centrally-evoked patterns of behaviour and some peripheral afferent signals lead to selective and or differential effects on regional sympathetic outflow. The classic example of this phenomenon in terms of behaviour is the stereotypic response evoked by defensive reactions; so called 'fight or flight'. This is characterised by redistribution of blood flow away from the gut and skin to skeletal muscle and coronary beds in preparation for sudden activity. Some homeostatic reflexes also require specific circulatory adaptations. The 'volume reflex' elicits reductions in renal and increases in cardiac sympathetic outflow in response to reduced blood volume, for example during haemorrhage or water deprivation. Hypoxia or the 'diving reflex' selectively constricts blood vessels supplying viscera and muscle with the aim of preserving blood flow to the major vital organs, the brain and heart.

One hypothesis is that neurons that preferentially control muscle or visceral vasoconstrictors are topographically distributed in the RVLM *(McAllen et al., 1995)*. There is some support for this hypothesis based upon anatomical *(Pyner and Coote, 1998)* and microinjection studies *(McAllen and Dampney, 1990; McAllen and May, 1994; Ootsuka and Terui, 1997)*. Neurons projecting to the kidney or adrenal gland appear to be found most rostrally *(Pyner and Coote, 1998)* and the largest increase in renal blood flow could also be elicited from GABA injections centered rostrally in the RVLM *(Ootsuka and Terui, 1997)*. Neurons controlling other vascular beds appear to be more widely distributed in the RVLM, although neurons that control sympathetic outflow to the heart muscle are a special case. Different positive effects on inotropy, dromotropy or chronotropy are evoked following glutamate microinjection into either the left or right RVLM or following stimulation of the left or right cardiac nerve in vagotomised cats *(Campos and McAllen, 1999a)*.

An intriguing hypothesis is that RVLM neurons controlling different vascular beds are coded either by their neurochemical content or neurotransmitter inputs *(Pilowsky and Goodchild, 2002)*. For example, δ-opioid receptor activation in the RVLM selectively inhibited lumbar but not splanchnic SNA *(Miyawaki et al., 2002b)*. Microinjection of 8-OHDPAT into the RVLM at rostral injection sites selectively inhibited renal sympathetic activity; whereas at caudal sites muscle sympathetic activity was selectively inhibited *(Bago et al., 1999)*. An enduring question is whether or not expression of PNMT or various

neuropeptides including preproenkephalin or NPY encodes separate populations of RVLM neurons that drive different sympathetic outflows.

Input from different presympathetic cell groups to SPN may control not only blood flow but also different aspects of organ function. The stimulus for different functional effects may be encoded in frequency versus amplitude responses of peripheral sympathetic nerves; for example, as is observed in the renal nerve following stimulation of A5 or RVLM in rabbit *(Malpas et al., 1996; Maiorov et al., 2000)*. Fine control of renal function (ie. renal vascular resistance, hormone release or sodium / water re-absorption) may be achieved via alterations of renal nerve frequency and or amplitude *(Malpas et al., 1996; Janssen et al., 1997; Maiorov et al., 2000)*. For example, moderate (10 %) but not mild (13 %) hypoxia increased renin excretion, which depended upon increased amplitude and low frequency bursting of renal SNA *(Janssen et al., 1997)*.

Some afferent reflexes may selectively recruit different premotor units to evoke differential patterns of sympathetic activation or withdrawal. For example, the gut polypeptide cholecystokinin is released following food intake and, via a vagal afferent pathway, evokes intestinal vasodilatation by inhibiting of a subpopulation of sympathoexcitatory RVLM neurons *(Sartor and Verberne, 2002, 2003; Verberne and Sartor, 2004; Sartor et al., 2006)*. The volume reflex is triggered by reduced venous filling pressure and atrial stretch receptor activation *(Bainbridge, 1915)* and probably elicits differential effects on renal and cardiac sympathetic activity via a central synapse in the PVN *(Lovick et al., 1993)*.

Sympathetically-mediated dilatation or constriction of cutaneous blood vessels is essential for control of body temperature. Neurons in the RVLM and raphé are labeled from the rat tail artery *(Smith et al., 1998)*; in rat the tail is a major thermoregulatory organ because of its large surface area and lack of hair. Heat loss and heat preservation mediated by modulation of cutaneous blood flow depends on the level of input to cutaneous SPN from the raphé nuclei; in contrast, input from the RVLM is thought to be only minor or redundant *(Nalivaiko and Blessing, 2002; Nakamura et al., 2004; Ootsuka et al., 2004)*. The recent work of Ootsuka and McAllen suggests that in fact the RVLM, although not concerned with temperature, is crucial to regulation of cutaneous blood flow *(Ootsuka and McAllen, 2005)*. Muscimol inhibition of the RVLM in rat reduced the temperature threshold and sensitivity of tail fibre activation in response to lowering of core body temperature *(Ootsuka and McAllen, 2005)*. The authors conclude that, although the raphé

determines the temperature-sensitivity of cutaneous SPN, the ability to finely regulate their activity is dependent upon a background excitatory drive from the RVLM that raises the threshold and hence excitability of cutaneous SPN *(Ootsuka and McAllen, 2005)*. A similar system could account for high gain control of numerous sympathetic outflows in response to different afferent signals.

Medullary Raphé and Rostral Ventromedial Medulla (RVMM)

Midline and parapyramidal regions of the medulla contain a large population of neurons that provide descending input to SPN supplying diverse sympathetic beds *(Strack et al., 1989)*. These neurons are largely distributed within the serotonergic medullary raphé nuclei (raphé magnus, pallidus and obscurus) and the neighbouring nucleus reticularis gigantocellularis or rostral ventromedial medulla (RVMM) *(Steinbusch, 1981; Strack et al., 1989)*. The medullary raphé nuclei are the largest source of serotonin input to the cord *(Dahlstrom and Fuxe, 1964; Pilowsky et al., 1986; Minson et al., 1990b; Jensen et al., 1995; Pilowsky et al., 1995a)*. Dual labeling experiments in rat demonstrate diverse neurotransmitter content colocalised with 5-HT, including thyrotropin-releasing hormone, substance P, enkephalin and GABA *(Kachidian et al., 1991)*. There are also many non-serotonergic cells intermingled within these areas.

Neurons in the raphé project monosynaptically to SPN the IML *(Bacon et al., 1990)* and may have axon collaterals that synapse on catecholamine-containing neurons in the RVLM *(Nicholas and Hancock, 1990)*. Functional evidence indicates a polysynaptic pathway to the RVLM since stimulation of a depressor region within the raphé inhibits barosensitive RVLM neurons but raphé neurons could not be antidromically activated from the RVLM *(McCall, 1988; Verberne et al., 1999b)*. Serotonin- and substance P-containing neurons in the raphé project directly to the ventrolateral medulla *(Holtman and Speck, 1994)* and may be implicated in 5-HT or NK-1 receptor-mediated cardiovascular or respiratory effects *(Gray et al., 1999; Miyawaki et al., 2001; Makeham et al., 2005)*. Raphé neurons receive projections from the dorsal horn, NTS, RVLM, lateral tegmental field, ventrolateral periaqueductal grey and preoptic hypothalamic area *(Snowball et al., 1997; Nogueira et al., 2000; Wang and Wessendorf, 2002)* and a subset of 5-HT-containing cells is inhibited

by baroreceptor discharge *(Pilowsky et al., 1995b; Gao and Mason, 2001)*. Hence, a wide array of visceral, nociceptive and somatic information reaches raphé neurons.

The effects on sympathetic vasomotor outflow elicited by stimulation of the raphé are often contradictory and appear to reflect a mixed population of sympathoexcitatory and -inhibitory neurons *(Coleman and Dampney, 1995; Henderson et al., 1998)*. Pressor responses are evoked from the RVMM *(Minson et al., 1987)* whereas depressor or pressor effects are evoked from the caudal midline medulla depending on species or anaesthesia *(Coleman and Dampney, 1995; Henderson et al., 1998; Verner et al., 2004)*. Microinjection of GABA or muscimol into the raphé does not alter renal sympathetic activity or AP *(Coleman and Dampney, 1995)*, suggesting that it does not contribute to vasomotor tone generation.

The functional role of 5-HT in control of SPN activity is still unclear *(Minson et al., 1990b; Jensen et al., 1995)*. Glutamatergic raphé neurons are the largest source of temperature-sensitive excitatory drive to cutaneous SPN and brown adipose tissue (see above and *(Nakamura et al., 2004)*. Most raphé neurons that were activated by cold exposure or fever that expressed the type 3 vesicular glutamate transporter (vGLUT3) did not contain 5-HT *(Nakamura et al., 2004)*, suggesting that these populations of neurons are functionally and morphologically separate. Raphé neurons also play a role in cardiovascular responses to haemorrhage *(Heslop et al., 2002)*, descending control of nociception *(Mason, 2001)* and respiration *(Verner et al., 2004)*. However, the precise role of 5-HT in many of these functions is unclear. 5-HT-containing neurons in the raphé are very sensitive to changes in pH and are associated with medullary arteries suggesting that they may function as central chemosensors *(Bradley et al., 2002; Nattie et al., 2004)*.

Pontine A5

The A5 cell group is located within the caudal ventral pons between the facial nucleus and its emerging fibre bundle and the caudal pole of the superior olivary nucleus. By definition it contains cells that synthesize noradrenaline and traditionally it was defined by immunoreactivity to the catecholamine synthetic enzymes TH or DβH *(Byrum et al., 1984; Byrum and Guyenet, 1987)*. Using this approach, several authors have estimated that approximately 90 % of the A5 neurons project to the spinal cord IML and central

autonomic area *(Byrum et al., 1984)*. Goodchild and colleagues showed, however, that some cells in the A5 region contain DβH but not TH and do not project to the thoracic cord or the RVLM *(Goodchild et al., 2001)*, suggesting that A5 is not a homogeneous cell population. Nevertheless, it is well established that the A5-spinal projection plays a role in control of sympathetic outflow and is presumably the only supraspinal source of noradrenaline regulating activity of SPN.

Byrum, Stornetta and Guyenet proposed a method for identifying sympathoregulatory A5 cells *in vivo* in rat based upon their location, antidromic activation from the spinal cord and inhibition by clonidine *(Byrum et al., 1984)*. Some A5 cells are inhibited by baroreceptor discharge but are unaffected by nociceptive input *(Byrum et al., 1984; Guyenet, 1984; Huangfu et al., 1991)*. Some A5 cells also have extensive ascending and intramedullary projections *(Byrum et al., 1984; Byrum and Guyenet, 1987)*. Connections to the RVLM have been disputed, although the best evidence is that A5 cells are destroyed after toxin uptake following injection of DβH-saporin into the RVLM *(Madden et al., 1999)*. A recent study also revealed labeling in A5 following CTB injection into the retrotrapezoid nucleus in rat, which overlaps the rostral tip of the group of C1 RVLM neurons *(Rosin et al., 2006)*.

Despite this knowledge the functional role of A5 cells in cardiovascular regulation is unclear. Electrical stimulation of the region produced large increases in AP in anaesthetised rabbits *(Woodruff et al., 1986; Drye et al., 1990; Maiorov et al., 1999)*. Studies using chemical stimulation showed clearly, however, that activation of A5 evokes depressor responses or minimal effects on AP in anaesthetised *(Drye et al., 1990; Maiorov et al., 1999)* or conscious rabbits *(Maiorov et al., 1999; Maiorov et al., 2000)* and anaesthetised rats *(Stanek et al., 1984; Loewy et al., 1986; Huangfu et al., 1992)*. These responses may be due to differential effects on regional blood flow *(Stanek et al., 1984)* and sympathetic activity *(Huangfu et al., 1992)*. For example, injection of NMDA into the A5 region increased splanchnic and renal SNA but reduced lumbar SNA and AP *(Huangfu et al., 1992)*. Depletion of spinal cord noradrenaline using injections of 6-OHDA in rat attenuated the depressor response to A5 stimulation *(Loewy et al., 1986)*. Blockade of spinal GABA-A receptors using intrathecal injection of bicuculline also prevented depressor responses to glutamate stimulation of A5 *(Hara et al., 1997)*. This suggests that sympathoinhibition produced by A5 is mediated by activation of an intraspinal inhibitory

interneuron to at least some SPN. The putative role of A5 neurons in chemoreflex control of the circulation is discussed in Section V.

Paraventricular Nucleus of the Hypothalamus (PVN)

The PVN is located around the dorsolateral edges of the 3rd ventricle and contains neurons important in autonomic and neurosecretory function. Together with several other hypothalamic nuclei it provides descending input to SPN *(Luiten et al., 1985)* but it is unique in that it targets the entire sympathetic outflow *(Strack et al., 1989)*. Direct synaptic connections have been demonstrated between PVN neurons and SPN supplying the SCG *(Hosoya et al., 1991)*, stellate ganglion *(Ranson et al., 1998)* and adrenal gland *(Motawei et al., 1999)*.

The PVN is subdivided into five parvocellular and three magnocellular subdivisions *(Swanson and Kuypers, 1980)*. PVN neurons that target SPN are concentrated in the dorsal and posterior parts of the parvocellular PVN *(Swanson and Kuypers, 1980; Swanson et al., 1980; Strack et al., 1989)*. PVN neurons transneuronally labeled from the stellate ganglion or SCG were located medially; whereas those labeled from the adrenal gland or celiac ganglion were located dorsolaterally within the parvocellular subdivision *(Strack et al., 1989; Jansen et al., 1995)*. Neurons in the magnocellular PVN secrete vasopressin, oxytocin and corticotrophin-releasing factor (CRF) directly into the portal circulation via terminals that synapse in the posterior pituitary. This vascular access allows indirect neurohumoral control of autonomic function in addition to direct regulation of autonomic outflow via parvocellular neurons.

Around a third of spinally projecting PVN neurons also contain vasopressin and oxytocin *(Sawchenko and Swanson, 1982; Cechetto and Saper, 1988)*. 22 % of PVN neurons transneuronally labeled from the superior cervical ganglion but only 6 % of neurons labeled from the adrenal or celiac ganglion contained vasopressin *(Strack et al., 1989)*. The PVN is probably the only supraspinal source of vasopressin within the spinal cord *(Cechetto and Saper, 1988)*. Other peptides and neurotransmitters expressed by spinally projecting PVN neurons include somatostatin *(Sawchenko and Swanson, 1982)*, met-enkephalin *(Sawchenko and Swanson, 1982; Cechetto and Saper, 1988)*, angiotensin II and CRF *(Jansen et al., 1995)*.

The PVN also has extensive projections to other autonomic cell groups in the brainstem *(Luiten et al., 1985; Toth et al., 1999)*. PVN fibres descend through the ventrolateral midbrain and pons synapsing in the substantia nigra, periaqueductal grey and pontine reticular nuclei [dorsal raphe, pedunculopontine and parabrachial nuclei, locus coeruleus and A5]. Posterior to the pons, PVN fibres traverse the floor of the medulla and send branches into the dorsal medulla (NTS, DMX), ventrolateral medulla (RVLM, CVLM, NA), and midline raphe. Most fibres terminate bilaterally via segmental decussations with the exception of exclusively ipsilateral input to the RVLM *(Toth et al., 1999)*.

Presympathetic PVN neurons do not appear to be concerned with changes in AP level, with very few neurons showing c-fos activation after hypotensive stimuli *(Badoer et al., 1993; Dampney et al., 2003a)*. Some PVN neurons are reported to be barosensitive and display tonic activity *(Lovick and Coote, 1988; Chen and Toney, 2003)*. Most PVN neurons are extremely sensitive to changes in blood volume or plasma osmolality *(Badoer et al., 1993; Pyner et al., 2002; Stocker et al., 2006)*. Blood volume expansion causes a distinct efferent response characterised by an increase in sympathetic outflow to the heart and a corresponding decrease in sympathetic outflow to the renal bed. This response is thought to be mediated in part by activation of PVN neurons via input from circumventricular organs or from vagal afferent pathways responsive to changes in right atrial venous filling pressure *(Bainbridge, 1915)*. Ibotenic acid lesion of the PVN inhibited the effect of blood volume expansion on renal vasodilatation in rat *(Lovick et al., 1993)*. Expansion of a balloon catheter located at the junction of the superior vena cava and right atrium in rats inhibited renal sympathetic activity and induced *c-fos* expression in a small number of PVN neurons *(Pyner et al., 2002)*. A reduction in renal and increase in cardiac or splanchnic sympathetic nerve activity was observed following discrete injections of excitatory amino acids into the PVN *(Deering and Coote, 2000)*.

A role for the PVN in tonic AP regulation is controversial. In rats deprived of water for two days, inhibition of the PVN with the GABA-A receptor agonist muscimol dramatically reduces AP and renal or lumbar sympathetic nerve discharge; whereas it has little effect in control animals *(Stocker et al., 2004; Stocker et al., 2005)*. Thus descending input from the PVN may be critical for AP maintenance in certain circumstances. In spontaneously hypertensive rats (SHR) injection of muscimol bilaterally into the PVN reduced sympathetic nerve discharge and AP much more markedly compared to normotensive

animals *(Allen, 2002)*. Reduced inhibition or increased excitation of PVN neurons via glutamatergic or angiotensinergic inputs may contribute to the tonic elevation of sympathetic activity that occurs in SHR or experimental heart failure *(Dampney et al., 2005)*.

II. Central Control of Cardiac Vagal Outflow

Introduction

Vagal efferent outflow to the heart mediates negative chronotropic, dromotropic and ionotropic effects. Vagal fibres project to ganglia located on epicardial fat pads on right and left atria that selectively regulate sinoatrial node rate and atrioventricular conduction, respectively *(Randall and Ardell, 1985; Ardell and Randall, 1986; Gatti et al., 1995)*. A third intracardiac cranioventricular ganglion was identified in cat that mediates effects of vagal stimulation on left ventricular contractility *(Gatti et al., 1997)*. Vagal tone is subject to powerful reflexogenic mechanisms that produce strong vagal activation during lung inflation, pulmonary C-fibre and arterial baroreceptor activation *(Haymet and McCloskey, 1975; Davidson et al., 1976; Daly, 1993)*. In addition, vagal efferent discharge is coupled to respiration being most active during post-inspiration / expiration *(Davidson et al., 1976)*.

Cardiac Vagal Preganglionic Neurons (CVPN)

In mammals the level of background activity in vagal nerves is determined by groups of cardiac vagal preganglionic neurons (CVPN) in two regions of the medulla, the DMX and ventrolateral NA illustrated in Fig 1.2.1 *(Hopkins and Armour, 1984; Hopkins et al., 1984; Izzo et al., 1993; Taylor et al., 1999)*. Separate pools of motoneurons in the NA are labeled following dual injection of retrograde tracers into the sinoatrial and atrioventricular nodes *(Blinder et al., 1998b)* or sinoatrial node and cranioventricular ganglion in cat *(Blinder et al., 1998a)*. Hence, the NA may contain separate groups of cardioinhibitory neurons that control different cardiac functions via parallel but morphologically distinct pathways.

Input from the DMX or NA can independently affect heart rate, atrioventricular conduction and ventricular contractility *(Jones et al., 1995; Garcia Perez and Jordan, 2001; Jones, 2001)*. Cheng and Powley demonstrated a largely convergent pattern of inputs to atrial

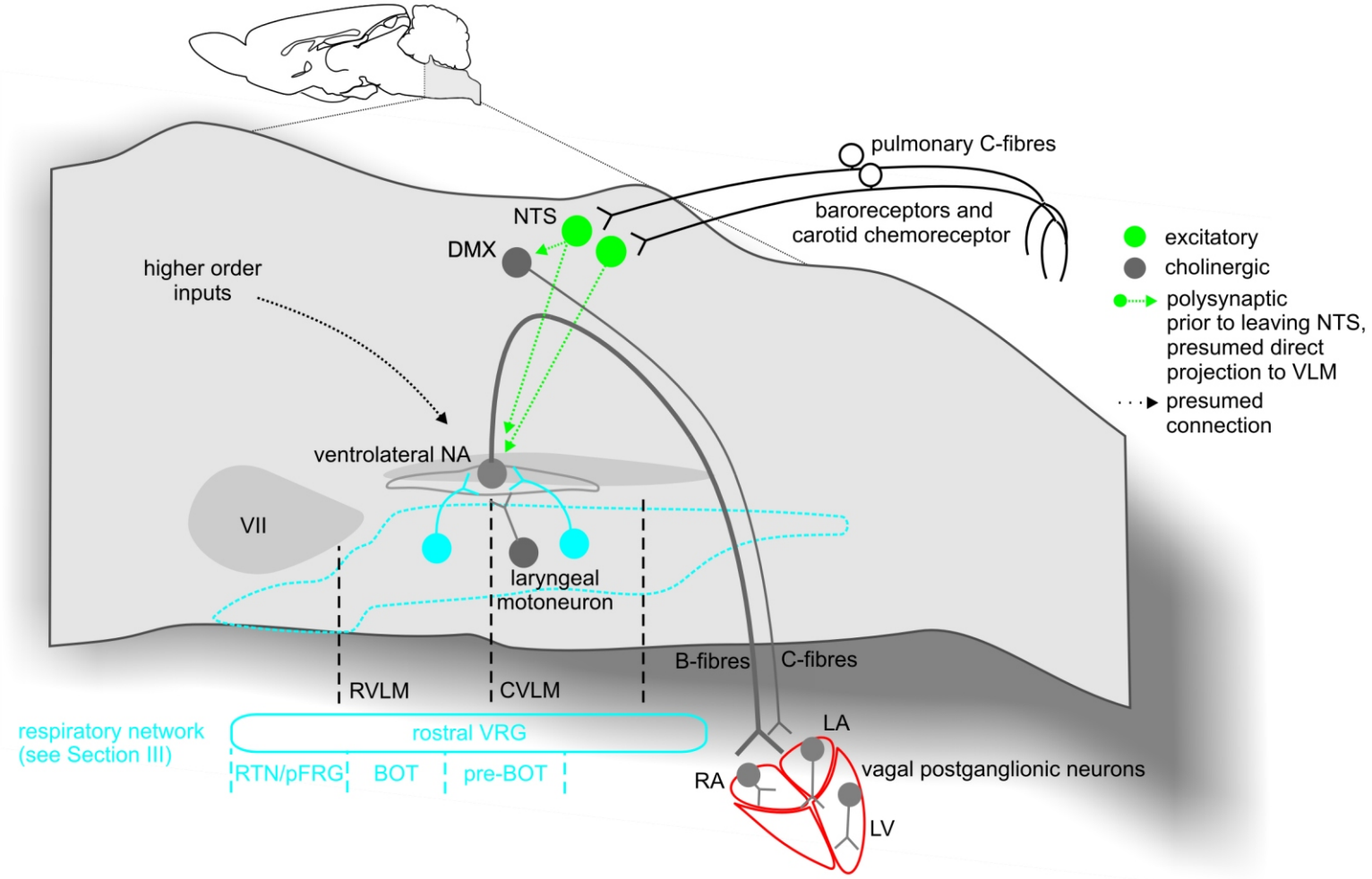

Figure 1.2.1. Major afferent and efferent connections of cardiac vagal preganglionic neurons (CVPN) in the dorsal and ventral medulla and location of neighbouring respiratory groups. CVPN located mainly in the ventrolateral NA receive ongoing input from arterial baroreceptors, chemoreceptors and central respiratory neurons and have fast-conducting axons. These neurons depend on synaptic inputs to drive their activity and presumably are the main source of ongoing reflexogenic discharge in vagal efferent fibres characterised by strong inhibition during inspiration and powerful baroreflex-evoked increases in their activity. CVPN in the DMX have slower conducting axons, receive more specialised afferent input (including from pulmonary C-fibres) and have less potent effects on vagal activity. CVPN in the NA and DMX provide largely convergent input to vagal postganglionic neurons located in epicardial fat pads on the right and left atria and also within the left ventricle that control heart rate, conduction and ventricular contractility, respectively.

ganglia following anterograde tracing from the NA and DMX in rat *(Cheng et al., 1999; Cheng and Powley, 2000)*. Their results show, however, that axons arising from the NA target greater numbers of postganglionic neurons and exhibit greater divergence (more postganglionic neurons contacted / axon) compared to axons arising from the DMX *(Cheng et al., 1999; Cheng and Powley, 2000)*. These anatomical differences may reflect functional specializations of the two preganglionic neuronal pools. Neurons in the NA are thought to be the major source of reflex cardioinhibitory input based upon their short latency antidromic activation from branches of the cardiac vagus that mediate rapid cardiac slowing in cat *(McAllen and Spyer, 1976)*. The activity of NA neurons is strongly coupled to the cardiac cycle and respiration and their small myelinated axons suggest that they probably comprise the majority of fast-conducting (10-30 m/s) vagal B-fibres *(McAllen and Spyer, 1976, 1978a, 1978b; Gilbey et al., 1984; Jones, 2001)*. Neurons in the DMX do not display baroreflex or respiratory modulation and have unmyelinated axons; hence they probably comprise the majority of slower conducting (< 2 m/s) vagal C-fibres *(Jones et al., 1995, 1998)*.

Synaptic Inputs to CVPN – Critical Role of Amino Acids

CVPN are intrinsically silent and require synaptic inputs to drive their activity *(Mendelowitz, 1999)*. Intracellular recordings from CVPN in the NA revealed that they receive ongoing excitatory and inhibitory synaptic inputs *(Gilbey et al., 1984)*. Very few NA neurons recorded *in vivo* are spontaneously active *(McAllen and Spyer, 1976, 1978a, 1978b)*; when present they fire most strongly during expiration and have a strong pulse-modulated activity being most active during the rising phase of the AP wave *(McAllen and Spyer, 1976, 1978b; Gilbey et al., 1984)*.

Strong increases in CVPN activity are mediated by iontophoretic application of excitatory amino acids or activation of arterial baroreceptors *(McAllen and Spyer, 1978b)*. A direct projection to CVPN from the NTS has been reported in cat *(Blinder et al., 1998b)*. Electrical stimulation of the NTS in medullary slices results in excitatory amino acid receptor-dependent EPSPs in retrogradely labeled CVPN *(Neff et al., 1998a)*. Hence a direct excitatory pathway from the NTS to CVPN in the NA is likely to mediate bradycardia following baroreflex activation.

Patch-clamp recordings from rat CPVN in medullary slices revealed GABA and glycinergic inhibitory postsynaptic potentials during inspiration *(Neff et al., 2003)*. Consistent with this, intracellular recordings in cat showed that inspiratory inhibition was mediated by chloride-mediated IPSPs *(Gilbey et al., 1984)*. The source of central inspiratory-related inhibition of CVPN is at present unclear. Some CVPN in the NA receive excitatory input from superior laryngeal neurons *(Mendelowitz, 2000)*, which may impose their own respiratory rhythmicity onto CVPN. The synaptic inputs to CVPN are illustrated in Fig 1.2.2.

Peptide and Amine Inputs to CVPN

The NA receives diverse aminergic and peptidergic inputs that contribute to the ongoing and occasional regulation of CVPN activity in concert with changes in behaviour, arousal or metabolic requirements *(Jordan, 2005; Paton et al., 2005)*. The origin of many of these inputs is unknown, given that the utility of neuronal tracers is limited because of the small size of the NA and diverse functions of vagal preganglionic neurons clustered together in the NA.

In medullary slices patch-clamp recordings of retrogradely labeled CVPN showed that the frequency of GABAergic and glycinergic IPSPs was enhanced by bath application of orexin-A *(Wang et al., 2005)*. Input to CVPN from orexin-synthesising neurons in the lateral / perifornical hypothalamus *(Saper et al., 2005)* may hence contribute to the profound tachycardia evoked by stimulation of this region *(McDowall et al., 2006)*. Other peptides including substance P injected into the NA evoke bradycardia without altering atrioventricular conduction *(Massari et al., 1996)*. Numerous substance P immunoreactive terminals form synapses in the NA but not directly with CVPN *(Blinder et al., 1998c)*, indicating a site of action presynaptic to CVPN.

5-HT-containing terminals closely appose CPVN within the NA in rat *(Izzo et al., 1993)*. Antagonism of 5-HT1A receptors using intracisternal injection of WAY prevents baroreflex reductions in heart rate in rabbit *(Skinner et al., 2002)*. Activation of presynaptic 5-HT1A receptors located on GABA inputs to CVPN is thought to facilitate baroreflex-evoked bradycardia via disinhibition *(Skinner et al., 2002; Jordan, 2005)*. Serotonergic medullary raphé nuclei have projections to airway vagal preganglionic neurons in the NA *(Haxhiu et al., 1993)*, although whether or not they also target CVPN is at present unclear.

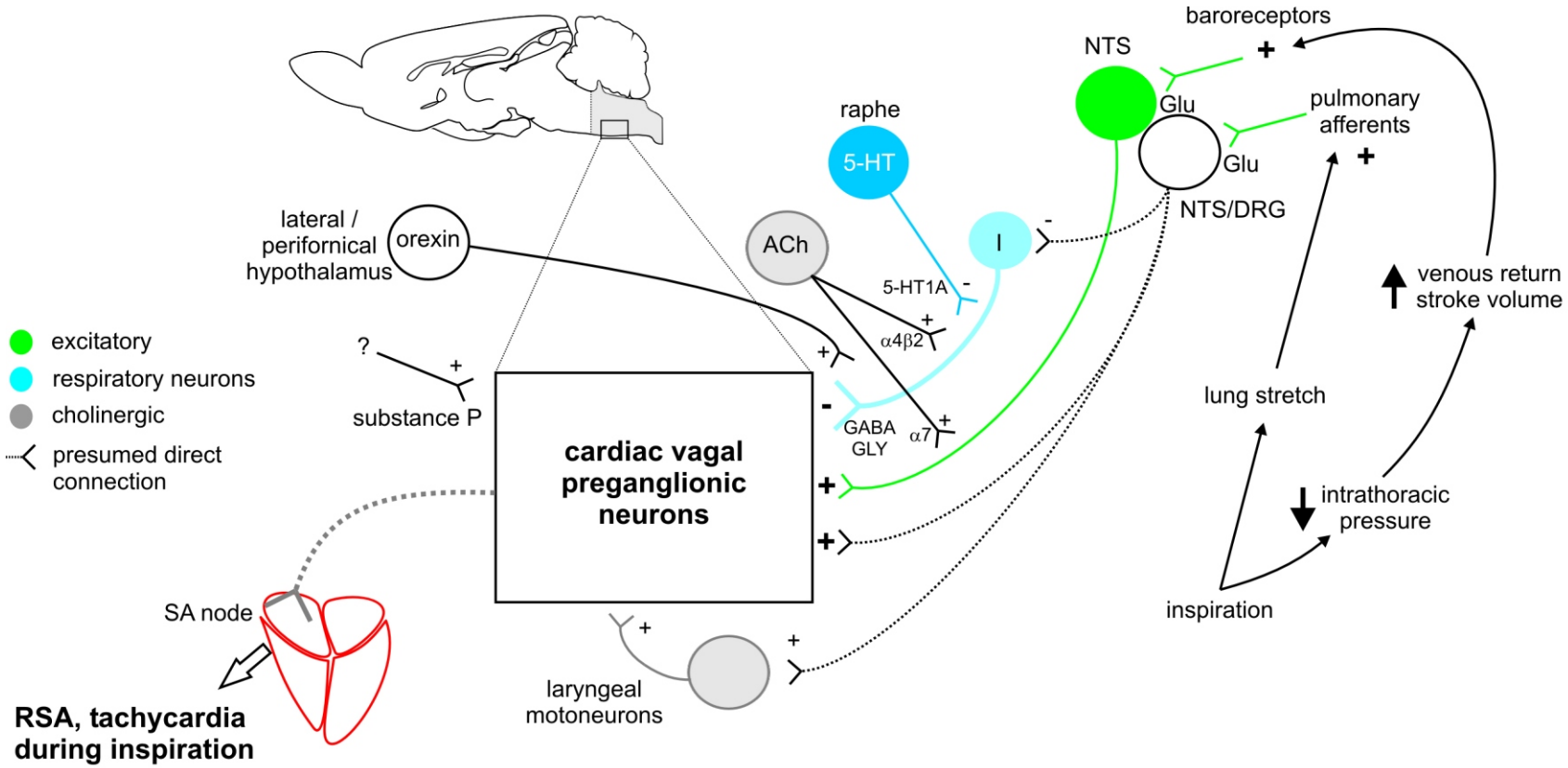

Figure 1.2.2. Synaptic inputs to CVPN in the NA. Cardioinhibitory CVPN are dependent upon ongoing synaptic inputs to drive their activity, which generate rhythmic fluctuations of vagal efferent discharge and heart rate. Rhythmic heart rate fluctuations synchronous with respiration (respiratory sinus arrhythmia, RSA) result from the summation of inspiratory synaptic nhibition (via direct inputs from central respiratory neurons) and post-inspiratory excitation of CVPN. The mechanisms of the latter are numerous and include pulmonary afferent reflex inputs triggered by lung stretch (which also reflexly inhibit inspiration and excite larygneal adductor motoneurons) and excitatory baroreflex inputs triggered by increases in stroke volume due to a transient reduction in intrathoracic pressure. Serotonergic and cholinergic inputs facilitate rhythmic respiratory-timed inhibition and excitation of CVPN via receptors located presynaptically on respiratory or baroreflex-related inputs (for illustration purposes the specific nicotinic and 5-HT receptor subtypes involved are shown next to the terminal from which their endogenous ligand is released). Numerous other peptide and amine inputs (eg. orexin) modulate activity of CVPN under specific circumstances (eg. sleep/wake, distress).

Acetylcholine acting at pre- and post-synaptic nicotinic receptors within the NA has a powerful excitatory influence on CVPN *(Mendelowitz, 1998)*. Collateral inputs from ambiguual motoneurons colocalised within the NA may be an important source of cholinergic inputs to CVPN *(Mendelowitz, 2000)*. Nicotinic receptors appear to be activated phasically to facilitate glutamatergic excitation of CVPN by baroreceptor inputs, and conversely to facilitate GABAergic inhibition of CVPN during inspiration *(Neff et al., 1998b; Wang et al., 2001; Neff et al., 2003; Wang et al., 2003)*. For details see Section VI.

Inspiratory Gating of Reflex Bradycardia

Vagal bradycardia elicited by baroreceptor or carotid chemoreceptor activation is attenuated during lung inflation or central inspiration *(Haymet and McCloskey, 1975; Davidson et al., 1976; Daly, 1993)*. CVPN in the NA that receive both reflex and respiratory inputs are likely to be involved since single CVPN are less sensitive to baroreceptor activation during inspiration, when they are actively inhibited *(McAllen and Spyer, 1978b; Gilbey et al., 1984)*. Hence, the gating of reflex bradycardia during inspiration most likely reflects a reduced capacity of reflex excitatory inputs to induce activation of CVPN when their membrane is relatively hyperpolarized at this stage of the respiratory cycle. In contrast, reflex bradycardia mediated by pulmonary C-fibre activation is equally effective during inspiration *(Daly, 1993)*. Neurons in the DMX at least partly mediate this response, since they are activated by phenylbiguanide and are not inhibited by central respiratory inputs *(Jones et al., 1998)*.

Respiratory Sinus Arrhythmia

In all mammals there are rhythmic variations of heart rate at the frequency of respiration characterised by tachycardia during inspiration. The mechanisms of this respiratory sinus arrhythmia (RSA) are of immense interest since a reduction in the amplitude of RSA is strongly predictive of early mortality in several clinical settings *(TaskForce, 1996)*. The amount of RSA is thought to reflect the level or degree of reflex control of vagal efferent activity, which protects the heart against ischaemic damage and arrhythmia (see Section VII).

RSA arises in part from the centrally generated pattern of inspiratory inhibition of CVPN *(McAllen and Spyer, 1976; Gilbey et al., 1984; Neff et al., 2003)*. Secondly, lung stretch receptor afferents reflexly activate CVPN following inspiration *(Paton and Nolan, 2000)*.

Thirdly, respiratory muscular movements cause oscillations of AP that lead to phasic baroreflex activation, which in turn modulates CVPN activity in time with respiration (see Section V). Baroreceptor and cardiopulmonary afferents also modulate sympathetic input to the heart. However, vagal activity is thought to largely determine beat-to-beat control of heart rate because ACh is released and degraded rapidly compared to the slower rate of release and clearance of noradrenaline from sympathetic nerve terminals *(Levy et al., 1993)*. Supporting evidence for central respiratory-vagal coupling in humans has come from studies demonstrating that respiratory oscillations of heart rate persist in the absence of respiratory movements during voluntary apnoea *(Passino et al., 1997; Cooper et al., 2003; Cooper et al., 2004)*. Support for baroreflex involvement in humans was demonstrated by showing that sinusoidal neck suction, to damp respiratory AP oscillations reaching carotid baroreceptors, effectively damped RSA *(Piepoli et al., 1997)*.

III. Central Control of Respiration

Introduction

Rhythmic respiratory activity is generated by a network of respiratory neurons in the dorsal and the ventral medulla *(Ezure, 1990; Feldman et al., 1990; Bianchi et al., 1995; Pilowsky, 1995; Onimaru et al., 1997; Ballanyi et al., 1999; Feldman et al., 2003; Duffin, 2004; Ramirez and Viemari, 2005)*. Respiratory neurons in general have firing patterns synchronous with three major phases of the respiratory cycle; inspiration (I), post-inspiration (post-I) and expiration (E) *(Salmoiraghi and Burns, 1960; Salmoiraghi and vonBaumgarten, 1961)*. The coordinated firing of populations of I and E neurons generates rhythmic motor outflow to primary muscles of respiration (diaphragm, abdominal wall and intercostal muscles) and the airways. Different components of the network determine respiratory rate (rhythm) and amplitude *(McCrimmon et al., 2000; Monnier et al., 2003)*. Intrinsic chemosensitivity of the respiratory network (or some of its neurons) and afferent inputs from peripheral O_2-sensitive chemoreceptors determine appropriate levels of ventilation *(Hayashi and Fukuda, 2000; Mahamed et al., 2001; Mulkey et al., 2004; Richerson, 2004)*.

From birth the respiratory network is capable of generating respiratory-like activity in phrenic and hypoglossal nerves recorded in isolated slice or brainstem-spinal cord preparations *(Smith et al., 1991; Onimaru et al., 2003)*. A hybrid network-pacemaker model originally proposed by Smith et al has provided an enduring theoretical framework for understanding respiratory rhythm generation, with some caveats *(Smith et al., 2000)*. Normal inspiratory activity is generated by some neurons with bursting pacemaker-like potentials that excite a group of synaptically interconnected glutamatergic interneurons *(Smith et al., 1991; Koshiya and Smith, 1999)*. The activity of this network recruits inspiratory muscles, presumably via separate premotor pathways supplying cranial and phrenic motorneurons *(Peever et al., 2001)*.

In adults, transitions between inspiration and expiration are dependent upon mutual inhibitory synaptic connections between various components of the network. Blockade of glycine receptors with strychnine or Cl^--mediated inhibition abolishes rhythmic respiratory output in adults *(Feldman and Smith, 1989; Hayashi and Lipski, 1992; Paton and Richter, 1995)*. Early postnatally the inspiratory 'off switch' appears to depend more on the bursting properties of the pacemaker network driving inspiration *(Onimaru et al., 1997)*. Glycinergic IPSPs are recorded in numerous respiratory neurons at this stage of development *(Shao and Feldman, 1997; Brockhaus and Ballanyi, 1998)*; however, blockade of synaptic inhibition *(Onimaru et al., 1989)* or glycine receptors *(Paton and Richter, 1995; Shao and Feldman, 1997)* in neonates does not abolish rhythmic respiratory output. Hence, postnatal development of the respiratory network is dependent upon maturation of respiratory neurons and their synaptic connections.

The Dorsal Respiratory Group

Large pools of medullary respiratory neurons are found in a dorsal (DRG) and ventral respiratory group (VRG) identified in cat, rat, rabbit and several other species *(Bianchi et al., 1995)*. The DRG is located at the level of the obex within the ventrolateral NTS and contains I neurons that are an important source of excitatory drive to spinal motorneurons in cat *(Cohen et al., 1974)*. Although early studies in rat found very few respiratory neurons in this area *(Ezure et al., 1988; Zheng et al., 1991)*, those that are clustered here seldom project to the spinal cord suggesting that the DRG may be functionally less relevant for premotor control of respiration in rat *(de Castro et al., 1994)*. The DRG is likely to be an important site of integration of somatic and visceral reflex input into the

respiratory network in many species. Several I neurons in the DRG in rat project to the spinal cord and are activated by lung deflation *(Ezure and Tanaka, 2000)*.

The Ventral Respiratory Group

In the ventral medulla, respiratory neurons form a lateral column extending from the pyramidal decussation to the caudal pole of the facial nucleus; collectively they form the VRG. Neurons within this region are vital for generating normal and adaptive breathing patterns *(Smith et al., 1991; Lieske et al., 2000; Lieske et al., 2001; Paton et al., 2006)*. The location and major connections of neurons in the VRG are illustrated in Fig 1.3.1.

In general there is a distinct topographic distribution of respiratory neurons in the VRG in adults *(Ezure et al., 1988; Connelly et al., 1992; Sun et al., 1998; McCrimmon et al., 2000)*, although in neonatal animals different classes of respiratory neuron are distributed throughout the VRG *(Onimaru et al., 1997)*. The caudal most part of the VRG caudal to the obex (equivalent to the nucleus retroambigualis as defined in cat) contains predominantly E neurons that project to the spinal cord *(Ezure et al., 1988)*. Rostral to this region and contiguous with the emergence of the NA are a large pool of I neurons that project monosynaptically to the cervical cord *(Ezure et al., 1988)*. They form the major excitatory output pathway driving inspiratory diaphragmatic activity.

The Bötzinger Complex

Immediately caudal to the facial nucleus there is a concentration of inhibitory E neurons, many of which project to the cord *(Merrill and Fedorko, 1984)* and have widespread inhibitory connections with other neurons of the DRG and VRG *(Kalia et al., 1979; Lipski and Merrill, 1980)* as well as with themselves *(Duffin and van Alphen, 1995)*. This region is termed the Bötzinger complex (BOT) *(Lipski and Merrill, 1980)*. In rat it occupies about 600 μm caudal to the facial nucleus *(Sun et al., 1998)*. The majority of BOT neurons are located dorsal to the presympathetic catecholamine-synthesising neurons of the RVLM *(Pilowsky et al., 1990; Kanjhan et al., 1995)* and are immunoreactive for the type 2 glycine transporter *(Schreihofer et al., 1999; Ezure et al., 2003)*. BOT neurons may function as an inspiratory off switch and prolong expiratory time via widespread glycinergic inhibition of I neurons and phrenic motorneurons *(Duffin and Douse, 1993; Tian et al., 1999)*.

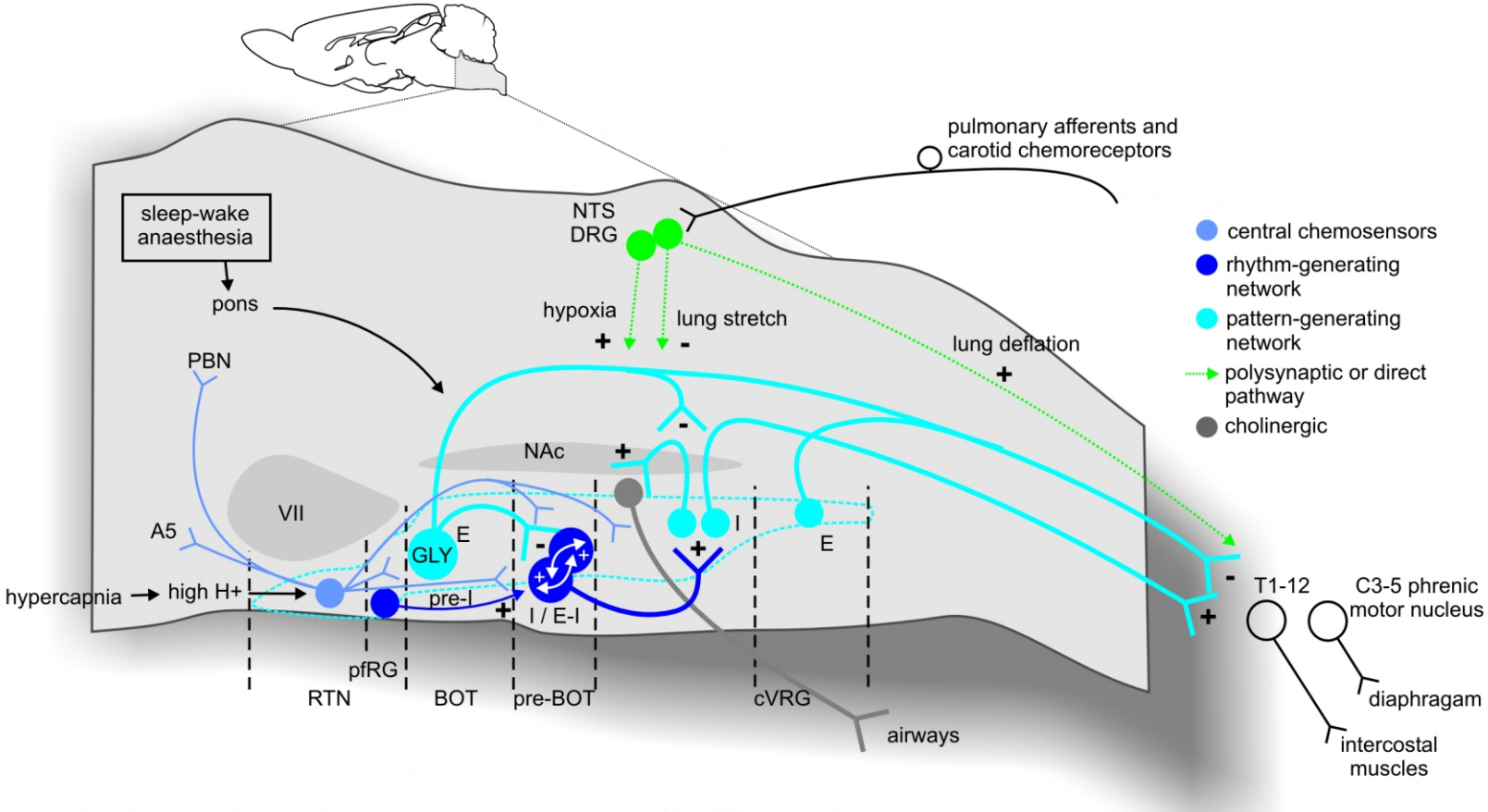

Figure 1.3.1. Schematic showing the location and major efferent projections and interconnections of neurons in the ventral respiratory group (VRG) that generate patterns of normal breathing. The schema is an oversimplification of compartmentalised respiratory neurons that differ in location within the VRG, firing patterns and putative functional role in generating respiratory rhythm or pattern or chemosensitive drive to the respiratory network. The major compartments in adult are as indicated below the ventral surface. The RTN contains neurons sensitive to H+ that have extensive projections throughout the VRG and into the pons. Pre-I neurons in the pfRG and the synaptically interconnected network of propriobulbar excitatory neurons in the pre-BOT are part of the kernel for respiratory rhythm generation. Glycinergic E neurons in the BOT provide widespread inhibitory input to the VRG that is thought to play an important role in switching off inspiratory activity. I neurons of the VRG and E neurons of the cVRG have projections to spinal cord motorneuronal groups supplying inspiratory and expiratory muscles. Major sensory inputs to the respiratory network include pulmonary afferents sensitive to lung stretch and deflation that have inhibitory (-) or excitatory (+) effects on inspiratory activity, respectively; peripheral chemoreceptors that reflexly increase inspiratory activity in response to low PaO2; and higher order inputs that modulate respiratory activity during sleep-wake cycles and anaesthesia.

The Pre-Bötzinger Complex

Between the BOT and the caudally located premotor I neurons lies a transition zone containing a concentration of I, E and E-I phase-spanning neurons whose connections are mainly propriobulbar *(Connelly et al., 1992; Sun et al., 1998)*. This region has been termed the pre-Bötzinger complex (pre-BOT); its anatomical equivalent is the caudal most part of the retrofacial nucleus as defined in cat *(Connelly et al., 1992)* or the rostral part of the CVLM depressor region in rat *(Sun et al., 1998)*. The neurons of the pre-BOT fire rhythmically in the absence of synaptic inputs and lesion of the area results in severely distorted patterns of breathing *(Smith et al., 1991; Koshiya and Smith, 1999; Gray et al., 2001)*. It is thought that this region plays a critical role in generation of respiratory rhythm (see following section).

Retrotrapezoid Nucleus / Parafacial Respiratory Group

At the rostral tip of the VRG are neurons located at the medial border of the facial nucleus close to the ventral surface that provide afferent input to both the DRG, VRG and several other brain regions *(Rosin et al., 2006)*. This area is referred to as the retrotrapezoid nucleus (RTN) or parafacial respiratory group (pfRG) and contains neurons that are intrinsically sensitive to H+ and can generate, via their connections to the VRG, graded ventilatory responses to low pH *(Mulkey et al., 2004; Guyenet et al., 2005a)*. Although other elements of the central respiratory network are chemosensitive *(Bradley et al., 2002; Nattie et al., 2004)*, the RTN is emerging as an important site of central and peripheral chemoreception *(Guyenet et al., 2005b)*.

Numerous neurons with pre-I firing patterns are found within the pfRG in neonates, usually close to the ventral surface *(Onimaru et al., 1989; Onimaru and Homma, 2003)*. Rhythmic activity of these neurons is preserved after cooling of the pre-BOT, which abolishes phrenic discharge, suggesting that the pre-BOT may be driven by these rostrally-located pre-I neurons *(Onimaru et al., 1997)*. Also within the pfRG are putative pacemaker neurons that can drive activity of expiratory muscle groups independent of inspiratory activity *(Janczewski and Feldman, 2006)*. Mammals may have evolved separate rhythm generators driving inspiratory and expiratory activity with a major evolutionary transition in breathing, either from water to air breathing or with the origin of the diaphragm *(Feldman et al., 2003; Janczewski and Feldman, 2006)*.

Reciprocal connections of the VRG

The VRG is reciprocally connected with all levels of the VRG on both sides of the medulla demonstrated using combined retrograde and anterograde tract tracing *(Ellenberger and Feldman, 1990)* and functionally using cross-correlation analysis in rat *(Duffin and van Alphen, 1995; Duffin et al., 2000)*. In addition, anatomical connections have been demonstrated between the VRG and NTS, lateral gigantocellular field (RVMM) and midline raphé *(Ellenberger and Feldman, 1990)*. It is unclear if these areas provide input into respiratory neurons in the ventral medulla, as colocalised in this region are neurons with functionally diverse roles in control of the airways, circulation and organ function.

Respiratory Rhythm Generation

Normal respiratory rhythm depends on the bursting discharge of one or more groups of neurons. The kernel for respiratory rhythm generation was originally thought to reside in the pre-BOT. A thin section (~ 350 μm) of the medulla from neonatal rat containing only this region and lacking any afferent input is capable of generating rhythmic discharge in XIIn roots emerging from the slice *(Smith et al., 1991)*. The pre-BOT contains at least two classes of pacemaker-like neurons; some depend on a persistent sodium current whereas others depend on calcium to drive their intrinsic bursting activity *(Pena et al., 2004)*. Either class of pacemaker appears to be able to maintain normal breathing based upon studies where rhythmic respiratory output was maintained after selective blockade of calcium currents with cadmium *(Thoby-Brisson and Ramirez, 2001)* or persistent sodium currents with riluzole *(St-John et al., 2006)*. Pacemakers that utilise this latter current to drive their bursting activity appear to be crucial to certain patterns of respiratory activity, including gasping evident under severe hypoxia *(Paton et al., 2006)*.

In less reduced preparations, eg brainstem-spinal cord or *en bloc* brainstem, the activity of pre-BOT neurons appears to be driven at least partly by pre-I neurons in the RTN/pfRG that fire up to 500 ms prior to inspiration *(Ballanyi et al., 1999; Onimaru and Homma, 2003)*. Whether or not there are morphologically distinct groups of pacemaker neurons in adult is unclear. Selective inhibition of the pre-BOT using opiate administration in juvenile rats is thought to uncouple their activity, resulting in quantal reductions in breathing frequency due to failure of the pre-I cell group to trigger pre-BOT activity *(Takeda et al., 2001; Mellen et al., 2003)*.

Reciprocal excitatory and inhibitory connections between the network of I neurons in the pre-BOT are necessary to drive rhythmic inspiratory activity. In slice preparations from neonatal rat containing pre-BOT neurons, rhythmic XIIn discharge was abolished by bath application of the non-NMDA receptor antagonist CNQX *(Smith et al., 1991; Funk et al., 1993)*. Release of glutamate acting predominantly at AMPA receptors appears to be essential for this to occur *(Smith et al., 1991; Funk et al., 1993)*. I and E neurons within the pre-BOT also have reciprocal inhibitory connections that are glycinergic *(Shao and Feldman, 1997)*.

Peptide inputs converge on pre-BOT neurons and are important for bidirectional modulation of respiratory rhythm. In slice preparation from neonatal rats and mice, injection of substance P depolarized pre-I neurons in the pre-BOT whereas opiate administration hyperpolarized these neurons *(Gray et al., 1999)*. Expression of the substance P neurokinin-1 receptor (NK1-R) may distinguish a key group of ~ 600 glutamatergic neurons with a pre-I firing pattern in pre-BOT *(Gray et al., 1999; Gray et al., 2001; Guyenet and Wang, 2001; Guyenet et al., 2002)*. Selective destruction of NK1-R pre-BOT neurons by microinjection of the neurotoxin saporin conjugated to substance P led to severely ataxic breathing patterns during wakefulness in adult rat *(Gray et al., 2001)*. However, many of the caudal most NK1-R containing neurons in rat are bulbospinal *(Makeham et al., 2001)* and contain preproenkephalin (PPE) mRNA *(Guyenet et al., 2002)*, suggesting that NK-1R is not a specific marker of propriobulbar glutamatergic pre-BOT neurons.

Respiratory-Sympathetic Integration

Adrian, Bronk and Philips first identified respiratory rhythmicity in cervical and abdominal sympathetic nerves in rabbit and cat that persisted following sensory denervation and under paralysis *(Adrian et al., 1932)*. All vasoconstrictor sympathetic outflows are modulated by central respiratory drive *(Numao et al., 1987; Janig and Habler, 2003)*, although the pattern of respiratory modulation varies considerably depending on the outflow, acid-base balance and animal species. In cat cervical preganglionic fibres are most active during inspiration *(Boczek-Funcke et al., 1992b)*; whereas lumbar sympathetic fibres showed a post-inspiratory peak *(Boczek-Funcke et al., 1992a)*. In rat cervical and lumbar nerves have a post-inspiratory peak; whereas most others have a predominant I peak *(Numao et al.,*

1987; Bartsch et al., 1999; Miyawaki et al., 2002b). Muscle and visceral sympathetic fibres are in general strongly modulated by respiration; whereas fibres supplying cutaneous beds are weakly modulated *(Janig and Habler, 2003)*. Integration between control of respiration and regional and systemic blood flow is thought to be critical to the efficiency of O_2 uptake *(Taylor et al., 1999)*. In rat more sympathetic fibres with predominantly inspiratory activity are recruited by hypoventilation *(Bartsch et al., 1999)*.

SPN in rat show at least four different respiratory-modulated firing patterns; they are most active during either i) inspiration, ii) post-inspiration, iii) expiration or iv) have no respiratory modulation *(Zhou and Gilbey, 1992; Pilowsky et al., 1994a)*. Neurons in presympathetic cell groups RVLM and A5 also exhibit similar patterns of respiratory-modulated activity (Fig. 1.3.2) *(Haselton and Guyenet, 1989a; Guyenet et al., 1993; Miyawaki et al., 1995)*. Hence, it is likely that presympathetic neurons receive direct inputs from respiratory neurons with different firing patterns. E and I neurons in the BOT have extensive local arborisations; their dendrites often project towards the ventral surface and their terminals intermingle with TH-containing neurons in the RVLM *(Pilowsky et al., 1990; Pilowsky et al., 1994b; Kanjhan et al., 1995)*. Some filled intracellularly recorded E neurons of the BOT formed close appositions with TH or spinally projecting neurons in the RVLM in rat *(Sun et al., 1997)*. This input may explain the respiratory modulation of some RVLM neurons that show an expiratory-related depression of their activity, although this population is relatively small *(Miyawaki et al., 1995)*.

Excitatory inputs to presympathetic neurons in the RVLM are a potent source of post-inspiratory excitation of SNA. Blockade of non-NMDA receptors using CNQX in the RVLM selectively abolished the post-inspiratory peak in splanchnic nerve activity *(Miyawaki et al., 1996a)*. Blockade of GABA-A receptors in the RVLM with bicuculline enhanced post-inspiratory discharge of splanchnic and lumbar nerves, suggesting that excitatory post-inspiratory inputs are also tonically inhibited within the RVLM *(Miyawaki et al., 2002a)*. The source of these inputs is unclear. Recently, four types of respiratory modulation were demonstrated in extracellularly-recorded GABAergic neurons in the CVLM *(Mandel and Schreihofer, 2006)*. Hence it is possible that some neurons that relay inhibitory baroreceptor drive to the RVLM also transmit respiratory-related inputs.

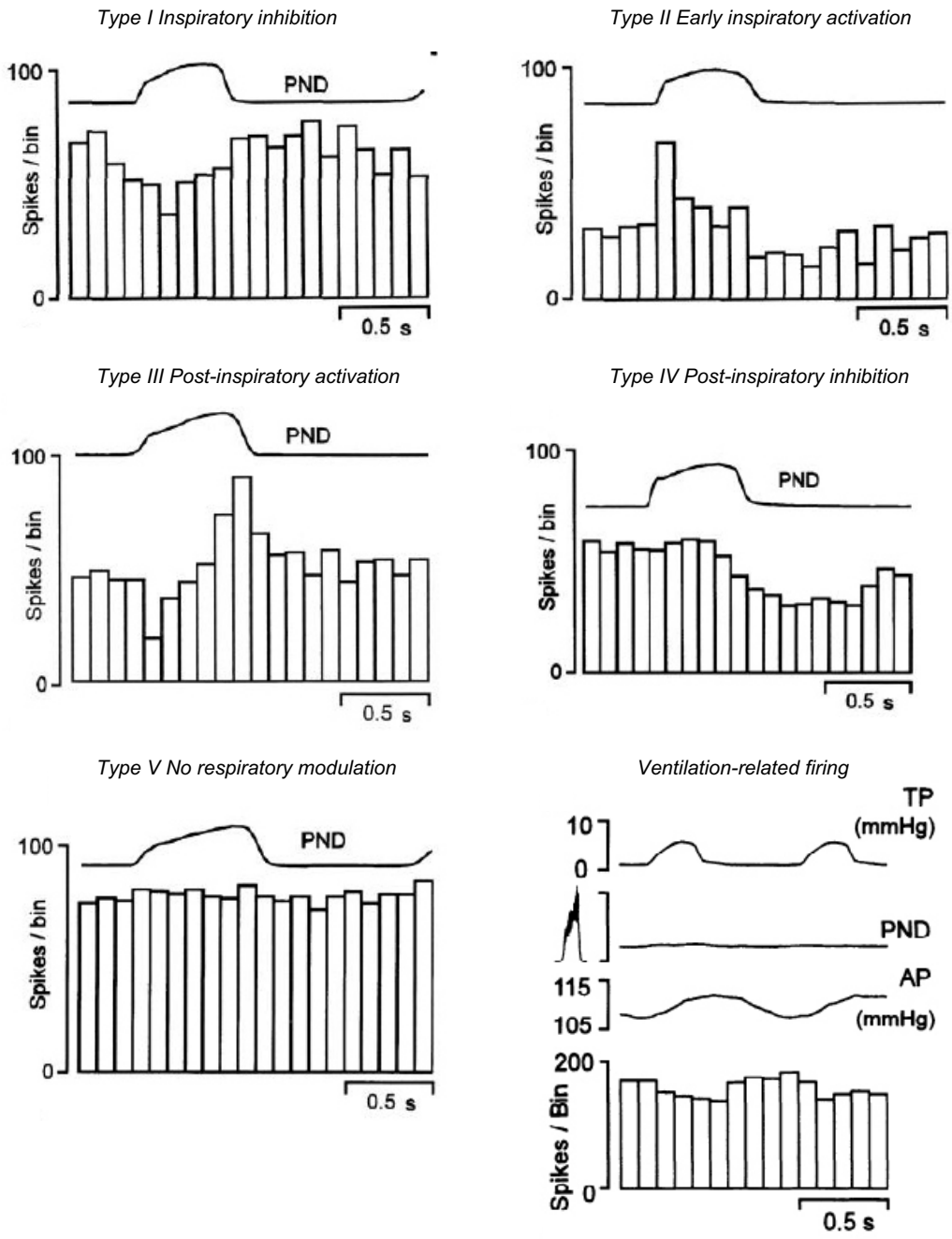

Figure 1.3.2. Different patterns of respiratory modulation and ventilation-related firing of presympathetic RVLM neurons in anaesthetised rats (adapted from Miyawaki et al. 1995). These patterns of activity drive respiratory-synchronous discharges in peripheral sympathetic nerves. Most sympathetic fibres exhibit an inspiratory and or post-inspiratory burst discharge. In the absence of central respiratory drive there is activity in RVLM neurons and sympathetic nerves coupled to the ventilator: this pattern is due to reflex activation of lung stretch receptors and feedback from arterial baroreceptors due to changes in AP generated by positive airway pressure. Natural respiration also generaters rhythmic fluctuations of AP due to an inspiration-induced decrease in intrathoracic pressure, which momentarily increases venous return and stroke volume. Abbreviations: AP, arterial pressure; PND, phrenic nerve discharge; TP, tracheal pressure.

Fluctuations of AP arise due to the mechanical effects of respiration and produce feedback effects on SNA via the baroreflex. AP oscillations result primarily from a reduction in intrathoracic pressure during inspiration that momentarily increases venous return and stroke volume *(Dornhorst et al., 1952)*. In vagotomised, ventilated animals where respiration is out of phase with ventilation, oscillations of SNA can be seen to be coupled both to central respiratory activity recorded in the phrenic nerve and to the rate of the ventilator (eg *(Miyawaki et al., 1995)*. The latter is dependent upon intact baroreceptor afferents *(Habler et al., 1996)*. Activity of single units in the RVLM is also entrained independently to phrenic activity as well as to ventilation *(Miyawaki et al., 1995)*.

IV. Cardiovascular Reflex Function

Cranial and Spinal Afferent Reflex Pathways

Several cranial and spinal afferent pathways modulate peripheral vasomotor and cardiac sympathetic and vagal outflow via inputs to autonomic nuclei in the brainstem. In the following sections the peripheral afferent and central pathways subserving several powerful cardiovascular reflexes (the baroreflex, peripheral chemoreflex and somatosympathetic reflex) are briefly reviewed.

Arterial Baroreceptors

Acute changes in AP are sensed by stretch-sensitive baroreceptors located in the wall of the aortic arch and bifurcation of the internal and external carotid arteries. Aortic and carotid baroreceptor afferents run in the glossopharyngeal (IX) and vagal (X) nerves, via branches known as the sinus and aortic nerves that also carry chemoreceptor information in most species. In rat, rabbit and mouse, aortic nerves only carry baroreceptor information *(Kobayashi et al., 1999)* (see below). Baroreceptor activation caused by increases in AP results in reductions in peripheral sympathetic activity and heart rate; conversely, baroreceptor deactivation elicits opposite compensatory changes. Activity in sympathetic nerves supplying the spleen, heart and renal beds was silenced at different AP (148, 167 and 173 mmHg, respectively), suggesting non-uniform control of regional sympathetic outflow by baroreceptors *(Ninomiya et al., 1971)*.

Central pathways and neurotransmitters subserving the arterial baroreflex have been extensively reviewed *(Kumada et al., 1990; Chalmers and Pilowsky, 1991; Pilowsky and Goodchild, 2002)*. The first central synapse is in the caudal NTS where primary baroreceptor afferents terminate in the dorsolateral and medial subdivisions *(Lipski et al., 1975; Ciriello, 1983)*. Glutamate appears to be an important transmitter relaying baroreceptor information, as baroreflexes are largely eliminated by blockade of excitatory amino acid receptors in the NTS in the anaesthetised adult rat *(Leone and Gordon, 1989)*.

The central baroreflex pathway from the NTS is presumed to include a direct connection with CVPN (see Section II) and indirect connections with the RVLM sympathetic premotor neurons that relay via GABAergic neurons in the CVLM (see Section I) (Fig 1.4.1). NTS neurons have monosynaptic excitatory connections with CVLM neurons *(Bailey et al., 2006)*; however, at this stage it is still not clear if CVLM neurons receive direct input from NTS neurons that are contacted by baroreceptor afferents. It is likely that baroreceptor information is first relayed to interneurons within the NTS, some of which are inhibitory *(Pilowsky and Goodchild, 2002)*. Some barosensitive presympathetic neurons in the PVN and A5 presumably also receive baroreceptor input along with several other central sites including A1, midline raphé, pontine reticular nuclei (LC and PBN), lateral tegmental field and supra-optic nucleus of the hypothalamus *(Yamashita, 1977; Pilowsky et al., 1995b; Barman et al., 2002; Bailey et al., 2006)*. The baroreflex is hence not only integrated within the lower brainstem but also modulates several higher brain areas including, amongst others, those connected with hormonal control and arousal.

Contribution of the Baroreflex to Long Term Levels and Short Term Variability of AP

At normal levels of AP the majority of carotid and aortic baroreceptor fibres are tonically active *(Coleridge and Coleridge, 1980)*. At least in the short term, tonic baroreceptor firing contributes to setting resting levels of sympathetic activity *(Horiuchi and Dampney, 1998)*. The importance of the baroreflex in long term control of AP has been debated. McCubbin and colleagues originally showed that baroreceptor function in dogs with chronic renal hypertension was reset to higher AP, such that baroreceptor afferents fired at higher

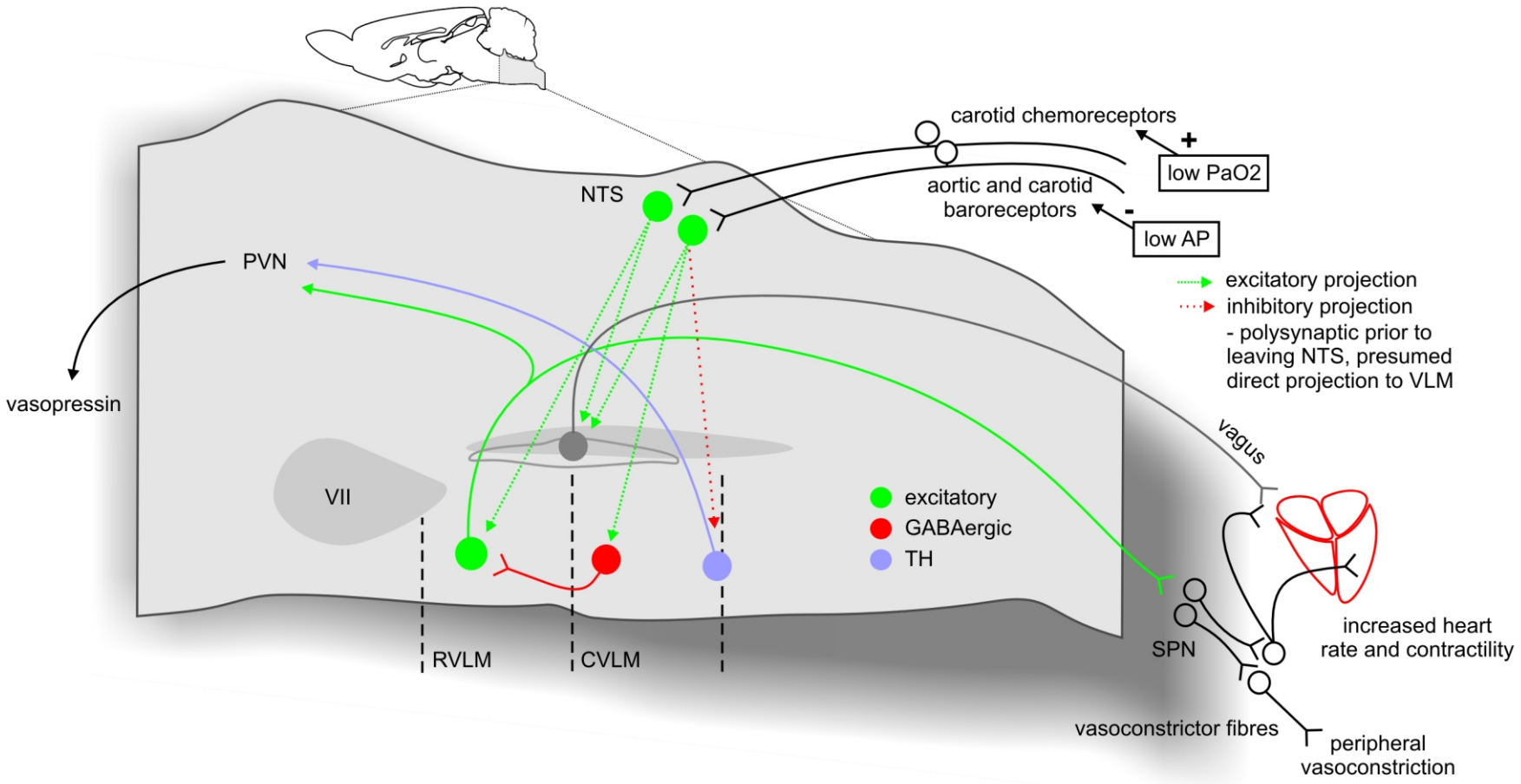

Figure 1.4.1. Schematic representation of central pathways involved in cardiovascular responses to hypotension or hypoxia. Low AP leads to countermeasures designed to restore homeostasis; including a reduction in efferent cardiac vagal outflow and increase in sympathetic outflow to the heart and blood vessels. This occurs via withdrawal of excitatory NTS input to CVPN and GABAergic neurons in the CVLM, which leads to disinhibition of the ongoing activity of presympathetic neurons in the RVLM. Baroreceptor unloading also leads to disinhibition of A1 cells in the caudal VLM that project to the magnocellular secretory neurons in the PVN leading to release of vasopressin, which promotes water resorption in the kidney and has direct vasoconstrictor effects. Low PaO2 elicits peripheral vasoconstriction (mainly in skeletal muscle and abdominal organs) and bradycardia to preserve blood flow to vital organs (the brain and heart). This occurs via activation of NTS excitatory input to both CVPN and presympathetic neurons in the RVLM. The same circuits are recruited in response to hypertensive and hyperoxic stimuli to elicit opposite effects on vagal and sympathetic outflow and inhibit release of posterior pituitary hormones.

stimulus threshold and had normal phasic responses to changes in AP *(McCubbin et al., 1956)*. Baroreceptor resetting occurs rapidly and has been argued to preclude any contribution of the baroreflex to setting long term levels of AP *(Coleridge et al., 1984)*. Rather, baroreflex resetting is thought to be a key mechanism promoting higher levels of AP in several forms of hypertension *(Krieger, 1989)*.

Loss of baroreceptors, on the other hand, would presumably result in chronically elevated sympathetic activity and sustained increases in AP. However, mean levels of AP remain fairly normal for many weeks following complete baroreceptor denervation in dog *(Cowley et al., 1973)*, rabbit *(Saito et al., 1986)* or rat *(Norman et al., 1981; Schreihofer et al., 2005)*. Thrasher recently re-addressed this question in a novel preparation in dog by denervating both sets of aortic and one set of carotid baroreceptors: the common carotid artery was chronically ligated on the side with intact carotid baroreceptors *(Thrasher, 2002)*. Chronic baroreceptor unloading tested in this way led to a sustained increase in mean AP (~ 20 mmHg) recorded over 7 days *(Thrasher, 2002)*). Raised sympathetic activity was indicated by a sustained increase in HR and, despite a presumed increase in renal perfusion pressure, normal sodium excretion and elevated plasma renin *(Thrasher, 2002)*. Hence, despite the phenomenon of resetting, baroreceptors appear capable of long term adjustments of the level of sympathetic outflow. The error signal for the baroreceptors is still unclear, however, since although carotid sinus *pulse* pressure was reduced chronically, *mean* carotid sinus pressure remained normal throughout the 7 days *(Thrasher, 2002)*.

Studies are in full agreement, however, that chronic baroreceptor denervation results in marked increases in short term fluctuations of AP (Fig 1.4.2) *(Cowley et al., 1973; Norman et al., 1981; Saito et al., 1986; Schreihofer et al., 2005)*. Hence, baroreceptor activity plays a critical role in buffering beat-to-beat and daily perturbations in AP. In animals with sinoaortic denervation there is evidence for left ventricular hypertrophy and impaired contractility and endothelial stress *(Eto et al., 2003; Martinka et al., 2005)*. Hence, increased blood pressure variability is an important factor predisposing to organ damage even in the absence of overt hypertension *(Mancia and Grassi, 2000)*.

The dynamic properties of the baroreflex show that it is a high gain system operating over a limited range of sympathetic and vagal nerve firing *(Sato et al., 1999; Petiot et al., 2001; Kawada et al., 2004)*. Baroreflex function is described using logistic curves based on four

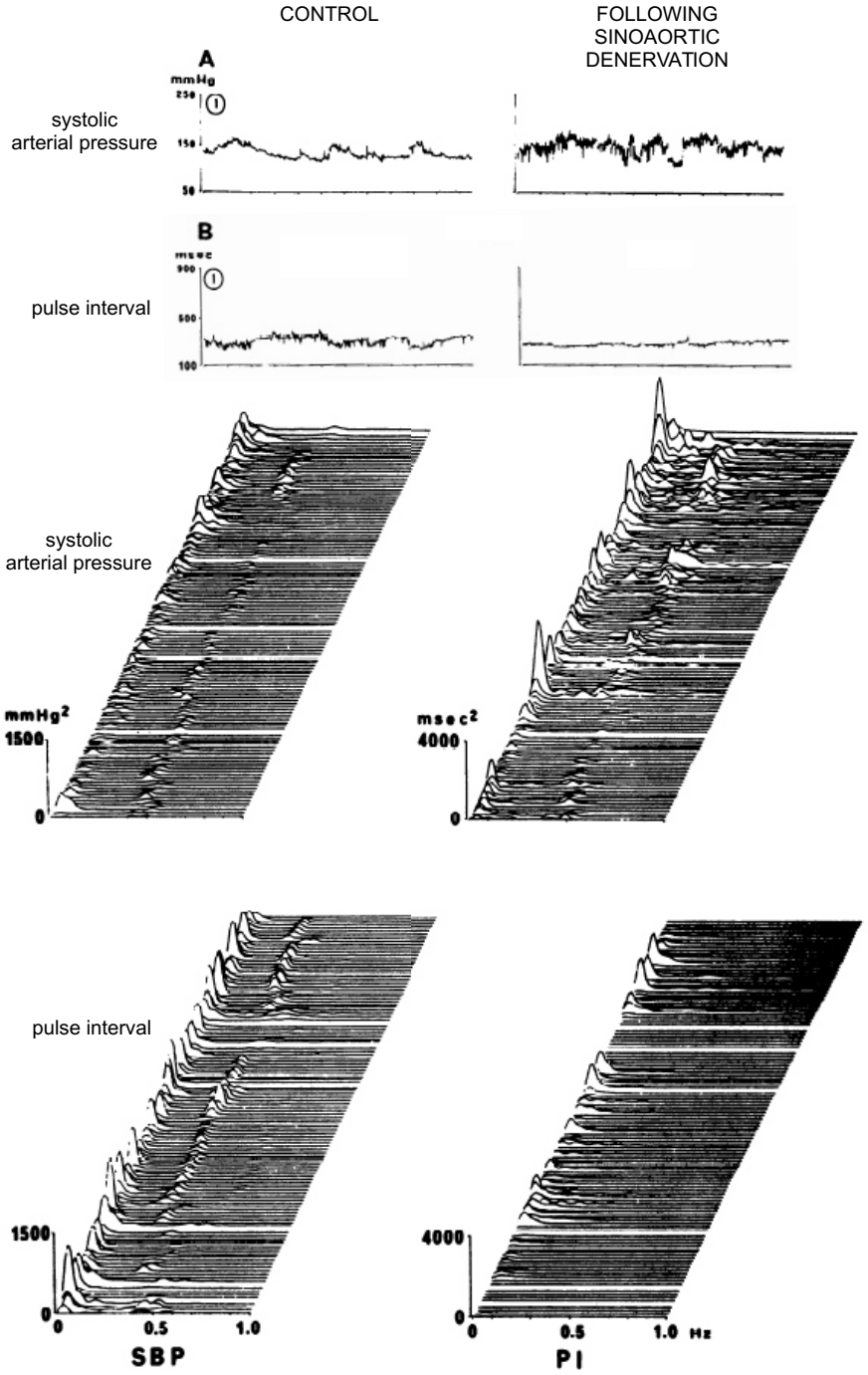

Figure 1.4.2. Effect of sinoaortic denervation on arterial pressure and heart rate variability in awake cats (adapted from Di Rienzo et al. 1991). Mean systolic pressure (A) and heart rate (pulse interval, B). Systolic pressure is much more erratic, whereas there is less variability in heart rate 7-10 days following sinoaortic denervation (right panels) compared to the control period (left panels). Lower panels illustrate individual systolic pressure and pulse interval power spectra over time showing a marked increase in power at ~0.3 Hz in systolic pressure, and a corresponding reduction in power at this frequency in heart rate. These data indicate that baroreceptors are critical for buffering short term fluctuations of AP and that a proportion of heart rate variability is driven by baroreceptor input. Similarly, sinoaortic denervation results in marked reductions in the amplitude of low frequency periodic discharges in vasoconstrictor sympathetic nerves (see text), indicating that baroreceptors provide rhythmic feedback to CNS pathways in order to reflexly modulate regional blood flow and buffer variations of systemic pressure.

or five parameters that describe threshold and saturation points and the gain of changes in sympathetic activity or heart rate throughout a range of arterial pressures *(Ricketts and Head, 1999; McDowall and Dampney, 2006)*. The resting level of AP is also referred to as the set-point of the baroreflex. This is usually situated at a point of high baroreflex gain, close to the midpoint of the curve; presumably this enables maximum buffering of AP around its resting level.

Baroreceptor-effector coupling has an inherent time delay due to integration within the neural arc and delayed responses of efferent organs *(Sato et al., 1999; Keyl et al., 2001)*. This is in part thought to generate slow regular fluctuations of AP at a frequency slower than respiration, originally observed by Mayer – so-called low frequency (LF) oscillations *(Mayer, 1876)*. The frequency is close to 0.1 Hz in humans *(Pagani et al., 1986)*, dogs *(Akselrod et al., 1981; Pagani et al., 1986)* and cats *(Di Rienzo et al., 1991)*, 0.3 Hz in rabbits *(Head et al., 2001)* and 0.4 Hz in rats and mice *(Julien et al., 2003; Baudrie et al., 2007)*. Mayer waves are coupled to LF oscillations of SNA and HR *(Bertram et al., 1998; Ringwood and Malpas, 2001)*. Changes in HR at this frequency tend to oppose; whereas changes in sympathetic activity reinforce Mayer waves in AP *(Cerutti et al., 1991; Ringwood and Malpas, 2001)*. The amplitude of Mayer waves is greatly reduced after alpha-adrenergic *(Cerutti et al., 1991)* or chronic ganglionic blockade *(Julien et al., 1995)* or sinoaortic denervation *(Kunitake and Kannan, 2000; Julien et al., 2003; Barres et al., 2004)*. Thus the generation of Mayer waves is related both to phasic changes in sympathetic outflow and to normal operation of the baroreflex.

Peripheral Chemoreceptors

Acute mild hypoxia is detected as a change in PaO_2 by peripheral chemoreceptors located in the carotid and aortic bodies in cat and dog; only the former are present in rabbit, mouse and rat *(Comroe and Mortimer, 1964; Marshall, 1994)*. Chemoreceptor activation triggers cardiorespiratory adjustments that function to maintain oxygenation in vital organs including the brain and heart *(Marshall, 1994)*. Generally, the response is characterised by an increase in ventilation, bradycardia and vasoconstriction in the skeletal muscle and splanchnic beds. An increase in ventilation has secondary effects on the circulation characterised by tachycardia and peripheral vasodilatation. These effects are mediated secondary to hyperventilation due to resulting hypocapnia, reflex effects of lung inflation, and increased activity of central inspiratory neurons *(Daly, 1993; Daly and Cook, 1994)*. In

rat direct chemoreceptor influences appear to predominate over these secondary effects. For example, the magnitude of bradycardia and vasoconstriction evoked by N_2 inhalation in spontaneously breathing rats was unaffected by vagotomy or constant ventilation under paralysis *(Marshall, 1987)*.

Chemoreceptor afferents run in the IX and X cranial nerves that also carry baroreceptor information and synapse in the medial and commissural NTS. The integrated circuitry that coordinates sympathetic (and phrenic) responses to chemoreceptor activation is thought to be contained wholly within the lateral pons and medulla (see Fig 1.4.1) *(Koshiya and Guyenet, 1994a; Guyenet, 2000)*. Select neuronal groups express *c-fos* following hypoxia in conscious rabbits; these include mainly the K-F nucleus in the caudolateral pons and medial NTS and RVLM in the medulla *(Hirooka et al., 1997)*. Blockade of glutamatergic inputs into the RVLM using kynurenate *(Koshiya et al., 1993)* or selective blockade of AMPA/Kainate receptors using CNQX *(Miyawaki et al., 1996b)* abolished the sympathoexcitatory response to hypoxia (see Section I).

The origin of peripheral chemoreceptor drive to RVLM neurons is unclear. In part the sympathetic activation that occurs during hypoxia is transmitted via increased inspiratory drive from central respiratory neurons. Muscimol inhibition of the pre-BOT, which eliminates the increase in inspiratory-related sympathetic discharge, does not however alter the magnitude of excitation of RVLM neurons in response to hypoxia *(Koshiya and Guyenet, 1996b)*. More caudally, muscimol inhibition of the CVLM also has no effect on sympathoexcitatory responses to N_2 inhalation in rat *(Koshiya et al., 1993)*. Hence, RVLM neurons must receive direct excitatory chemoreceptor-related inputs, probably directly from the NTS *(Aicher et al., 1996; Koshiya and Guyenet, 1996b)*. The commissural part of the NTS contains neurons that are excited by hypoxia, are antidromically activated from the RVLM and have axon collaterals in the NA *(Koshiya and Guyenet, 1996a)*. A monosynaptic connection between some NTS neurons and C1 RVLM neurons has also been documented anatomically *(Aicher et al., 1996)*.

Guyenet and colleagues proposed that the A5 region is a critical synaptic relay in the sympathetic chemoreflex since unit activity and post-inspiratory modulation of A5 neurons increased along with splanchnic SNA during N_2 inhalation *(Guyenet et al., 1993)*. Bilateral inhibition of A5 using muscimol in anaesthetised rats markedly reduced the splanchnic sympathoexcitatory response to hypoxia *(Koshiya and Guyenet, 1994b)*. In conscious

rabbits, however, muscimol inhibition of A5 enhanced renal sympathetic activation under 20 min of 10 % O_2 inhalation *(Maiorov et al., 2000)*. Recently, it was shown that pressor responses to cyanide-induced hypoxia were unaffected by destruction of the A5 cell group using localised injection of 6-hydroxydopamine in rat *(Madden and Sved, 2003)*. Hence, A5 may play a modulatory, but not obligatory role in the peripheral chemoreflex.

Somatic Afferents

Somatic nerves are mixed nerves containing numerous motor and sensory fibres. The reflex effects on circulation of stimulating somatic nerves under experimental conditions has been of considerable value in understanding mechanisms that operate to adjust cardiovascular function in response to pain or muscle contraction. Single afferent volleys in muscle or cutaneous nerves elicit sympathetic reflex discharges and post-excitatory depression of their activity *(Sato and Schmidt, 1973)*. Short trains of stimulation at 100 – 200 Hz augment the reflex sympathoexcitation. Electrical stimulation of myelinated low-threshold cutaneous afferents evokes strong increases in sympathetic activity *(Sato and Schmidt, 1973)*. Stimulation of high-threshold group II muscle afferents evokes responses only at higher stimulus strength; whereas group I afferents (muscle spindle and Golgi tendon organ) have no excitatory or inhibitory influence on the sympathetic system *(Coote and Perez-Gonzalez, 1970; Sato and Schmidt, 1973)*. This is in contrast to effects of metaboreceptor activation in active muscle; for example, tetanic contraction of hindlimb muscle evokes increases in BP *(Ally et al., 1994)*. This latter reflex is thought to be part of the feedback pathway contributing to elevated blood flow to active muscle during exercise *(Fisher and White, 2004)*.

Brief high voltage low frequency stimulation of somatic nerves in rat produces characteristic two peak responses in sympathetic nerves with latencies of about 70 and 170 ms *(Morrison and Reis, 1989; Miyawaki et al., 2001, 2002b)*. The origin of different latency peaks involves properties of both the afferent and efferent pathways (Fig 1.4.3). For example, early vs late peaks are in part mediated by a short-latency spinal component and longer latency medullary and pontine components arising from branches of the ascending sensory spinothalamic pathway. A critical nodal point in this pathway is the RVLM *(Morrison and Reis, 1989)*. Increased activity of bulbospinal neurons in this region precedes and corresponds to early and late peaks in splanchnic discharge seen following sciatic nerve stimulation in rat *(Morrison and Reis, 1989)*. Tested in this way, the two clear

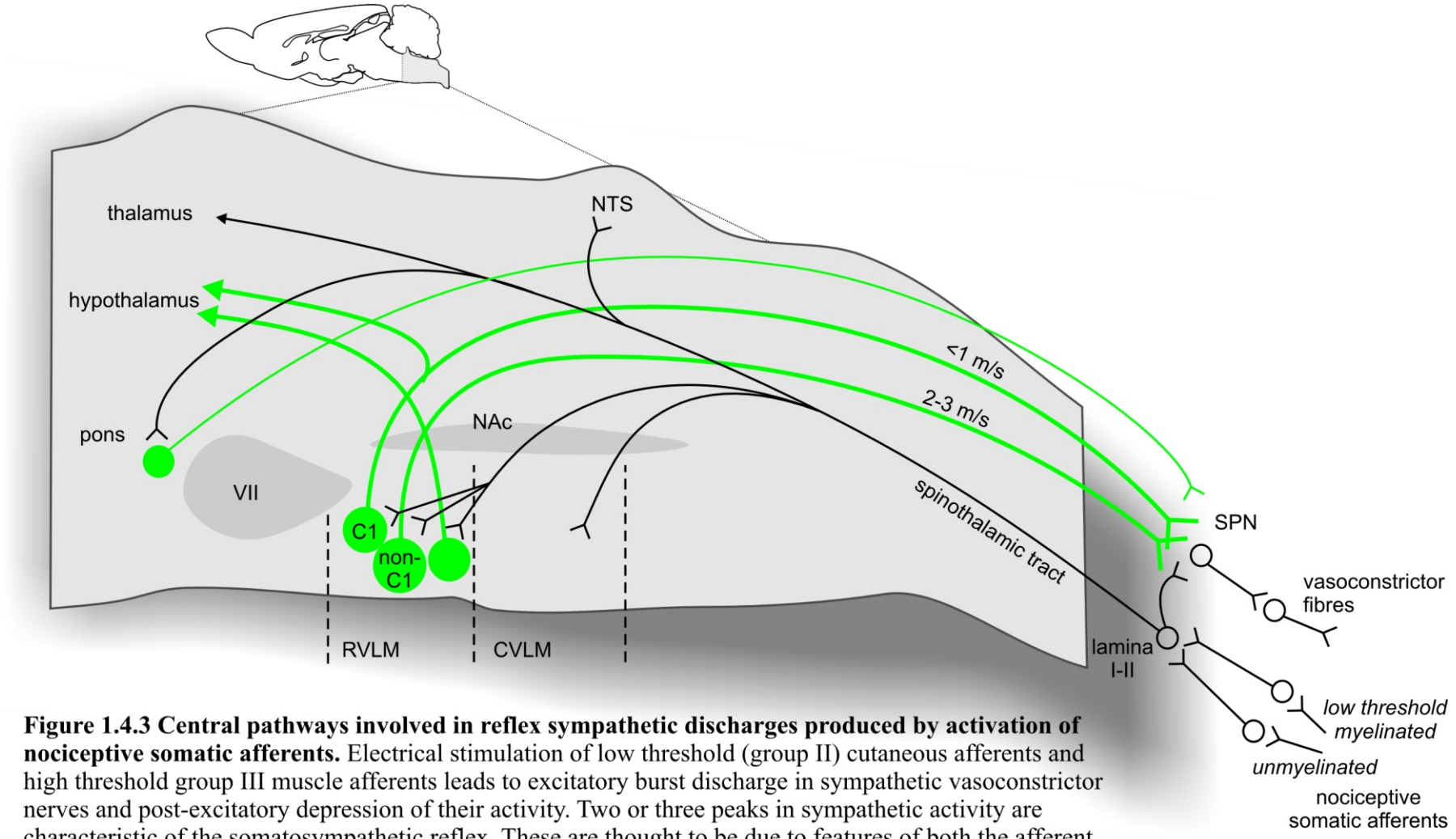

Figure 1.4.3 Central pathways involved in reflex sympathetic discharges produced by activation of nociceptive somatic afferents. Electrical stimulation of low threshold (group II) cutaneous afferents and high threshold group III muscle afferents leads to excitatory burst discharge in sympathetic vasoconstrictor nerves and post-excitatory depression of their activity. Two or three peaks in sympathetic activity are characteristic of the somatosympathetic reflex. These are thought to be due to features of both the afferent pathway (sensory fibres with different conduction velocities), ascending branches of the spinothalamic tract at different levels of the neuraxis (spinal, medullary and pontine components) and efferent pathways. A key synapse in this pathway is the RVLM. Two peaks in sympathetic discharge are thought to be due in part to early and or late activation of neurons in this region with direct projections to SPN that are fast-conducting (mainly non-C1 neurons) or slow conducting (mainly C1 neurons).

peripheral discharges characteristic of the somatosympathetic reflex may result from early and late activation of RVLM neurons with fast-conducting axons, as well as late activation of neurons with slower conducting axons *(Morrison and Reis, 1989; Verberne et al., 1999a)*.

V. The Central Cholinergic Nervous System

Cholinergic Innervation of the CNS

Cholinergic cell bodies are located in a loosely contiguous axis arising from the cranial nerve nuclei of the brainstem to cholinergic cell groups in the mesopontine tegmentum and basal forebrain. Ascending cholinergic pathways are organized in six projection systems originally designated Ch1-Ch6 based upon combined immunohistochemistry and tract tracing studies in macaque and rat *(Mesulam et al., 1983a; Mesulam et al., 1983b)* (Figure). Ch1-Ch4 systems are located within various basal forebrain nuclei, including the medial septal nucleus, diagonal band and nucleus basalis, and provide the major cholinergic projections to the hippocampus, olfactory bulb, cortex and amygdala. In addition, intrinsic cholinergic projections richly innervate the striatum. The Ch5 and Ch6 systems arise from the pedunculopontine tegmental nucleus of the pontomesencephalic reticular formation (PPT) and the laterodorsal tegmental grey of the periventricular area (LDT) and provide the major cholinergic innervation of the thalamus *(Mesulam et al., 1983b)*. Cholinergic neurons in the PPT and LDT are also the major source of descending cholinergic projections to the caudal pons and medulla (Fig. 1.5.1) *(Rye et al., 1988; Woolf and Butcher, 1989; Jones, 1990; Yasui et al., 1990)*.

Fundamental Aspects of Cholinergic Neurotransmission

Acetylcholine (ACh) is synthesized in the presynaptic terminal from choline and acetyl-CoA by the cytoplasmic protein choline acetyl transferase (ChAT) and subsequently transported into synaptic vesicles by the vesicular acetylcholine transporter (vAChT). Co-expression of both ChAT and vAChT is required for a neuron to be *cholinergic*, ie whose terminals contain a releasable pool of ACh. The vAChT gene lies within the first intron of the ChAT gene and both have the same transcriptional orientation *(Tanaka et al., 1998)*.

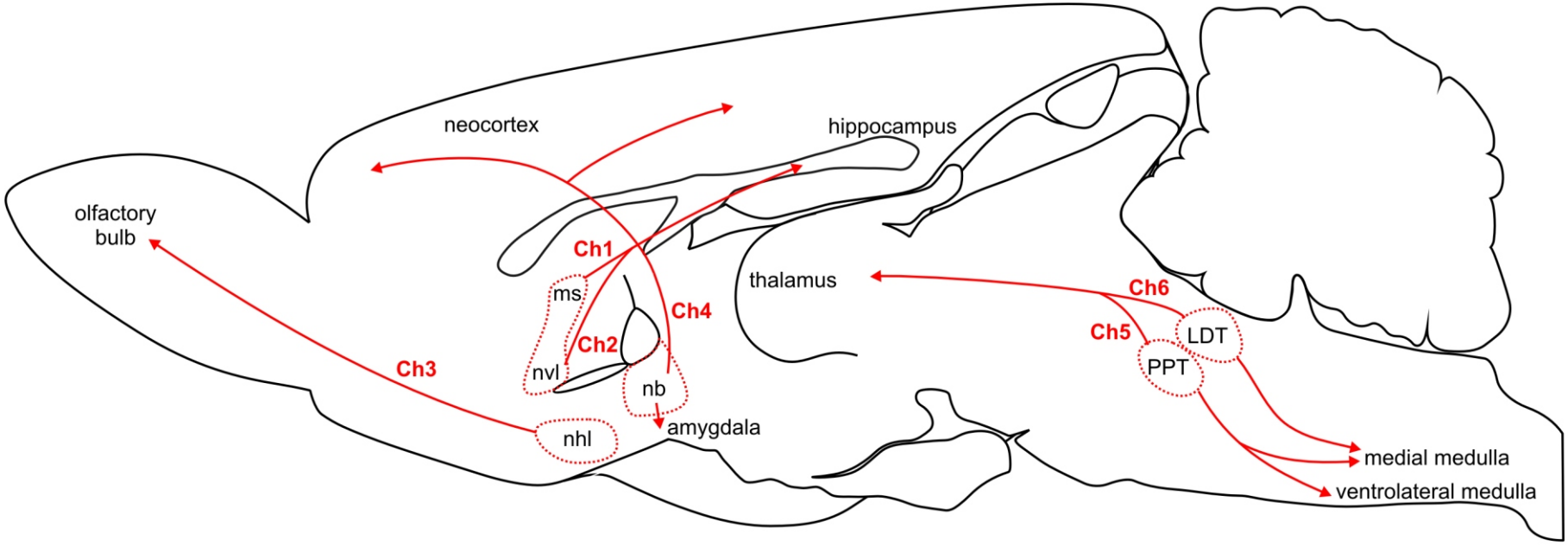

Figure 1.5.1. Schematic representation of the major cholinergic projection systems in the rat brain. Ascending projections adapted from Mesulam et al. 1983. Cholinergic cell groups most closely associated with the projection systems are indicated in dotted outlines. The Ch4 projection is also made up of neurons in the globus pallidus, diagonal band and preoptic nucleus. The Ch5 projection is made up of neurons found mostly within the PPT and those closely associated with the PPT lying ventrally in the cuneiform nuclues and caudally within the parabrachial nucleus. Abbreviations: ms, medial septal nucleus, nb, nucleus Basalis of Meynert; nhl, horizontal limb nucleus of the diagonal band; nvl, vertical limb nucleus of the diagonal band. Omitted are the cholinergic projections intrinsic to the striatum and cholinergic cranial nerve nuclei of the brainstem. Schematic of sagittal rat brain adapted from Paxinos and Watson (1996).

This conserved structure enables the coordinated expression of both genes, which are also thought to share common upstream regulatory sequences *(Berrard et al., 1995; Shimojo et al., 1998; Tanaka et al., 1998)*.

Cholinesterases terminate the synaptic action of ACh through hydrolysis and acetylcholinesterase (AChE) is widely distributed throughout the CNS. AChE is found in the cell bodies, axons and dendrites of cholinergic neurons as well as in the cell bodies of many non-cholinergic cholinoceptive neurons *(Mesulam and Geula, 1992)*. The hydrolysis of ACh leads to liberation of choline, whose reuptake by the presynaptic terminal is the main mechanism regulating choline availability for *de novo* synthesis of ACh. A key regulator of choline reuptake is Na^+-dependent transport via the high affinity choline transporter (HAChT) *(Parsons, 2000)*.

ACh mediates synaptic transmission via binding to ion channel-gated nicotinic (nAChR) and G-protein coupled muscarinic receptors (mAChR). Neuronal nAChR are composed of five transmembrane subunits surrounding a water-filled pore that gates the selective passage of cations into the cell *(Dani and Bertrand, 2006)*. In mammals, nAChR composed of heteromeric αβ or homomeric α7 subunit combinations are widely distributed in the CNS *(Dani and Bertrand, 2006)*. MAChR exist as five molecularly distinct subtypes (M1-M5) whose structures are otherwise highly conserved, consisting of seven α-helical transmembrane segments and an extracellular N-terminal portion that recognises and binds ACh *(Caulfield and Birdsall, 1998)*. Sequence divergence in the second or third intracellular cytoplasmic loops probably determines the preferential coupling of different subtypes either to $G\alpha_{q/11}$ (M1, M3, M5) or $G\alpha_{i/o}$ proteins (M2, M4) *(Caulfield and Birdsall, 1998)*. In general, these subgroups mediate intracellular excitation and inhibition, respectively, via activation of phospholipase C (M1, M3, M5) or inhibition of adenylyl cyclase (AC) (M2, M4) *(Caulfield and Birdsall, 1998)*. There is also evidence for direct K+ channel activation mediated by M2 receptor-activated $G\alpha_{i/o}$ subunits *(Wickman and Clapham, 1995)* or M2/M4 receptor-mediated stimulation of AC *(Onali and Olianas, 1995)* and others also report excitatory responses linked to M2 receptor activation in the periphery *(Eglen et al., 1994; Ehlert, 2003)*. For example, the contractile response in gut smooth muscle is linked to synergistic activation of M2 and M3 receptors leading to increased Ca2+ influx and enhanced Ca2+ sequestration from intracellular stores, respectively *(Ehlert, 2003)*.

The diversity of cholinergic receptors and their pre- and postsynaptic and axonal locations contribute to the varied roles these receptors play in modulating neuronal excitability. In the CNS mAChR play fundamental roles in several higher processes including learning, memory and attention and extrapyramidal motor control *(Bymaster et al., 2003a)*. Some mAChR subtypes located centrally are also linked to control of body weight and temperature regulation *(Bymaster et al., 2003a)*, cardiovascular function *(Sundaram et al., 1988; Giuliano et al., 1989)* and respiration *(Nattie and Li, 1990; Boudinot et al., 2004)*. This is supported by the fact the administration of AChE-inhibitors and direct acting mAChR agonists evoke profound autonomic effects including hypertension and hypothermia and respiratory disturbances in several species including man (see following sections). The anatomical substrates involved in central cholinergic effects on circulation and respiration are less clear, and in most cases their physiological importance is unknown. The following sections discuss the evidence for descending cholinergic innervation of the ventral medulla and interactions with neurons important in control of cardiovascular and respiratory function.

Cholinergic Innervation of the Ventrolateral Medulla

Descending projections to the ventral medulla from pontomesencephalic cholinergic neurons have been demonstrated using anterograde or retrograde tracing and combined immunohistochemical detection of ChAT or AChE *(Rye et al., 1988; Woolf and Butcher, 1989; Jones, 1990; Yasui et al., 1990)*. These cells are located in diffuse and discrete cell clusters within the PPT and periventricular LDT *(Mesulam et al., 1983b)*. Cholinergic PPT neurons are found as far caudal as the parabrachial nucleus and occasionally embedded in the superior cerebellar peduncle; more rostrally they are found clustered adjacent to the lateral lemniscus and in a more diffuse medial group *(Mesulam et al., 1983b)*. Neurons in the PPT appear to provide most of the cholinergic input to ventrolateral regions; whereas both the PPT and LDT provide input to medial and midline regions of the ventral medulla *(Rye et al., 1988; Yasui et al., 1990)*. Following Fluorogold injection into the RVLM in rat, approximately 10 % of ChAT-positive PPT neurons were labeled on the ipsilateral side but very few were found in the LDT *(Yasui et al., 1990)*. Descending projections from the PPT to the ventral medulla are predominantly ispilateral but always have a contralateral component *(Woolf and Butcher, 1989; Yasui et al., 1990)*. Cholinergic input to the RVLM may also arise from small ChAT-labeled somata in the gigantocellular field of the medial medulla that send fibres into the neighbouring VLM *(Ruggiero et al., 1990)*.

A dense plexus of cholinergic terminals innervates the VLM revealed by immunohistochemical detection of ChAT *(Jones and Beaudet, 1987; Giuliano et al., 1989; Milner et al., 1989; Ruggiero et al., 1990)*, vAChT *(Arvidsson et al., 1997; Schafer et al., 1998)* or HAChT *(Kus et al., 2003)*. Antibodies to AChE also densely stain the VLM and subjacent ventral surface in rat *(Satoh et al., 1983)* and cat *(Jones and Webster, 1988)*. The colocalisation of many of the components required for cholinergic neurotransmission indicates an active turnover of ACh and the existence of local cholinoceptive neurons within the VLM. At rostral levels containing the majority of sympathoexcitatory RVLM neurons, femtomolar amounts of ACh could be continuously microdialysed from the region following neostigmine injection in freely moving rats *(Taguchi et al., 1999)*. In micropunches of RVLM resting ChAT enzyme activity is high relative to medullary somatomotor nuclei (eg. hypoglossal nucleus) *(Arneric et al., 1990)*.

ChAT-immunoreactive (IR) terminals interdigitate with TH/PNMT labeled cells in the RVLM *(Milner et al., 1989; Ruggiero et al., 1990)*. According to an ultrastructural study in sections of rat VLM, ChAT-IR terminals rarely form synapses with TH/PNMT labeled cells (8 %) *(Milner et al., 1989)*. In contrast, ChAT-IR terminals form abundant synaptic contacts with non-TH cell bodies and dendrites (77 %) and ChAT-IR perikarya (15 %) and occasionally with unlabeled terminals that contact other unlabeled perikarya *(Milner et al., 1989)*. These findings are not definitive, however, with regard to neurons located specifically in the rostral region of the RVLM since quantitation was only conducted on sections taken from 0.5 - 2 mm caudal to the facial nucleus *(Milner et al., 1989)*. This would exclude the majority of C1 neurons with descending projections to the spinal cord *(Verberne et al., 1999a; Phillips et al., 2001)*. The abundance of synaptic contacts formed by ChAT-labeled terminals in the VLM caudal to this area, however, reflects cholinergic innervation of other regions essential to control of circulation and breathing including the CVLM and pre-BOT.

Muscarinic Receptor Genes and Protein in the Ventrolateral Medulla

Genes encoding the mAChR subtypes M1 – M5 were cloned in the late 1980s and were found to have a strong sequence homology *(Kubo et al., 1986; Bonner et al., 1987; Bonner et al., 1988)*. Gene expression of mAChR in the VLM has been investigated using PCR

amplification of cDNA from tissue punches of the RVLM from spontaneously hypertensive and Wistar Kyoto rats; all mAChR subtypes were found to be expressed although their relative abundance was not calculated *(Gattu et al., 1997b)*.

Antisera specific to each subtype were produced by bacterial expression of proteins incorporating the non-conserved third cytoplasmic loops *(Levey et al., 1991; Levey, 1993)*. According to subtype-specific immunoprecipitation, 80 % of mAChR protein in the brainstem is made up of M2 receptors with equal amounts of the other subtypes making up the remaining 20% *(Levey, 1993)*. The localisation of mAChR subtypes in the medulla was reported to mostly presynaptic based upon M2 receptor binding confined to terminals and fibres rather than cell bodies in human infant medulla *(Mallard et al., 1999)*. Using the radioligand quinuclidinyl benzilate (QNB) to preferentially bind M2 receptors, a high density of M2 receptor was reported in rat RVLM *(Ernsberger et al., 1988a; Ernsberger et al., 1988b)* and a proportion of these were present extrasynaptically *(Ernsberger et al., 1988b)*. In other regions of the brain M2 receptors are located mainly on presynaptic terminals *(Quirion et al., 1995)* but are also often found clustered at the postsynaptic membrane *(Hersch et al., 1994)*. The precise cellular and subcellular locations of M2 or other receptor subtypes within the RVLM is unknown. Expression or binding of mAChR in more caudal regions of the medulla has not been investigated.

Cholinergic Influences on Blood Pressure

The profound pressor effects of central mAChR activation are well established and have been reviewed in detail *(Hornykiewicz and Kobinger, 1956; Brezenoff and Giuliano, 1982; Buccafusco, 1996; Kubo et al., 1997; Kubo, 1998)*. It was known as early as 1867 that eserine (physostigmine) produced a central pressor effect in dogs that could be blocked by atropine (see *(Hornykiewicz and Kobinger, 1956)*. It was not until the early 1900s that specific effects of physostigmine were related to prolongation of the synaptic actions of ACh (see *(Dale, 1962)*. In several species, including man, dose-dependent increases in AP are evoked by cholinesterase inhibitors (carbamates such as physostigmine, neostigmine or organophosphates including di-isopropyl fluorophosphate and sarin) or direct acting cholinomimetics (including carbachol, oxotremorine, arecoline) when administered into the systemic circulation or directly into the CSF (*cat: (Day and Roach, 1977)*; *dog: (Lang and Rush, 1973)*; *man: (Petrie et al., 2001)*; *rat: (Varagic, 1955; Walker and Weetman, 1970; Brezenoff, 1972; Brezenoff and Rusin, 1974; Buccafusco and Brezenoff, 1978; Kubo*

and Tatsumi, 1979; Buccafusco and Spector, 1980; Giuliano et al., 1989). This pressor response is consistently antagonised by atropine or scopolamine administered via the same route (eg *(Brezenoff and Caputi, 1980)*. The magnitude of the pressor response is similar in anaesthetised or conscious animals; an exception is in cat where under anaesthesia the pressor response to carbachol reverts to a depressor effect *(Armitage and Hall, 1967)*.

The CNS sites that mediate cholinergic pressor responses are thought to include hypothalamic and lower brainstem regions. Regions of the forebrain and hypothalamus are activated in response to intracereberoventricular administration of physostigmine *(Li et al., 1997)*. The posterior hypothalamus contains mAChR that when activated lead to vasopressin release and increases in AP *(Buccafusco and Brezenoff, 1979)*, although atropine injected into this region did not prevent pressor responses to physostigmine in rat *(Brezenoff et al., 1982)*. Moreover, pressor responses to intravenous physostigmine *(Varagic, 1955; Willette et al., 1984)* or oxotremorine *(Walker and Weetman, 1970)* or intracerebroventricular injection of oxotremorine *(Ozawa and Uematsu, 1976)* were completely unaffected by transection rostral to the medullary sympathetic outflow. In contrast, pressor effects were completely abolished by cervical transection or blockade of ganglionic transmission *(Sundaram and Sapru, 1988)* or peripheral adrenoceptors *(Varagic, 1955)*. Hence, a key site of action was likely to be in the medulla within regions involved in generating or modulating sympathetic outflow.

Microinjection of ACh or carbachol into the NTS lowered AP in anaesthetised rats *(Criscione et al., 1983)*. In contrast, microinjections of ACh, physostigmine or cholinomimetics directly into the RVLM produce a profound increase in AP, heart rate and sympathetic nerve activity in anaesthetised rats *(Willette et al., 1984; Punnen et al., 1986; Sundaram et al., 1988; Sundaram and Sapru, 1988; Giuliano et al., 1989; Kubo, 1998)*. Moreover, blockade of mAChR bilaterally within the RVLM with scopolamine abolished the increase in sympathetic activity and AP evoked by intravenous physostigmine in anaesthetised rats *(Giuliano et al., 1989)*. Hence, the RVLM is a key site of action of systemically administered cholinesterase inhibitors responsible for producing sympathetically-mediated increases in AP.

Cholinergic Influences on Cardiovascular Reflexes

Despite extensive investigation of the central pathways subserving the baroreflex and other major cardiovascular reflexes including the somatosympathetic and peripheral and central chemoreflex, little is known about the involvement of central cholinergic receptors. One study reported that the late peak of the somatosympathetic reflex evoked by intercostal nerve stimulation was inhibited by intravenous oxotremorine in anaesthetised cats *(Baum and Shropshire, 1978)*. MAChR are thought to play an important role in central and peripheral chemosensitivity *(Nattie and Li, 1990; Shao and Feldman, 2000; Boudinot et al., 2004)*; for example, conscious mice lacking the M3 receptor displayed reduced compensatory ventilatory responses to hypercapnia or moderate hypoxia using whole-body plethysmography *(Boudinot et al., 2004)*. The involvement of mAChR in cardiovascular components of these reflexes is unknown.

Other data point to the involvement of mAChR in central integration of the arterial baroreflex. In conscious rats intracerebroventricular injection of physostigmine enhanced reflex bradycardia but inhibited reflex tachycardia evoked by noradrenaline and sodium nitroprusside, respectively *(Caputi et al., 1980)*. This reflects an acute resetting of the baroreflex, presumably to the higher pressures evoked by physostigmine, without marked changes in range or sensitivity of the cardiac component of the reflex. In anaesthetised rats, intracerebroventricular or intravenous injection of physostigmine potentiates the carotid arterial occlusion reflex (CAOR) *(Brezenoff et al., 1982; Park and Long, 1991)*, which produces an increase in AP in part via carotid baroreceptor unloading. Park and Long also found a parallel reduction in the fall in AP produced by 45º head-up tilt *(Park and Long, 1991)*, suggesting that physostigmine may act centrally to enhance the gain of the vasomotor component of the baroreflex. The conclusions of these previous studies, however, are limited given that the reflex pathway evoked by CAOR is complex and probably not limited to arterial baroreflex activation. Carotid occlusion unloads carotid baroreceptors, signaling for a rise in AP, but the opposite occurs for aortic baroreceptors, limiting the increase in AP. Moreover, carotid occlusion leads to central ischaemia as well as local deoxygenation that could activate carotid body chemoreceptors *(Franchini and Krieger, 1992)*.

The central sites responsible for effects on baroreflex function evoked by physostigmine are not clear. Potentiation of the carotid occlusion reflex by physostigmine was prevented by atropine injected into the posterior hypothalamus *(Brezenoff et al., 1982)*. The potential involvement of medullary sites where mAChR activation alters AP is unclear.

The NTS may be involved as it receives input from baroreceptor afferents and transmits baroreceptor information to both vagal and sympathetic premotor nuclei. NAChR containing homomeric α7 subunits are located presynaptically on terminals of primary baroreceptor afferents in the medial NTS, indicated by the dramatic reduction in α-bungarotoxin binding in this region following unilateral nodose ganglionectomy in rat *(Ashworth-Preece et al., 1998a)*. Whether or not nAChR or mAChR in the NTS play a role in the baroreflex is unclear. Local administration of the α7-nAChR antagonist mecylamine reduced glutamate release in the NTS following aortic nerve stimulation *(Ashworth-Preece et al., 1998b)* although central administration of hexamethonium or mecylamine *(Caputi et al., 1980)* or microinjection of atropine directly into the NTS *(Tsukamoto et al., 1994)* has little effect on baroreflex-evoked bradycardia.

The RVLM may also be involved since barosensitive neurons here are excited by local mAChR activation (see following sections). One study claimed that the amount of ACh microdialysed from the RVLM increased following tetanic stimulation of aortic baroreceptor afferents or injection of phenylephrine in anaesthetised rats *(Kubo et al., 1998d)*, suggesting that mAChR activation may contribute to normal baroreflex responses. The involvement of RVLM mAChR in the sympathetic baroreflex or other sympathoexcitatory reflexes mediated within the region is unknown.

Muscarinic Cholinergic Modulation of RVLM Neuronal Activity

Increases in sympathetic activity and AP evoked via mAChR activation in the RVLM appear to be mediated via the inhibitory M2 receptor subtype; M2 receptor-preferring antagonists injected into the RVLM prevent cardiovascular effects following local injection of cholinergic agonists *(Sundaram et al., 1988; Sundaram and Sapru, 1988)* or intravenous physostigmine *(Giuliano et al., 1989)*. It is well recognised that there are no antagonists specific for mAChR subtypes, although some show higher affinity for certain subtypes (Table. 1.5.1) *(Caulfield and Birdsall, 1998)*. Some studies also showed that nicotine evoked a pressor response when injected into the RVLM *(Tseng et al., 1994)*; however, in anaesthetised rats the sympathoexcitatory response to physostigmine or carbachol was unaffected by blockade of nAChR with hexamethonium *(Giuliano et al., 1989)*.

Antagonist affinity constants (log affinity constants or pK_B values) for mammalian muscarinic receptors[a]

Antagonist	Receptor subtype				
	M_1	M_2	M_3	M_4	M_5
Atropine	9.0–9.7	9.0–9.3	8.9–9.8	9.1–9.6	8.9–9.7
Pirenzepine	7.8–8.5	6.3–6.7	6.7–7.1	7.1–8.1	6.2–7.1
Methoctramine	7.1–7.8	7.8–8.3	6.3–6.9	7.4–8.1	6.9–7.2
4-DAMP	8.6–9.2	7.8–8.4	8.9–9.3	8.4–9.4	8.9–9.0
Himbacine	7.0–7.2	8.0–8.3	6.9–7.4	8.0–8.8	6.1–6.3
AF-DX 384	7.3–7.5	8.2–9.0	7.2–7.8	8.0–8.7	6.3
Tripitramine	8.4–8.8	9.4–9.6	7.1–7.4	7.8–8.2	7.3–7.5
Darifenacin	7.5–7.8	7.0–7.4	8.4–8.9	7.7–8.0	8.0–8.1
Guanylpirenzepine	7.7	5.5	6.5	6.5	6.8
PD 102807	5.3	5.7	6.2	7.3	5.2
MT3[b]	7.1	<6	<6	8.7	<6
MT7[b]	9.8	<6	<6	<6	<6

Table 1.5.1 Antagonist affinity constants for mammalian muscarinic receptors. Data are from a variety of mammalian species including human. Last two drugs are toxins from Eastern Green Mamba venom. Adapted from Caulfield and Birdsall (1998).

Carbachol enhanced the firing rate of spinally projecting barosensitive neurons recorded *in vivo* and presumed AP-regulating neurons *in vitro (Huangfu et al., 1997; Kubo et al., 1997; Wang et al., 2000)*. Many of the cells recorded *in vitro* (~70%) were also immunoreactive for TH *(Huangfu et al., 1997)*. Voltage clamp recordings of the same neurons showed that carbachol produced an inward current (ie. carried by a cation), which was unaffected by a low Ca^{2+} / high Mg2+ perfusate or tetrodotoxin, indicating a direct postsynaptic site of action (Huangfu *et al.*, 1997). Carbachol-evoked depolarisation could also result from an increase in discharge of local interneurons, or possibly even direct depolarisation of presynaptic terminals *(McGehee et al., 1995; Huangfu et al., 1997)*. In neonates activation of RVLM neurons produced by carbachol is inhibited by either nAChR or mAChR antagonists *(Huangfu et al., 1997)*. In contrast, mAChR effects predominate in adult *(Huangfu et al., 1997; Kubo et al., 1997; Wang et al., 2000)*, which could reflect maturation of the neurons or synaptic environment in the RVLM.

Sensitivity to carbachol in the RVLM is not restricted to presympathetic neurons. In fact a large majority of cells, many of which display respiratory-related discharge, respond to iontophoretically-applied carbachol *in vivo (Huangfu et al., 1997)*. Pressor responses to local activation of mAChR could result from direct and or indirect effects on sympathoexcitatory RVLM neurons (Fig. 1.5.2). Since M2 receptors are in general coupled to inhibitory G proteins, it is thought that one likely mechanism explaining cholinergic sympathoexcitatory responses is that M2 receptors are located presynaptically on inhibitory inputs to RVLM neurons *(Arneric et al., 1990)*. In many other brain regions, cholinergic receptors usually modulate neuronal excitability via a combination of receptors located pre- and postsynaptically. The receptor subtypes and site/s of action underlying cholinergic effects in RVLM remain to be fully resolved.

A tentative conclusion that could be drawn from the robust pressor effects of physostigmine is that ACh is constitutively released in the RVLM. Whether or not this is physiologically significant (as it pertains to vasomotor tone generation) remains questionable. Bilateral antagonism of mAChR or nAChR in the RVLM produces negligible reductions in AP in the majority of studies *(Willette et al., 1984; Sundaram et al., 1988; Sundaram and Sapru, 1988; Giuliano et al., 1989; Nattie and Li, 1990)*. The effects of iontophoretically applied antagonists on the firing rate of RVLM neurons are also inconsistent *(Kubo et al., 1997; Wang et al., 2000)*.

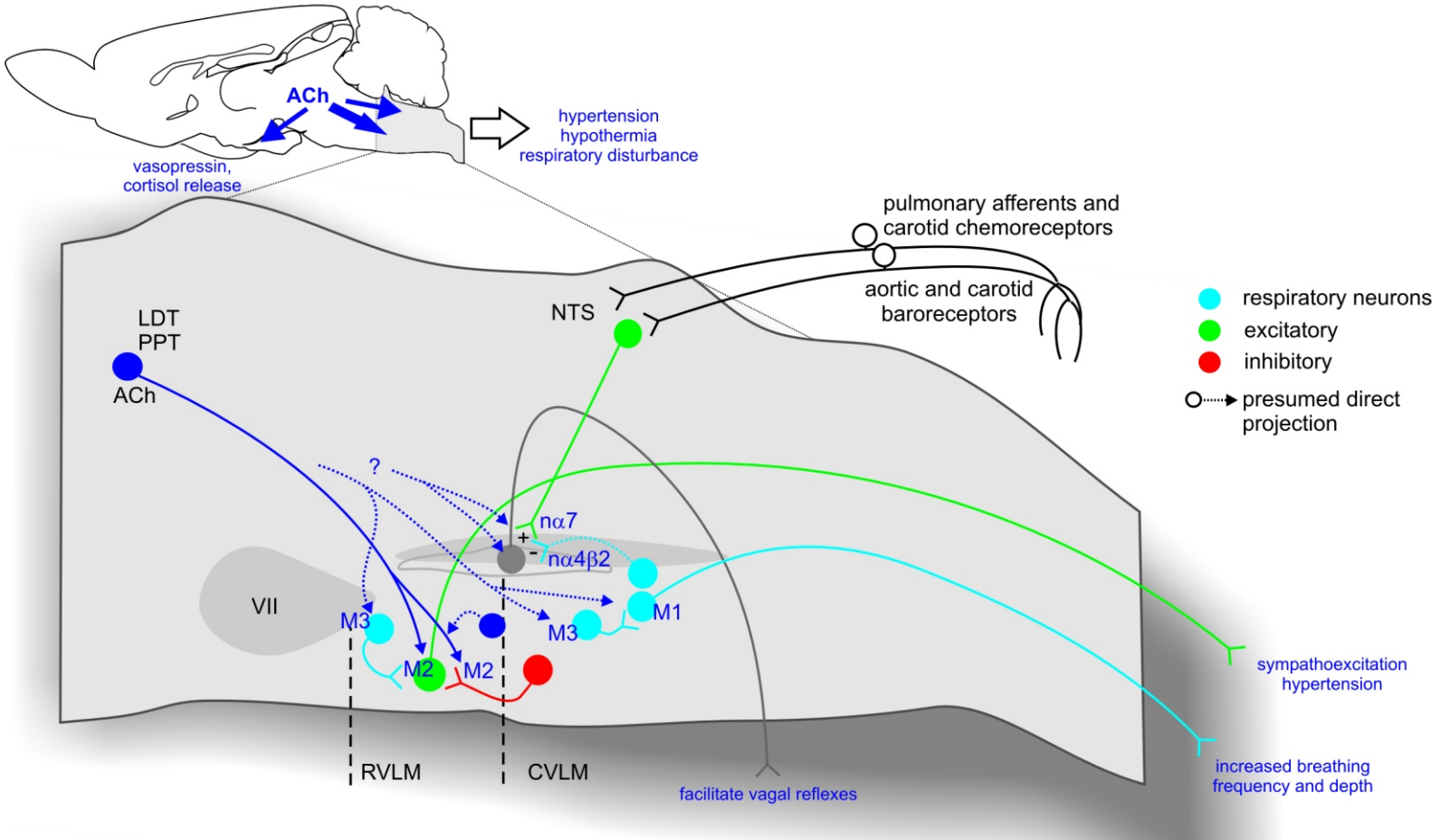

Figure 1.5.2. Sites of action and cholinergic receptor subtypes involved in eliciting cardiorespiratory responses within the ventral medulla. Direct or systemic application of cholinergic agonists to the ventral medulla elicits increases in arterial pressure, heart rate and ventilation via diverse effects on neurons located within the RVLM, VRG and NA. Descending cholinergic inputs are presumed to originate mostly from mesopontine cholinergic cell groups shown in dark blue. There may also be intrinsic sources of cholinergic input to the VLM possibly from neurons in the medial medulla (see Ruggiero et al. 1990), or intrinsic cholinergic projections from cholinergic vagal motorneurons to CVPN in the NA. The major receptor subtypes implicated in modulation of activity in different medullary areas are shown in dark blue. M2 receptors appear to be located pre and postsynaptically in the RVLM according to mainly *in vitro* data; their activation leads to excitation of presympathetic neurons and increases in sympathetic activity and arterial pressure.

Bilateral blockade of mAChR in the RVLM with atropine or scopolamine does, however, produce a large reduction in AP in spontaneously hypertensive rats (SHR) compared to their normotensive controls *(Lee et al., 1991; Kubo et al., 1995a)*. This suggests that release of ACh in the RVLM may contribute to basal levels of sympathetic activity under conditions where AP is elevated. Similar doses of physostigmine also generate larger increases in AP in hypertensive animals (SHR: *(Kubo and Tatsumi, 1979; Buccafusco and Spector, 1980; Lee et al., 1991; Kubo et al., 1995a)*; Dahl-salt-sensitive hypertension: *(McCaughran et al., 1983)*; DOCA salt-sensitive and renal hypertension: *(Kubo et al., 1996)*. This does not appear to be explained by differences in AChE enzymatic activity or spontaneous ACh release in the RVLM of SHR compared to Wistar Kyoto rats *(Arneric et al., 1990; Kubo, 1998)*. An increase in mAChR number may contribute since binding was enhanced in some studies *(Gattu et al., 1997a; Gattu et al., 1997b)* but not others *(Hernandez et al., 2003)*. An increase in receptor sensitivity is also possible, although again some studies report larger pressor responses to ACh or physostigmine in SHR *(Lee et al., 1991)* but others report no difference in SHR or DOCA-salt sensitive rats *(Kubo et al., 1995a; Kubo et al., 1996)*.

The most likely explanation for enhanced cholinergic tone in the RVLM of hypertensive animals is an increase in ACh synthesis and release. ChAT activity was increased in the RVLM but not other medullary regions of SHR *(Kubo et al., 1995b; Kubo et al., 1998b)* or DOCA-salt-sensitive and renal hypertensive rats *(Kubo et al., 1996)*. DOCA-salt-sensitive hypertensive animals exhibited an increased number of ChAT-expressing neurons in RVLM *(Kubo et al., 1998c)*, although ChAT-IR was similar between SHR and WKY *(Xiong et al., 1998)*. Furthermore, high affinity uptake of free choline was greater in crude synaptosomal fractions from medulla/pons in mature SHR compared with WKY *(Trimarchi and Buccafusco, 1987)*.

The precise origin of cholinergic inputs that act to increase AP via the RVLM is unknown. Pressor responses evoked by glutamate or D-L-homocysteic acid stimulation of the PVN *(Kubo et al., 2000)*, midbrain central grey *(Kubo et al., 1999)* or lateral PBN *(Kubo et al., 1998a)* were reportedly prevented by scopolamine injected bilaterally into the RVLM. All of these sites project directly or indirectly to the RVLM, although they conspicuously lack any cholinergic neurons with demonstrated projections to the RVLM. An exception is the lateral PBN / Kölliker-Fuse nucleus, whose rostral extension contains ChAT-positive neurons that are part of the diffuse caudal part of the PPT *(Mesulam et al., 1983b; Yasui et*

al., 1990). Kubo argued, however, that the cholinergic projection from the PPT to the RVLM does not increase AP, since the pressor response evoked by unilateral injection of glutamate within the PPT was not prevented by mAChR blockade ispilaterally in the RVLM *(Kubo et al., 1999)*. It is clearly possible that fibres projecting contralaterally from the PPT *(Rye et al., 1988; Woolf and Butcher, 1989; Yasui et al., 1990)* may have been able to evoke equivalent pressor effects in this study. Alternatively, the lateral PBN may be functionally distinct from the PPT but many cholinergic PPT neurons are in fact located within this area *(Mesulam et al., 1983b)*. Li and Ku have also documented a cholinergic pressor effect mediated via the RVLM that is initiated within the amygdala and relays via the hypothalamus *(Li and Ku, 2002)*.

Nicotinic Cholinergic Modulation of CVPN

The phasic release of ACh in cardiac vagal premotor nuclei may play an important role in modulating reflex and respiratory inputs to CVPN and hence contribute to the genesis of naturally-occurring sinus arrhythmias. Vagal preganglionic neurons receive ongoing excitatory inputs from arterial baroreceptor-related afferents and inhibitory inputs from respiratory neurons and pulmonary afferents (see Section II). Neff et al. demonstrated that respiratory-related inhibitory inputs were abolished by bath application of the nAChR antagonist dihydro-β-erythroidine in α4β2 subunit-selective concentrations in slice preparations of rat medulla (Neff et al. 2003). Hence, normal respiratory sinus arrhythmia is dependent upon fast nAChR-gated facilitation of inhibitory inputs to CVPN. A similar mechanism appears to facilitate excitatory baroreceptor-related inputs to CVPN but is dependent upon activation of nAChR containing α7 subunits *(Neff et al., 1998b)*.

Cholinergic Influences on Respiration

Activation of mAChR *(Shao and Feldman, 2000; Bellingham and Ireland, 2002)* or nAChR in the ventral medulla *(Shao and Feldman, 2001)* modulates central respiratory output and airway patency. Topical application of atropine to the chemosensitive zones of the ventral medulla *(Dev and Loeschcke, 1979)* or injections of M3 or M1 receptor-preferring antagonists under the VLM surface in anaesthetised cats *(Nattie and Li, 1990)* reduced resting ventilation and phrenic nerve output and blunted CO_2 sensitivity. Constitutive activation of M3 receptors on pre-Bötzinger neurons in the caudal VLM contributes to their ongoing phasic activity based upon *in vitro* preparations recording hypoglossal motor output *(Shao and Feldman, 2000, 2005)*. M3 receptor knockout mice

also show reduced compensatory ventilatory responses to increases in CO_2 or moderate hypoxia *(Boudinot et al., 2004)*. M1 receptor knockout mice had elevated tidal volume but normal frequency and normal ventilatory responses to hypoxia and hypercapnia *(Boudinot et al., 2004)*. Hence, M3 receptors are likely to be involved in central chemoreception; whereas M1 receptors may modulate activity of respiratory premotor units. In contrast, medullary M2 receptors do not appear to modulate respiration *(Nattie and Li, 1990)*.

ACh applied to the ventral medullary surface increases ventilation *(Haxhiu et al., 1984)*; whereas application to the dorsal surface depresses respiration (see *(Bianchi et al., 1995)*. In several species direct iontophoresis of ACh has been shown to either excite or inhibit different medullary respiratory neurons. Jordan and Spyer reported that expiratory neurons with spinal or propriobulbar projections were inhibited by ACh but inspiratory neurons were unaffected *(Jordan and Spyer, 1981)*. Several others have reported mixed effects on inspiratory and excitatory neurons. Bohmer et al. reported that ACh inhibited inspiratory neurons, inhibited and excited expiratory neurons and excited most neurons with phase-spanning activity *(Bohmer et al., 1987)*. ACh excites, via activation of mAChR, mainly laryngeal motorneurons or bulbospinal premotor neurons; whereas equal numbers of respiratory neurons with intrinsic medullary projections are excited or inhibited *(Haji et al., 1996)*. Hence, overall respiratory responses to cholinergic stimulation may arise from mixed effects on different populations of respiratory neurons.

Muscarinic Cholinergic Influences on Thermoregulation

It is well established that systemic or central application of cholinesterase inhibitors or cholinomimetics lowers body temperature in several species *(Gordon, 1994)*. The mAChR subtypes involved in the cholinergic hypothermic response are still unresolved. M2 receptors appear to be crucial since hypothermic responses evoked by oxotremorine in mice selectively deficient in this subtype are present but markedly attenuated compared to wildtype *(Bymaster et al., 2003a)*. Cholinergic hypothermia appears to involve a combination of increased heat loss mechanisms (eg. evaporative water loss and increased cutaneous blood flow) and reduction in heat-generating mechanisms (shivering / non-shivering thermogenesis) *(Gordon, 1994)*.

The major central sites responsible for control of body temperature include the preoptic hypothalamic area, which is thought to primarily regulate whole-body responses to

changes in ambient temperature, and medullary sites including the RVLM and midline raphé that directly control cutaneous sympathetic fibres *(McAllen, 2004)*. Thermoregulatory raphé neurons are an important source of excitatory input to SPN supplying cutaneous beds necessary for temperature-dependent regulation of their activity *(Nalivaiko and Blessing, 2002; Nakamura et al., 2004; Ootsuka et al., 2004)*. RVLM neurons are considered non-essential for thermoregulatory sympathetic functions, although it is likely that they provide the background excitatory drive to cutaneous SPN *(Ootsuka and McAllen, 2005)*. Reductions or increases in body temperature have been reported following microinjection of cholinergic agonists into the preoptic hypothalamus *(Gordon, 1994)*. Whether or not there are direct cholinergic effects on body temperature mediated by the RVLM or raphé has not been investigated.

VI. The Flinders Sensitive Line

Origin of the Flinders Lines

Whilst at Flinders University in the early 1970s, Janowsky and Overstreet established a selective breeding program where Sprague Dawley (SD) rats were selected for low and high responses to the anticholinesterase di-isopropyl fluorophosphate (DFP) *(Overstreet et al., 1979)*. Several selection criteria were used; in particular a robust marker was the reduction in body temperature, one of several well known sequelae of anticholinesterase agents *(Gordon, 1994)*. Originally, these lines were generated in order to establish tolerance to the effects of DFP in the resistant rats (Flinders Resistant Line, FRL). This was not the case, however, with successive generations of FRL rats continuing to display fairly normal responses *(Overstreet et al., 1979)*. On the other hand, they found that rats bred for sensitivity to DFP (Flinders Sensitive Line, FSL) showed markedly increased physiological and behavioural responses to DFP, physostigmine or direct acting muscarinic agonists compared to both control lines (FRL and SD) *(Overstreet and Russell, 1982; Overstreet et al., 1992b)*. At around the same time, Janowsky and colleagues published work showing that patients with symptoms of major depression exhibited enhanced sensitivity to some specific central effects of cholinergic agonists, including arecoline-induced REM sleep *(Gillin et al., 1991)* and physostigmine-induced ACTH and beta-

endorphin release *(Risch et al., 1983)*. Subsequent testing revealed key behavioural differences in FSL compared to FRL and SD rats (Table 1.6.1), igniting enduring interest in the FSL rat as a genetic model of depression.

Neurochemical Abnormalities in FSL Rats

Cholinergic hypersensitivity in FSL rats was originally thought to involve predominantly changes in central mAChR function. This was based on the finding that AChE activity was not different in whole brains from FSL and FRL rats *(Overstreet et al., 1979)*; whereas mAChR binding with saturating concentrations of QNB was increased in adult FSL rats in the striatum and hippocampus but was unchanged in the cortex *(Overstreet et al., 1984; Pepe et al., 1988)*. FSL rats display greater sensitivity to the hypothermic and locomotor suppressant effects of muscarinic agonists as early as postnatal day 13 *(Daws and Overstreet, 1999)*. However, QNB binding in animals around this age revealed no differences in mAChR number in any brain region *(Daws et al., 1991; Daws and Overstreet, 1999)*. Increases in binding were apparent in the hippocampus and striatum only at later stages of development (~ postnatal day 60) and in the hypothalamus only at postnatal day 120 *(Daws et al., 1991; Daws and Overstreet, 1999)*.

There is limited evidence for changes in specific mAChR subtypes in FSL rats. Based upon displacement of specific QNB binding using pirenzepine, the ratio of M1:M2 binding increased from 2:1 at postnatal day 13 to 4:1 at day 120 in striatal preparations from FSL rats; whereas the ratio remained fairly constant in FRL rats or other brain regions of FSL rats *(Daws and Overstreet, 1999)*. Others examined ChAT and mAChR subtype expression levels in tissue pooled from pontine reticular nuclei including the locus coeruleus, LDT and PPT in FSL rats using semi-quantitative PCR (Southern analysis and radiolabeling of the cDNA oligonucleotide) *(Greco et al., 1998)*. There were no differences in the relative expression levels of ChAT, M2 or M5 receptor mRNA; whereas M3 receptor mRNA expression tended to be reduced in FSL rats compared to FRL and SD rats *(Greco et al., 1998)*.

Several genes are likely to be involved in inheritance of muscarinic supersensitivity in FSL rats *(Overstreet et al., 1992b)*. Supersensitivity to the hypothermic effects of arecoline,

Table 1.6.1. Key behavioural differences between FSL and FRL rats. Adapted from Overstreet et al (2002). [a]Interpretations are the candidate's and also indicated from reviews on this subject (Overstreet et al. 2002; 2005)

Behavioural task	% Difference (FSL v FRL)	Interpretation[a]
Bar-pressing for water	61	Psychomotor retardation
Bar-pressing for food	61	
Active avoidance	52	Tendency to adopt passive behavioural strategy, behavioural 'despair'
Passive avoidance	262	
Swim test immobility	167 - 457	
Elevated Plus Maze	100	No anxious behaviour
Accuracy in matching task	100	Normal cognition
Saccharin preference (SP)	100	Normal basal response to pleasurable stimuli; stress precipitates anhedonia
SP after Chronic Mild Stress	57	
REM sleep	161, 141	

Table 1.6.2. Similarities and differences between neurobiological abnormalities in FSL rats and those reported in human depression. Adapted from Overstreet et al. (2005).

Key finding in FSL rat	Key observation in depression
Cholinergic hypersensitivity **No change in swim test immobility with cholinergic antagonist**	**Cholinergic hypersensitivity** **No antidepressant effect of cholinergic antagonists**
Increased sensitivity to hypothermic effects of 5-HT1A agonists, BUT reduced accumbal dopamine release induced by 5-HT	*Reduced 5-HT1A sensitivity*
Altered TH expression	**Altered noradrenaline sensitivity**
Reduced dopamine transporter	**Reduced dopamine transporter**
Not assessed	Reduced GABA levels
Normal corticosterone	*Elevated* / normal cortisol
Reduced NPY levels	**Reduced NPY**
Normal levels of neurotrophin **Increase with antidepressant**	*Reduced levels of neurotrophin* **Increase with antidepressant**

Bold in both columns indicates match; *italics* indicates mismatch

oxotremorine or physostigmine was lost after crossbreeding FSL and FRL and was partially restored by mating their progeny with FSL but not with each other *(Overstreet et al., 1992b)*. This indicated that predominantly additive and recessive genes contribute to the FSL phenotype.

The polygenic phenotype of FSL rats may also explain why several neurotransmitter systems are affected in these animals. It was demonstrated early on that FSL rats are more sensitive to the hypothermic effects of nicotinic receptor agonists *(Dilsaver et al., 1992)*. FSL rats exhibited increased binding of cytisine (selective for nicotinic $\alpha 4\beta 2$ subunits) but not α-bungarotoxin (selective for $\alpha 7$ subunits) in frontal cortex, striatum, midbrain and colliculi compared to FRL rats *(Tizabi et al., 1999)*. Chronic nicotine exposure, which normally readily evokes nicotinic receptor desensitization, fails to do so in FSL rats *(Tizabi et al., 2000)*.

FSL rats are also more sensitive to dopaminergic and serotonergic receptor agonists and amine pathways appear to be altered centrally *(Yadid et al., 2000; Overstreet et al., 2005)*. FSL rats were found to be more sensitive to the hypothermic and behavioural effects of the serotonergic agonist l(m-chlorophenyl) piperazine *(Wallis et al., 1988)* or the selective 5-HT1A receptor agonist 8-OHDPAT *(Overstreet et al., 1992a; Overstreet et al., 1994; Shayit et al., 2003)*. In adults there appear to be overall increases in 5-HT1A receptor numbers indicated initially by elevated 8-OHDPAT binding in cortex of FSL rats *(Schiller et al., 1991)*. 5-HT1A receptor expression is moderately increased whereas 5-HT2C receptor expression is reduced in several brain regions of FSL rats compared to FRL rats, with the exception of selective increases in 5-HT2C receptor mRNA in the CA2-3 regions of the hippocampus in FSL rats *(Osterlund et al., 1999)*.

The amount of 5-HT and its metabolite 5-HT1AA was increased 3 to 8-fold in tissue punches from limbic regions (nucleus accumbens, prefrontal cortex or hippocampus) and hypothalamus but not the striatum or dorsal or median raphé in FSL compared to FRL rats *(Zangen et al., 1997)*. The ratio of 5-HT1AA to 5-HT was lower in FSL rats indicating reduced 5-HT turnover *(Zangen et al., 1997)*. Despite the high tissue content of 5-HT, a recent study using regional autoradiographic detection of α-[^{14}C]methyl-L-tryptophan demonstrated reduced 5-HT synthesis throughout the brain of FSL rats *(Hasegawa et al., 2006)*. Somewhat paradoxically, the amounts of extracellular 5-HT dialysed from the nucleus accumbens was similar in FSL and FRL rats *(Zangen et al., 2001; Dremencov et*

al., 2005), despite the previous report of dramatic increases in tissue content of 5-HT and 5-HT1AA in this region in FSL rats *(Zangen et al., 1997)*. Although appearing disparate, the various data point towards a reduction in the releasable pool of 5-HT. It is possible that this is a consequence of enhanced numbers or sensitivity of 5-HT1A receptors, which are usually associated with inhibitory autocrine regulation of serotonergic neurons.

Noradrenaline levels were also found to be 2 to 3-fold higher in tissue punches from limbic regions and median raphé; whereas dopamine levels were 6-fold higher in nucleus accumbens and 2-fold higher in striatum, hippocampus and hypothalamus of FSL rats *(Zangen et al., 1999)*. Gene expression of the catecholamine biosynthetic enzyme TH was similar in substantia nigra but elevated two-fold in the adrenal medulla and ventral tegmental area of FSL rats compared to SD rats *(Serova et al., 1998)*. Again paradoxically, extracellular dopamine levels were 40 % lower in nucleus accumbens in microdialysates from FSL rats compared to SD rats *(Zangen et al., 2001)* despite the high tissue content in this region *(Zangen et al., 1999)*. It is likely that impaired 5-HT regulation of accumbal dopamine release can explain the lower extracellular levels since microinjection of 5-HT into the accumbens fails to release dopamine *(Zangen et al., 2001)* and inhibition of accumbal dopamine release mediated by 5-HT2C receptors is enhanced in FSL rats compared to controls *(Dremencov et al., 2005)*.

FSL rats also exhibit changes in pharmacological sensitivity and expression of components of several neuropeptide systems, including NPY *(Caberlotto et al., 1999)*, endorphins *(Zangen et al., 2002)*, vasopressin *(Overstreet and Griebel, 2005)* and corticotrophin-releasing factor *(Owens et al., 1991)*. The underlying mechanisms leading to alteration of multiple neurotransmitter systems in FSL rats are unknown. It may be a consequence of how these systems interact functionally with central mAChR or from changes in second messenger signaling common to specific neurotransmitter receptors. For example, the M2 and 5-HT1A receptors activate a common pool of Gi/o proteins leading to inhibition of adenylyl cyclase *(Odagaki and Fuxe, 1995)*.

Behavioural and Physiological Sequelae of Cholinergic Hypersensitivity

The specific neurotransmitter abnormalities present in FSL rats appear to result in a distinct phenotype in these animals. So far attention has been directed towards their

performance in behavioural tasks thought to reflect anxiety or depressed-like behaviour. For example, key features of the FSL rat are their high immobility time in the Porsolt forced swim test or following exposure to mild stressors including footshock *(Overstreet, 1986; Pucilowski and Overstreet, 1993; Overstreet et al., 1994)*, psychomotor retardation characterised by reduced operant responding for food or water reward *(Russell et al., 1982; Bushnell et al., 1995)*, and reduced active and increased passive behaviours in avoidance tasks *(Overstreet et al., 1990; Overstreet et al., 1992b)*. Moreover, abnormal behaviour in these tasks can be normalised by chronic but not acute treatment with conventional antidepressants *(Zangen et al., 1997; Overstreet et al., 2005)*. Together with evidence for early postnatal development of some depressed-like behaviours *(Daws and Overstreet, 1999; Shayit et al., 2003)*, the FSL rat appears to reflect the long time course and delayed response to treatment that are hallmarks of depression in humans. In contrast, their adequate performance in the elevated plus maze and similar responses to benzodiazepines suggests that FSL rats lack an anxious phenotype *(Overstreet et al., 1995; Braw et al., 2006)*.

A key feature of depression is anhedonia, which in rodents is modeled by preference for sucrose but which is normal in FSL rats *(Pucilowski et al., 1993)*. Their preference for sucrose is markedly reduced compared to controls, however, following exposure to chronic mild stress *(Pucilowski et al., 1993)*, one of the traditional methods for inducing anhedonia as a model of depressed-like behaviour. Hence, these observations appear to strengthen the value of the FSL rat as a model of depression in which some of the core symptoms of depression are innate and others are precipitated by environment. Similarly, maternal separation in FSL rats leads to exacerbation of depressed symptoms *(El Khoury et al., 2006)*.

FSL rats also model changes in sleep architecture and somatic symptoms of depression. They have elevated amounts of REM sleep and shorter latency between REM episodes consistent with a depressed phenotype *(Shiromani et al., 1988; Shiromani et al., 1991b)*, but normal slow wave sleep unlike human depression *(Shiromani et al., 1991b)*. FSL rats also exhibit reduced body weight *(Overstreet, 1993; Friedman et al., 1996)* and required smaller food pellets for training to bar-press for reward *(Bushnell et al., 1995)* suggesting that they have reduced appetite. Evidence for gastric dysmotility *(Djuric et al., 1995; Mattsson et al., 2005)*, immune dysfunction *(Friedman et al., 1996; Friedman et al., 2002)*

and airway hyperresponsiveness *(Djuric et al., 1995; Djuric et al., 1998)* in FSL rats is also indicative of a complicated somatic disease.

The importance of cholinergic abnormalities in the expression of some behavioural changes in FSL rats has been questioned. When FSL and FRL rats were crossbred to produce F1 progeny, which were then mated or crossed back to produce three additional groups, it was found that immobility time in adults was strongly correlated to the hypothermic responses to 8-OHDPAT but not oxotremorine in juvenile animals *(Overstreet et al., 1994)*. Hence, this is an important indication that behavioural changes in FSL rats may not be a direct result of muscarinic supersensitivity; rather they appear to involve 5-HT1A receptor supersensitivity.

Disturbances in sleep architecture *(Shiromani et al., 1988; Shiromani et al., 1991b; Benca et al., 1996)* and possibly related changes in circadian rhythms of body temperature *(Shiromani et al., 1991a; Shiromani and Overstreet, 1994)* and activity *(Shiromani and Overstreet, 1994)*, may also be unrelated to a primary cholinergic abnormality. It is clear that FSL rats exhibit increased amounts of REM and corresponding reductions in NREM sleep *(Shiromani et al., 1988; Shiromani et al., 1991b; Benca et al., 1996)*. The amount of REM sleep induced by intermittent exposure to brief periods of dark was similar in FSL and FRL rats, however, casting doubt over the importance of putative differences in cholinergic activity responsible for producing this rapid phase-switching between wake, NREM and REM *(Benca et al., 1996)*.

It is possible that diminished HPA axis reactivity is linked to changes in stress-responsiveness in FSL rats, although this is controversial. Lower plasma ACTH concentrations were reported in some studies *(Owens et al., 1991)* but not others *(Friedman et al., 1996)* and levels of plasma corticosterone are consistently similar between FSL and FRL rats *(Owens et al., 1991; Friedman et al., 1996)*. Lower plasma ACTH as well as corticosterone levels, however, were reported in juvenile (30-41 day old) FSL compared to SD rats *(Malkesman et al., 2006)*. Putative neural substrates of diminished HPA axis activity may include changes in peptides involved in control of anterior pituitary hormone release. For example, FSL rats had lower CRF concentrations in the median eminence, locus coeruleus and prefrontal cortex but displayed elevated CRF binding in the anterior pituitary *(Owens et al., 1991)*.

Neurochemical abnormalities in pontine, hypothalamic, limbic and basal forebrain structures may underlie behavioural abnormalities and sleep-disturbances in the FSL rat *(Yadid et al., 2000; Overstreet et al., 2005)*. In many cases there is support for the notion that similar neurotransmitter differences occur in human depression (Table 1.6.2), providing support for the potential value of the FSL rat as a model of endogenous depression *(Yadid et al., 2000; Overstreet et al., 2005)*. Despite extensive investigation, there are currently no data on the consequences of selective breeding for cholinergic sensitivity on mAChR or other neurotransmitter systems in regions of the lower brainstem concerned with control of cardiovascular, thermoregulatory or respiratory function. Whether or not there are changes in physiological regulation of these vital systems in FSL or FRL rats is unknown.

VII. Depression: an Internal Dialogue

Depression and Cardiovascular Disease

Depression is a debilitating illness affecting more than one million Australians each year and contributing to premature death by suicide, cardiovascular disease and other health problems *(Mathers et al., 1999; Bunker et al., 2003; Hickie, 2004)*. Depressive illnesses are complex and have varied clinical presentations that range in severity. Hallmarks of depression include low mood, loss of motivation, low self esteem or excessive guilt, and feelings of hopelessness *(Mann, 2005)*. Fundamentally, depression is a central nervous system disorder that also influences cognition, behaviour and physiological regulation of sleep, appetite, immune, gastrointestinal and cardiovascular functions *(DSM-IV, 1994; Nestler et al., 2002)*.

A link between depression and increased incidence of cardiovascular disease has been known for a long time. Symptoms of depression are much more common in patients with coronary heart disease (CHD) (~ 25 %) compared to the general population *(Rudisch and Nemeroff, 2003)*. Depression is now widely regarded as an important risk factor for development of CHD in previously disease-free individuals *(Bunker et al., 2003; Wulsin, 2004)* and appears to be strongly predictive of subsequent early mortality *(Ahern et al., 1990; Frasure-Smith, 1991)*.

CHD is defined by the presence of coronary atherosclerosis but often the first clinical signs are angina and myocardial infarction (MI). Sudden death with evidence for underlying CHD is the most common cause of mortality from cardiovascular disease *(Zipes and Wellens, 1998)*. Sudden death is usually precipitated by the rapid onset of lethal ventricular arrhythmias resulting from underlying tissue damage or following a subsequent MI *(Greene et al., 1989; Zipes and Wellens, 1998)*.

Depression and CHD may share a common genetic basis *(McCaffery et al., 2006)*. The mechanisms linking depression with increased incidence and severity of CHD are unknown. Several biological and social factors are hypothesised to play a role, including increased propensity to smoke or drink alcohol, lack of social support and medical non-compliance and links with prevalence of inflammatory and immune disorders *(Freedland et al., 2005; Gehi et al., 2005a; Lett et al., 2005; McCaffery et al., 2006)*. The association between depression and increased mortality has also been directly attributed to exacerbated autonomic nervous system (ANS) dysfunction *(Frasure-Smith et al., 1993; Carney et al., 2005a)*. A recent study has indicated that a proportion of the risk associated with depression in post-MI patients is directly attributable to low heart rate variability (HRV), an index of impaired cardiac autonomic control *(Carney et al., 2005b)*. This hypothesis is controversial, however; here the evidence for increased risk of arrhythmia and abnormal ANS function in depression is carefully reviewed and scrutinized.

Depression and Mortality Following MI

In most but not all studies symptoms of depression have been associated with increased risk of cardiac mortality in patients with CHD *(Ahern et al., 1990; Frasure-Smith, 1991; Stewart et al., 2003)*. It is likely that the effect of depression is greatest in some patient groups particularly those at risk of MI. The seminal studies of Frasure-Smith et al. showed that depression is associated with a 4 – 5 fold increase in the risk of mortality in the first 6 months following an MI *(Frasure-Smith et al., 1993, 1995)*. Its predictive value is equivalent to that of left ventricular dysfunction or previous history of MI *(Frasure-Smith et al., 1993)*. Severity of depression at admission for MI is positively correlated with risk of mortality over the subsequent 5 years *(Lesperance et al., 2002)*. Although not studied as extensively, depression has been found to have similar prognostic value in patients with

unstable angina *(Lesperance et al., 2000)* or following coronary artery bypass graft surgery *(Connerney et al., 2001)*.

Depression and Arrhythmia

Following acute MI, ventricular electrical instability characterised by frequent premature ventricular complexes (PVC) or non-sustained ventricular tachycardia (VT) is predictive of subsequent death *(Hallstrom et al., 1992; Moss et al., 1996; La Rovere et al., 1998)*. In the 18 months following MI the increased risk of mortality associated with depression was greatest in patients with frequent PVCs (≥ 10 per hour) *(Frasure-Smith et al., 1995)*. In 103 patients with stable CHD, ventricular tachycardia (VT) during 24 hr Holter monitoring was more common in patients with mild-severe depression symptoms (23 %) compared to non-depressed subjects (3.5 %) *(Carney et al., 1993)*. In a larger study in 645 patients recruited following surgery for an implantable cardioverter defibrillator (ICD), moderate-severe depression scores were significantly associated with time to first shock and total occurrence of shocks for VT or fibrillation *(Whang et al., 2005)*. In a recent study of 940 patients with documented CHD receiving cardiac catheterization and followed up for a median of 3 years, in-hospital depression scores were significantly related to subsequent incidence of ventricular arrhythmias *(Watkins et al., 2006)*. In contrast, in the five years following MI, depression was not associated with readmission to hospital for angioplasty, bypass surgery or recurrence of non-fatal MI *(Lesperance et al., 2002)*. These studies suggest that in the post-MI patient group in particular, the risk associated with depression may be explained by a pro-arrhythmic rather than pro-ischaemic mechanism.

In patients with CHD depression symptoms are often associated with conventional cardiac risk factors including hypertension *(Jonas et al., 1997)* and left ventricular dysfunction *(van Melle et al., 2005)*. Underlying cardiovascular abnormalities have been widely reported in depressed patients with or without existing cardiac disease; these include an increase in platelet aggregability *(von Kanel, 2004)*, impaired brachial artery flow-mediated dilatation *(Rajagopalan et al., 2001; Broadley et al., 2002)*, elevated plasma noradrenaline *(Esler et al., 1982; Veith et al., 1994)*, reduced HRV *(Carney et al., 1995; Stein et al., 2000; Agelink et al., 2001; Agelink et al., 2002; Guinjoan et al., 2004; Carney et al., 2005b)*, reduced baroreflex sensitivity (BRS) *(Watkins and Grossman, 1999; Broadley et al., 2005)* and increased QT interval variability *(Carney et al., 2003)*. Several of these factors may contribute to the higher incidence of mortality in depression. In

particular, ECG abnormalities or autonomic dysfunction indicated by elevated plasma noradrenaline and low HRV and BRS could explain the higher incidence of arrhythmia *(Zipes and Wellens, 1998)*.

The Autonomic Nervous System and Ventricular Arrhythmia

Several models of arrhythmia have been used to uncover potential substrates of susceptibility to lethal ventricular arrhythmia *(Walker et al., 1988; Barron and Lesh, 1996; Hamlin, 2006)*. The model developed by Schwartz and coworkers has arguably provided the most information about the role of the autonomic nervous system (ANS). In this model, conscious dogs receive an anterior MI and following a month long recovery are subjected to an exercise stress test and transient ischaemia induced by occlusion of the left circumflex coronary artery *(Schwartz et al., 1984)*: the incidence of ventricular fibrillation (VF) and sudden death is about 50 % *(Schwartz et al., 1984; Schwartz et al., 1988; De Ferrari et al., 1991; Vanoli et al., 1991)*.

Schwartz and coworkers made the seminal observation that reflex changes in heart rate induced by the combination of exercise and ischaemia reflect arrhythmia susceptibility; heart rate reduced in resistant animals and increased in susceptible animals *(Schwartz et al., 1984)*. Moreover, differences in autonomic outflow were directly responsible for inducing or protecting from arrhythmias: left stellate ganglionectomy prevented sudden death, whereas stimulation of the right cervical vagus prevented recurrence of fibrillation *(Schwartz and Stone, 1980; Schwartz et al., 1984; Vanoli et al., 1991)*. Beta-adrenergic receptor blockade with propranolol was effective in lowering heart rate and preventing arrhythmias *(De Ferrari et al., 1993)*; whereas vagomimetic effects of oxotremorine *(De Ferrari et al., 1992; De Ferrari et al., 1993)* or low dose pirenzepine *(Pedretti et al., 2003)* were partially effective. Hence, reductions in heart rate in dogs resistant to fibrillation appeared to reflect reflex vagal activation during ischaemia that was cardioprotective. In contrast, heart rate increases reflected sympathetic overactivity and impaired reflex vagal activation that was arrhythmogenic. The reduction in heart rate *per se* may not be imperative, however, since vagal stimulation conferred a protective effect even when heart rate was kept constant by atrial pacing *(Vanoli et al., 1991)*.

Markers of Cardiac Autonomic Control in Prediction of Cardiac Risk

The clinical utility of monitoring moment to moment variations of heart rate as a marker of neural autonomic control was first noted by Hon and Lee in the 1960s. They observed in perinatal recordings of fetal ECG that a reduction in variations of fetal heart rate predicted fetal distress and death *in utero (Hon and Lee, 1963b*, *1963a)*. In babies prone to fetal distress there are episodes of profound bradycardia prior to delivery due to reflex vagal activation. Most commonly these are the result of transient hypoxic episodes *(Parer and Livingston, 1990)*. Reductions in heart rate variability (HRV) were thought to reflect a shutdown of the mechanisms responsible for reflexly modulating heart rate, which pre-empted fetal death linked to the inability to compensate for hypoxia.

In the conscious dog model of sudden death, HRV was found to be reduced 1 month after anterior MI and low values predicted susceptibility to VF *(Hull et al., 1990)*. BRS, assessed by the reflex reduction in heart rate following phenylephrine infusion, was also much lower in dogs susceptible to VF *(Schwartz et al., 1988)*. Lower BRS prior to the initial MI predicted sudden death in the month allowed for recovery *(Schwartz et al., 1988)*.

It is now well established that low HRV and BRS are strong prognostic markers in several clinical settings *(Kleiger et al., 1987; Bigger et al., 1992a; Bigger et al., 1993; La Rovere et al., 1998; La Rovere et al., 2001)*. Following MI, HRV < 70 ms and BRS < 3 ms/mmHg were associated with a 3.2 and 2.8 times higher risk of cardiac mortality, respectively (ATRAMI; *(La Rovere et al., 1998)*). Risk of cardiac mortality is substantially increased with the combination of reduced BRS or HRV and frequent PVC (> 10 per hour) *(La Rovere et al., 1998)* or episodes of non-sustained VT *(La Rovere et al., 2001)*. HRV is also temporally related to the incidence of ventricular arrhythmia; HRV indices were markedly depressed in the minutes preceding onset of VT/VF in post-MI patients who received an ICD *(Pruvot et al., 2000)*. Although the majority of studies have measured HRV and BRS early after MI (~ two weeks), when measured late after infarction (1 year) a reduction in HRV is independently associated with subsequent mortality *(Bigger et al., 1993)*.

Interpretation of the Predictive Value of HRV and BRS

The predictive value of reduced HRV and BRS is widely interpreted to reflect an autonomic imbalance that favours pro-arrhythmic sympathetic activity *(Pagani et al., 1984; Pagani et al., 1986; Lombardi et al., 1987; Pagani et al., 1991; Lombardi et al., 1996; Lombardi, 2002)*. HRV and BRS are predominantly markers of autonomic input to

the sinus node. As such, how a reduction in HRV or BRS predicts ventricular electrical instability is unclear, since autonomic innervation of the atria and ventricles can be easily dissociated *(Chiou and Zipes, 1998)*. Furthermore, HRV and BRS only reflect the end-organ response to a complex, interconnected collection of afferent, neural and efferent pathways that regulate autonomic activity (see Sections I – IV). A substantial problem that remains is elucidating the causes of autonomic dysfunction related to a specific disease process.

The complexity of the physiological components of HRV is an additional challenge to the interpretation of abnormal HRV *(TaskForce, 1996)*. HRV is in large part a product of reflex influences on autonomic outflow to the heart related to respiration that occur at high frequencies (HF) and baroreflex buffering of LF Mayer wave oscillations of AP (see Sections I – IV). It has been argued that HRV is in large part driven via feedback from arterial baroreceptors in response to spontaneous fluctuations of AP *(Bertinieri et al., 1985; Sleight et al., 1995; Persson et al., 2001; Laude et al., 2004)*. This is based mainly on the fact that there is good agreement between values for BRS measured using traditional methods (eg. phenylephrine, carotid neck suction) versus modern techniques based on computing the gain of spontaneous beat-to-beat fluctuations of R-R interval with corresponding AP fluctuations (eg. sequence method, α-coefficient) *(Persson et al., 2001; Laude et al., 2004)*. Very low frequency (VLF) variations of heart rate may be related to activity of the renin-angiotensin system or temperature *(Akselrod et al., 1981; Taylor et al., 1998)*. There is also evidence for non-neural mechanisms generating HRV. In heart transplant recipients who unavoidably have an initial complete autonomic denervation, a small amount of HRV was generated by deep breathing or exercise *(Bernardi et al., 1990; Radaelli et al., 1996)*. This suggested that respiratory-related heart rate oscillations could also result from direct mechanical effects of ventilation on the myocardium.

Phasic vagal activity has a strong influence on beat-to-beat variations of sinus cycle length (see Section II). The magnitude of HRV is correlated to vagal tone and it is mostly abolished by atropine in human *(Fouad, 1994; Medigue et al., 2001)*, dog *(Akselrod et al., 1981)*, rat *(Elghozi et al., 2001)* and mouse *(Mansier et al., 1996; Baudrie et al., 2006)*. The SA node pacemaker cells respond in a non-linear fashion to increasing concentrations of ACh *(Zaza and Lombardi, 2001)*, indicating that vagal activity is non-linearly related to HRV. This does not detract from its predictive validity but does complicate its physiological interpretation.

Current understanding of physiological components of HRV suggests that specific frequencies reflect vagal activity or the relative balance of sympathetic and vagal activity *(TaskForce, 1996)*. Oscillations of heart rate occurring at HF (RSA) typically dominate the HRV spectrum; they are almost entirely vagally mediated (see Section II) although as mentioned above there is evidence for a small non-neural component *(Bernardi et al., 1990)*. LF oscillations of heart rate are synchronous with Mayer wave oscillations of AP (see Section IV). They appear to be due to combined activities of sympathetic and vagal activities, since their amplitude is reduced by atropine or beta-adrenergic receptor blockade *(Akselrod et al., 1981)*. In controlled experiments the VLF component of HRV has been shown to depend largely on vagal activity *(Taylor et al., 1998)* and power at these frequencies is increased by blockade of the renin-angiotensin system *(Akselrod et al., 1981; Taylor et al., 1998)*.

Experimental findings of changes in HRV associated with increased sympathetic activity have been difficult to reconcile. For example, HRV is virtually absent during intense exercise *(Arai et al., 1989)* or in heart failure *(Kienzle et al., 1992)* where there is marked cardiac sympathetic activation. One explanation for these findings is that saturating levels of sympathetic activity may completely antagonise vagal actions at the sinus node and hence eliminate the predominate source of HRV *(Malik, 1998)*. Clearly, in pathophysiological settings, an interpretation of the predictive value of HRV must reconcile how the causes of a reduction in variability lead to an increase in ventricular electrical instability.

Reduced HRV in Depression

HRV can be defined using measures of the variation of R-R intervals around a mean recorded from the ECG or pulse interval of AP; these include the standard deviation of R-R intervals (SDNN) or other measures including the root mean square of successive differences (RMSDD) *(TaskForce, 1996)*. HRV can also be measured as the variations occurring at specific frequencies by using fast-Fourier or related transformations *(Akselrod et al., 1981)*. This analysis relies on blocks of R-R interval data ranging from a few minutes up to 24 hrs that contain enough of the relevant oscillations. A third technique, time-frequency analysis, has been used to examine spectral parameters of HRV as continuous variables *(Bianchi et al., 1993; Mainardi et al., 2002)*, much like one would

examine continuous recordings of AP or heart rate. Finally, healthy subjects' HRV displays scale-invariance *(Guzzetti et al., 1996; Braun et al., 1998)*, a fundamental feature of a complex system that appears erratic but is in fact non-randomly organized. Although all of these measures have been studied in detail in cardiovascular and other diseases, the depression literature covers only time and frequency domain parameters of HRV. Hence, attention is focused on these techniques.

HRV measured using SDNN was reduced in depressed patients who were otherwise medically well compared to controls *(Rechlin et al., 1994)*. Severe depression rated according to the Hamilton Depression scale (HAM-D) was associated with reduced RMSSD and HF power in patients with no history of cardiovascular-related disease compared to moderately depressed and control groups *(Agelink et al., 2002)*. The relationship between HRV and depression symptoms has been examined using 24 hour ambulatory ECG measurements *(Carney et al., 1995; Stein et al., 2000)*. in patients with stable CHD moderate-severe depression (Beck Depression Inventory (BDI)) was associated with reduced 24 hr average SDNN and VLF power compared to mildly depressed or control subjects *(Stein et al., 2000)*. Similarly, patients undergoing elective coronary angiography with major or minor depression showed reduced 24 hr average SDNN compared to non-depressed patients *(Carney et al., 1995)*. LF but not HF power was significantly reduced in patients with stable CHD with moderate-severe depression scores *(Stein et al., 2000)*. In contrast, HF but not LF power was reduced in older patients (> 60 yo) with recent MI or unstable angina and depression according to HAM-D *(Guinjoan et al., 2004)*. In the latter study there was a significant correlation between total and HF power and severity of depression *(Guinjoan et al., 2004)*.

In the largest study so far, however, there was no association between HRV and depression symptoms in 24 hr ECG recordings from 873 patients with stable CHD *(Gehi et al., 2005b)*. Patients in this study were mostly men (82 %) and were included on the basis of either a recent MI or revascularization procedure, or diagnosis of CHD based on angiography or exercise treadmill test *(Gehi et al., 2005b)*. It is possible that differences in HRV in these patients are not apparent because of improvements in treatment intervention for CHD that could have positive effects on HRV. Secondly, it may be that there are no detectable differences in HRV in this cohort because most patients had stable CHD and differences are manifest only in patients at risk of MI. In support of this there is a strong association between depression symptoms and reduced HRV in at-risk CHD patients, as

demonstrated in 24 ambulatory ECG monitoring of patients screened for the Enhancing Recovery In Coronary Heart Disease (ENRICHD) trial who had a recent acute MI *(Carney et al., 2001)*. All spectral parameters of HRV (ULF, VLF, LF and HF) were significantly reduced in patients with major or minor depression compared to non-depressed controls *(Carney et al., 2001)*. After adjusting for age, gender, smoking and diabetes, which were also associated with HRV, depression remained significantly associated with all parameters except HF power ($P<0.07$) *(Carney et al., 2001)*.

In a follow-up study, the impact of depression on survival in the 30 month follow-up period was adjusted for the log of VLF power of HRV *(Carney et al., 2005b)*. The reduction in VLF power accounted for a proportion of the increased risk of mortality associated with depression *(Carney et al., 2005b)*. Reduced VLF power is also strongly related to reduced survival in patients with a recent acute MI independent of depression *(Bigger et al., 1992a; Bigger et al., 1993)*. In depressed patients there appears to be a correlation in a majority of studies between severity of depression and risk of cardiac events and a reduction in HRV at frequencies associated with autonomic input to the heart.

Reduced BRS in Depression

BRS measured using the sequence method has been reported to be reduced *(Broadley et al., 2005)* or unchanged *(Broadley et al., 2002)* in patients with treated depression and no history of CHD or conventional risk factors for CHD. Interestingly, in these two studies BRS was similar in the depressed group (19.5 and 19.3 ms/mmHg) but differed in controls (25.4 and 20.9 ms/mmHg), suggesting that an ambient factor, possibly the recording environment, may have contributed to the negative finding. In a small study of 66 patients with stable CHD, age-adjusted BRS measured using cross-spectral analysis was significantly reduced (4.5 vs 6.5 ms/mmHg) in patients with high vs. low BDI scores *(Watkins and Grossman, 1999)*.

Direct Evidence for Differences in Autonomic Outflow in Depression

Several small studies have reported changes in peripheral noradrenaline kinetics in depression. Two studies using the isotope dilution technique have reported increased noradrenaline spillover in five *(Esler et al., 1982)* and seventeen *(Veith et al., 1994)*

depressed patients compared to controls. Noradrenaline clearance from the plasma is reported to be higher *(Esler et al., 1982)* or unchanged *(Veith et al., 1994)* in depressed patients compared to controls. Carney et al. (1999) reported no difference in plasma noradrenaline levels in 50 depressed vs. 39 non-depressed patients with CHD *(Carney et al., 1999)*. Agelink et al. reported a reduction in the Valsalva ratio; the ratio of longest (during recovery) to shortest (during Valsalva) R-R intervals, in medically well depressed patients [the Valsalva manoeuver is a maximum inspiratory capacity-forced expiration against a closed glottis] *(Agelink et al., 2001; Agelink et al., 2002)*. Presumably, this reflects a reduction in maximum vagal activation in the recovery phase of the Valsalva when AP increases rapidly.

Summary

In a majority of studies there appears to be a correlation between severity of depression, risk of cardiac events, a reduction in 24 hr average HRV and reductions in LF and HF in short term recordings. The reduction in HRV in depression appears to reflect a reduction in reflex vagal activity and relative increase in sympathetic activity, which is in part supported by direct evidence for changes in the level of peripheral noradrenaline (see above). The finding that 24 hr average SDNN and RMSSD correlate to short term spectral components of HRV *(Bigger et al., 1992b)* also supports the conclusion that the reduction in HRV in depression is not spurious but is due to abnormal physiological regulation of heart rate. Recent studies provide some support for a reflex origin of the reduction in HRV, for example 2 out of 3 studies found that BRS was reduced in depressed patients with or without cardiac disease compared to control subjects *(Watkins and Grossman, 1999; Broadley et al., 2005)* and reflex vagal activation during Valsalva also appeared to be reduced *(Agelink et al., 2001; Agelink et al., 2002)*. These studies support the possibility that depression is associated with an autonomic imbalance, possibly of reflex origin, that may explain the increased susceptibility to arrhythmia and sudden death. Figure 1.7.1 illustrates possible mechanisms in depressed individuals that disrupt normal cardiovascular regulation and predispose to arrhythmia.

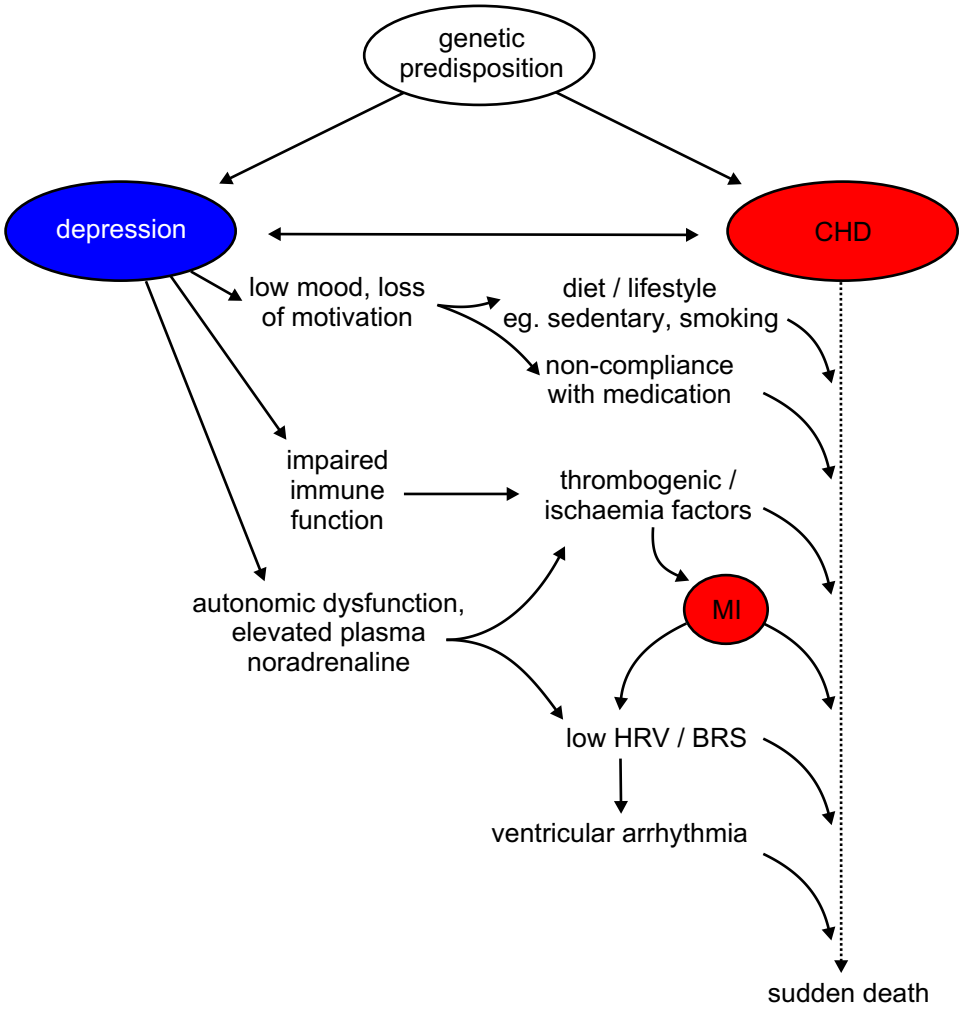

Figure 1.7.1. Hypothetical flow diagram illustrating biological factors affecting the progression and severity of coronary heart disease (CHD) and the influence of depression. Depression is a neurobiological disorder that affects mood, behaviour and cognition and physiological regulation of immune and cardiovascular function. In depressed patients with or without existing cardiac disease there is evidence of impaired immune and autonomic function, which can heighten sensitivity to inflammation and endothelial dysfunction and lead to abnormal cardiovascular regulation. In patients with CHD the presence of depression symptoms is predictive of early mortality, particularly following an initial MI. Depression is thought to promote development of fatal arrhythmias rather than further thrombus formation or ischaemia. Autonomic dysfunction characterised by low HRV and BRS may be directly linked to higher incidence of arrhythmia in post-MI patients with depression. Low HRV and BRS reflect an imbalance in autonomic outflow to the heart, characterised by reduced reflex vagal activity and a relative predominance of sympathetic activity, which promotes ventricular electrical instability.

VIII. Aims and Objectives

Although the basic organisation of cardiorespiratory neural networks in the lower brainstem is well established, the significance of the diverse range of amines and peptides that modulate their activity is unclear. In particular, the role of cholinergic inputs to the RVLM in control of circulation is poorly understood. Local mAChR activation in the RVLM evokes potent sympathoexcitatory responses, although the receptor subtypes and neurochemical phenotype/s of RVLM neurons that mediate this response are unknown. The first aims of this thesis were firstly to further elucidate the neurochemical and -anatomical substrates underlying cholinergic sympathoexcitatory effects in the RVLM and, secondly, to determine the physiological role of cholinergic inputs to the RVLM in control of the circulation.

FSL and FRL rats were originally bred from SD rats for increased or reduced hypothermic responses, respectively, to cholinesterase inhibitors and direct acting muscarinic agonists. FSL rats exhibit a number of central changes in mAChR and other neurotransmitter receptors that influence behaviour, sleep architecture and appetite. In FRL rats the integrity of major CNS functions appears to be unaltered compared to SD rats. No previous studies have determined the effect of this selective breeding protocol in FSL or FRL rats on the expression or function of mAChR involved in control of peripheral circulation or breathing. Hence, the second aim of this thesis was to determine if there are alterations in tonic or reflex cardiorespiratory regulation in FSL or FRL rats and to determine if this involves genetic disturbances in mAChR function within the lower brainstem.

Depression symptoms are associated with impaired autonomic control of heart rate (reduced HRV and BRS) and increased susceptibility to arrhythmia. The causes of autonomic dysfunction in depression are unknown. Previous data show that the FSL rat models many of the behavioural and somatic symptoms seen in human depression. Hence, this strain has potential value in further understanding biological factors associated with a depressed phenotype that predispose to cardiac complications. Hence, the final aims of this thesis were firstly to determine if FSL rats exhibit autonomic abnormalities that resemble those reported in human depression and, secondly, to determine if vulnerability to ventricular arrhythmia is increased in FSL rats compared to control strains.

Chapter 2 General Materials and Methods

I. Ethical Approval

All studies were approved by the Animal Care and Ethics Committee of Royal North Shore Hospital and University of Technology Sydney. Rats were killed whilst deeply anaesthetised, unconscious and unresponsive to noxious stimuli with overdose of anaesthetic or potassium chloride (KCl, 3 M) or toxic doses of the cardiac glycoside ouabain (see Chapter 6).

II. Animals

Male rats were used in all experiments. Rats were maintained in local breeding colonies at Gore Hill Research Laboratories in a 12 hour light-dark cycle with access to food and water *ad libitum*. Sprague Dawley (SD) rats aged 10 – 15 weeks were used. FSL and FRL rat breeders were imported from the University of North Carolina in September 2003 and used to establish local breeding colonies (importation and liaison with AQIS organized by candidate). All rats were tested for differences in their sensitivity to hypothermia induced by the mAChR agonist oxotremorine prior to their use in experimental procedures, as described previously *(Daws and Overstreet, 1999)*. Briefly, conscious (or lightly halothane-anaesthetised, 1 % in O_2) animals were administered the peripheral mAChR antagonist atropine methylnitrate (2 mg / kg) followed by oxotremorine (0.2 mg / kg) intraperitoneally (ip) and the change in rectal temperature from baseline recorded after 30 minutes. Cholinergic hypersensitive FSL rats (> 2 ºC fall in rectal temperature) and FRL rats (<1 ºC fall) aged 10 – 15 weeks, and in some cases younger rats (~4 wks) (see Chapter 4), were used.

III. Surgical Procedures

Anaesthesia and Maintenance

For non-recoverable procedures animals were anaesthetised with urethane (ethyl carbamate, 1.2 – 1.5 g / kg ip, Sigma) diluted to 10 % to minimize peritoneal irritation. Depth of anaesthesia was continuously assessed by testing withdrawal responses to strong hindpaw pinch and by stroking the cornea with a cotton bud. Additional anaesthetic (urethane 30mg) was administered when required. Rectal temperature was maintained

between 37 and 38 ºC with an infrared lamp and thermoregulated heating blanket (Harvard Apparatus, USA).

Intra-Arterial AP Measurement and Intravenous Drug Administration

AP was measured via an intra-arterial cannula containing heparinised saline (heparin 3-5 drops, 5000 IU in 1 ml, David Bull Laboratories) placed into the right common carotid or deep or superficial femoral arteries, depending upon the procedure. The internal carotids and vertebral arteries join the circle of Willis at the base of the brain; this arrangement allows collateral circulation into the cerebral arteries such that ligation of one carotid artery will not greatly hinder cerebral perfusion. In most animals the circle of Willis is well developed. In humans, however, there is considerable congenital anatomical variability, which has been linked to differences in susceptibility to cerebral aneurysm and stroke *(Kayembe et al., 1984)*. The superficial femoral artery was cannulated in recovery experiments in order to maximise blood supply to the limb.

Drugs were administered via intravenous cannulas containing saline placed into the right jugular or femoral vein. The latter was preferred for experiments where the cardiac component of the baroreflex was analysed; since intrajugular injections elicit transient volume expansion in the right atrium and briefly perturb the ECG and recordings of HR. The arterial and venous catheters used were clear polyvinylchloride tubing ID 0.58 mm, OD 0.96 mm; superficial femoral catheters were ID 0.28 mm, OD 0.61 mm.

Nerve Isolation and Placement of Blood Flow Probes and ECG and EMG Electrodes

The left greater splanchnic nerve was isolated via a retroperitoneal approach and cut at its junction with the celiac ganglion in order to record from sympathetic preganglionic fibres supplying the mesenteric and abdominal beds. The left phrenic nerve was also isolated using a subscapular approach and cut distally. The left aortic nerve (AN) was also isolated using the same approach, tied and cut distally in some studies (Chapters 3 and 6). In one study the right tibial nerve (TN) was also isolated and left intact (Chapter 3).

Nerves were placed onto bipolar silver wire electrodes and bathed in paraffin oil (the TN was covered in cotton wool soaked with an approximately 1:1 mixture of paraffin oil and Vaseline). In most experiments the electrocardiogram (ECG) was also recorded using a 3-lead placement: a ground lead was inserted subcutaneously in the neck and positive and negative leads inserted on either side of the chest through the right atrial-ventricular apical axis. In some studies a laser Doppler flow probe ($\lambda = 780 \pm 10$ nm, power = 0.5 – 1.0 mW, Oxford Optronics, UK) was placed within a ventral incision close to the base of the tail, overlying the ventral tail artery (Chapters 3 and 5). In some experiments Teflon-coated stainless steel filaments were inserted into the left biceps femoris in order to record electromyographic activity (EMG) (Chapter 3). In young animals (Chapter 4) respiratory activity was recorded by placement of bipolar electrodes into the diaphragm or intercostal muscles.

Recording and Data Acquisition

The arterial line was connected to a pressure transducer and the AP signal was sampled at 200 Hz. Splanchnic sympathetic nerve activity (SNA), phrenic nerve activity (PNA) and EMG were recorded differentially (Bioamplifier, CWE Inc., USA). Raw signals were amplified (x5000), band pass filtered (30-1000 Hz) and sampled at 1000 Hz. ECG recordings containing clear P and QRS deflections were usually obtained by filtering the raw signal between 10-100 Hz and ECG was sampled at 1000 Hz. Tail blood flow (TBF) was also sampled at 1000 Hz using laser Doppler flowmetry. All signals were acquired online using an analog-to-digital converter (1401 Plus, Cambridge Electronic Design (CED) Ltd, UK) and analysed online and offline using Spike2 software (CED Ltd, UK).

Stimulation and Activation of Cardiovascular Reflexes

Arterial baroreflexes were activated by sequential intravenous injection of sodium nitroprusside (SNP) and phenylephrine (PE) (10 μg / kg) (Chapters 3 – 5). Submaximal baroreflex inhibition of SNA was achieved by electrical stimulation of the AN with tetanic 100 Hz pulses (pulse width 1 ms, 0.5-2 V) (Chapter 6) or intermittent 0.5 Hz pulses (100 sweeps, twin pulses separated by 2.5 ms) (pulse width 1 ms, 5-10 V) (Chapter 3). The somatosympathetic reflex was evoked by intermittent electrical stimulation of the TN (0.5 Hz x 100, twin pulses separated by 2.5 ms, pulse width 1 ms, 15-20 V) (Chapter 3). Carotid chemoreceptor activation was achieved by substitution of the inhaled gas mixture for 100% N_2 for a period of 15s.

Microinjection

For microinjection of drugs into discrete brain regions, animals were placed in a stereotaxic frame, mechanically ventilated via a tracheostomy (14G cannula) and paralysed with pancuronium dibromide (0.8mg + 0.4mg/hr, 2mg/ml). Adequacy of neuromuscular blockade was assessed by monitoring PNA and chest wall movements. Rats were ventilated with 100% O_2 mixed with room air (Ugo Basile, Italy). End-tidal CO_2 was monitored using a CO_2 analyser (Capstar-100, CWE Inc., USA) and maintained between 4 – 5 % of expired gases. In Chapter 3 drugs were microinjected into the pons before and after paralysis; in these animals the cervical vagus was cut bilaterally in order to stabilise AP recordings and breathing movements.

For microinjection into the RVLM the dorsal surface of the medulla was exposed via an atlanto-occipital craniotomy and the head angled forward to give a horizontal medullary surface. For microinjections into the pons, animals were placed in a flat-skull position and the calvarium was partially removed to expose the parietal cortex bilaterally. For microinjection into the IML, a laminectomy was performed between T1 and T2 vertebral segments to expose the dorsal surface of the spinal cord bilaterally.

Single or triple-barrel glass micropipettes were manufactured under high temperature using a moving-coil single electrode puller (Camden Instruments Ltd) or programmable multi-electrode puller (Micro Data Instruments Inc, USA). Pipettes were filled with drugs for microinjection and lowered using a micromanipulator (Narishige, Japan) into the brain or spinal cord using previously defined coordinates (**RVLM,** 2 mm rostral, 2 mm lateral to calamus scriptorious and 3.5 – 3.8 mm ventral to the dorsal surface: **IML,** 0.4 mm lateral to midline, 0.9 mm ventral; **Lateral pons and PPT,** the region explored was from 6.5 – 10 mm caudal to Bregma, 1.5 – 2 mm lateral to midline and 5 – 9 mm below the dorsal surface of the parietal cortex) *(Paxinos and Watson, 1996)*. The RVLM was identified functionally as the site where glutamate (100 mM, 50 nl) evoked a profound transient increase in AP (>50 mmHg) and SNA (>200 %). In recovery experiments (pentobarbital anaesthesia) injections of retrograde tracer were made into the RVLM identified functionally as the site where glutamate evoked pressor responses >80 mmHg.

Drugs were administered via pressure microinjection by monitoring movement of the fluid meniscus against a calibrated grid viewed through an operating microscope. Other delivery methods include iontophoretic ejection of drug through the pipette achieved by passing current through the solution. These techniques were pioneered for delivering small volumes of excitatory amino acids to evoke responses from restricted brain regions. Microinjection of glutamate, for example, has the distinct advantage over electrical stimulation in that in activates only cell bodies rather than axons of passage *(Goodchild et al., 1982)*. Any drug can theoretically be administered in this way, although there are several considerations including determining an effective *in vivo* concentration based on receptor-binding studies, endogenous uptake mechanisms and the chemical nature of the compound (eg. size, lipophilic?). Depending on the diffusion characteristics of the drug, small volumes occupy extracellular space within an approximate 'sphere' of influence (a 50 nl injection corresponds to a sphere with radius of ~360 μm, assuming volume fraction $\alpha = 0.21$) *(Nicholson, 1985; Tao and Nicholson, 1996)*. However, small or highly lipophilic molecules may diffuse rapidly. Moreover, spread of drug (even glutamate) to regions distal from the injection site can result in additional late responses not associated with the region of interest *(Lipski et al., 1988)*. Despite these considerations, microinjection remains a relatively simple and powerful technique for modulating neurotransmission within discrete brain regions.

Drugs

All drugs for iv injection were dissolved in saline (0.9% NaCl, pH 7.4): atropine methylnitrate (mATR, a peripheral mAChR blocker, $t_{1/2}$ 4 hrs, Sigma, 5 mg/ml); oxotremorine sesquifumarate salt (OXO, a broad spectrum mAChR agonist, $t_{1/2}$ 1.6 hrs, Sigma, 0.5 mg/ml); (-) scopolamine hydrobromide (SCOP, a broad spectrum mAChR antagonist, $t_{1/2}$ 8 hrs, 5 mg/ml); sodium nitroprusside (SNP, Faulding) and phenylephrine (PE, ICN Biomedicals Inc.); prazosin hydrochloride (a selective α1-adrenoceptor antagonist, Sigma, 2.5 mg/ml); atenolol (a selective β-adrenoceptor antagonist, Sigma, 2.5 mg/ml). All drugs were administered in a volume of 0.4 ml/kg. Ouabain (cardiac glycoside selective for Na^+/K^+ ATPase, Sigma) was dissolved in saline and prepared for infusion in a 20 ml syringe.

The following drugs were used for microinjection; all were dissolved in phosphate buffered saline (PBS, 0.01M, pH 7.4): l-glutamic acid (glut, monosodium salt, Sigma, 100 mM (5

nmol / 50 nl)); (-) scopolamine hydrobromide, (SCOP, a broad spectrum mAChR antagonist, Sigma, 60 mM (3 nmol / 50 nl)); DL-homocysteic acid (DLH, an excitatory amino acid, MP Biomedicals USA, 100 mM); (-)-bicuculline methiodide (a selective GABA-A receptor antagonist, Sigma, 4 mM); injection site markers, either colloidal gold (Sigma, 20 nM) or methylene blue (4%). See below for details of retrograde tracer microinjections.

IV. Histological Procedures

In microinjection studies brains and spinal cords were removed and fixed overnight in 4 % formaldehyde in saline and sectioned (50 μm) using a vibrating microtome (Leica VT1000S, Germany). Brain sections were either mounted immediately onto gelatinized slides (RVLM sites marked with methylene blue or injection sites in the pons) or processed for detection of gold-labeled injection sites in the RVLM using a silver intensification reaction (Silver Enhancer Kit, Sigma). Briefly, gold-labeled sections were developed under agitation in a silver salt and an initiator for 10 mins; these solutions were extracted and the reaction was fixed in 2.5 % aqueous sodium thiosulphate. Mounted sections were counterstained in Cresyl Violet following dehydration (ascending concentrations of ethanol), removal of lipids (chloroform), hydration and differentiation (95 % EtOH / acetic acid). Sections were observed under light microscopy (Leica, Germany) and compared to standard sections of Paxinos and Watson (1996), photographed and images adjusted for brightness and contrast using SPOT2 software (Diagnostic Instruments). Injection of retrograde tracers in the RVLM and IML were confirmed using immunohistochemical procedures described below.

V. Retrograde Tracing and Immunohistochemical Procedures

Retrograde Tracing and Transcardial Perfusion

Rats were anaesthetised with sodium pentobarbital (60 mg / kg ip) and received long-lasting analgesia pre-operatively (carprofen (non-steroidal), 2.5 mg ip). Small pressure injections of the retrograde tracing agent cholera toxin β subunit (CTB, 1 %) were made into the pressor region of the RVLM on one side (20 nl) or bilaterally into the IML (200 nl

/ side). Wounds were sutured and rats were allowed to recover for 36 hrs (RVLM group) or 3 – 5 days (IML group). Following recovery, rats were deeply anaesthetised with sodium pentobarbital (70 mg / kg ip). The chest was opened and the animal was perfused through the ascending aorta with tissue culture medium (ph 7.4, Dulbeco's Modified Eagle's Medium, Sigma) followed by 4 % formaldehyde in 0.1 M phosphate buffer (PB). Brains and spinal cords were removed and post-fixed overnight.

Light and Fluorescence Immunohistochemistry

Serial transverse sections (50 μm) were cut using a vibrating microtome (Leica VT1000S). Sections were washed in 50 % ethanol (30 min) and Tris-phosphate-buffered saline (TPBS; Tris-HCl 0.01 M, sodium PB 0.01 M, 0.9 % NaCl, pH 7.4) (3 x 30 min). Sections were processed for detection of single or multiple proteins using light and fluorescence immunohistochemistry.

For fluorescence immunohistochemistry, sections were incubated with three primary antibodies (see below) diluted in 5 % normal horse serum (NHS) prior to overnight incubation with fluorophore-conjugated secondary anti-sera diluted 1:500 in 2 % NHS (see below). For light immunohistochemistry, sections were reacted with species-specific primary antibodies and biotinylated secondary antibodies. For detection of multiple proteins using light microscopy, sections were incubated with ExtrAvidin peroxidase (Sigma, 1:1000 in TPBS) for 3 – 4 hrs and proteins detected using enhanced diaminobenzidine (DAB) reactions (nickel and imidazole). DAB reactions consisted of pre-incubation of sections in a mixture of DAB-tetrahydrochloride (10 mg, Sigma), glucose (20 %), ammonium chloride (0.4 % NH_4Cl), distilled water and nickel ammonium sulphate (1 %, 800 μl) + sodium PB (0.4 M) *or* imidazole (1 M, 100 μl) + Tris-HCl (100 mM). Sections were reacted with glucose oxidase (1 μl / ml, Sigma) for 10 – 30 mins until reaction product was visible (nickel – black; imidazole – brown). Each reaction was stopped by removing reaction mix and washing sections in buffer.

Spinally projecting neurons were visualised using goat anti-CTB (light 1:50 000, fluorescence 1:1000, List). Cholinergic perikarya and terminals were visualised using rabbit anti-vAChT (light 1:500, fluorescence 1:800, Chemicon, USA) or sheep anti-ChAT (light, 1:500, Chemicon). Catecholaminergic neurons were visualised using mouse anti-TH (fluorescence 1:2000, Sigma, Australia). All secondary antisera (Jackson Immunoresearch)

were diluted 1:500 in TPBS-merthiolate (TPBS-M) containing 2% NHS. Sections incubated with single primary antibodies were incubated with donkey anti-rabbit IgG to detect vAChT or biotinylated donkey anti-goat IgG to detect ChAT. Sections for light microscopy containing vAChT and CTB primary antibodies were incubated sequentially with biotinylated donkey anti-rabbit IgG or biotinylated donkey anti-goat IgG and the order of addition of secondaries (and subsequent DAB reactions) was varied. Sections for fluorescence microscopy containing two or three primary antibodies were incubated overnight in a mixture of fluorescein isothiocyanate (FITC)-conjugated donkey anti-rabbit IgG to detect vAChT, Texas Red (TR)-conjugated donkey anti-goat IgG to detect CTB and 7-amino-4-methylcoumarin-3-acetic acid (AMCA)-conjugated donkey anti-mouse IgG to detect TH. All sections were mounted onto slides with Prolong anti-fade (Molecular Probes, Invitrogen, Australia) and viewed using a fluorescent microscope (Leica DML or Zeiss imager Z.1, Germany). Images were acquired using a SPOT2 digital camera (Diagnostic Instruments). Fluorescence images were merged using SPOT2 and brightness and contrast adjusted using Zeiss Imaging software.

VI. Data Analysis

All data were analysed post-hoc using Spike 2 software (CED Ltd, UK). Heart rate (HR) was derived from the R-R interval of ECG or pulse interval (PI) from the AP wave. Mean AP (MAP) and systolic AP (SAP) were recorded from the AP wave. SNA and PNA were full wave rectified and smoothed with a time constant of 40 ms.

Drug Effects

Cardiovascular, blood flow and respiratory responses to various drugs were expressed as the peak change in each variable from a control period (2 – 5 min) expressed as units or percent baseline (MAP (mmHg), HR (bpm), tail blood flow (TBF, % baseline), mean SNA amplitude (% baseline), PNA amplitude (% baseline) or frequency (Hz) or minute inspiratory activity (PNA amplitude x frequency x 60)). In some chapters the time course of responses was evaluated (see Chapters 5 and 6 for details).

Cardiovascular Reflexes

Electrical Stimulation of Aortic Baroreceptor and Somatic Afferents

Reflex responses of SNA to intermittent AN or TN stimulation (0.5 Hz, 100 sweeps) were quantified by peri-stimulus averaging. The peak changes in average SNA were expressed as a percent of baseline taken over 200 ms prior to the stimulus. The magnitude of the respiratory-related modulation of SNA was quantified by phrenic-triggered averaging of SNA over at least 50 phrenic cycles. The magnitude of the post-inspiratory peak in average SNA was quantified as percent baseline taken over 200 ms prior to onset of phrenic discharge (late expiration), which shows the most constant amplitude during the respiratory cycle *(Miyawaki et al., 2002b)*.

Tetanic stimulation of the AN (100 Hz) was used to quantify the magnitude of reflex bradycardia evoked by submaximal stimulation of the baroreflex (Chapter 6). To control for differences in preparation of the nerve and resulting stimulus strengths (3 x threshold), the amount of bradycardia was calibrated to the fall in AP elicited by AN stimulation (ms/mmHg).

Peripheral Chemoreceptor Activation with Brief Hypoxia

Following brief hypoxia maximal changes in SNA and MAP were expressed as a percent of baseline SNA or MAP (mmHg) taken over 10 s prior to the stimulus.

Baroreflex Function Curves

Sympathetic baroreflex function curves were generated by plotting the relationship between reflex changes in SNA evoked by maximal changes in MAP following sequential bolus injection of SNP and PE (10 μg / kg iv). AP and SNA were averaged with a time constant of 1 s. SNA was normalized by setting maximum SNA inhibition following PE as 0 % and resting SNA as 100 %. Normalized values of SNA vs MAP were fitted to a four-parameter sigmoid logistic function (Eq 1.) by non-linear regression (GraphPad Prism®) over the duration of the baroreflex stimulus. Goodness of fit was shown by r^2 values ≥ 0.95.

Eq 1. $$y = P4 + \frac{P1}{(1 + 10^{[P2\,(P3 - x)]})}$$

where y is SNA and x is MAP, P1 is the range of SNA response, P2 is the slope coefficient, P3 is MAP at 50% SNA range (MAP_{50}) and P4 is the lower plateau. The first derivative of the logistic function was used to calculate maximal gain (G_{max}; gain at MAP_{50}), and gain at resting MAP (G_{MAP}).

In Chapter 4, heart rate baroreflex gain in response to ramp changes in MAP was also calculated. Unlike SNA, however, peak HR responses following SNP or PE were delayed and hence did not initially correspond to the rate of change in MAP. A linear rather than a logistic approach was used to overcome this problem, although this is likely to have underestimated HR gain. R-R interval and MAP were averaged with a time constant of 0.2 s. Linear regression analysis was applied to R-R interval and MAP data over a defined change in MAP (40 mmHg).

Spontaneous Baroreflex Sensitivity (BRS)

The sequence method was used to calculate spontaneous heart rate BRS from R-R interval time series and the AP wave using an easily applied script in Spike 2 (see Appendix 1). The algorithm detects all sequences of three consecutively lengthening or shortening R-R intervals that correspond to an increase or decrease in MAP of at least 0.5 mmHg, respectively, and calculates the slope of individual regression lines through these points. Spontaneous BRS was calculated as the average slope of R-R interval sequences for all sequences detected during 5 minute segments of data.

Heart Rate Variability (HRV)

In Chapter 4, a time domain measure of HRV was calculated from R-R interval time series generated from the ECG. The standard deviation of R-R intervals (SDNN) was calculated over 5 minute segments of data. All data segments were visually inspected for stationarity (no wandering baseline or large deviations from baseline) and lack of artefacts or ectopic beats.

Spectral Analysis

Spectral analysis was performed using fast Fourier transformation (FFT, size 256, resolution 0.04 Hz) of R-R interval, PI, SAP or SNA time series that had been uniformly

resampled at 10 Hz. The length of segments for spectral analysis varied in different studies. In anaesthetised animals spectra were determined over 2-5 minutes of resting data; in conscious animals spectra were calculated over 80 s of data to maximize suitable periods for analysis where animals were quiescent. Summed power was calculated at low frequencies containing sympathetic and baroreflex-related oscillations (LF; 0.25 – 0.75 Hz) and high frequencies synchronous with ventilation and central inspiratory activity (HF; 1-2.5 Hz); and occasionally VLF (< 0.2 Hz). Where possible, HF power was calculated at the exact frequency of phrenic discharge (Chapter 3). Baroreflex gain was also estimated using the α-coefficient, calculated as the square root of the ratio between PI and SAP power in the LF or HF range *(Pagani et al., 1988; Persson et al., 2001)*. See Appendix 2 for further details and an easily applied Excel® spreadsheet for calculating various spectral parameters.

Ouabain Infusion and Classification of Arrhythmia

Ouabain was infused through the right femoral vein at 3 ml / hr at a dose of 200 μg / kg / min. Cardiovascular parameters were acquired continuously prior to and throughout infusion. BRS was calculated using the reflex bradycardia induced by stimulation of the AN over three similar trials separated by 100 s conducted prior to and during ouabain infusion. Average AP, PI and BRS were taken immediately prior to and every 5 minutes throughout ouabain infusion. The maximal change in these variables was recorded as the difference from control levels to the level prior to conduction block. All analysis was blinded to strain by random coding of data files. Ventricular arrhythmias were identified from the ECG using Lambeth conventions *(Walker et al., 1988)*. Ventricular premature beats (VPB) were classified as a premature QRS complex without a preceding P-wave and ventricular tachycardias (VT) as a run of four or more consecutive VPBs (see Chapter 6).

Definition of Appositions

Cholinergic terminal appositions with neurons in the RVLM were detected at high magnification using light and fluorescence microscopy. Light microscopic sections were viewed at 100 x to identify close appositions between vAChT-positive terminals (black reaction product) and CTB-labelled neurons in the RVLM (brown reaction product). An apposition was defined as a site where there was no discernible gap between a bouton and neuron (soma or proximal dendrite) that appeared to make contact in the same plane of view. Similarly, close appositions were detected under fluorescence microscopy;

appositions between vAChT-positive boutons and CTB-labeled neurons or dual labeled CTB and TH neurons in the RVLM were quantified as described below.

Cell Counts

Cells immunoreactive (IR) for CTB or TH and the number of cells / section that were closely apposed by vAChT were counted in serial sections of medulla (separated by 200 μm) extending caudally from the caudal pole of the facial nucleus (VII) (Bregma -11.60 to -13.40 mm). The RVLM was defined anatomically as being bordered dorsally by the nucleus ambiguus pars compacta, laterally by the spinal trigeminal tract, and medially by the lateral edge of the inferior olive (at caudal levels) or pyramidal tract (at most rostral levels).

VII. Statistical analysis

See Chapters 3 – 6 for statistical tests used appropriate to each data set.

VIII. Additional Materials and Methods

The following procedures were not performed by the candidate and are included for completeness, with respect to manuscripts published during the period of candidature.

Combined *In Situ* Hybridisation Immunohistochemistry

For immunohistochemical detection of mRNA as well as protein, floating brain sections were processed with a combined method of *in situ* hybridisation (ISH) and fluorescence immunocytochemistry *(Li et al., 2005)*. Sections were firstly hybridized with preproenkephalin (PPE), M2 or M3 receptor antisense riboprobe, washed in descending concentrations of salt, then reacted with primary antibodies against digoxigenin (DIG, alkaline phosphatase conjugated) and other proteins (see below) for 48 hrs at 4ºC. The proteins were then detected by fluorophore-conjugated secondary antibodies (1:500, Jackson); DIG-labelled *in situ* neurons were detected by a histochemical reaction using

nitroblue tetrazolium and 5-bromo-4-chloro-3-indolyl phosphate salts described in detail previously *(Li et al., 2005)*.

For visualisation of enkephalinergic neurons in the RVLM sections were reacted with primary antibodies against DIG (alkaline phosphatase-conjugated sheep anti-DIG (1:1000, Roche, Germany), mouse anti-neuron-specific nuclear protein (NeuN, 1:2000, Chemicon, USA) and rabbit anti-vAChT (1:800). For visualisation of M2 or M3 receptor mRNA within the RVLM sections were reacted with primary antibodies against DIG, mouse anti-TH (1:2000) and rabbit anti-CTB (1:5000, Virostat, USA).

For visualisation of enkephalinergic neurons and cholinergic terminals in the RVLM, sections were incubated overnight in Cy3-conjugated donkey anti-mouse IgG (for NeuN), FITC-conjugated donkey anti rabbit (for vAChT) and DIG-labelled *in situ* neurons (for PPE mRNA) were detected as described above *(Li et al., 2005)*. For visualisation of M2 or M3 receptor mRNA colocalised with catecholaminergic and spinally projecting neurons in the RVLM, sections were incubated for 24 hrs at 4ºC with Cy3-conjugated donkey anti-mouse IgG (for TH) and FITC-conjugated donkey anti-rabbit IgG (for vAChT). DIG-labelled neurons (for M2 or M3 mRNA) were detected as described above *(Li et al., 2005)*.

Synthesis of DIG-labeled Riboprobes for M2, M3 Receptor and PPE

DNA fragments for PPE was firstly amplified by PCR from rat brain cDNA using forward and reverse primers with SP6 and T7 promoters attached at the 5′ end, respectively. Homology analysis using nucleotide BLAST searches of the National Centre for Biotechnology Information (NCBI, USA) were carried out to ensure that the RNA probe sequence was specific to the mRNA of interest only. Antisense sequences, riboprobe length and GeneBank accession source numbers for M2 receptor, M3 receptor and PPE mRNA are shown in Table 2.1.

Table 2.1. Sp6- and T7-tagged primer sequences for DIG-labelled riboprobes

Gene	Primer	GenBank	Nucleotide sequence (5'-->3')*	Size (bp)
M2	fwd	NM_031016	ATTTAGGTGACACTATAGAAGtgcctccgttatgaatctcc	750
	rvse		TAATACGACTCACTATAGGGAGAcgacccaactagttctacagt	
M3	fwd	NM_012527	ATTTAGGTGACACTATAGAAGatcaaaggaaacgctgtgct	514
	rvse		TAATACGACTCACTATAGGGAGAgtcggctgtaaacaccacct	
PPE	fwd	BC083563	GGATCCATTTAGGTGACACTATAGAAGctaaatgcagctaccgcctg	743
	rvse		GAATTCTAATACGACTCACTATAGGGAGAttccatctcgggaacttcttt	

*Upper case denotes Sp6 and T7 tag sequences and lower case denotes primer sequence

The antisense and sense riboprobes were then transcribed *in vitro* using DIG-11-UTP (Roche Applied Sciences) and Ampriscibe T7 or Sp6 transcription Kit (Epicenter, USA).

All sections were mounted onto slides with Prolong anti-fade (Molecular Probes, Invitrogen, Australia) or Vectorshield Hard Set (Vector laboratories, USA) and viewed using a fluorescent microscope (Leica DML or Zeiss imager Z.1, Germany). Images were acquired using a SPOT2 digital camera (Diagnostic Instruments). Fluorescence images were merged using SPOT2 and contrast adjusted using Zeiss Imaging software.

Quantitative RT-PCR

Rats were deeply anaesthetized with sodium pentobarbital (70 mg/kg ip) and transcardially perfused with ice-cold sterile saline (0.9 % NaCl in phosphate buffer, PB) as described previously *(Kumar et al., 2006)*. The brainstem and spinal cord was cut into 350 µm sections in freezing conditions using a vibratome (Leica VT1000S). Single sections were visualised using a dissecting microscope; tissue was isolated from the rostral (Bregma -11.7 to -12.4) and most caudal medulla (Bregma -15.0 to 15.7) ventral to the nucleus ambiguus, and from the posterior cerebellum.

Total RNA was extracted from each tissue section using the SV total RNA isolation system (Promega, USA) *(Nuyts et al., 2001)*. Total RNA (150 ng) was reverse transcribed (ImProm-II™, Promega, USA) and gene-specific target amplification was performed using quantitative real time PCR in 20 µl reactions containing 1 µl cDNA and 100 µmol/l each primer (RotorGene-2000, Corbett Research, Australia). The reaction conditions consisted of an initial 10 min denaturation at 95ºC followed by 40 cycles of denaturation at 95ºC, annealing at 62ºC for 20 s, extension at 72ºC for 20 s, then 82 ºC for 10 s to allow for data acquisition.

Primers specific for M1 - M5 receptor mRNA and GAPDH were designed from GenBank sequences using commercially available software and obtained from Sigma-Genosys (Australia) (Table 2.2). Samples of the amplified M1-M5 receptor gene products were electrophoresed in an ethidium bromide-stained 2% agarose gel. Gene products were recovered enzymatically using QiaQuick gel extraction kit (Qiagen, Australia) and the DNA was sequenced using the ABI Prism 3730 platform (SUPAMAC, Australia) to confirm specificity to the GenBank sequence. Expression levels of M1 - M5 receptor mRNA were evaluated by normalizing relative to expression of the housekeeping gene glyceraldehyde-3-phosphate dehydrogenase (GAPDH) as previously described *(Li et al., 2003)*.

Table 2.2. Primer sequences for RT-PCR detection of M1-M5 receptor mRNA

Gene	Primer	GenBank	Nucleotide sequence (5'-->3')	Size (bp)
M1	fwd	NM_080773	GCCTACAGCTGGAAGGAAGA	105
	rvse		GGGCATCTTGATCACCACTT	
M2	fwd	NM_031016	TGCCTCCGTTATGAATCTCC	192
	rvse		TCCACAGTCCTCACCCCTAC	
M3	fwd	NM_012527	TGCTAGCCTTCATCATCACG	202
	rvse		TCACACTGGCACAAGAGGAG	
M4	fwd	D78485	CGCCCAGAGACTACAGGAAC	155
	rvse		GGGCTCAGGAATACCTCAAA	

M5	fwd	NM_017362	ACCATCACTTTTGGGACTGC	104
	rvse		TCCTTGGTTCGCTTCTCTGT	
GAPDH	fwd	X02231	TGCACCACCAACTGCTTAGC	87
	rvse		GGCATGGACTGTGGTCATGAG	

Radiotelemetric Probe Implantation

A Dataquest (IV) telemetry system (Data Science Int., MN) consisting of an implantable transmitter, radio receiver, ambient pressure monitor, data matrix and acquisition software was used to measure blood pressure (BP) and temperature in FSL, FRL and SD rats ($n \geq 5$ per group). Rats were housed individually and received pre and post-operative antibiotics (amoxicillin trihydrate (9.3 mg/L) and tylosin tartrate (6.2 mg/L) po). Probes were implanted aseptically under general anaesthesia (sodium pentobarbitone, 60 mg/kg ip) following intraperitoneal administration of analgesia (carprofen, 2.5 mg) and an antibiotic (cephazolan, 0.55 g/kg). Depth of anaesthesia was continuously monitored by testing withdrawal responses to hindpaw pinch and corneal reflexes and additional doses of sodium pentobarbitone (6 mg ip) were administered as required. The probes were implanted into the aorta via the femoral artery and the body of the probe was sutured in place in the peritoneal cavity. All wounds were closed with interrupted sutures and topical tissue adhesive (cyanoacrylate). Rats were kept under close supervision in a warm environment until ambulatory and allowed to recover for 7 – 14 days. Recovery was confirmed by the presence of circadian rhythms in blood pressure, adequate food and water intake, increased body weight and adequate wound healing *(Leon et al., 2004)*.

Chapter 3 Function and Neurochemistry of Cholinergic Inputs to the RVLM

I. Abstract

Central command is a feedforward neural mechanism that evokes parallel modifications of motor and cardiovascular function during arousal and exercise. The neural circuitry involved has not been elucidated. We have identified a cholinergic neural circuit that when activated mimics effects on tonic and reflex control of circulation similar to those evoked at the onset of and during exercise. Central mAChR activation increased SNA as well as the range and gain of the sympathetic baroreflex via activation of mAChR in the RVLM in anaesthetised artificially ventilated SD rats. RVLM mAChR activation also attenuated and inhibited the peripheral chemoreflex and somatosympathetic reflex, respectively. Cholinergic terminals made close appositions with a subpopulation of sympathoexcitatory RVLM neurons containing either preproenkephalin mRNA or TH immunoreactivity. M2 and M3 receptor mRNA was present postsynaptically in non-TH RVLM neurons only. Cholinergic inputs to the RVLM arise only from the pedunculopontine tegmental nucleus (PPT). Chemical activation of this region produced increases in muscle activity, SNA and blood pressure and enhanced the SNA baroreflex: the latter effect was attenuated by mAChR blockade. These findings indicate a novel role for cholinergic input from the PPT to the RVLM in central cardiovascular command. This pathway is likely to be important during exercise where a centrally-evoked facilitation of baroreflex control of the circulation is required to maintain blood flow to active muscle.

II. Introduction

A distinct pattern of tonic and reflex cardiovascular adjustments is mediated by central command to ensure appropriate muscle and organ perfusion during different arousal or behavioural states, such as sleep and exercise *(Rowell and O'Leary, 1990; White et al., 2001; Williamson et al., 2006)*. Limited evidence implicates some regions within the pons and hypothalamus that could provide descending input to cardiovascular control sites *(Krout et al., 2003; Garcia-Rill et al., 2004; Dampney et al., 2005)*, however the neural circuitry and neurotransmitters involved are yet to be elucidated.

Activation of the central cholinergic system has a profound effect on cardiovascular and other autonomic functions. Systemic or central administration of acetylcholinesterase inhibitors or muscarinic agonists increases blood pressure *(Buccafusco and Brezenoff,*

1979; Brezenoff et al., 1982; Brezenoff and Giuliano, 1982; Giuliano et al., 1989; Kubo, 1998), lowers body temperature *(Daws and Overstreet, 1999)* and alters respiration *(Nattie and Li, 1990; Shao and Feldman, 2000)*. Pressor responses can be evoked via activation of mAChR within several cardiovascular nuclei, including the posterior hypothalamus *(Buccafusco and Brezenoff, 1979)*, NTS *(Criscione et al., 1983)* and RVLM *(Giuliano et al., 1989; Kubo, 1998)*. Effects of central mAChR activation on cardiovascular reflexes are less well understood *(Caputi et al., 1980; Brezenoff et al., 1982; Park and Long, 1991)*.

Sympathoexcitatory and hypertensive effects of intravenously administered physostigmine are largely mediated by excitation of RVLM neurons *(Giuliano et al., 1989; Huangfu et al., 1997; Kubo, 1998)*. The RVLM generates basal sympathetic vasomotor activity and is a critical synaptic relay in cardiovascular reflexes *(Pilowsky and Goodchild, 2002; Guyenet, 2006)*. Descending cholinergic projections to the RVLM arise from neurons in the pedunculopontine tegmental nucleus (PPT) *(Yasui et al., 1990)*, although local medullary neurons may also be a source of cholinergic input *(Ruggiero et al., 1990)*. The function of this input into the RVLM is unknown. A dense cholinergic terminal field is present within the RVLM *(Giuliano et al., 1989; Milner et al., 1989; Ruggiero et al., 1990)*, although supportive anatomical evidence that cholinergic terminals provide input to C1 or non-C1 spinally projecting neurons is lacking. Activation of the inhibitory M2 mAChR subtype in the RVLM is thought to mediate pressor responses *(Giuliano et al., 1989; Kubo, 1998)* but its cellular location or that of other mAChR subtypes within the RVLM is unknown.

We hypothesised that cholinergic input to the RVLM from the PPT is involved in central command-mediated effects on cardiovascular function. Previous studies have shown that the PPT is involved in initiation of movement and modulation of muscle tone during locomotion, exercise and arousal *(Bedford et al., 1992; Pahapill and Lozano, 2000; Garcia-Rill et al., 2004)*. Additionally, the PPT connects albeit indirectly with both motor and sympathetic outflows *(Krout et al., 2003)*.

We aimed, firstly, to determine the role of the RVLM in the autonomic responses and effects on reflex control of the circulation evoked by central mAChR activation. Secondly, we identified the mAChR subtypes involved by examining gene expression within phenotypically identified RVLM neurons and determined the exact sources of cholinergic

input to the RVLM. Finally, we determined the tonic and reflex cardiovascular effects generated by chemical stimulation of the PPT.

III. Materials and Methods

Anaesthesia, Surgical Procedures and Recording

SD rats (n = 17) were anaesthetised with urethane, intubated and instrumented for recording of AP, SNA, PNA and TBF as described in Chapter 2. Microinjections into the RVLM were made in 13 rats. Microinjections were made into the pons in 4 rats; in these experiments both vagi were cut and in two rats muscle EMG was recorded from the hindlimb. Rats were paralysed and ventilated as described in Chapter 2.

Activation of Cardiovascular Reflexes

Cardiovascular reflexes were activated as described in Chapter 2, via sequential iv injection of SNP and PE, intermittent electrical stimulation of the AN or TN, and brief hypoxia.

Experimental Protocol

All animals were pretreated with mATR to block peripheral mAChR (2 mg / kg). In nine rats, all reflexes were activated before and after central mAChR activation with iv injection of OXO (0.2 mg / kg). SCOP was injected bilaterally into the RVLM to determine if this reversed effects of OXO on SNA, AP and reflexes. Repeat doses of OXO were administered and reflexes were again tested. In four rats reflexes were not tested during experiments to examine effects of OXO on SNA, AP, PNA, TBF and spectral parameters of SAP and SNA before and after SCOP injection into the RVLM. In four additional rats, DLH (8 nmol) or bicuculline (0.2 nmol) was injected into the pons at 6.5 – 9.5 mm caudal and 2 mm lateral to Bregma at varying depths (5.5 – 9 mm ventral) to examine site-specific effects on AP, SNA and SNA baroreflex responses. In some animals effects on the SSR were also examined. Effects on EMG were examined in two rats prior to neuromuscular blockade and nerve recording. In three animals, sites within the PPT where stimulation evoked increases in SNA and SNA baroreflex responses were tested following SCOP (2 mg / kg) administered intravenously to block central mAChR.

Data Analysis

Data were analysed as described in Chapter 2 in order to examine baseline cardiorespiratory responses and effects on respiratory modulation of SNA and cardiovascular reflex responses of SNA and AP. SNA baroreflex function curves and their first derivatives were generated as described in Chapter 2. Spectral parameters were quantified at low (0.25 – 0.75 Hz) and phrenic nerve frequencies (1.0 - 2.5 Hz) as described in Chapter 2.

Retrograde Labeling from the Spinal Cord or RVLM and Immunolabeling of Protein and mRNA

CTB was injected into the RVLM in 3 rats and into the IML in 10 rats in order to retrogradely label neurons with projections to these areas. Following recovery, rats were transcardially perfused and brain and spinal cord sections processed for light or fluorescence immunohistochemistry or combined *in situ* hybridisation immunohistochemistry as described in Chapter 2. Sections were processed in order to visualise cholinergic neurons with projections to the RVLM, the location of ChAT or vAChT labelled neurons in the medulla, to visualise and quantify the number of cholinergic appositions on phenotypically identified sympathoexcitatory RVLM neurons (CTB +/- TH or PPE mRNA) or proportion of neurons containing M2 or M3 receptor mRNA. In some animals RNA was isolated from a tissue punch from the RVLM and RT-PCR carried out to detect M1-M5 receptor mRNA as described in Chapter 2.

Statistical analysis

All data are presented as mean ± standard error of the mean. A paired Students' t-test was used to calculate effects of treatment versus control or following SCOP and $P<0.05$ was considered significant.

IV. Results

RVLM mAChR Mediate Sympathoexcitatory but not Other Autonomic Effects Evoked by Central mAChR Activation

Central mAChR activation (OXO) significantly increased AP, mean and post-inspiratory-related discharge of SNA, HR and TBF and reduced PNA amplitude (Fig. 3.1A, B, D). Bilateral injection of SCOP into the RVLM (Fig. 3.1C) significantly attenuated the increase in AP (n=8, $P<0.01$), SNA (n= 8, $P<0.01$), HR (n=8, $P<0.05$) and post-inspiratory activation of SNA (n=4, $P<0.05$) but had no effect on changes in TBF (n= 4, n.s.) or PNA amplitude (n=4, n.s.) evoked by OXO (Fig. 3.1D).

Spectral analysis of systolic AP (SAP) and SNA revealed an increase in low frequency (LF, ~0.4 Hz) oscillations following OXO (0.3 ± 0.1 vs 36.5 ± 15.1 $mmHg^2$, $P<0.05$; 4.6 ± 1.4 vs 47.5 ± 17.9 $SNA\%^2$, $P<0.05$). Respiratory-related oscillations of SNA also tended to be increased ($P=0.051$). SCOP injected bilaterally into the RVLM had no effect on baseline parameters but prevented the increase in LF oscillations evoked by OXO (0.3 ± 0.1 vs 0.4 ± 0.1 $mmHg^2$; 3.3 ± 1.0 vs 7.3 ± 2.5 $SNA\%^2$, n=7, $P<0.05$) (Fig. 3.2).

Activation of RVLM mAChR Facilitates the Sympathetic Baroreflex and Inhibits the Somatosympathetic and Chemoreflexes

OXO significantly enhanced the reflex sympathoexcitatory and inhibitory responses evoked by equipotent doses of SNP and PE (Fig. 3.3). This effect was reproducible following repeat injection of OXO (Fig. 3.3A). OXO significantly increased the maximum plateau (146 ± 4 vs. 321 ± 12 %, $P<0.01$) and maximum gain of the SNA baroreflex (4.4 ± 0.5 vs. 8.2 ± 0.6 %/mmHg, $P<0.05$) (Fig. 3.3B, C). The operating point (resting MAP) also shifted closer to the point of maximum gain (Fig. 3.3C).

Figure 3.4 shows the effects of OXO on cardiovascular reflexes before and after blockade of mAChR bilaterally in the RVLM. OXO increased the magnitude of SNA inhibition evoked by AN stimulation (166 ± 13 % control, n=6, $P<0.01$) or excitation following SNP administration (4 ± 3 vs 217 ± 2 %SNA/50mmHg, n=4, $P<0.01$). In contrast, OXO inhibited both excitatory peaks of SNA evoked by TN stimulation (early peak 37 ± 3 % control, $P<0.01$, late peak 41 ± 5 % control, n=9, $P<0.01$). Sympathoexcitatory and pressor responses to brief hypoxia were attenuated and inhibited, respectively (53 ± 6 % control, $P<0.01$; +33 ± 2 mmHg vs -17 ± 5 mmHg, n=7, $P<0.01$). Bilateral injection of SCOP into the RVLM reversed effects of OXO on reflexes, such that they were mostly indistinguishable from controls. The early peak of the somatosympathetic reflex was only

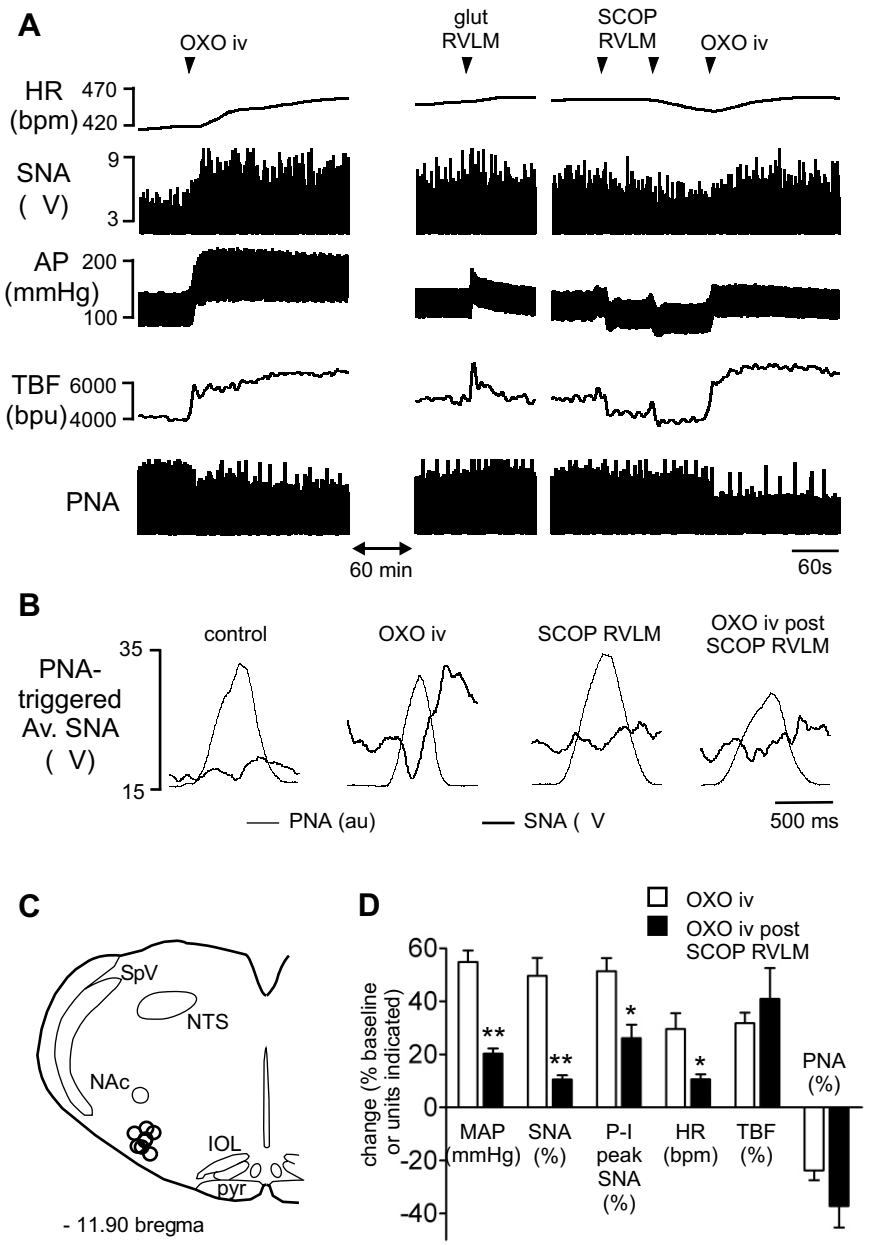

Figure 3.1 *The role of RVLM mAChR in mediating autonomic effects of central mAChR activation in urethane-anaesthetised rats.* A: Following pre-treatment with mATR, OXO (0.2mg/kg iv) evokes an increase in SNA, AP and TBF but a reduction in PNA amplitude. Following identification of RVLM pressor sites (glut), SCOP (9 nmol/site) is injected into the RVLM bilaterally substantially reducing the pressor, sympathetic and HR effects but not the TBF or PNA response to OXO. Increases in HR are due to sympathetic activation. B: Average SNA (bold line) and PNA (thin line) waveforms showing increase in post-inspiratory (P-I)-related discharge of SNA following OXO and blockade of this effect by SCOP injection in the RVLM. C: Injection sites in the RVLM (open circles, only unilateral sites shown). D: Group data from 8 animals illustrating effects seen in A and B. Data shown are mean ± SEM.

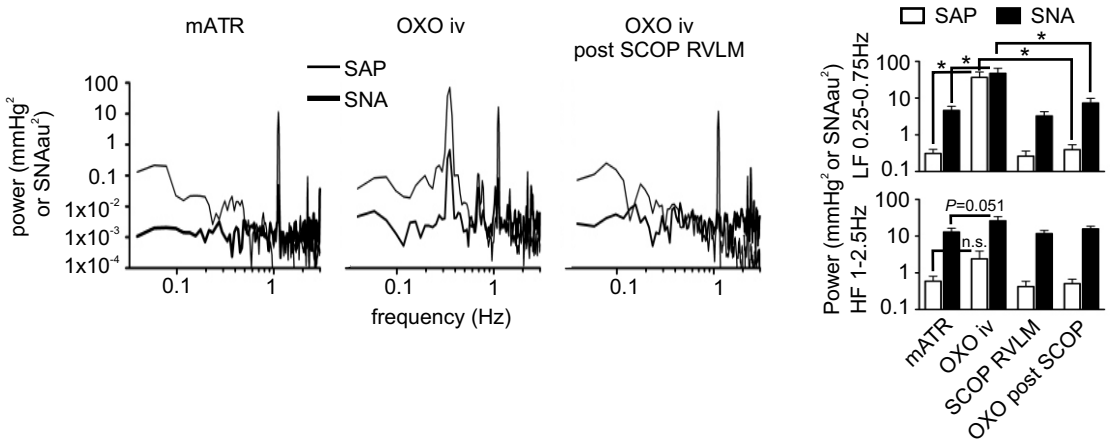

Figure 3.2 *MAChR activation within the RVLM enhances low frequency (0.4 Hz) and respiratory-related oscillations of SNA.* Power spectra of SNA and SAP (uniformly resampled at 10 Hz) are illustrated showing that the amplitude of the LF peak is increased following OXO. Grouped data from seven animals are shown on right illustrating the significant increase in LF power of SNA and SAP following OXO and blockade of this effect by prior injection of SCOP bilaterally into the RVLM. OXO also tended to increase HF oscillations of SNA but not SAP. Data are mean ± SEM, **P*<0.05, ** *P*<0.01, ns = non significant.

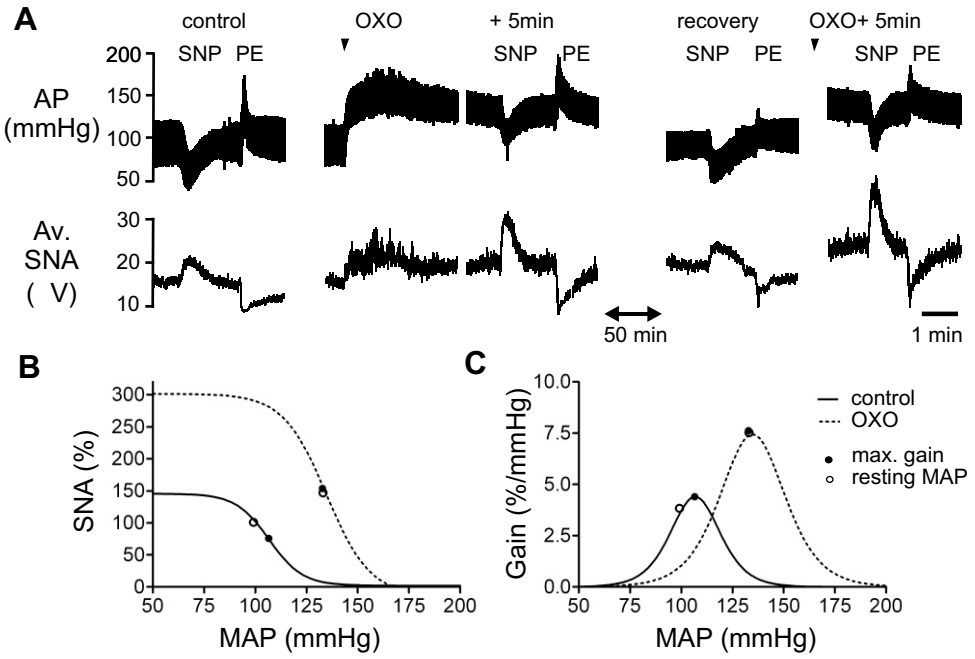

Figure 3.3 *Effects of central mAChR activation on sympathetic baroreflex function.* A: OXO (0.2mg/kg iv) evokes significant facilitation of the sympathetic reflex effects evoked by baroreceptor unloading (SNP) and loading (PE). This effect is reproducible. B: Average four-parameter sympathetic baroreflex function curves generated from data (n=3) including that shown in A and C: their first derivatives (error bars are omitted for clarity). Central mAChR activation with OXO shifts the SNA baroreflex to higher AP and SNA and increases its range and gain.

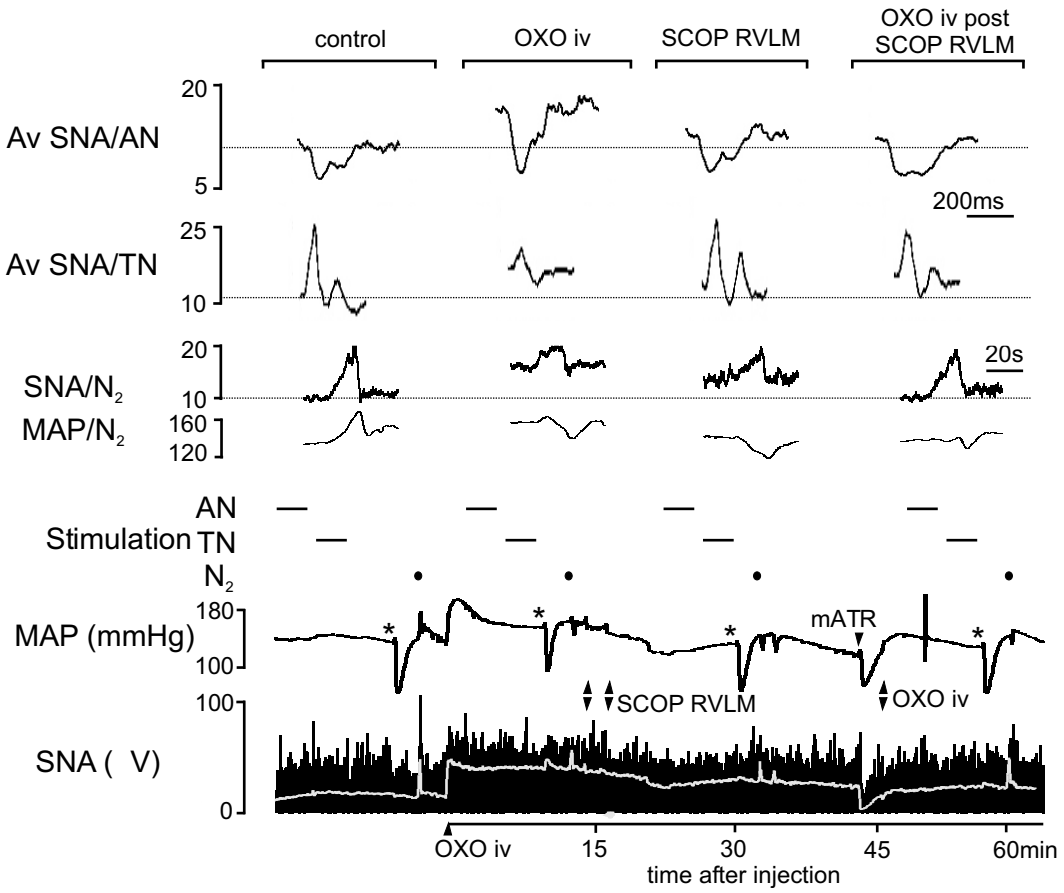

Figure 3.4 *The role of RVLM mAChR in mediating effects on cardiorespiratory reflex function following central mAChR activation.* A continuous recording of MAP and SNA (bottom two rows) illustrating differential effects of OXO (0.2 mg/kg iv) on the baroreflex (AN stimulation, top row), the somatosympathetic reflex (TN stimulation, 2nd row) and the peripheral chemoreflex (N_2 substitution, 3rd and 4th rows). The stimulus periods are indicated under the peristimulus-averaged SNA responses. OXO enhances SNA baroreflex responses, inhibits both early and late peaks of the somatosympathetic reflex and attenuates sympathoexcitatory and pressor effects of the peripheral chemoreflex. These effects are blocked by prior injection of SCOP bilaterally in the RVLM. Mean changes in SNA are overlaid on the raw SNA signal to illustrate effect of OXO on reflex responses to baroreceptor unloading with SNP (*). Dotted horizontal lines indicate the control level of SNA.

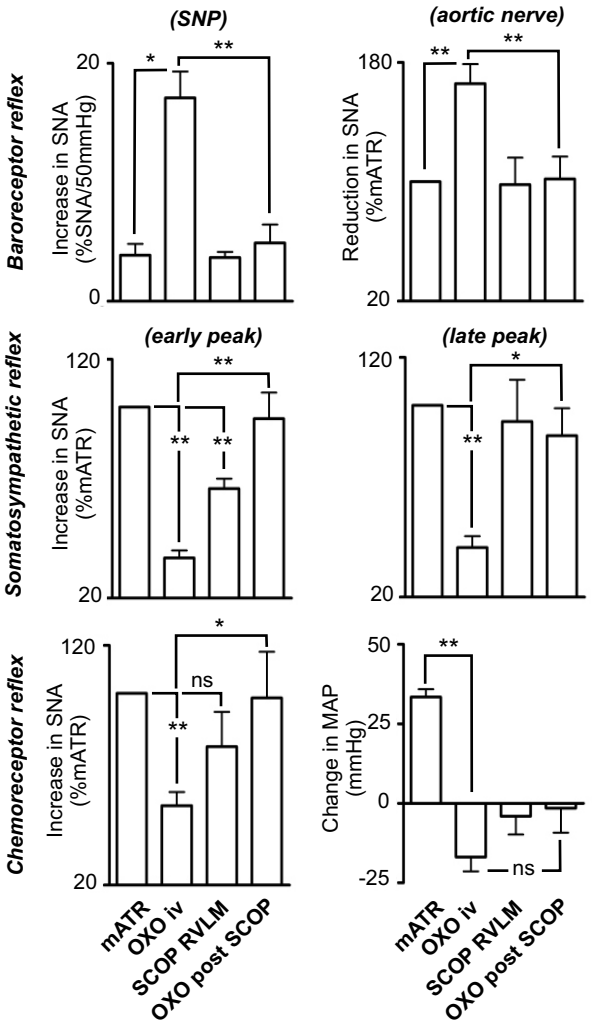

Figure 3.5 *MAChR activation within the RVLM enhances the baroreflex and inhibits the somatosympathetic and peripheral chemoreflex.* Grouped data from nine animals showing OXO-evoked effects on cardiorespiratory reflex function. OXO enhances SNA baroreflex responses, inhibits both early and late peaks of the somatosympathetic reflex and attenuates sympathoexcitatory and pressor effects of the peripheral chemoreflex. Most reflexes return to control level following SCOP injection bilaterally into the RVLM, although the early peak of the somatosympathetic reflex remains attenuated and chemoreflex activation evokes no change in AP. Prior injection of SCOP into the RVLM blocks all effects on cardiorespiratory reflexes evoked by OXO. Data are mean ± SEM, **P*<0.05, ** *P*<0.01, ns = non significant.

partially restored (66 ± 4 % control, $P<0.01$). A repeat injection of OXO 30 min following SCOP failed to elicit effects on any reflex similar to its initial robust effects (n≥4 per group). The pressor response to brief hypoxia did not return to normal after the initial dose of OXO. Grouped data are illustrated in Fig 3.5.

Cholinergic Terminals Closely Appose Sympathoexcitatory RVLM Neurons

vAChT-IR terminals were found throughout the VLM and in cell bodies within the facial and ambigual motor nuclei, consistent with previous reports *(Arvidsson et al., 1997; Schafer et al., 1998)*. A choline acetyltransferase (ChAT)-positive cell group previously identified in the ventromedial medulla *(Ruggiero et al., 1990)* was not present using vAChT labeling (Fig. 3.6). vAChT-IR terminals were closely apposed to CTB-labelled spinally projecting cells in the RVLM; 32.6 ± 7.4 % (379 / 1118 cells, n = 3) of all CTB-IR neurons and 31.1 ± 5.6 % (66 / 206 cells, n = 3) of TH-positive CTB-IR cells (Fig. 3.7, 3.8A). vAChT-IR varicosities also formed perisomatic appositions with NeuN-positive non-TH RVLM neurons that expressed PPE, as well as other PPE-negative NeuN-positive cells (Fig. 3.8B).

M2 and M3 Receptor mRNA is Expressed in Spinally Projecting Non-TH Neurons in the RVLM

All mAChR subtypes were expressed in an RVLM tissue punch (Fig. 3.9). We analysed the cellular distribution of M2 receptor expression in the RVLM and found that no spinally projecting TH neurons contained M2 receptor mRNA (0/310, n=5) (Fig. 3.10A). In contrast, 23 ± 4 % of spinally projecting non-TH RVLM neurons did express M2 receptor mRNA (78/367, n=5) (Fig. 3.10C). M3 receptor mRNA was also expressed in some TH-IR/non-CTB-IR and some CTB-IR/non-TH neurons (Fig. 3.10B, D).

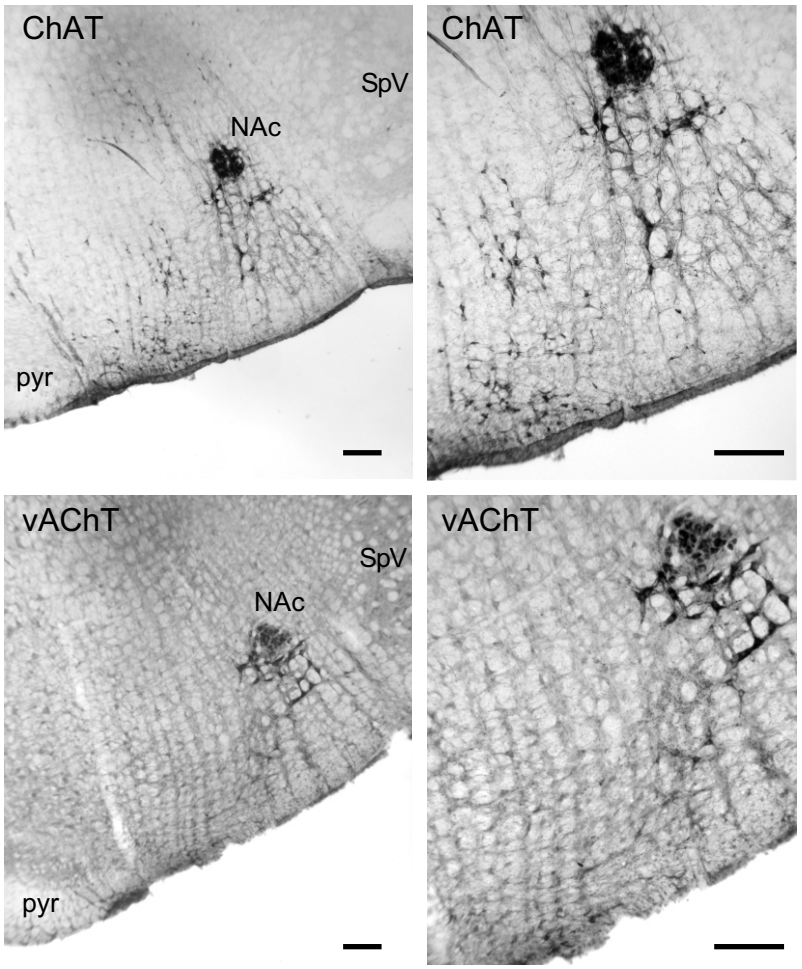

Figure 3.6 *Comparison of ChAT and vAChT immunoreactivity in the ventral medulla.* Coronal sections of the medulla at the same level of the RVLM are shown at low (left panel) and high power (right panel) from different SD rats that were perfused transcardially. 50 m brainstem sections were reacted for immunoreactivity against ChAT (sheep, 1:500, Chemicon, USA) or vAChT (rabbit 1:500, Chemicon, USA) and detected using nickel-intensified diaminobenzidine reactions [1]. ChAT labelling in the medulla identifies large motoneurons of the compact and loose formation of the nucleus ambiguus that can be seen to send fine ChAT containing fibres ventrally into the RVLM. Smaller ChAT-positive perikarya are clearly visible in the medial ventral medulla. In comparison, vAChT labelling identifies ambiguual motoneurons and cholinergic terminal fields in the RVLM but labelling in the ventromedial region is clearly absent. Scale bars = 200 m. *Abbreviations:* NAc, nucleus ambiguus pars compacta; pyr, pyramidal tract; SpV, spinal trigeminal tract.

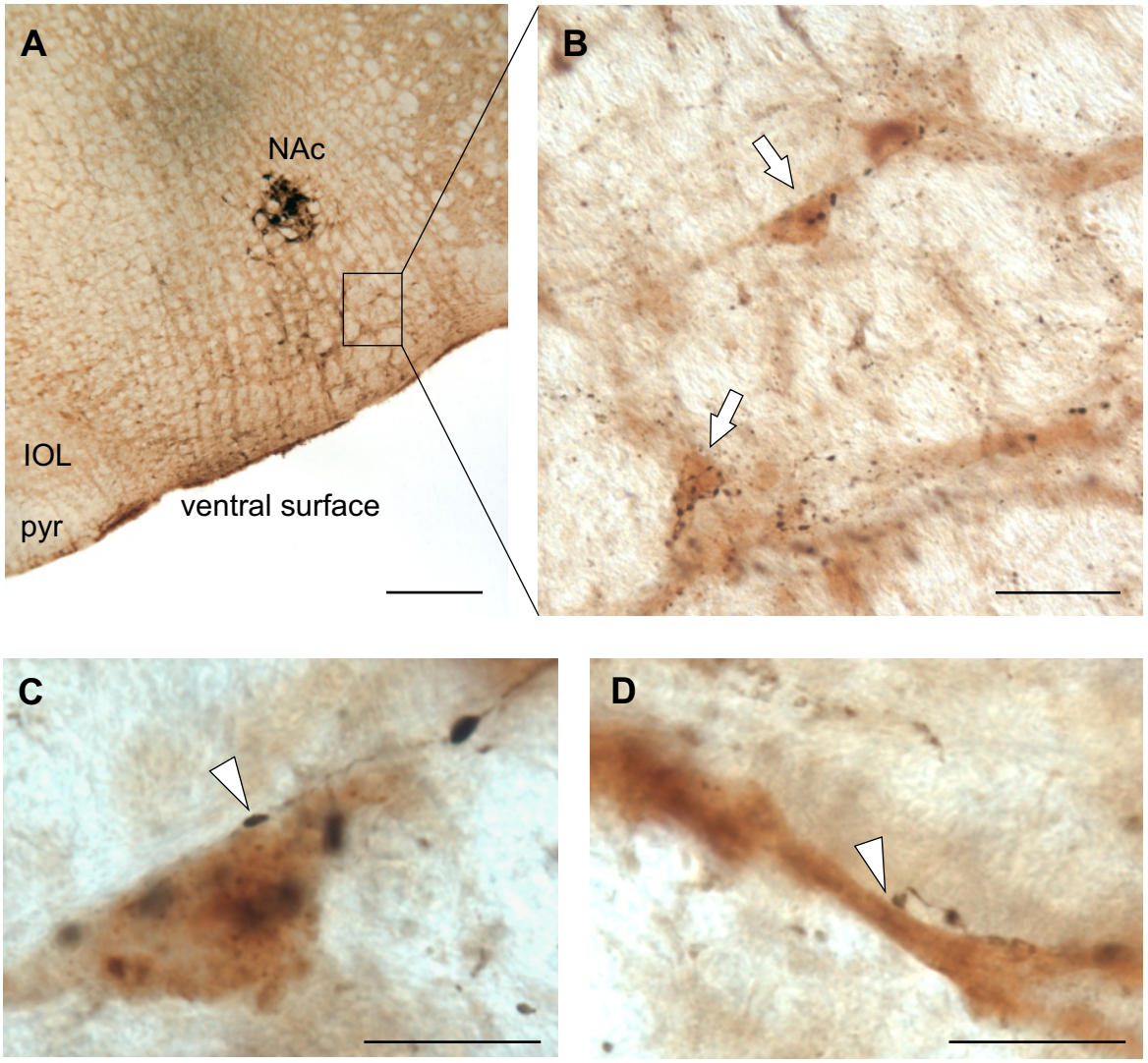

Figure 3.7 *Spinally projecting neurons in the RVLM are closely apposed by vAChT-IR varicosities.* A: Sagittal section of the medulla stained for immunoreactivity to CTB (brown reaction product) and vAChT (black reaction product). Note the neurons in the more dorsal nucleus ambiguus that are immunoreactive for vAChT. B: CTB-positive neurons in the RVLM (boxed area in A) retrogradely labeled from the thoracic IML surrounded by vAChT-IR terminals (arrows). C and D: Close appositions between vAChT-IR varicosities and CTB-labeled neurons in the RVLM (arrowheads). Scale bars: A; 400 m, B; 200 m, C and D; 50 m. Abbreviations: IOL, inferior olivary nucleus; NAc, nucleus ambiguus pars compacta; pyr, pyramidal tract.

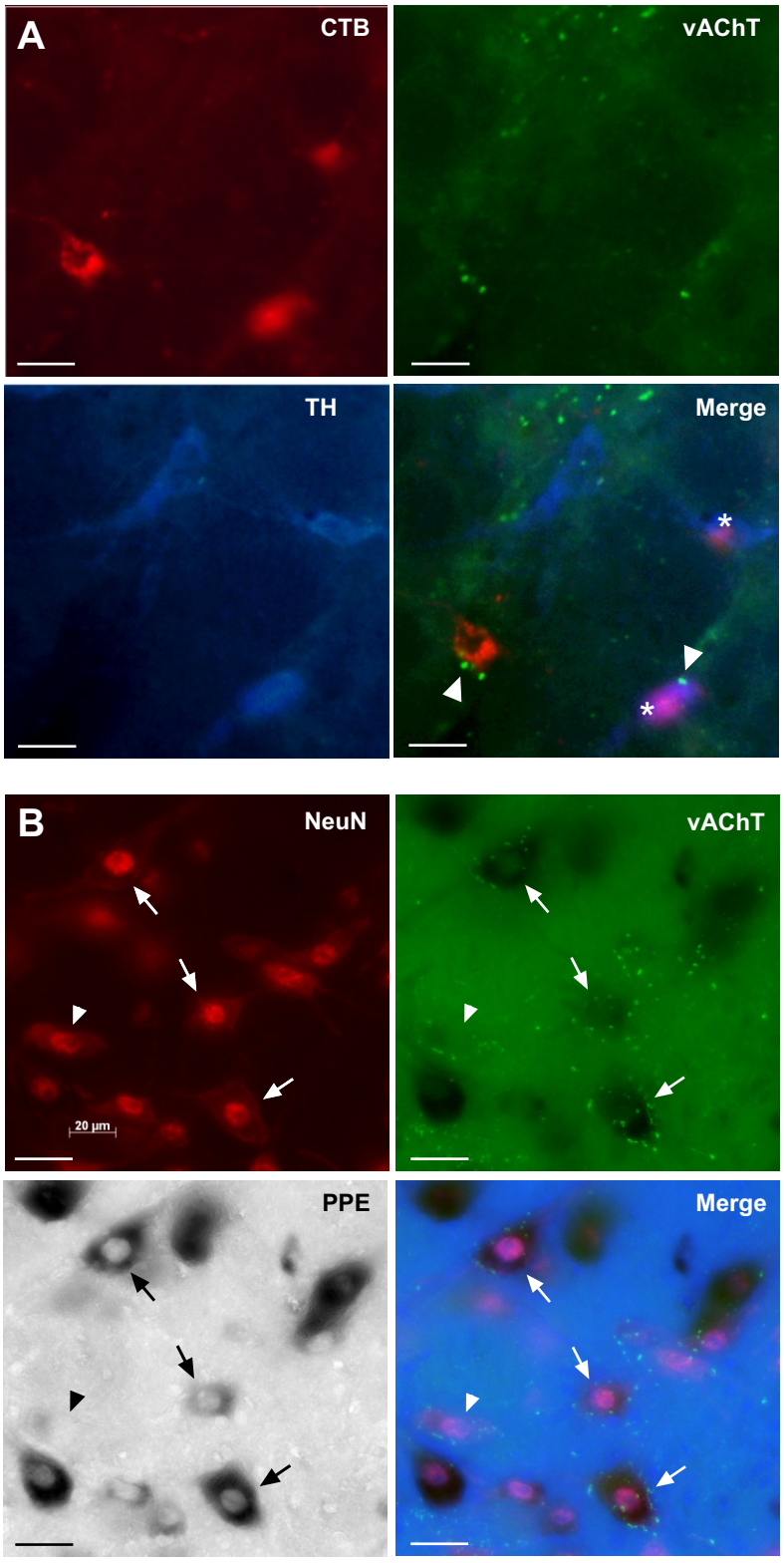

Figure 3.8 *Phenotypically identified sympathoexcitatory neurons in the RVLM are closely apposed by vAChT-IR varicosities.* A: CTB-labeled neurons in the RVLM that are immunoreactive to TH (*) or negative for TH are closely apposed by vAChT-positive terminal varicosities (arrowheads). B: Neurons in the RVLM identified by the neuron-specific marker NeuN that express PPE mRNA (arrows) are closely apposed by vAChT-IR, as are PPE-negative neurons (arrowheads). Scale bars: A and B; 25 m.

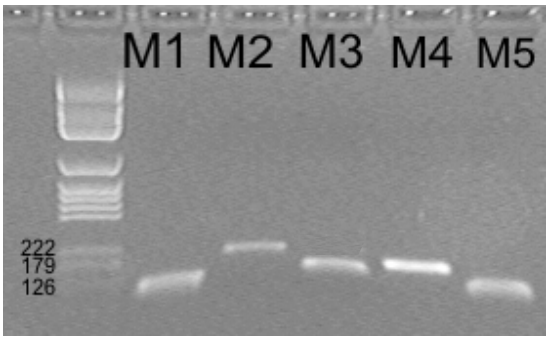

Figure 3.9 *M1-M5 receptor subtypes are expressed in the RVLM*. 2% Ethidium bromide stained agarose gel with high intensity amplicons confirming the presence of M1-M5 receptor mRNA in a tissue punch taken from the RVLM in an SD rat.

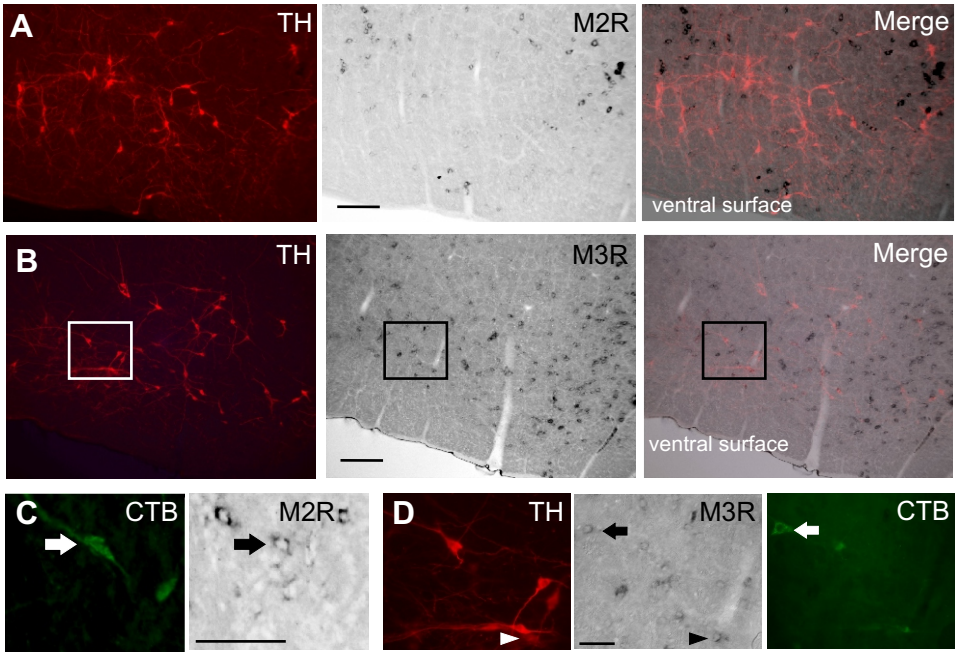

Figure 3.10 *Cellular distribution of M2 (A, C) or M3 receptor mRNA (B, D) and TH-IR neurons in the RVLM.* M2 receptor mRNA is colocalised in RVLM neurons that project to the thoracic IML (CTB-IR) (C) but none of these contain TH-IR. M3 receptor mRNA is expressed in some CTB-IR neurons (arrows) or in TH-IR cells lacking CTB-IR (arrowheads) (boxed area in B shown in D). Scale bars: A and B 250 m; C and D 100 m.

Direct Cholinergic Projections to the RVLM from the PPT

To determine the source of cholinergic input to the RVLM, discrete injections of CTB were made unilaterally into the RVLM (Fig. 3.11A) and cholinergic neurons were identified by vAChT-IR. CTB-IR neurons were found in regions previously described including the parabrachial nucleus, the paraventricular nucleus of the hypothalamus (Fig. 3.11B), central nucleus of the amygdala and the cortex *(Yasui et al., 1990; Horiuchi et al., 1999)*. vAChT-IR neurons were also found in regions previously described *(Arvidsson et al., 1997; Schafer et al., 1998)* (Fig. 3.11C, D). Neurons that were double-labeled for CTB and vAChT had a restricted distribution and were confined within the PPT (Fig. 3.11C, D).

Chemical Stimulation of the PPT Increases Muscle Activity and SNA and Facilitates the Sympathetic Baroreflex via mAChR Activation

Bilateral injection of bicuculline into the PPT evoked increases in AP and EMG activity (Fig. 3.12A). EMG activity but not the increase in AP was abolished by subsequent neuromuscular (NM) blockade (Fig. 3.12A). Injection of DLH into the PPT produced an increase in SNA and AP and increased the magnitude of SNA excitation produced by injection of SNP (Fig. 3.12B). These effects could be evoked throughout the rostrocaudal extent of the PPT (~7 to 9 mm caudal to Bregma). Smaller increases in SNA were evoked at sites dorsal or ventral but facilitation of baroreflex-evoked SNA responses was restricted to the PPT (6.5-7.5 mm ventral) (Fig. 3.12B). Transient alterations in PNA frequency were observed following stimulation of the PPT and surrounding brain areas; whereas the somatosympathetic reflex was unaffected. Prior blockade of central mAChR receptors with SCOP iv prevented the facilitation of baroreflex-evoked SNA responses (n=3, $P<0.05$) but did not abolish sympathoexcitation produced by DLH injection into the PPT (Fig. 3.12C).

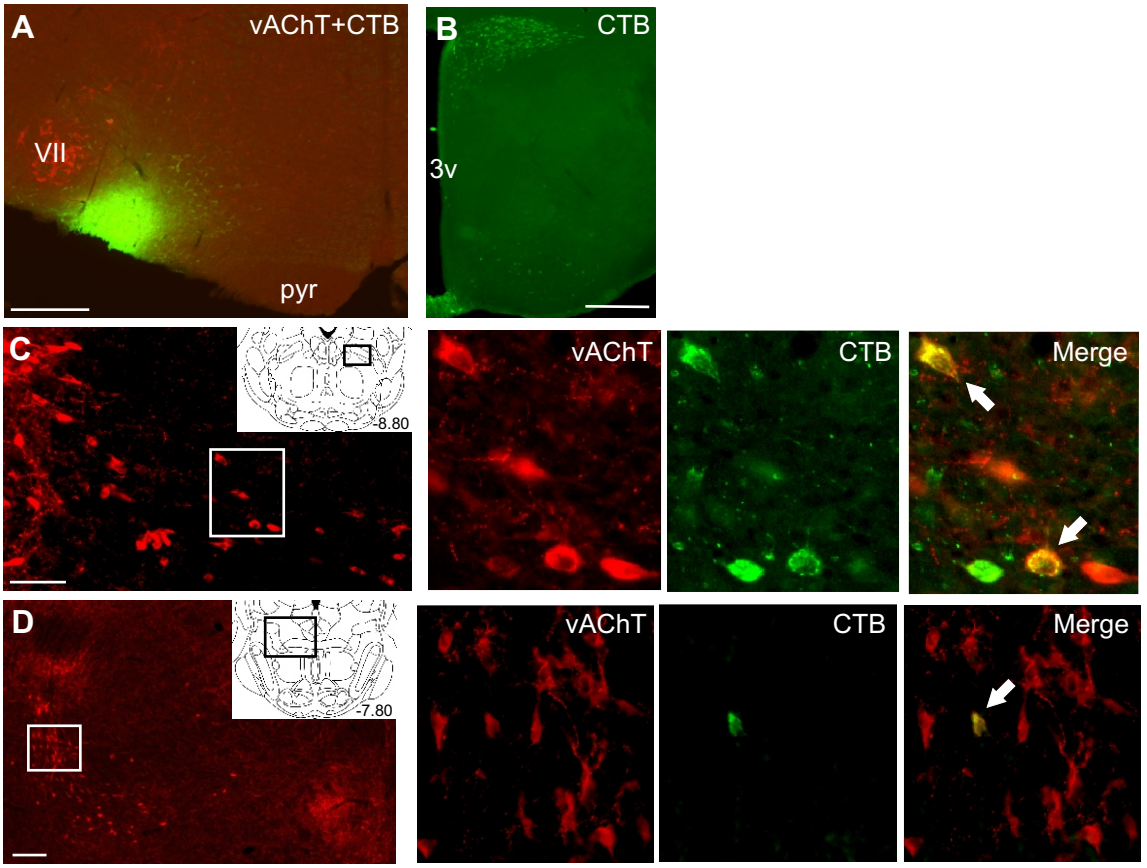

Figure 3.11 *Distribution of retrogradely labelled neurons in the hypothalamus (B) and pons (C and D) following injection of CTB into the pressor region of the RVLM (A, CTB green).* Neurons double-labelled (arrows) for CTB and vAChT (red) were found only within rostral and caudal parts of the PPT (C, D, schematics adapted from Paxinos and Watson, 1996). Scale bars: A and B 500 m; C 100 m; D 200 m. 3v, 3rd ventricle; pyr, pyramidal tract; VII, facial nucleus.

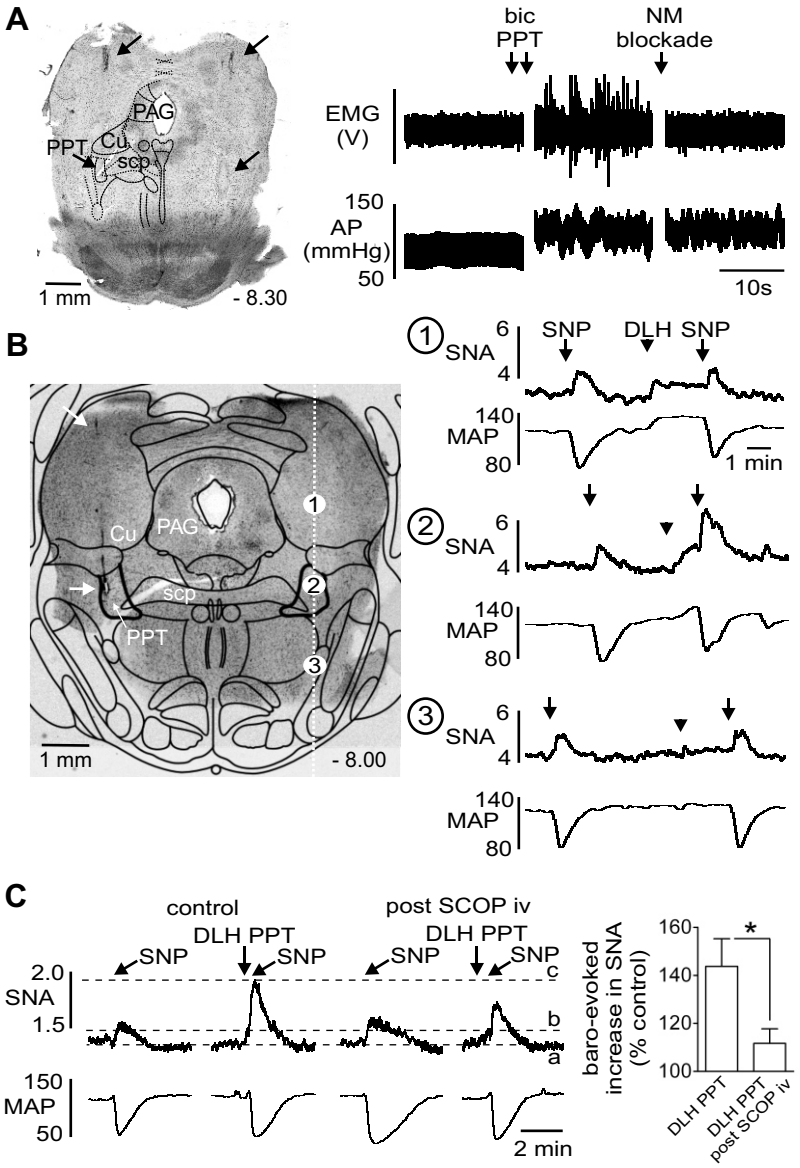

Figure 3.12 *Activation of the PPT elicits increases in muscle activity, SNA and baroreflex responses.* Coronal sections of the pons showing tracks and injection sites of bicuculline (bic 4mM, A) and DLH (100mM, B) (arrows) and cardiovascular responses evoked from the PPT. A: Disinhibition (bic) of the PPT increases AP and EMG activity. B: Unilateral injection of DLH into the PPT (2), but not more dorsally (1) or ventrally (3), increases SNA and AP and enhances the reflex increase in SNA following SNP injection. C: Pre-treatment with SCOP (2 mg/kg iv) blocks the facilitation of the baroreflex evoked by PPT stimulation (lowercase letters indicate reference levels of SNA; *a:* baseline, *b:* new level reached following DLH injection into the PPT, *c:* peak level reached following SNP injection before SCOP. Data are mean ± SEM. Schematics adapted from Paxinos and Watson (1996). Cu,

V. Discussion

The novel findings of this study are 1) mAChR activation in the RVLM facilitates the sympathetic baroreflex and attenuates and inhibits the sympathetic chemoreflex and somatosympathetic reflex, respectively; 2) identified sympathoexcitatory neurons in the RVLM receive cholinergic input and differentially express M2 and M3 receptor subtypes; 3) Chemical stimulation of the PPT, which provides the only direct cholinergic input to the RVLM, evokes a similar pattern of tonic and baroreflex SNA responses to that seen following RVLM mAChR activation. Neurons in the PPT control muscle tone during locomotion, exercise and arousal *(Bedford et al., 1992; Pahapill and Lozano, 2000; Garcia-Rill et al., 2004)*. Our findings indicate that tonic and reflex cardiovascular adjustments are also evoked from the PPT via direct cholinergic projections to the RVLM. These data support our hypothesis that cholinergic input to the RVLM is involved in central command.

RVLM mAChRs mediate the increase in SNA and HR evoked by centrally acting OXO, in agreement with previous studies *(Giuliano et al., 1989; Kubo, 1998)*. Post-inspiratory-related discharge of SNA was also enhanced, indicating a direct effect on respiratory-related inputs to the RVLM *(Miyawaki et al., 1996a)* that presumably contributes to the mean increase in SNA evoked by OXO. This effect was elicited independently of the OXO-evoked depression of phrenic amplitude, which is mediated by sites other than the RVLM *(Nattie and Li, 1990; Shao and Feldman, 2000)*. The OXO-evoked increase in TBF, presumably contributing to the well described hypothermic effect of this drug *(Daws and Overstreet, 1999)*, is also mediated via other central sites. These may include the preoptic area of the hypothalamus as it receives cholinergic input and carbachol microinjections here evoke hypothermia *(Tanaka et al., 2002)*.

We show for the first time that the reflex responses of SNA to baroreceptor loading or unloading, demonstrated following vasoactive drug administration and by direct stimulation of baroreceptor afferents, were markedly enhanced by OXO and were mediated by RVLM mAChRs. Furthermore, baroreflex-related LF oscillations of both SAP and SNA *(Ringwood and Malpas, 2001)* were enhanced.

Our findings show that RVLM mAChR activation resets the SNA baroreflex to higher pressures and increases its range and gain. Earlier studies showed that the pressor effect of bilateral carotid occlusion was greater after central or systemic administration of physostigmine *(Brezenoff et al., 1982; Park and Long, 1991)*. Caputi et al. (1980) demonstrated an upward shift in baroreflex HR responses without changes in range or gain following intracerebroventricular injection of physostigmine *(Caputi et al., 1980)*. A limitation of the present study was that pretreatment with mATR to block peripheral mAChR precluded analysis of vagally-mediated HR responses. Our findings indicate that RVLM mAChR activation facilitates sympathetic vasomotor responses to baroreflex activation; whereas cholinergic effects at brain sites important in reflex vagal control, including the nucleus ambiguus *(Wang et al., 2001)*, may evoke resetting of the HR baroreflex without changing its gain.

OXO evoked differential effects on cardiovascular reflexes via RVLM mAChR activation. Baroreflex SNA responses mediated by direct inhibition or disinhibition of RVLM neurons *(Lipski et al., 1996)* were enhanced. Somatosympathetic and chemoreflex SNA responses mediated by direct excitation of RVLM neurons *(Miyawaki et al., 1996a)* were inhibited and attenuated, respectively. The clear inhibition of the somatosympathetic reflex suggests that these effects were not indirectly due to raised sympathetic activity. To our knowledge, one study in anaesthetised cats also showed that a somatosympathetic reflex evoked by intercostal nerve stimulation was inhibited by OXO *(Baum and Shropshire, 1978)*. As single RVLM neurons receive largely convergent input from baroreceptors, peripheral chemoreceptors, somatic afferents and central respiratory neurons *(Guyenet et al., 1990; Miyawaki et al., 1995; Pilowsky et al., 1996; Verberne et al., 1999a)* three mechanisms are possible to explain our data: OXO activates inhibitory presynaptic mAChRs located on reflex inputs to RVLM neurons, postsynaptic excitatory mAChRs on RVLM neurons, or a combination of both. Pre- and postsynaptic effects of carbachol on RVLM neurons have been demonstrated *in vitro (Huangfu et al., 1997)*.

Phenotypically-identified sympathoexcitatory (CTB+TH) and putative sympathoexcitatory (CTB+non-TH, or PPE+) neurons in the RVLM were closely apposed by vAChT-IR varicosities. This is the first anatomical evidence indicating that cholinergic terminals may synapse with sympathoexcitatory RVLM neurons. Milner et al (1989) showed that ChAT-IR terminals formed abundant synaptic contacts in the ventral medulla but these were rarely seen with TH-containing neurons. In Milner's study, however, only caudal sections

of the RVLM were examined (0.5 – 2.0 mm caudal to the facial nucleus); these contain few spinally projecting TH neurons *(Phillips et al., 2001)*. Furthermore, compared to ChAT, immunoreactivity to vAChT as used here gives better cholinergic terminal labeling *(Arvidsson et al., 1997; Schafer et al., 1998)*.

Our results show for the first time that the M2 receptor was not expressed in TH neurons but was expressed in a subpopulation of spinally projecting non-TH neurons. M2 receptor-preferring antagonists prevent pressor effects of RVLM mAChR activation *(Giuliano et al., 1989)*. The ligands used, however, do not display high affinity for any one particular subtype *(Caulfield and Birdsall, 1998)*. If M2 receptors do mediate OXO-evoked sympathoexcitatory responses then they are most likely located presynaptically in the RVLM or this effect is mediated by non-TH spinally projecting neurons. Huangfu et al. (1997) showed in neonatal RVLM that both C1 and non-C1 cells depolarized in response to mAChR activation. Because vAChT-IR terminals apposed both classes of RVLM neurons we sought evidence for expression of other receptor subtypes. A subpopulation of spinally projecting non-TH RVLM neurons also contain M3 receptor mRNA. We have further demonstrated that mRNA for all 5 mAChR subtypes was present in the RVLM, confirming earlier studies in WKY and SHR *(Gattu et al., 1997b)*. Our results suggest that different or multiple mAChR subtypes may be expressed by sympathoexcitatory RVLM neurons.

In agreement with Yasui and coworkers *(Yasui et al., 1990)* we found that the projection from the PPT to the RVLM is cholinergic. In addition, we show that the PPT is the only cholinergic cell group that provides input to the RVLM. Local inputs from ChAT-positive neurons in the ventromedial medulla *(Ruggiero et al., 1990)* are not functionally cholinergic since we found that these cells did not contain vAChT.

We demonstrated for the first time that chemical stimulation of the PPT facilitates baroreflex-evoked excitation of SNA, mimicking effects of RVLM mAChR activation. Blockade of mAChR with SCOP prevented this effect but did not completely abolish sympathoexcitation generated by PPT activation. Electrical stimulation of the PPT increases AP, HR and renal SNA (with a lesser increase in lumbar SNA) in decerebrate animals *(Chong and Bedford, 1997; Koba et al., 2006)*. Sympathoexcitatory responses are also evoked from surrounding brain areas including the cuneiform nucleus *(Verberne,*

1995). At present we cannot explain the lack of effect of stimulating the PPT on other reflex responses that are modified by activation of RVLM mAChR.

Disinhibition of the PPT increased EMG activity, consistent with studies that reported increases in muscle activity following electrical or chemical stimulation of the PPT in anaesthetised or decerebrate animals *(Chong and Bedford, 1997; Pahapill and Lozano, 2000; Koba et al., 2006)*. Single cholinergic neurons in the PPT have dual connections with the motor cortex and stellate ganglion, as revealed by polysynaptic viral tracing*(Krout et al., 2003)*. The PPT may therefore be a key nodal point where changes in motor signals can be coordinated with descending modulation of sympathetic function. The simplest explanation of our data is that stimulation of the PPT evokes muscular activity and releases acetylcholine activating RVLM mAChR pre and/or postsynaptically located on sympathoexcitatory neurons causing an increase in AP and SNA as well as increasing the range and gain of the sympathetic baroreflex.

Functional Implications

The involvement of the PPT in initiating and modulating movement related to arousal and locomotion, including exercise, is well recognised *(Bedford et al., 1992; Pahapill and Lozano, 2000; Garcia-Rill et al., 2004)*. The present findings indicate that the cholinergic projection to the RVLM may be activated in parallel to elicit tonic and reflex cardiovascular adjustments that are appropriate to different behaviours. The pattern of effects bears a striking similarity to those evoked by central command during exercise *(Rowell and O'Leary, 1990; Raven et al., 2002; Williamson et al., 2006)*.

Exercise is accompanied by a resetting of baroreflex control of SNA and HR to higher AP *(Kamiya et al., 2001; Raven et al., 2002; Miki et al., 2003; Williamson et al., 2006)*. This is thought to be crucial to AP elevation at exercise onset and AP stabilization during exercise and can oppose other reflex influences on circulation, including nociceptive and peripheral chemoreflexes *(Rowell and O'Leary, 1990)*. In addition to an increase in AP and SNA, the increase in the range and gain of the sympathetic baroreflex as seen here strongly resembles that evoked during treadmill exercise in conscious rats *(Miki et al., 2003)*. Studies showing complete sympathetic baroreflex function curves during exercise in humans are sparse, although some studies have demonstrated large increases in linear baroreflex gain of muscle SNA during static exercise *(Kamiya et al., 2001)* or no change

during moderate intensity arm cycling *(Fadel et al., 2001)*. In contrast, exercise appears to reset the cardiac component of the baroreflex to higher AP without changing its gain *(Raven et al., 2002)*, also resembling effects on the HR baroreflex evoked by central administration of physostigmine *(Caputi et al., 1980)*. Recent evidence indicates that the cardiac baroreflex is transiently inhibited at exercise onset, which may facilitate immediate vagal withdrawal *(Matsukawa et al., 2006)*.

In conclusion, our data indicate that the cholinergic projection from the PPT to the RVLM is an integral component of the central command pathway that regulates circulatory function during exercise, and possibly other arousal or behavioural states.

Chapter 4 Cardiovascular Autonomic Function in Anaesthetised FRL and FSL Rats

I. Abstract

AChR are important in premotor and efferent control of autonomic function; however, the extent to which cardiovascular function is affected by genetic variations in AChR sensitivity is unknown. We assessed HRV and BRS in rats bred for resistance (FRL) or sensitivity (FSL) to cholinergic agents compared to SD rats, confirmed using hypothermic responses evoked by the muscarinic agonist OXO ($n \geq 9$ / group). AP, ECG, SNA and PNA were acquired under urethane anaesthesia. HRV was assessed in time and frequency domains from short term R-R interval data and spontaneous heart rate BRS was obtained using a sequence method at rest and after mATR (2 mg/kg iv). HR and SNA baroreflex gains were assessed using conventional pharmacological methods. FRL and FSL were normotensive but displayed elevated heart rates, reduced HRV and HF power and spontaneous BRS compared to SD rats. In FRL and FSL rats, mATR had no effect on these parameters, indicating a reduction in cardiovagal tone. FSL rats exhibited reduced PNA frequency, longer baroreflex latency and reduced baroreflex gain of HR and SNA compared to FRL and SD rats, indicating dual impairment of cardiac and circulatory baroreflexes in FSL rats. These findings indicate that AChR resistance results in cardiovagal insufficiency, presumably as a result of reduced cardiac mAChR function. In contrast, AChR sensitivity results in autonomic and respiratory abnormalities arising from alterations in central mAChR and or other neurotransmitter receptors.

II. Introduction

Baroreflex and respiratory modulation of HR and AP are important homeostatic mechanisms and can be severely impaired in cardiac and non-cardiac disease *(Kleiger et al., 1987; Grassi et al., 1995; La Rovere et al., 1998; La Rovere et al., 2001; Laude et al., 2004)*. In the human population interindividual differences in responses to drugs that influence cardiac autonomic function have been shown to have an inherited basis *(Kirstein and Insel, 2004)*. These differences are likely to be polygenic and may significantly influence susceptibility to cardiac disease *(Kirstein and Insel, 2004)*. Loss of function of ganglionic or smooth muscle AChR results in profound impairment of cardiac autonomic function *(Fisher and White, 2004)*. However, the importance of smaller genetic variations in AChR function is not known.

AChR exist as ligand-gated ion channels (nAChR) or G-protein coupled receptors (mAChR) and are expressed as subtypes differing in subunit composition or G-protein signalling, respectively (for review *(Caulfield and Birdsall, 1998)*). AChR subtypes are widely distributed throughout the autonomic nervous system and contribute differentially to control of sympathetic and vagal outflow. With respect to cardiac autonomic control, nicotinic α7 subunits mediate fast synaptic transmission in ganglia supplying the heart and muscarinic M2 receptors in the sinoatrial node are the target of vagal stimulation *(Fisher and White, 2004; Kirstein and Insel, 2004)*. In the central nervous system nAChR modulate cardiovagal premotor activity via baroreflex- and respiratory-related inputs to the NA *(Neff et al., 1998b; Neff et al., 2003; Wang et al., 2003)*. Cholinergic mechanisms (both nicotinic and muscarinic) play a significant role in control of sympathetic vasomotor tone mediated at both central and peripheral sites *(Giuliano et al., 1989; Arneric et al., 1990; Kubo, 1998; Sartori et al., 2005)*.

FSL and FRL rat lines were bred for differential sensitivity to the hypothermic effects of cholinesterase inhibition from SD rats *(Overstreet, 1986)*. FSL rats are more sensitive to the behavioural and physiological effects of muscarinic agonists, whereas responses are attenuated in FRL compared to SD rats *(Overstreet, 1986; Daws and Overstreet, 1999; Overstreet et al., 2005)*. FRL and FSL rat also exhibit differential binding of mAChR ligands in striatum and hippocampus with some evidence for subtype-specific alterations *(Overstreet, 1986; Daws and Overstreet, 1999)*. FRL are otherwise genetically similar to SD *(Overstreet et al., 1992b)*, thus either the resistant line or outbred SD has been considered an appropriate control for FSL. Muscarinic sensitivity develops early postnatally in FSL *(Daws and Overstreet, 1999)* and is likely to be polygenic *(Overstreet et al., 1992b)*. This results in increased sensitivity to nicotine *(Tizabi et al., 1999; Tizabi et al., 2000)*, dopaminergic agonists *(Yadid et al., 2000)* and 5-HT1A receptor agonists *(Overstreet et al., 1998)*; occurring via functional interactions with mAChR or from changes in G-protein signalling common to specific neurotransmitter receptors *(Overstreet et al., 1998)*. At present there is no data demonstrating functional or genetic differences in AChR in cardiovascular brain regions, ganglia or target organs in FRL or FSL rats.

In light of these inherited differences in AChR sensitivity, we hypothesised that vagal and sympathetic control of cardiovascular function would be altered in FRL and FSL compared to SD. In order to test this we used analysis of HR, HRV and BRS in response to endogenous or induced changes in blood pressure under anaesthesia. Analysis of HRV and

BRS is used extensively to examine cardiovascular autonomic function in normal subjects and in patients with cardiac and non-cardiac disease *(Kleiger et al., 1987; Grassi et al., 1995; La Rovere et al., 1998; La Rovere et al., 2001; Lombardi, 2002; Laude et al., 2004)*.

III. Methods

Anaesthesia, Surgical Procedures and Recording

SD (n = 10), FRL (n = 11) and FSL rats (n = 9) and 4 wk old FRL (n = 3) and FSL rats (n = 3) were used in this study. Adult animals were anaesthetised with urethane and instrumented for recording of AP, ECG, SNA and PNA as described in Chapter 2. Animals were allowed to freely breathe room air mixed with 100 % 0_2 delivered through a nose cone placed close to the animal. Juvenile FRL and FSL rats were anaesthetised as above and instrumented for recording of AP and respiratory EMG activity as described in Chapter 2.

Experimental Protocol

Cardiorespiratory parameters were acquired at rest for 30 – 60 mins. Baroreflexes were activated using injection of SNP and PE as described in Chapter 2. After a period of recovery (~ 10 min), a subset of rats ($n \geq 5$ / group) was administered mATR and cardiorespiratory parameters were monitored for a further 10 mins. Young FRL and FSL rats were administered mATR (2 mg / kg), atenolol (1 mg / kg) and prazosin (1 mg / kg), with at least 15 min separating each drug and the order of administration of the first two drugs switched in different animals. Resting cardiorespiratory parameters were calculated on three 5 minute segments of data per animal, between 3 and 4 hours after anaesthesia induction.

Heart Rate Variability (HRV)

HRV was assessed in both time and frequency domains as described in Chapter 2 before and after mATR. Overall spectral power was divided into three frequency ranges; VLF (≤0.2 Hz), LF (0.2-1 Hz) and HF (1-3 Hz) and recorded as absolute values or in normalized units as a proportion of combined LF and HF power (excluding VLF component). For each animal, VLF, LF and HF power from the three separate 5 minute spectra were averaged.

Sympathetic and Heart Rate Baroreflex Function

Spontaneous heart rate BRS was calculated using the sequence method (see Chapter 2 and Appendix 1). Separate values of mean BRS were recorded for lengthening (bradycardia) and shortening (tachycardia) interval sequences and only when at least 3 sequences per 5 minute segment were present. BRS was recorded before and after mATR.

SNA baroreflex function curves and HR-MAP regression lines were generated as described in Chapter 2. For HR, separate values for BRS (SNP) and BRS (PE) were recorded for each animal. For SNA, the first derivative of the logistic function was used to calculate maximal gain (G_{max}; gain at MAP_{50}), and gain at resting MAP (G_{MAP}).

Statistical Analysis

All data are presented as individual data points or mean ± standard error. Data were analysed using one-way analysis of variance (ANOVA) and a *post-hoc* test for significance performed with Bonferroni's correction, an unpaired *t*-test on individual means or a paired *t*-test to compare effects of mATR.

IV. Results

Sensitivity to Oxotremorine-induced Hypothermia

Administration of OXO (0.2 mg / kg i.p.) following mATR (2 mg / kg i.p.) produced a fall in rectal temperature in FSL rats (- 2.5 ± 0.1 ºC, n = 9) that was significantly greater ($p < 0.001$) and non-overlapping compared with FRL (- 0.7 ± 0.1 ºC, n = 11) and SD rats (- 0.6 ± 0.2 ºC, n = 10). Changes in rectal temperature in FRL rats compared with SD rats were not significantly different. Juvenile FSL rats exhibited larger OXO-evoked falls in temperature (3.4 ± 0.2 ºC, n = 3) compared to age-matched FRL rats (1.2 ± 0.1 ºC, n = 3).

Resting Cardiovascular Parameters

MAP was similar in SD, FRL and FSL rats (Table 4.1). In contrast, resting HR was significantly elevated ($p < 0.01$) in FRL and FSL rats compared with SD rats (Table 4.1). Mean heart rate in SD rats exhibited significantly greater variance ($p < 0.001$) compared with FRL and FSL rats (Table 4.1, Fig 4.1C). In the presence of mATR (2 mg / kg) there

was no significant change in MAP, HR or PNA frequency in FRL and FSL rats. MATR had a significant effect ($p < 0.01$) on heart rate in SD rats producing a sustained tachycardia (Δ 95 ± 12 bpm). In the presence of mATR, MAP and HR were similar between SD, FRL and FSL rats (Table 4.1).

Resting Respiratory Parameters

The frequency of phrenic nerve discharge was significantly reduced in FSL rats compared with FRL ($p < 0.01$) and was not different between FRL and SD rats (Table 4.1). In the presence of mATR, respiratory frequency was unchanged in all groups and remained significantly lower in FSL compared to FRL ($p < 0.05$) and SD rats ($p < 0.01$) (Table 4.1).

HRV

Time Domain Analysis

HRV in the time domain (SDNN) was markedly reduced in FRL and FSL rats compared with SD rats ($p < 0.01$) (Table 2, Figure 4.1A). SDNN in SD showed greater variance ($p < 0.001$) compared with FRL and FSL rats. In the presence of mATR (2 mg / kg), SDNN was unchanged in FSL and FRL rats but significantly reduced in SD rats ($p < 0.01$). In the presence of mATR SDNN was similar in all three groups (Table 4.2).

Frequency Domain Analysis

Spectral analysis of HRV showed distinct VLF, LF and HF components in SD rats with central frequencies around 0.1, 0.6 and 2 Hz, respectively (Figure 4.1B). HF was synchronous with mean phrenic nerve frequency during the 5 minute segment, consistent with work showing coupling of the HF band and respiratory sinus arrhythmia *(Pomeranz et al., 1985; Medigue et al., 2001)*. HRV spectra from FRL and FSL rats showed a reduction in spectral power over all frequencies (Figure 4.1B). Total spectral power, LF and HF power were significantly reduced ($p < 0.01$) in FSL and FRL rats compared with SD rats (Table 4.2). Normalized LF power was also reduced, whereas normalized HF power was increased in FSL and FRL rats compared with SD rats (Table 4.2). HF predominance was also evident as a reduction in LF / HF ratio in FSL and FRL rats compared with SD rats (Table 4.2).

Table 1. *Resting cardiorespiratory parameters in Sprague Dawley (SD), Flinders Resistant (FRL) and Sensitive Line rats (FSL) at rest under urethane anaesthesia (n ⩾ 6 / group)*

		Resting	*Methylatropine (2 mg / kg)*
MAP (mmHg)	*SD*	102 ± 4	96 ± 4
	FRL	113 ± 4	105 ± 4
	FSL	105 ± 4	106 ± 6
Heart rate (bpm)	*SD*	335 ± 17	432 ± 14 $^{\#}$
	FRL	459 ± 4 **	459 ± 12
	FSL	451 ± 16 **	446 ± 19
PNA frequency (Hz)	*SD*	2.1 ± 0.1	2.2 ± 0.1
	FRL	2.2 ± 0.1	2.1 ± 0.4
	FSL	1.7 ± 0.1 ††	1.6 ± 0.1 $^{** \dagger}$

Values are mean ± SE. See Methods for calculation. Abbreviations: MAP, mean arterial pressure; PNA, phrenic nerve activity. ** $p < 0.01$, * $p < 0.05$ (vs. SD); †† $p < 0.01$, † $p < 0.05$ (vs. FRL); $^{\#}$ $p < 0.01$ (significant effect of methylatropine).

Table 2. *Time and frequency domain analysis of heart rate variability in Sprague Dawley (SD), Flinders Sensitive (FSL) and Resistant Line rats (FRL) under urethane anaesthesia (n ⩾5 group)*

	SD	*FRL*	*FSL*
5-min resting			
SDNN (ms)	2.19 ± 0.31	0.50 ± 0.04 **	0.48 ± 0.03 **
Total power (ms^2)	5.05 ± 1.33	0.07 ± 0.01 **	0.10 ± 0.01 **
VLF (ms^2)	0.95 ± 0.20	0.01 ± 0.002 **	0.02 ± 0.005 **
LF (ms^2)	0.90 ± 0.20	0.01 ± 0.001 **	0.01 ± 0.001 **
HF (ms^2)	3.57 ± 0.92	0.05 ± 0.01 **	0.08 ± 0.01 **
LF / HF	0.34 ± 0.06	0.14 ± 0.02 **	0.14 ± 0.04 **
LF (nu)	25 ± 3	12 ± 2 **	11 ± 3 **
HF (nu)	75 ± 3	88 ± 2 **	89 ± 3 **
5-min mATR (2 mg/kg)			
SDNN (ms)	0.65 ± 0.20 $^{\#}$	0.41 ± 0.07	0.69 ± 0.16

Values are mean ± SE. See Methods for calculation. Abbreviations: nu, normalized units. ** $p < 0.01$ (vs. SD); $^{\#}$ $p < 0.01$ (significant effect of methylatropine).

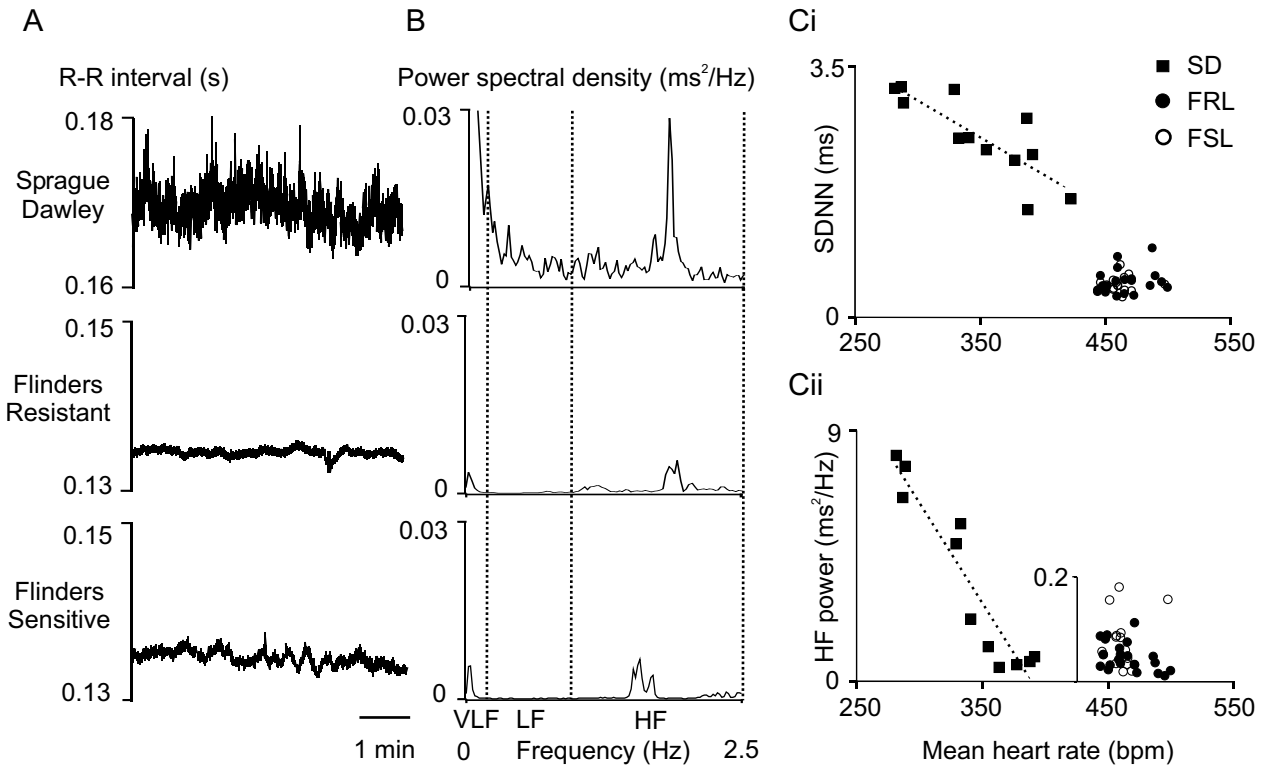

Figure 4.1. *Time and frequency domain analysis of heart rate variability and the relationship with mean heart rate in SD, FRL and FSL under urethane anaesthesia.* Representative R-R interval time series (A) and power spectra (B) show that in FRL and FSL fluctuations of R-R interval around the mean were markedly reduced as was total power within the frequency range 0 to 2.5 Hz, low frequency power (LF, 0.2 to 1 Hz) and high frequency power (HF, 1 Hz to 3 Hz) compared with SD. Linear regression (dashed lines) of data from SD (filled squares) indicates that heart rate was inversely correlated with SDNN (Ci) and HF power (Cii). In contrast, SDNN (Ci) and HF power (Cii) were consistently clustered at high mean heart rate in FRL (filled circles) and FSL (open circles).

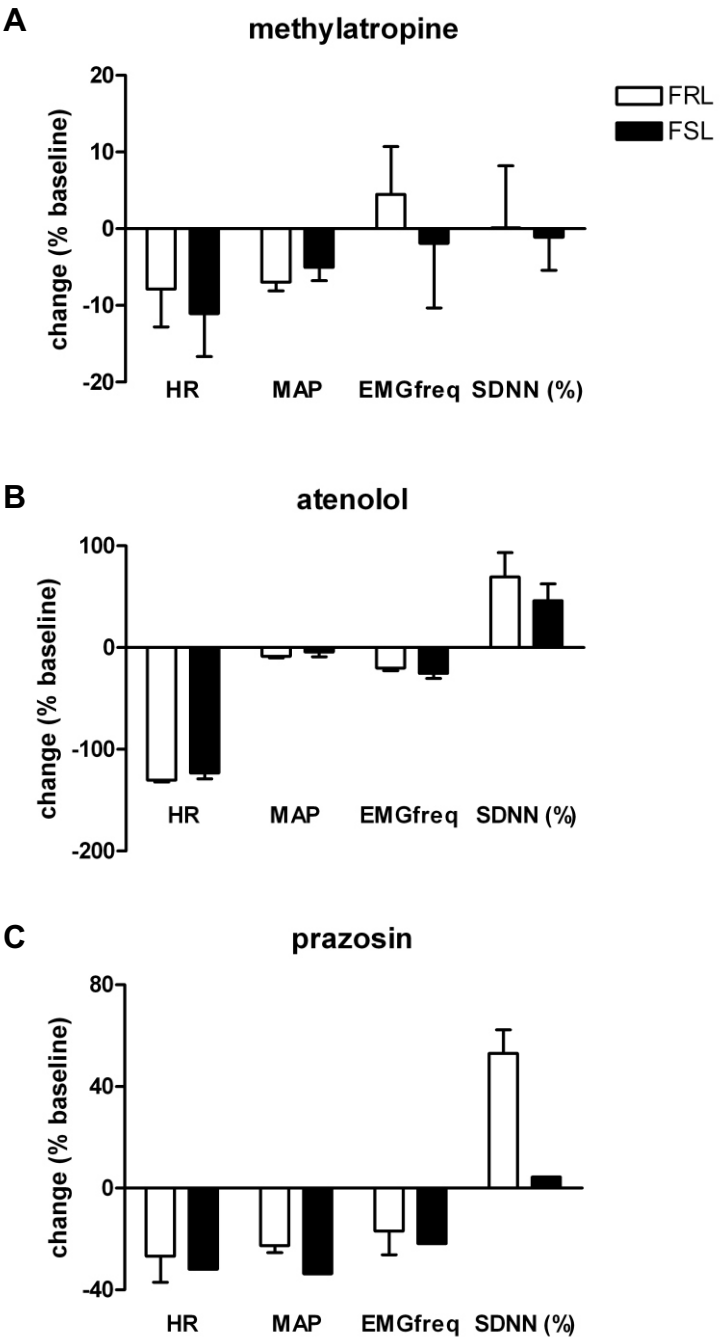

Figure 4.2 *Cardiorespiratory responses to sequential autonomic blockade in urethane-anaesthetised 4 wk old FRL and FSL rats.* A: Methylatropine (2 mg/kg iv) did not significantly alter cardiorespiratory parameters in either FRL (n=3) or FSL rats (n=3). B: Atenolol (1 mg/kg iv) evoked a large reduction in HR, an increase in HRV (SDNN) and small reduction in respiratory frequency; these effects did not differ in FRL (n=3) and FSL rats (n=3). C: Prazosin (1mg/kg iv) evoked a reduction in MAP, HR and respiratory frequency in FRL (n=3)and FSL rats (n=2); the reduction in MAP appeared to be larger in FSL rats. Prazosin evoked a much larger increase in HRV in FRL compared to FSL rats. Data are mean ± SEM.

Heart Rate-Dependency of HRV Parameters

In SD rats there was a significant inverse correlation between mean HR and SDNN ($p < 0.01$, Figure 4.1Ci), HF power ($p < 0.01$, Figure 4.1Cii) and LF power ($p < 0.01$, data not shown) and a non-significant positive correlation between mean heart rate and LF / HF ratio (data not shown). HRV parameters were clustered at high mean heart rates in FRL and FSL rats and there was no correlation with heart rates in these animals (Figure 4.1Ci, ii). In all three groups high mean HR was associated with low SDNN and reduced LF and HF power.

Comparison with Autonomic Outflow in Young FRL and FSL Rats

In order to determine whether or not there are differences in cardiac or vascular sympathetic outflow between FRL or FSL rats early in development, the effect of sequential autonomic blockade was examined in 4 wk old rats. MATR had little effect on MAP, HR, respiratory frequency or SDNN in either FRL or FSL rats (Figure 4.2A). Atenolol caused large reductions in HR, no change in MAP and increases in SDNN in both FRL and FSL rats (Figure 4.2B). Prazosin was successfully administered in two FSL and three FRL rats. Prazosin caused larger falls in MAP in FSL rats but similar reductions in HR in both FRL and FSL rats; whereas in FRL rats, prazosin caused a much larger increase in SDNN compared to FSL rats (Figure 4.2C).

Spontaneous Heart Rate BRS

Spontaneous BRS for lengthening and shortening interval sequences combined was significantly reduced ($p < 0.01$) in FRL (0.41 ± 0.04 ms / mmHg) and FSL rats (0.17 ± 0.02 ms / mmHg) compared to SD rats (1.52 ± 0.19 ms / mmHg). In SD mean HR was inversely correlated with spontaneous BRS for both lengthening and shortening interval sequences ($p < 0.01$, Figure 4.3A). Spontaneous BRS was clustered at high mean heart rates in FRL and FSL rats; however, BRS was significantly reduced ($p < 0.01$) in FSL compared to FRL rats (Figure 4.3A). Administration of mATR significantly reduced ($p < 0.05$) spontaneous BRS in SD but not in FRL or FSL rats (Figure 4.3B). In the presence of mATR spontaneous BRS of lengthening interval sequences was compared between groups and found to be significantly reduced ($p < 0.05$) in FSL rats (0.16 ± 0.05 ms / mmHg)

compared to FRL (0.62 ± 0.19 ms / mmHg) and SD rats (41 ± 0.10 ms / mmHg) (Figure 3B).

Baroreflex Sensitivity Derived from Ramp Changes in AP

Ramp decreases and increases in MAP and corresponding reflex changes in HR and SNA produced by intravenous injection of SNP or PE (10 μg / kg) are illustrated in Figure 4.4A. SNP evoked very similar reductions in MAP in all groups (SD, 43 ± 3 mmHg; FRL, 38 ± 2 mmHg; FSL, 41 ± 2 mmHg; n ≥ 8 / group). Similarly, increases in MAP evoked by PE were not significantly different between groups (SD, 50 ± 3 mmHg; FRL, 46 ± 2 mmHg; FSL, PE, 54 ± 3 mmHg; n ≥ 8 / group).

Heart Rate Baroreflex Latency

The time delay to peak change in HR following peak change in MAP evoked by SNP or PE was significantly increased in FSL rats (SNP; 24 ± 4 s, PE; 2.6 ± 0.3 s) compared to FRL (SNP; 11 ± 2 s, PE; 1.0 ± 0.4 s) and SD rats (SNP; 5 ± 1 s, PE; 0.7 ± 0.2 s) ($p < 0.05$).

Heart Rate BRS

Heart rate baroreflex gain, assessed as the slope of R-R interval and MAP following SNP or PE, was reduced in FSL rats (SNP 0.14 ± 0.03; PE; 0.42 ± 0.10 ms / mmHg) compared to FRL (SNP 0.36 ± 0.09; PE 0.69 ± 0.08 ms / mmHg) and SD rats (SNP 0.49 ± 0.10; PE 0.80 ± 0.17 ms / mmHg); however, reduced gain in FSL only reached significance compared to SD ($p < 0.05$, n = 3 / group) (Figure 4.4C).

Splanchnic Sympathetic Baroreflex Sensitivity

The range and mid-point of average baroreflex function curves for SNA were not significantly different between SD, FRL or FSL rats (Figure 4.4B, n ≥ 6 / group). Resting MAP was close to threshold (MAP_{50}) in all groups. However, G_{MAP} was reduced in FSL rats (2.27 ± 0.15 % nu / mmHg) compared to FRL rats (3.21 ± 0.51 % nu / mmHg) and significantly reduced ($p < 0.05$) compared to SD rats (3.98 ± 0.36 % nu / mmHg). G_{max} was significantly reduced ($p < 0.05$) in FSL rats (2.54 ± 0.10 % nu / mmHg) compared to both SD (4.59 ± 0.45 % nu / mmHg) and FRL rats (4.04 ± 0.45 % nu / mmHg) (Figure 4.4C).

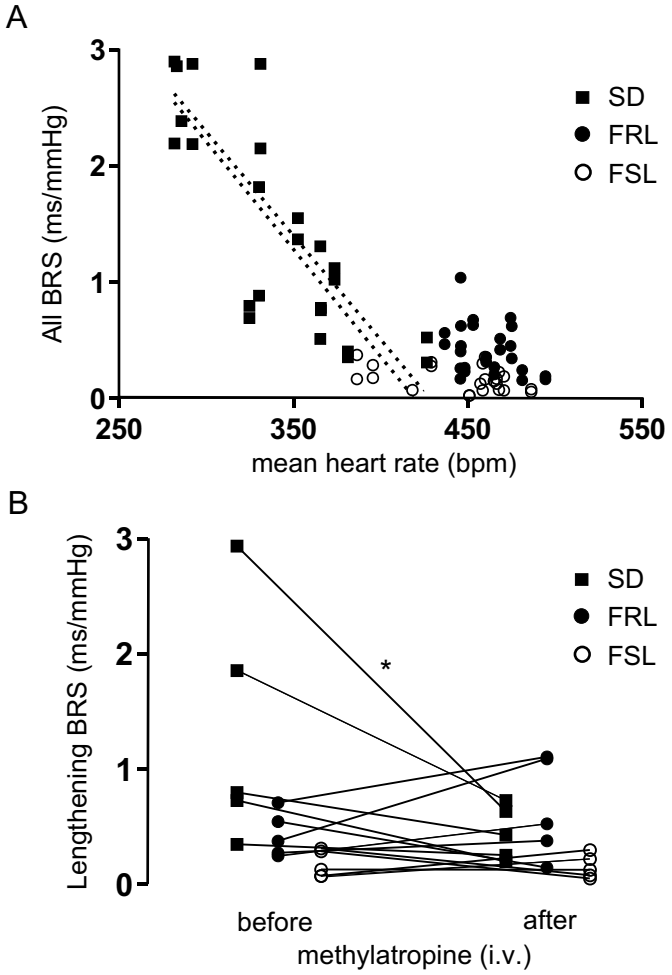

Figure 4.3. *Spontaneous baroreflex sensitivity measured using the sequence method and its relationship with mean heart rate in SD, FRL and FSL under anaesthesia (n = 8 / group).* Linear regression (dashed lines) of data from SD (filed squares) shows that heart rate was inversely correlated with the slope of lengthening and shortening sequences (A). The slope of lengthening and shortening sequences was reduced in FRL (filled circles) and FSL (open circles), and despite comparably high heart rates values for baroreflex sensitivity were reduced in FSL compared with FRL (A). The slope of lengthening sequences detected using the sequence method was significantly reduced (* $p < 0.05$) after treatment with methylatropine (2 mg / kg i.v.) in SD (filled squares) whereas it had little effect on the low values for slope obtained in FSL (open circles) (B). After methylatropine administration the slope of lengthening sequences was reduced in FSL compared with FRL (filled circles) and SD whereas slope was similar in FRL and SD (B).

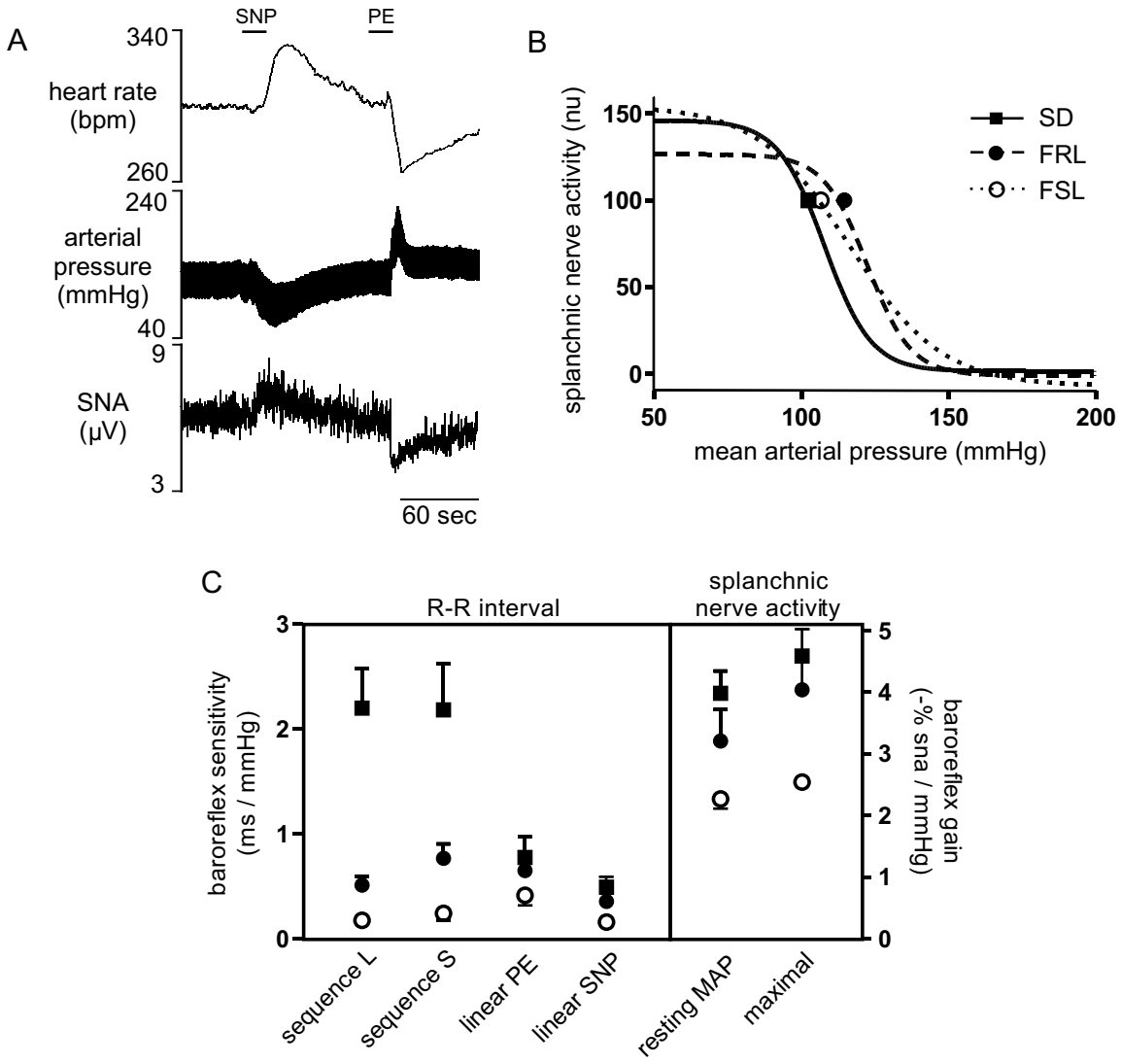

Figure 4.4. Changes in heart rate and splanchnic nerve activity (SNA) evoked by sequential administration of sodium nitroprusside (SNP) and phenylephrine (PE) (i.v.) are illustrated in a representative trace from an SD rat (A). Splanchnic logistic function curves in SD (solid line, filled square), FRL (dashed line, filled circle) and FSL (dotted line, open circle) (n = 6 / group) were in general similar, although gain was selectively reduced in FSL (B). Heart rate baroreflex sensitivity was reduced in FSL compared with FRL ($p < 0.05$) and SD ($p < 0.01$) using the slope of lengthening (sequence L) or shortening intervals (sequence S) or gain of R-R interval responses to ramp increases (linear PE) or decreases (linear SNP) in arterial pressure ($p < 0.05$ vs. SD) (C). Resting (ie. at mean arterial pressure (MAP)) and maximal splanchnic nerve baroreflex gain was also selectively reduced in FSL compared with FRL and SD ($p < 0.05$) (C).

Comparison of Baroreflex Sensitivity Measurements

FRL and FSL rats showed a reduction in spontaneous BRS compared to SD rats (Figure 4.3A, 4.4C); however, spontaneous BRS was significantly reduced in FSL compared to FRL also (Figure 4.3A, 4.4C). Considering the rate-dependency of spontaneous BRS (Figure 4.3A), higher mean HR was not a factor skewing BRS to lower values in FSL versus FRL rats. HR baroreflex gain following ramp changes in pressure was significantly reduced in FSL compared to SD rats (Figure 4.4C) and SNA baroreflex gain obtained using similar methods was significantly reduced in FSL rats compared to both FRL and SD rats (Figure 4.4C). There was general agreement in values of HR BRS obtained using lengthening or shortening interval sequences or using pharmacological methods. A notable exception was that in three SD spontaneous BRS was greater than BRS obtained using ramp changes in MAP (Figure 4.4C).

V. Discussion

We show that in anaesthetised FRL and FSL rats normal AP is maintained but cardiovagal tone and spontaneous baroreflex control of HR are diminished. Additionally in adult FSL rats, baroreflex control of sympathetic activity and respiratory frequency is reduced compared to FRL and SD rats. These findings indicate that selective breeding for reduced or increased AChR sensitivity results in specific cardiorespiratory deficits. FRL rats have reduced muscarinic sensitivity and may exhibit a reduction in functional cardiac mAChR required for vagal modulation of sinus rhythm *(Fisher and White, 2004)*. In contrast, FSL rats show a number of central changes in ACh (nicotinic and muscarinic) and aminergic receptors *(Yadid et al., 2000; Overstreet et al., 2005)* that accompany increased muscarinic sensitivity and these may be linked to the vagal, baroreflex and respiratory abnormalities described. In addition, similar impairments of autonomic control are present in young rats that also differ in hypothermic muscarinic sensitivity.

In the present work we characterized HRV and BRS (both spontaneous and pharmacological gains) in SD rats compared to FRL and FSL rats under anaesthesia. These methods predominantly reflect reflex vagal and sympathetic modulation of sinus rhythm, and where applicable AP, but do not directly reflect levels of autonomic tone. Reduced HRV and BRS are powerful predictive markers of prognosis and cardiac mortality in clinical settings *(La Rovere et al., 1998; La Rovere et al., 2001)* and have been interpreted

as indicators of sympathovagal balance as it pertains to cardiac autonomic modulation *(Pagani et al., 1986; Lombardi, 2002)*.

Cardiac vagal activity was reduced in adult FRL and FSL rats compared to SD rats, indicated by reduced HRV in the time domain and reduced HF power. HF oscillations in heart rate originate from vagal modulation as they are synchronous with vagally-mediated respiratory sinus arrhythmia and are abolished after atropine *(Pomeranz et al., 1985; Fouad, 1994)*. Cardiac vagal tone was markedly diminished in both lines, indicated by elevated resting heart rates unresponsive to mATR. Under these conditions it is likely that sympathetic modulation of HR predominates and risk of ventricular arrhythmia is increased *(Pagani et al., 1986; Hull et al., 1990; Lombardi, 2002)*. In juvenile FRL and FSL rats we also found that heart rates were unresponsive to mATR and blockade of beta-adrenoceptors using atenolol evoked a large reduction in HR that was similar in the two strains.

The reduction in vagal activity was the clearest difference between FRL rats and their parent strain SD. Vagal efferent modulation of HR is mediated almost entirely by M2 receptors in the sinoatrial node *(Fisher and White, 2004)*. It is likely that a reduction in functional cardiac M2 receptors accounts for reduced vagal activity in FRL rats compared to SD rats, particularly since they are otherwise genetically and phenotypically similar *(Overstreet et al., 1992b; Yadid et al., 2000; Overstreet et al., 2005)*. Furthermore, apart from their resistance to mAChR agonists, multiple chemical sensitivities are unaltered in FRL rats *(Overstreet et al., 1992b; Yadid et al., 2000; Overstreet et al., 2005)*. Opposite effects on vagal modulation of HR were not seen in FSL rats, suggesting that cardiac M2 receptors in this strain are not more sensitive to vagal stimulation. Peripheral muscarinic sensitivity is evident in FSL rats in some tissues; for example, methacholine-induced intestinal and bronchial constriction were enhanced in FSL compared to FRL rats *(Djuric et al., 1995; Djuric et al., 1998)*. Since M3 receptors predominantly mediate the contractile response in these tissues *(Matsui et al., 2002)* FSL rats may show enhanced M3 but not M2 receptor-mediated effects in the periphery. Subtype-selective differences in muscarinic sensitivity in FSL rats have also been observed in striatum, where M1 but not M2 receptor binding was found to be elevated *(Daws and Overstreet, 1999)*.

The diminution of vagal activity seen in FSL rats may result from changes in central pathways regulating vagal premotor output. This could also potentially mask any change in

muscarinic sensitivity at the level of the heart. Furthermore, it is possible that mAChR are not involved as FSL rats exhibit increased nicotinic *(Tizabi et al., 1999; Tizabi et al., 2000)* and 5-HT1A receptor sensitivities *(Wallis et al., 1988; Overstreet et al., 1998)* that could contribute to vagal inhibition. For example, nicotinic α4β2 subunits *(Neff et al., 2003)* and 5-HT1A receptors *(Skinner et al., 2002)* strongly modulate the tonic and reflex inhibition of CVPN in the NA. Nicotinic α4β2 subunit binding is increased in brains of FSL rats *(Tizabi et al., 1999)* and chronic nicotine exposure fails to evoke receptor desensitization in FSL compared to FRL rats *(Tizabi et al., 2000)*. However, the precise mechanisms underlying reduced vagal activity in FSL rats remain to be elucidated.

FSL rats exhibited a significantly slower rate of phrenic nerve discharge, indicating a reduction in central respiratory drive compared to FRL and SD rats. Although blood-gas analysis was not performed phrenic activity exhibited a typical augmenting pattern in all cases indicating normocapnic conditions. M1 and M3 receptors are important in neural control of breathing where they strongly modulate activity of ventral medullary cell groups controlling respiratory rhythmogenesis *(Nattie and Li, 1990; Shao and Feldman, 2000)*. This may indicate abnormal rhythmogenic control of breathing by mAChR in FSL rats. Respiratory patterns also influence cardiovagal activity; however, whether or not reduced respiratory frequency in FSL rats contributes to diminished cardiac vagal nerve traffic is unclear *(Pomeranz et al., 1985; TaskForce, 1996)*.

Normal AP appeared to be maintained in FRL and FSL rats compared to SD rats under anaesthesia, indicating an absence of cholinergic tone in AP regulation. Descending cholinergic input to the VLM may influence long term levels of blood pressure as local mAChR activation evokes sustained increased in sympathetic vasomotor activity *(Giuliano et al., 1989)*. This pathway does not appear to be tonically active under normotensive conditions *(Willette et al., 1984; Giuliano et al., 1989)* but it is strongly activated in animals with spontaneous *(Kubo et al., 1995b)* or deoxycorticosterone acetate-salt hypertension *(Kubo et al., 1996)*. Our findings indicate that increased AChR sensitivity alone is not sufficient to produce hypertension in FSL rats, at least at the ages tested. However, since sympathetic tone was not directly assessed it is possible that compensatory mechanisms (renal or neurohumoral) act to maintain normal blood pressure. Of note is that blockade of alpha-adrenoceptors in juvenile FSL rats produced a larger fall in MAP compared to FRL rats, suggesting that peripheral vascular sympathetic activity may be enhanced in FSL rats at least at this young age.

Baroreflex control of HR and AP were markedly and differentially affected in FRL and FSL rats. Diminished cardiovagal activity in both lines is likely to account for the observed reduction in spontaneous (HR) BRS compared to SD rats, as in the latter group BRS was sensitive to mATR and was correlated with mean HR. Following ramp changes in AP, FSL rats alone showed reduced HR baroreflex gain and longer latency to peak changes in HR. Sympathetic and vagal activities contribute relatively equally to HR gain under these latter conditions *(Head and McCarty, 1987)*, suggesting that FSL rats show a disturbed sympathetic component. This was also apparent as a selective reduction in the gain of splanchnic SNA following baroreflex activation in FSL rats compared to FRL and SD rats. Furthermore, SNP and PE elicited comparable blood pressure changes in SD, FRL and FSL rats indicating no differences in vascular α-adrenoreceptor sensitivity. Since responses to peripheral β-adrenergic agonists are also similar in FRL and FSL rats (above and *(Yadid et al., 2000)*) the sympathetic effects seen in FSL rats appear to be generated centrally. Reduced sympathetic baroreflex gain may result from changes in AChR, 5-HT1A or other aminergic receptors involved in the central integration and modulation of the baroreflex *(Pilowsky and Goodchild, 2002)*. For example, baroreflex activation evokes release of ACh in the rat RVLM *(Kubo et al., 1998d)*. Muscarinic M2 and 5-HT1A receptors also strongly modulate activity of presympathetic neurons in this region *(Huangfu et al., 1997; Miyawaki et al., 2001)*.

Anaesthesia is an important consideration in this study; firstly, since urethane anaesthesia affects cardiorespiratory function in general and respiratory sinus arrhythmia in particular *(Bouairi et al., 2004)*. Furthermore, FRL and FSL rats may be more or less sensitive to the cardiovascular effects of anaesthesia. Confirmation of the present observations will require similar studies in conscious animals. An advantage of the use of anaesthesia here is to enable comparison of autonomic regulation in the absence of locomotor activity, higher order inputs and stress reactivity that are known to differ between FRL and FSL rats *(Ayensu et al., 1995; Yadid et al., 2000; Overstreet, 2002)*.

In conclusion, the present study shows that autonomic control of the heart and circulation is impaired in rats differing in AChR sensitivity. FRL rats may exhibit a functional reduction in cardiac mAChR resulting in reduced vagal control of HR. Given that FRL are otherwise genetically and phenotypically similar to their parent strain SD, FRL rats may provide a novel model of innate vagal insufficiency. Furthermore, this indicates that care

should be taken in future studies using FRL as a control for FSL. In contrast, FSL rats show a number of central changes in ACh (nicotinic and muscarinic) and aminergic receptors that may be linked to concomitant alteration of vagal, sympathetic baroreflex and respiratory functions observed here. FRL and FSL may have an increased susceptibility to arrhythmia and myocardial damage and may provide a model for investigating an inherited basis of increased cardiac risk. FRL and FSL may be important also for evaluating the cardio-protective or -toxic effects of agents that differentially influence cardiac vagal and sympathetic outflow.

Chapter 5 Muscarinic Influences on Autonomic Function and Respiration in FSL Rats

I. Abstract

FSL rats selectively bred for exaggerated cholinergic hypothermic responses also exhibit cardiovascular abnormalities. Here, we quantified expression levels of M1 – M5 mAChR subtypes in the ventral medulla, cerebellum and spinal cord in FSL rats compared to FRL and SD rats. We also determined autonomic responses to central mAChR activation with OXO (0.2 mg/kg) in conscious animals using radiotelemetry to measure AP, HR and temperature, or under urethane anaesthesia to measure sympathetic and phrenic nerve activity and cutaneous blood flow. Baroreflex function curves for SNA before and after OXO were constructed using bolus injections of SNP and PE. FSL rats exhibited a three-fold increase in M2 and reduction in M3 receptor expression in 700 μm thick sections of the ventral medulla containing the rostral portion of the RVLM and midline and parapyramidal raphé nuclei. Pressor responses to OXO were significantly reduced in conscious or anaesthetised FSL rats compared to controls, whereas maximal SNA responses were not different between lines. The peak reductions in body temperature as well as peak increases in TBF under anaesthesia were enhanced in FSL rats compared to controls. These findings indicate a region- and subtype-specific alteration of mAChR gene expression in the lower brainstem of FSL rats. Muscarinic hypersensitivity seems to to be limited to the thermoregulatory system in FSL rats; however, disturbance of M2 and M3 receptor expression described here in the rostral medulla may contribute to altered respiratory or arterial baroreflex control seen in this strain.

II. Introduction

Acetylcholinesterase inhibitors and mAChR agonists evoke hypertension, respiratory disturbances and hypothermia via central actions in the hypothalamus and/or ventral medulla *(Brezenoff and Giuliano, 1982; Giuliano et al., 1989; Nattie and Li, 1990; Gordon, 1994)*. Five molecularly distinct mAChR subtypes exist that are coupled either to inhibitory (M2, M4) or excitatory G-proteins (M1, M3, M5) *(Caulfield and Birdsall, 1998)*. The precise mAChR subtypes mediating the autonomic responses described are unclear. Mice deficient in the M2 receptor, but not other subtypes, have an attenuated hypothermic response to the mAChR agonist oxotremorine (OXO) *(Bymaster et al., 2003a)*. Pharmacological studies have implicated M2 receptors in the ventral medulla in control of circulation *(Willette et al., 1984; Giuliano et al., 1989; Kubo, 1998)*; whereas

M1/M3 receptors in this area are involved in control of respiration *(Nattie and Li, 1990; Shao and Feldman, 2000).*

A key site of action of systemically administered cholinesterase inhibitors and mAChR agonists is the ventral medulla *(Giuliano et al., 1989; Nattie and Li, 1990)*, and see Chapter 3). Activation of mAChR on the ventral surface increases ventilation *(Haxhiu et al., 1984)*. Activation of mAChR in the RVLM increases sympathetic activity and arterial pressure and differentially modulates the sensitivity of cardiorespiratory reflexes including the arterial baroreflex *(Giuliano et al., 1989; Huangfu et al., 1997)*, and see Chapter 3). Only a subgroup of non-catecholamine containing sympathoexcitatory neurons in the RVLM contain M2 or M3 receptor mRNA (Chapter 3), suggesting that some mAChR important in autonomic functions may be located presynaptically.

We reported previously that FSL and FRL rats selectively bred for increased or reduced central muscarinic receptor sensitivity, respectively, have impaired autonomic function under anaesthesia (Chapter 4). FSL and FRL rats exhibited higher heart rates compared to their parent strain SD; whereas, FSL rats had reduced sympathetic baroreflex sensitivity and respiratory frequency compared to FRL and SD rats (Chapter 4). A defining feature of FSL rats is that they have exaggerated hypothermic responses to central mAChR activation; whereas, FRL rats have normal responses compared to their parent strain *(Overstreet et al., 1998; Daws and Overstreet, 1999)*. Limited evidence suggests that mAChR receptors levels and/or their kinetics are altered in FSL rats: M1 receptor binding is elevated in the striatum and hippocampus but not cortex of FSL rats *(Daws and Overstreet, 1999)*; whereas M1-M5 receptor expression levels were similar in the pons of FSL compared to FRL rats *(Greco et al., 1998)*. We sought to determine if in FSL rats cardiovascular or respiratory responses evoked by central mAChR activation differed, and whether or not these effects could be due to differences in mAChR gene expression.

Specifically, we determined whether or not there were differences in gene expression of M1 – M5 receptors in rostral and caudal regions of the ventral medulla in FSL and FRL compared to SD rats. Secondly, we determined whether or not there were altered tonic and reflex cardiovascular, thermoregulatory or respiratory responses to central mAChR activation in conscious and anaesthetised FSL, FRL and SD rats.

Quantitative PCR and *In Situ* Hybridisation Analysis of mAChR Subtype Expression

These experiments were not carried out by the candidate (see Chapter 2). FSL (n = 3), FRL (n = 3) and SD rats (n = 7) were anaesthetised with sodium pentobarbital, transcardially perfused with ice-cold sterile saline (0.9 % NaCl in PB) and tissue extracted from the rostral (RVM) and caudal ventral medulla (CVM) and cerebellum as described in Chapter 2. Expression levels of M1 - M5 receptor mRNA were evaluated using RT-PCR as described in Chapter 2.

Conscious RadioTelemetric Recording

This procedure was not carried out by the candidate (see Chapter 2). FSL (n = 9), FRL (n = 6) and SD (n = 7) rats were instrumented for radiotelemetric recordings of AP and temperature in conscious animals as described in Chapter 2.

Anaesthesia, Surgical Procedures and Recording

FSL, FRL and SD rats (n = 6 / group) were anaesthetised with urethane and instrumented for recording of AP, SNA, PNA and TBF as described in Chapter 2.

Experimental protocol

Anaesthetised and conscious rats were administered sequential doses of mATR (2 mg / kg) and OXO (0.2 mg / kg). Conscious animals received an ip injection of mATR and OXO was administered after 30 mins. In at least three animals per group, baroreflexes were tested under anaesthesia by administration of SNP and PE.

Data analysis

Cardiorespiratory parameters were continuously monitored following administration of mATR and OXO. In conscious animals mean values for AP, HR and temperature were acquired continuously with a moving average of 10 s. Peak response were taken 35 mins post-injection coinciding with the maximal temperature effects. Under anaesthesia, average values of MAP, SNA, TBF and minute inspiratory activity (PNA burst frequency x

amplitude x 60) were taken over 100 s segments following mATR (control) and at 2, 10 and 30 min following OXO. Peak changes in each variable as well as response area (area under curve from 0 to 30 min post OXO) were calculated. Logistic function curves describing the SNA-MAP relationship and their first derivatives for calculation of baroreflex gain were generated as described in Chapter 2.

Statistical analysis

Data were compared using one-way analysis of variance (ANOVA) and a post hoc test for significance with Bonferroni's correction. A paired t-test was used to compare changes in SNA baroreflex parameters within groups. All data are presented as mean ± standard error of the mean (SEM) and $P<0.05$ was considered statistically significant.

IV. Results

Region- and Subtype-Specific Alteration of mAChR Subtype Expression in Medulla and Spinal Cord of FSL Rats

M1 – M5 receptors were sometimes expressed at different levels relative to GAPDH in the same brain and spinal cord regions isolated from FSL, FRL and SD rats (Fig. 5.1). Our results do not show, however, the relative abundance of different subtypes compared between brain regions (i.e M1 vs. M2). In the RVM, M2 receptor mRNA levels were increased more than three-fold in FSL compared to FRL and SD rats ($P < 0.01$). In contrast, M3 receptor mRNA levels were reduced around three-fold in FSL compared to FRL and SD rats ($P < 0.05$). Expression levels of M1 and M4 receptors were similar between all three strains; whereas, M5 receptor mRNA levels were significantly lower in the RVM in FRL compared to SD rats ($P < 0.05$). In the caudal ventral medulla, M1 receptor mRNA was increased in FRL rats compared to SD rats ($P < 0.05$) and M3 receptor mRNA was reduced in FSL and FRL rats compared to SD rats ($P < 0.05$). In the posterior cerebellum in FSL and FRL rats, all mAChR subtypes were expressed at similar levels compared to SD rats (Fig. 5.1).

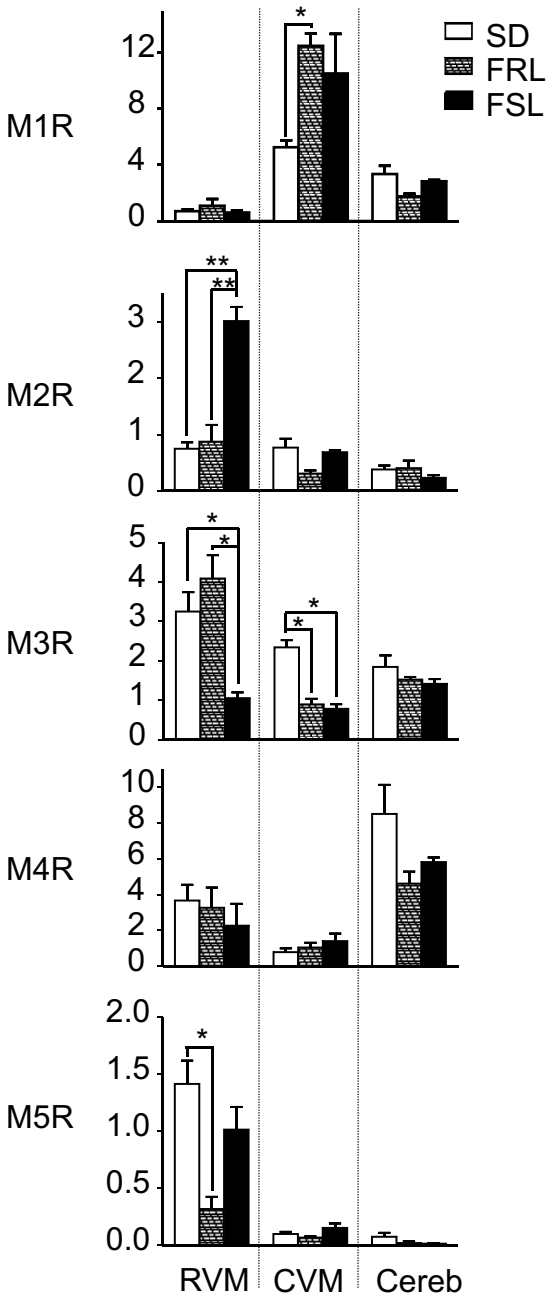

Figure 5.1 *Region- and subtype-specific alteration of mAChR subtype expression in rostral and caudal ventral medulla in FSL rats.* Comparison of gene expression levels of M1-M5 muscarinic receptor subtypes in FSL (n=3), FRL (n=3) and SD rats (n=5) using quantitative real-time PCR. Data are mean ± SEM, **P*<0.05, ***P*<0.01.

Reduced Pressor and Enhanced Hypothermic Responses to Central mAChR Activation in Conscious FSL Rats

Figure 5.2A shows that in conscious SD rats OXO evokes a pressor response accompanied by a bradycardia and a fall in temperature. Grouped data shows that although a pressor response was evoked in SD and FRL rats, a large depressor response was evoked in FSL rats (Fig. 5.2B). In all three strains of rat, the change in AP (pressor or depressor) was accompanied by bradycardia. In FSL rats, the onset of bradycardia preceded any change in AP. The magnitude of the bradycardia evoked in FSL rats (-75 ± 7 bpm) was greater compared with the response evoked in FRL (-11 ± 11 bpm, $P < 0.01$) or SD rats (-33 ± 11, $P < 0.05$) (Fig. 5.2B). Time course changes in the hypothermic response to OXO were different between FRL and SD rats ($P < 0.05$); however, peak hypothermic responses did not differ (FRL, -1.5 ± 0.2°C; SD, -1.9 ± 0.2, P = n.s.). The peak hypothermic response evoked by OXO in FSL rats (-2.7±0.2°C) was greater compared with both FRL and SD rats ($P < 0.05$) rats (Fig. 5.2B). The time course of hypothermia was also significantly longer in FSL rats compared to FRL ($P < 0.01$) and SD rats ($P < 0.01$).

Reduced Pressor, Equivalent Sympathoexcitatory and Enhanced Cutaneous Blood Flow Responses to Central mAChR Activation in FSL Rats

OXO evoked a large increase in AP, SNA and TBF in anaesthetised SD rats (Fig. 5.3). OXO evoked a marked tachycardia in anaesthetised SD rats, in contrast to the bradycardia evoked in conscious animals (compare Fig. 5.2 and 5.3). OXO produced the same pattern of responses in SD, FSL and FRL rats, but the magnitude of some effects differed between strains. The magnitude and response area of the increase in SNA and HR evoked by OXO was similar in FSL, FRL and SD rats (Fig. 5.3B). OXO evoked a smaller pressor response in FSL rats (29 ± 2 mmHg) compared to FRL (39 ± 3 mmHg, $P < 0.05$) and SD rats (50 ± 2 mmHg, $P < 0.01$) (Fig. 5.3B). In contrast, OXO evoked a much larger peak increase in TBF in FSL rats (62 ± 8 %) compared to FRL (19 ± 6 %, $P < 0.01$) and SD rats (16 ± 8 %, $P < 0.01$) (Fig. 5.3B).

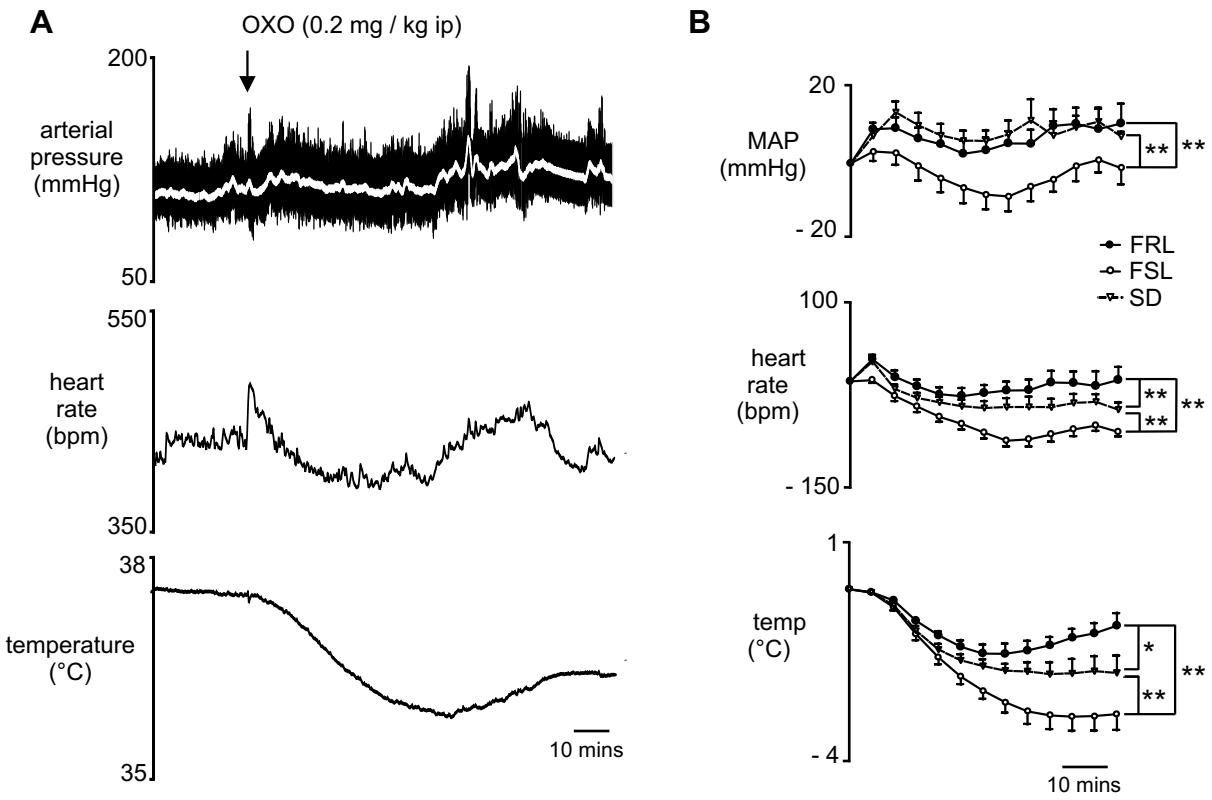

Figure 5.2 *Reduced pressor response but enhanced bradycardia and hypothermic response to central mAChR activation in conscious FSL rats.* **A:** Typical recording from a conscious unrestrained SD and **B:** group data from SD (n = 7), FRL (n = 6) and FSL rats (n = 9) illustrating changes in MAP, HR and temperature following intraperitoneal injection of OXO (0.2 mg/kg) after pre-treatment with mATR (2 mg/kg ip). Data are mean ± SEM, **P*<0.05, ***P*<0.01.

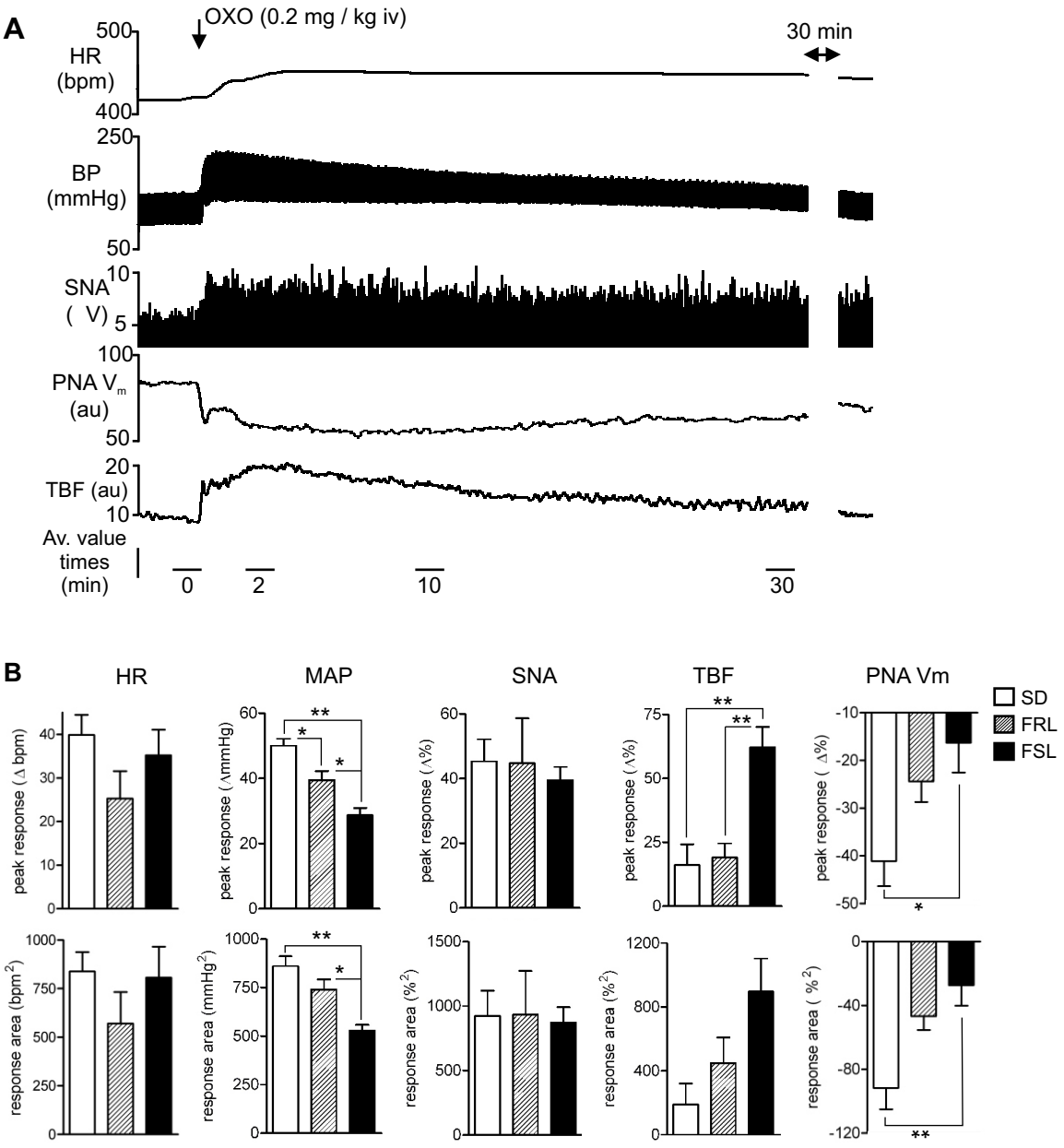

Figure 5.3 *Altered thermoregulatory, cardiovascular and respiratory responses to central mAChR activation in anaesthetised FSL rats.* **A:** Typical recording from a urethane-anaesthetised SD rat illustrating increases in HR, MAP, SNA and TBF and reductions in minute inspiratory activity (= PNA frequency (Hz) x amplitude (% baseline) x 60) in response to OXO (0.2 mg/kg iv) after pretreatment with mATR (2 mg/kg iv). **B:** Group data illustrating differences in magnitude of responses to OXO in SD, FRL and FSL rats (n = 6 / group) expressed as peak response or area under curve (response area) between 0 and 30 min post-injection. Data are mean ± SEM, **P*<0.05, ***P*<0.01.

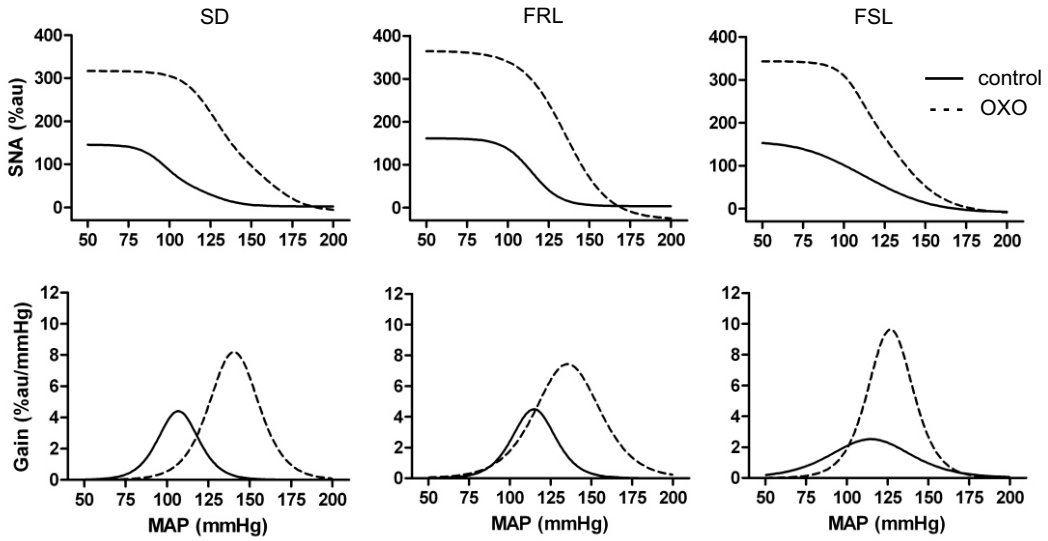

Figure 5.4 *Reduced sympathetic baroreflex sensitivity but no difference in maximal baroreflex responses to central mAChR activation in FSL rats.* Comparison of average SNA baroreflex function curves (top) and their first derivatives (bottom) before (control) and 5 min after OXO (0.2 mg/kg iv) in anaesthetised FSL, FRL and SD rats (n = 3 / group). Resting baroreflex gain is reduced in FSL rats compared to FRL and SD rats. OXO shifts the SNA-MAP relationship upward and to the right and markedly increases the maximum plateau of SNA and gain in all strains (see Results). Error bars are omitted for clarity.

Attenuated Respiratory Depressant Effects of Central mAChR Activation in FSL and FRL Rats

Under anaesthesia OXO produced a marked reduction in central inspiratory activity (Fig. 5.3A). The peak reduction and area under the curve of the depression of PNA was significantly attenuated in FSL rats (-16 ± 6 %) compared to SD rats (-41 ± 5 %, $P < 0.05$) (Fig. 5.3B). The magnitude of the respiratory depression evoked by OXO also tended to be lower in FRL rats (-24 ± 4 %, n.s.) compared to SD rats but this was not significantly different (Fig. 5.3B).

Reduced Resting SNA Baroreflex Sensitivity but Equivalent Maximal SNA Responses to Central mAChR Activation in FSL Rats

OXO shifted baroreflex function curves upward and to the right, producing a dramatic increase in the maximum plateau and gain of the SNA baroreflex (Fig. 5.4) as shown previously in SD (26). A similar effect in both direction and amplitude was seen in all strains (Fig. 5.4). Maximum SNA plateau in control conditions was similar in FSL (153 ± 13 %), FRL (160 ± 7 %) and SD rats (145 ± 6 %). Following OXO, maximum SNA plateau was increased around two-fold but was not significantly different in FSL (343 ± 19 %), FRL (310 ± 26 %) or SD rats (316 ± 18 %). SNA baroreflex gain in control conditions was significantly reduced ($P < 0.05$) in FSL rats (2.5 ± 0.2 %/mmHg) compared to FRL (4.7 ± 0.6 %/mmHg) and SD rats (4.4 ± 0.5 %/mmHg). Following OXO baroreflex gain was increased by around two-fold in SD (8.1 ± 0.6 %/mmHg) or FRL rats (6.7 ± 1.4 %/mmHg); whereas in FSL rats gain was increased by around three-fold (9.0 ± 1.7 %/mmHg). However, there was no significant difference in gain in FSL, FRL or SD rats following OXO.

V. Discussion

We demonstrated differences in gene expression of brainstem mAChR subtypes, using quantitative real time PCR, and in the thermoregulatory and respiratory responses to a mAChR agonist in FSL and FRL rats. M2 receptor expression was increased; whereas, M3 receptor expression was reduced in the RVM of FSL rats. Differences in gene expression

were restricted to the rostral part of the medulla, since M1 receptor expression was increased but M3 receptor expression was reduced in the CVM of both FSL and FRL rats; whereas, there were no line differences in subtype expression in the cerebellum. Our results indicate region- and subtype-specific differences in mAChR subtype expression in the ventral medulla of FSL rats that could account for differences in thermoregulatory or respiratory function in this strain. In contrast, differences in muscarinic regulation of cardiovascular function were less clear cut as we observed equivalent sympathoexcitatory responses but attenuated pressor effects in conscious or anaesthetised FSL rats.

The dramatic reduction in temperature after OXO was expected in FSL rats as this strain was bred for hypersensitivity to hypothermic effects of muscarinic agonists *(Overstreet et al., 1998; Daws and Overstreet, 1999)*. The exaggerated hypothermic response is suspected to be due to both reduced heat generation and dilatation of the peripheral circulation, causing heat loss to the ambient environment. In rats, the tail is the major thermoregulatory organ. Furthermore, blood flow to the tail is regulated by sympathetic vasoconstrictor fibres supplied by the RVLM and raphé nuclei *(Tanaka et al., 2002; Ootsuka et al., 2004)*. We demonstrate for the first time that there is a larger increase in TBF in FSL rats after OXO, indicating that enhanced peripheral vasodilatation contributes to the heightened hypothermic response. It is possible that M2 receptors in the rostral medulla are involved as mice deficient in this subtype have attenuated hypothermic responses to OXO compared to wildtype *(Bymaster et al., 2003b)*. We found that FSL rats exhibit increased levels of M2 receptor expression in the rostral medulla, which contains raphé neurons involved in thermoregulation *(Nakamura et al., 2004)*. The simplest explanation is that activation of M2 receptors in the raphé leads to increased cutaneous dilatation in FSL rats; however, it is not known if the cholinergic hypothermic response is mediated through the raphé in rat. This region is important in several CNS mechanisms that lead to heat loss and is a target of several centrally acting agents, including the 5-HT1A receptor agonist 8-OHDPAT, in evoking hypothermia *(Nakamura et al., 2004; Ootsuka and Blessing, 2006)*. Of note is that hypothermic responses to 8-OHDPAT are also exaggerated in FSL rats *(Overstreet et al., 1998)* suggesting that this strain may exhibit abnormal control of cutaneous blood flow by cholinergic as well as serotonergic mechanisms in the raphé. Other brain regions may be involved in FSL rats, including the preoptic hypothalamus where injection of cholinergic agonists has been reported to elicit either reductions or increases in body temperature *(Gordon, 1994)*. RVLM neurons supplying cutaneous sympathetic fibres are probably not involved, as we showed

previously that blockade of mAChR in the RVLM does not attenuate the increase in TBF evoked by OXO in SD rats (Chapter 3).

Given the dramatic differences in thermoregulatory responses to OXO, the lack of line differences in sympathoexcitatory responses after OXO was surprising. Moreover, pressor responses to OXO were markedly reduced in conscious and anaesthetised FSL rats compared to control strains. The simplest explanation for the attenuated pressor response in FSL rats, given equivalent levels of sympathetic activation, is an altered haemodynamic balance because of increased vasodilatation in the tail. Sympathoexcitation and increases in arterial pressure following OXO are mediated almost entirely via mAChR activation in the RVLM (see Chapter 3). M2 receptors are involved as M2-preferring antagonists prevent pressor responses to cholinergic agonists *(Giuliano et al., 1989)* and some sympathoexcitatory neurons express M2 receptor mRNA (Chapter 3). Although we observed increased M2 receptor expression levels in the RVM of FSL rats, the increases in HR and SNA following OXO under anaesthesia were virtually the same in FSL, FRL and SD rats. Two explanations are possible to explain our data. Firstly, the difference in gene expression seen in FSL rats may not be restricted to RVLM neurons. As we reported previously, mAChR are expressed only a small subpopulation of sympathoexcitatory RVLM neurons (Chapter 3). Secondly, both pre- and postsynaptic mAChR are involved in eliciting sympathoexcitatory effects in the RVLM *(Arneric et al., 1990; Huangfu et al., 1997)*. Hence, there may be changes in presynaptic mAChR levels in FSL rats that were not able to be detected using the methods here. If so, the relative balance of pre- versus postsynaptic effects on RVLM neurons may be altered in FSL rats. In support of this, we found that OXO evoked a relatively larger increase in baroreflex gain in FSL rats. This response is mediated presumably via presynaptic mAChR in the RVLM that modulate release of neurotransmitter from baroreceptor-related inputs.

In conscious rats we found that OXO evoked a bradycardia that was much larger in FSL rats compared to FRL or SD rats. The finding that anaesthesia reversed the direction of the change in HR evoked by OXO is consistent with previous studies *(Brezenoff and Giuliano, 1982)*. The simplest explanation is that anaesthesia blocks inhibitory muscarinic effects on HR. Both the tachycardia and bradycardia are mediated via sympathetic effects on HR as peripheral vagal effects were blocked with mATR. Activation of mAChR in the posterior hypothalamus or NTS has been shown to have variable effects on HR including bradycardia in conscious animals *(Brezenoff and Giuliano, 1982; Criscione et al., 1983;*

Tsukamoto et al., 1994). The reason for the exaggerated fall in HR seen here in FSL rats is not clear. Presumably, this is mediated by increased sympathoinhibitory effects on HR mediated by mAChR in sites such as the hypothalamus or NTS. The RVLM is unlikely to be involved as we noted that the bradycardia followed a different time course to the blood pressure profile.

OXO elicited a marked respiratory depression in SD rats, as reported in Chapter 3. Unexpectedly, the reduction in phrenic activity after OXO was attenuated in FSL rats compared to SD rats. FRL rats also tended to have attenuated respiratory depressant responses to OXO, suggesting that this may not be a specific cholinergic trait of FSL rats. These data indicate that FSL and FRL rat strains may have undergone genetic drift resulting in some phenotypic similarities compared to their parent strain. In support of this, we found similar differences in M1 and M3 receptor expression in the CVM of FSL and FRL rats compared to SD rats. Pharmacological and gene knockout studies implicate M3 and M1 receptors in the ventral medulla in control of respiratory rhythm and amplitude, respectively *(Nattie and Li, 1990; Shao and Feldman, 2000; Boudinot et al., 2004)*. The region of the RVM examined here contains inhibitory Bötzinger neurons that determine respiratory timing; the region of the CVM contains mainly expiratory neurons supplying spinal motorneurons *(Sun et al., 1997; McCrimmon et al., 2000)*. M3 receptor levels were reduced in both the RVM and CVM of FSL rats, supporting our finding that muscarinic agonists have less effect on respiration in this strain.

In summary, using telemetry in conscious animals and recordings made under anaesthesia, specific differences in the pattern of autonomic responses evoked by the muscarinic agonist OXO were found in FSL rats compared to FRL and SD rats. Secondly, using quantitative RT-PCR we demonstrated altered gene expression of certain mAChR subtypes in the rostral and caudal ventral medulla of FSL rats. Genetic differences, specific to FSL rats, were noted in the rostral medulla only and limited to some mAChR subtypes. We demonstrated that thermoregulatory but not sympathoexcitatory responses in FSL rats were enhanced. As both responses involve M2 receptors, the data indicate that genetic mechanisms regulating M2 receptors involved in either thermoregulation or cardiovascular function are inherited independently. These data provide support for the notion that cholinergic mechanisms that regulate body temperature are separate to those that regulate arterial pressure. Respiratory responses to OXO were attenuated in FSL rats indicating an opposite effect of cholinergic control on temperature versus respiration. This is supported

by the finding that M3 receptor expression was reduced rather than enhanced in the ventral medulla of FSL rats. Hence, our data demonstrate that functional mAChR supersensitivity in FSL rats is limited to the thermoregulatory system; whereas other muscarinic autonomic responses are either unaffected or attenuated.

Chapter 6 Cardiovascular Autonomic Function in Conscious FSL and FRL Rats and Susceptibility to Ventricular Arrhythmia

I. Abstract

Acetylcholine plays a role in control of cardiovascular function via interacting with central neurons that regulate vagal and sympathetic outflow. FRL and FSL rats bred for differences in cholinergic responses appear to have an altered level of vagal and or sympathetic input to the heart under urethane anaesthesia (Chapter 4). In the present study we investigated whether or not there were differences in diurnal patterns of AP, HR or activity in conscious freely behaving FRL and FSL rats compared to SD rats. Rats were implanted with telemetric probes under pentobarbital anaesthesia and, following recovery, cardiovascular variables were monitored for 24 hours by continuous samping of HR and AP for 5 mins, 4 times every hour. Spectral analysis of pulse interval (PI) and systolic AP (SAP) was used to investigate short-term regulation of AP and HR at high frequencies (HF, 1 – 3 Hz) that reflect vagal activity and low frequencies (LF, 0.25 – 0.75 Hz) associated with sympathetic outflow and baroreflex function. The results show that there was no difference in HR, AP or activity in conscious FSL rats compared to SD rats; whereas FRL rats selectively had an elevated HR during the day and night. FSL rats exhibited reduced HF power of HR during the day and night and an increased LF/HF ratio at night. BRS measured using the alpha-coefficient was also significantly reduced in conscious FSL rats compared to both FRL and SD rats. In addition, we hypothesised that FRL and / or FSL rats would be differentially susceptible to cardiovascular effects and arrhythmias produced by the cardiac glycoside ouabain, which inhibits the cardiac Na^+/K^+ ATPase leading to calcium overload in the myocardium and release of acetylcholine and noradrenaline from nerve terminals. FSL rats exhibited the highest incidence of ventricular premature beats and ventricular tachycardia during ouabain infusion. These findings indicate that reflex vagal input to the sinus node is reduced in FSL rats compared to control strains. In addition, FSL rats exhibit a predominance of sympathetic activity at night and increased susceptibility to arrhythmia under anaesthesia. In light of evidence that FSL rats resemble behavioural and neurochemical abnormalities associated with depressive disorders, the present findings may shed light on underlying mechanisms of autonomic dysfunction in depression.

II. Introduction

Depression symptoms are associated with autonomic dysfunction and early mortality in patients with CHD *(Frasure-Smith et al., 1993; Carney and Freedland, 2003)*. The underlying mechanisms are unclear but appear to involve increased susceptibility to arrhythmia rather than ischaemia or thrombosis *(Frasure-Smith et al., 1995; Lesperance et al., 2002; Watkins et al., 2006)*. An imbalance of autonomic inputs to the heart is proposed to generate electrical instability and promote arrhythmia formation *(Schwartz et al., 1992; Zipes and Wellens, 1998)*. Ongoing vagal activity is thought to be cardioprotective because it entrains the cardiac pacemaker and has powerful inhibitory effects on heart rate and atrioventricular conduction *(Vanoli et al., 1991; Jones, 2001)*. In contrast, sympathetic overactivity leads to ventricular electrical instability and predisposes to development of potentially fatal arrhythmias *(Schwartz et al., 1984; De Ferrari et al., 1993)*.

Spectral analysis of HRV has been widely used to discriminate between sympathetic and vagal components of HR modulation in humans and animals occurring at low or high frequencies (see Chapter 1) *(Akselrod et al., 1981; Medigue et al., 2001)*. A reduction in vagal activity and relative increase in sympathetic activity manifests as a reduction in HRV at low (LF) and high frequencies (HF) and an increase in the LF/HF ratio *(Pagani et al., 1991; Lombardi, 2002)*. Reduced HRV is often found in depressed subjects with or without history of CHD compared to controls *(Carney et al., 1995; Stein et al., 2000; Agelink et al., 2002; Guinjoan et al., 2004)*. Some studies also report a reduction in BRS measured using spectral and spontaneous indices in depressed subjects *(Watkins and Grossman, 1999; Broadley et al., 2005)*, suggesting that impaired reflexogenic control of HR may underlie the reduction in HRV.

FSL rats exhibit a number of physiological and behavioural abnormalities consistent with clinical depression, including psychomotor retardation *(Overstreet et al., 1986)*, reduced motivated behaviour (including eg. high immobility in the forced swim test) *(Overstreet and Russell, 1982; Overstreet, 1986)*, reduced appetite *(Bushnell et al., 1995)* and elevated REM sleep *(Shiromani et al., 1988; Benca et al., 1996)*. Depressed-like behaviour in FSL rats is alleviated by chronic, but not acute, treatment with antidepressants *(Zangen et al., 1997, 1999)*. FSL rats also exhibit somatic abnormalities including impaired immune responses and gastric dysmotility *(Friedman et al., 2002; Mattsson et al., 2005)*,

supporting the potential value of this strain in understanding the link between behavioural and somatic symptoms of depression.

In Chapter 4 we found that, under urethane anaesthesia, FSL rats exhibit a reduction in HRV in 5 minute data segments compared to outbred but not inbred control strains. Further interpretation of these data is limited by the presence of anaesthesia. In the present study we tested the hypothesis that freely behaving FSL rats would exhibit impaired cardiac autonomic control in 24 hr recordings of HRV and APV. Secondly, we determined and compared cardiovascular and cardiotoxic effects of the cardiac glycose ouabain in SD, FRL and FSL rats.

Ouabain selectively inhibits the cardiac Na+/K+-ATPase resulting in accumulation of intracellular Ca2+ and positive inotropic effects *(Hauptman and Kelly, 1999; Demiryurek and Demiryurek, 2005)*. Ca2+ overload can cause afterdepolarisations and increased automaticity that can lead to atrial and ventricular arrhythmias *(Hauptman and Kelly, 1999)*. Ouabain administration also leads to Ca2+ channel-mediated exocytotic release of ACh from vagal nerve terminals *(Kawada et al., 2001)* and release of noradrenaline from sympathetic nerve terminals *(Yamazaki et al., 1996; Yamazaki et al., 1999)*. Increases in autonomic activity lead to conduction slowing (due to release of ACh) and perturb ventricular electrical stability (mainly due to increased noradrenaline) *(Yamazaki et al., 1996; Hauptman and Kelly, 1999; Yamazaki et al., 1999)*. We hypothesised that FRL and FSL rats would be differentially susceptible to arrhythmias produced by ouabain due to differences in their resting levels of cardiac autonomic activity. We also determined whether or not there were differences in HR responses to aortic baroreceptor stimulation in FRL and FSL rats compared to SD rats prior to and during infusion of ouabain.

III. Materials and Methods

Conscious RadioTelemetric Recording

This procedure was not carried out by the candidate (see Chapter 2). FSL (n = 5), FRL (n = 5) and SD rats (n = 3) were instrumented for conscious radiotelemetric recording of ECG and AP as described in Chapter 2.

Anaesthesia, Surgical Procedures, Recording and Activation of Cardiovascular Reflexes

SD (n = 6), FRL (n = 6) and FSL rats (n = 7) were anaesthetised with urethane and instrumented for recording of AP, SNA and ECG. The AN was also isolated for stimulation of aortic baroreceptor afferents (pulse train 100 Hz, 5 – 10 V) as described in Chapter 2. Drugs and maintenance anaesthesia were infused into the femoral vein. Ouabain (Sigma) was dissolved in physiological saline and infused at 3 ml / hr at a dose of 200 μg / kg / min.

Data Analysis

Diurnal Changes in HR, AP and activity

HR, AP and activity were acquired continuously for 5 minutes every 15 minutes over a 24 hour period. Data were exported offline in 1 hour bins and averaged into quartiles, ie. during the day AM (6am – 12pm), day PM (12pm – 6pm), night PM (6pm – 12am) and night AM (12am – 6am) to incorporate changes in activity, feeding and sleep cycle *(van den Buuse, 1994; Head et al., 2004)*.

Spectral Analysis of HR and SAP

Spectral analysis was used to examine the variability of SAP and HR (pulse interval (PI)) in short term recordings from conscious animals using methods described in detail in Chapter 2 and Appendix 2. Over the entire 24 hrs of data, only segments that were stationary and did not include ectopic beats or noise artefacts were included (77 ± 5 % of total segments). Total power (0.04 Hz – 3 Hz), LF (0.25 – 0.75 Hz) and HF powers (1 – 3 Hz) were calculated within the defined frequency ranges. The LF / HF ratio of HRV was calculated from these data. Values for total power, LF and HF power, and LF / HF ratio were binned into hourly averages. 24 hr data were acquired and averaged into 6 hour-quartiles.

HR Baroreflex Sensitivity

BRS was estimated using the α-coefficient (see Chapter 2). Since indices of spontaneous BRS have been shown to be related to mean HR interval *(Zaza and Lombardi, 2001)* and see Chapter 4), we used analysis of covariance (ANCOVA, see below) to test whether

resting HR was a contributing factor. BRS was corrected for mean HR, using similar methods to Abrahamsson et al (2003), by first fitting individual linear regression lines between HR and BRS for data obtained from each strain *(Abrahamsson et al., 2003)*. The equations of the lines were then used to calculate BRS, at the mean HR of SD rats, in FRL and FSL rats.

Ouabain-Induced Cardiovascular Effects and Arrhythmia

Cardiovascular effects of ouabain and susceptibility to ventricular arrhythmia were examined as described in Chapter 2.

Statistical analysis

All values are expressed as mean ± SEM and were compared using two-way analysis of variance (ANOVA) to determine the effect of time of day (quartiles) and strain on physiological variables. One-way ANOVA was used for group comparisons with a post hoc test for significance performed with Bonferroni's correction. ANCOVA was used to test the degree to which HR (quantitative variable) and strain (categorical variable) contributed to variability of BRS (dependent variable) and linear regression was used to determine whether this was significantly non-zero.

IV. Results

Sensitivity to Oxotremorine-Evoked Hypothermia

FSL rats exhibited much larger hypothermic responses in response to OXO (2.2 ± 0.1 vs. 0.3 ± 0.1 ºC, $P<0.0001$) and had slightly lower body weights (314 ± 13 vs. 351 ± 14 g, $P=0.09$) compared to FRL rats.

Diurnal Changes in HR, AP and activity

All rats exhibited nocturnal elevations in HR, mean AP (MAP) and activity (Fig 6.1). Two-way ANOVA showed a highly significant effect ($P<0.001$) of time of day on HR and activity. Strain had a significant effect on HR ($P=0.039$) and activity ($P=0.024$). FRL rats had a predominantly higher resting HR compared to both FSL and SD rats (Fig. 6.1). FSL rats had a significantly elevated MAP compared to SD rats but not FRL rats (Fig. 6.1).

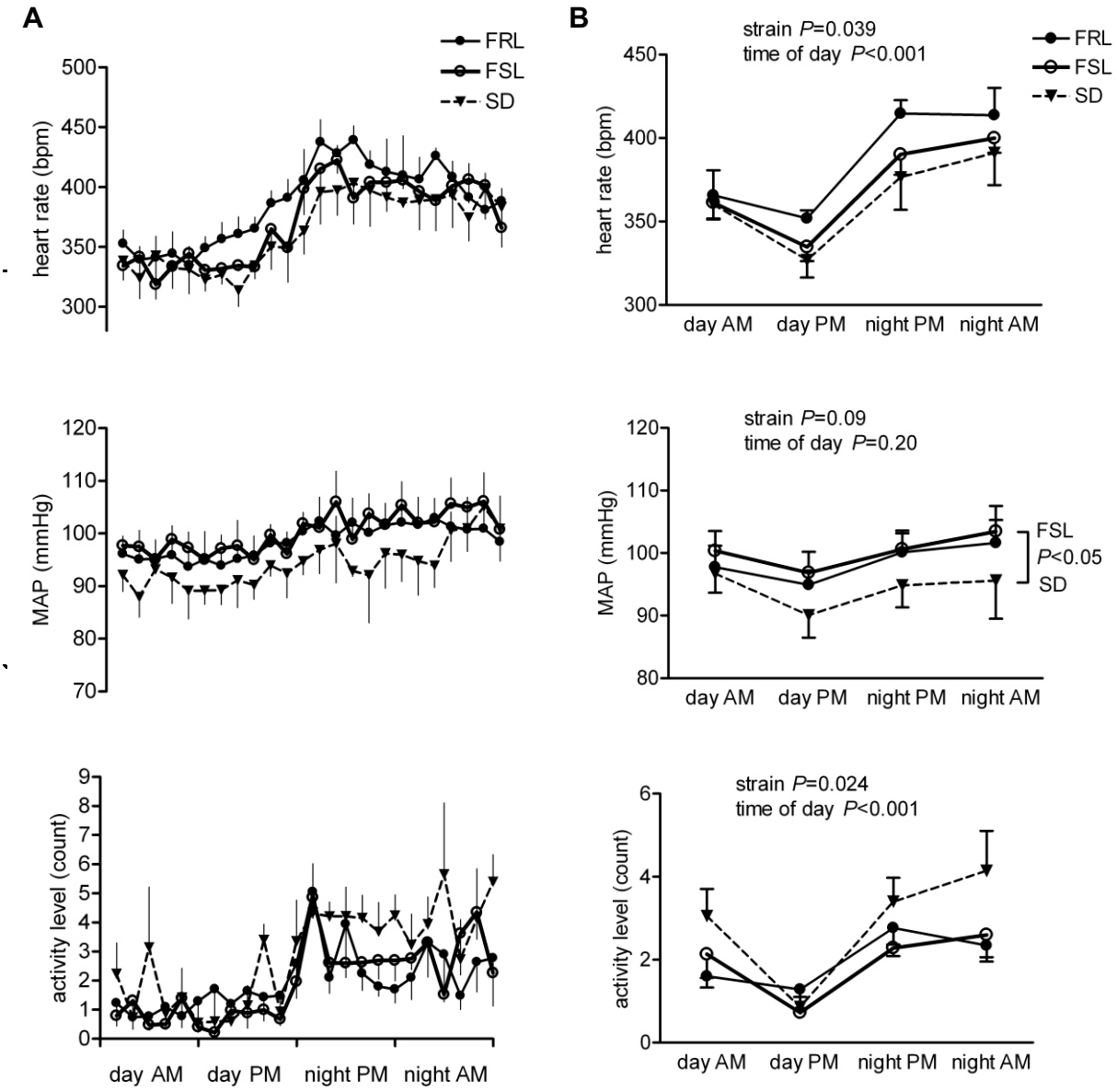

Figure 6.1 Diurnal patterns of HR, MAP and activity level in conscious SD (triangles, dashed line), FRL (filled circles, thin line) and FSL rats (open circles, bold line) recorded using radiotelemetric probes implanted into the abdominal aorta over 24 hrs in 1 hr averages (**A**) and 6 hr quartile averages (**B**). Values are mean ± SEM.

Locomotor activity was lowest in all strains in the second half of the day and highest in SD rats compared to FRL and FSL rats (Fig. 6.1).

Reduced HRV in FSL Rats during Day and Night

To obtain a snapshot of the pattern of variability during the day and night in FSL rats compared to controls, average SAPV and HRV spectra were taken at 12 pm and 3am from each animal. Figure 6.2 illustrates average spectra on log scales with error bars omitted for clarity. Power was clearly distributed in LF and HF bands. Frequencies < 0.25 Hz were included in the total power calculation but were not analysed separately. HRV was significantly reduced in FSL rats compared to FRL and SD rats in both LF and HF ranges at 12 pm and in the HF range at 3 am (Fig. 6.2). At these times SAPV was not different in FSL rats compared to FRL and SD rats (Fig. 6.2). SAPV was slightly but significantly elevated in the HF band at 12 pm in FRL rats compared to SD rats (Fig. 6.2).

Figure 6.3 shows that this pattern of a reduced HRV in FSL rats was maintained over the 24 hrs. Spectral parameters did not show consistent circadian variation between strains. There was a significant effect of strain on total power (P=0.023), HF power (P<0.001) and LF/HF ratio of PI (P=0.0098). During the day and night HRV was reduced in both LF and HF ranges in FSL rats compared to controls (Fig. 6.3). The difference was more marked within the HF range (P<0.01, Fig. 6.3). LF/HF ratio of PI was elevated ~ 1.5 fold in FSL rats compared to FRL and SD rats at night (P<0.05 vs FRL, Fig. 6.3). Total power of PI (0.04 – 3 Hz) was significantly higher in FRL rats compared to SD and FSL rats (Fig. 6.3). Total and LF power of SAP were not significantly different between strains although total SAPV was higher at night in FSL rats compared to controls (Fig. 6.3). HF power of SAP was significantly elevated in both FRL and FSL rats compared to SD rats (P<0.01, Fig. 6.3).

Reduced BRS in Conscious FSL Rats

BRS, estimated using α LF, was significantly reduced in FSL rats compared to FRL and SD rats (P<0.01 vs SD, P<0.05 vs FRL, Fig. 6.4A). There was no consistent circadian variation in α LF. ANCOVA showed a significant effect of mean HR on values of α LF (P<0.008). In FRL, but not FSL rats, α LF was inversely correlated to mean HR (P=0.014). Estimates of α LF corrected for mean HR showed that α LF was increased in FRL rats but remained unchanged in FSL rats (Fig. 6.4B).

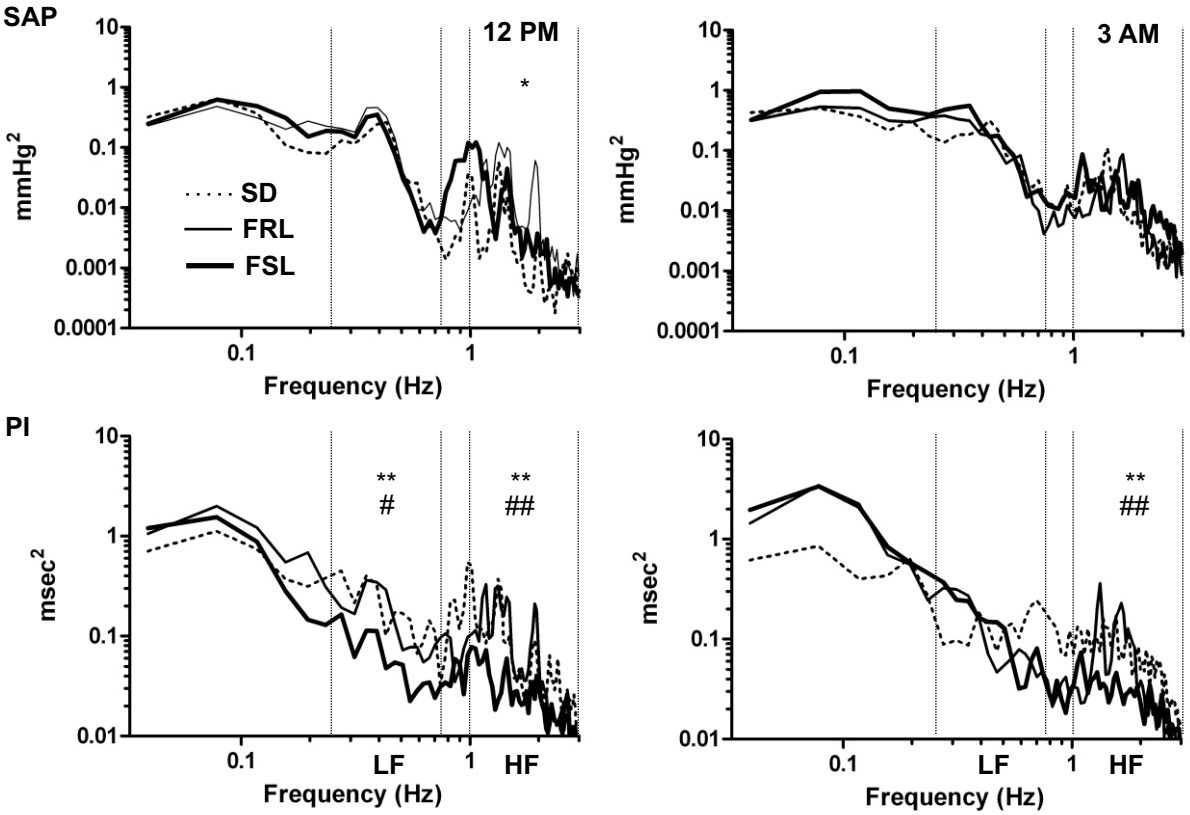

Figure 6.2 Average power spectral density functions of SAP *(top)* and PI *(bottom)* at two time points; 12PM *(left)* and 3AM *(right)*, in conscious SD (dashed line), FRL (thin line) and FSL rats (bold line). Vertical lines denote bandwidths for calculation of power in low frequency (LF, 0.25 0.75 Hz) and high frequency (HF, 1 3 Hz) components of variability. Error bars are omitted for clarity. **P*<0.05, ***P*<0.01 FSL vs. SD; $^{\#}P$<0.05, $^{\#\#}P$<0.01 FSL vs. FRL.

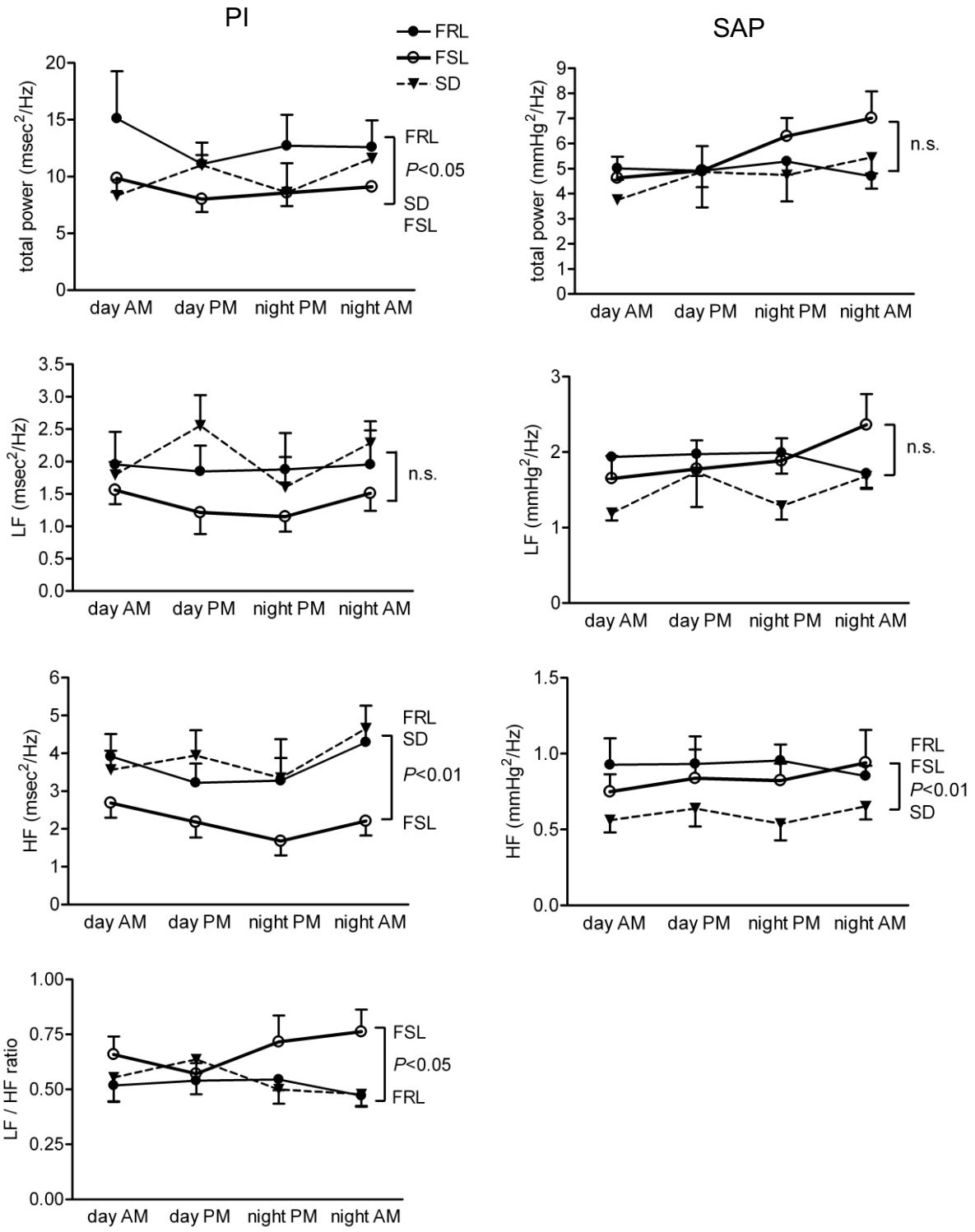

Figure 6.3 *Reduced HRV during the day and night and increased LF/HF ratio during the active night period in FSL rats.* Power spectral densities of PI (left) and SAP (right) for total (0.04 - 3 Hz), low frequency (LF, 0.25 - 0.75 Hz) and high frequency (HF, 1 - 3 Hz) components of variability and LF / HF ratio in conscious SD (triangles, dashed line), FRL (filled circles, thin line) and FSL rats (open circles, bold line) over 24 hrs. Power was calculated using fast Fourier transformation of 80 s stationary data segments four times every hour. Values are mean ± SEM.

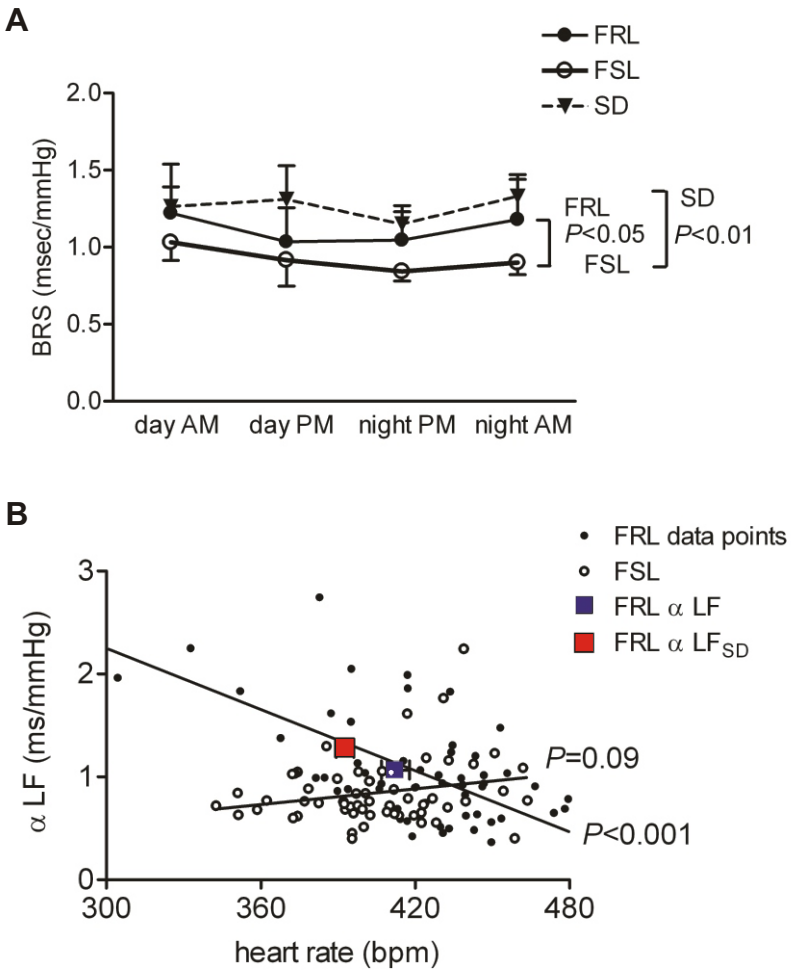

Figure 6.4 *Reduced BRS in FSL rats.* **A:** Values for BRS, calculated using the alpha-coefficient, in conscious SD (triangles, dashed line), FRL (filled circles, thin line) and FSL rats (open circles, bold line) over 24 hrs. **B:** Linear regression lines were fitted to individual data points showing that BRS is inversely related to heart rate in FRL rats but not FSL rats. Boxes indicate raw and heart rate-corrected BRS of FRL rats calculated as described in Materials and Methods. Values are mean ± SEM.

Ouabain-Induced Cardiovascular Effects

As described in Chapter 4, resting HR was higher in FRL and FSL rats compared to SD rats under urethane anaesthesia. Cardiovascular responses produced by continuous infusion of ouabain were compared between FRL, FSL and SD rats. Ouabain elicited a significant reduction in SAP in SD (124 ± 2 to 90 ± 3 mmHg), FRL (131 ± 7 to 99 ± 7 mmHg) and FSL rats (132 ± 9 to 99 ± 11 mmHg). In contrast, ouabain produced a significant shortening of R-R interval only in SD rats (175 ± 10 to 141 ± 4 ms) compared to FRL (132 ± 3 to 133 ± 2 ms) and FSL rats (140 ± 7 to 134 ± 4 ms). The change in R-R interval produced by stimulation of the AN was reduced in FRL and FSL rats compared to SD rats prior to ouabain infusion. Ouabain significantly reduced the reflex bradycardia evoked by AN stimulation in SD rats (0.83 ± 0.16 to 0.34 ± 0.08 ms/mmHg) to levels similar to those evoked at rest or following ouabain in FRL (0.19 ± 0.10 to 0.12 ± 0.05 ms/mmHg) and FSL rats (0.36 ± 0.11 to 0.19 ± 0.05 ms/mmHg). In contrast, the magnitude of SNA inhibition evoked by AN stimulation was unchanged by ouabain infusion in all strains (Fig. 6.5). There was a significant positive correlation between the reflex increase in R-R interval / mmHg evoked by AN stimulation prior to ouabain infusion and the dose of ouabain required to elicit conduction block ($r^2 = 0.83$, $P<0.05$, pooled data from all strains).

Ouabain-Induced Arrhythmia

Continuous infusion of ouabain produced conduction slowing indicated by prolongation of the P-R interval and increased duration of the QRS complex QRS (Fig. 6.5). Conduction block was elicited in all animals at cumulative doses of 883 ± 38 μg in SD, 747 ± 64 μg in FRL and 713 ± 72 μg in FSL rats. Preceding conduction block, isolated VPBs were present in 3 / 7 FSL, 0 / 6 FRL and 1 / 6 SD rats and non-sustained runs of VT in 5 / 7 FSL, 2 / 6 FRL and 0 / 6 SD rats (Fig. 6.6).

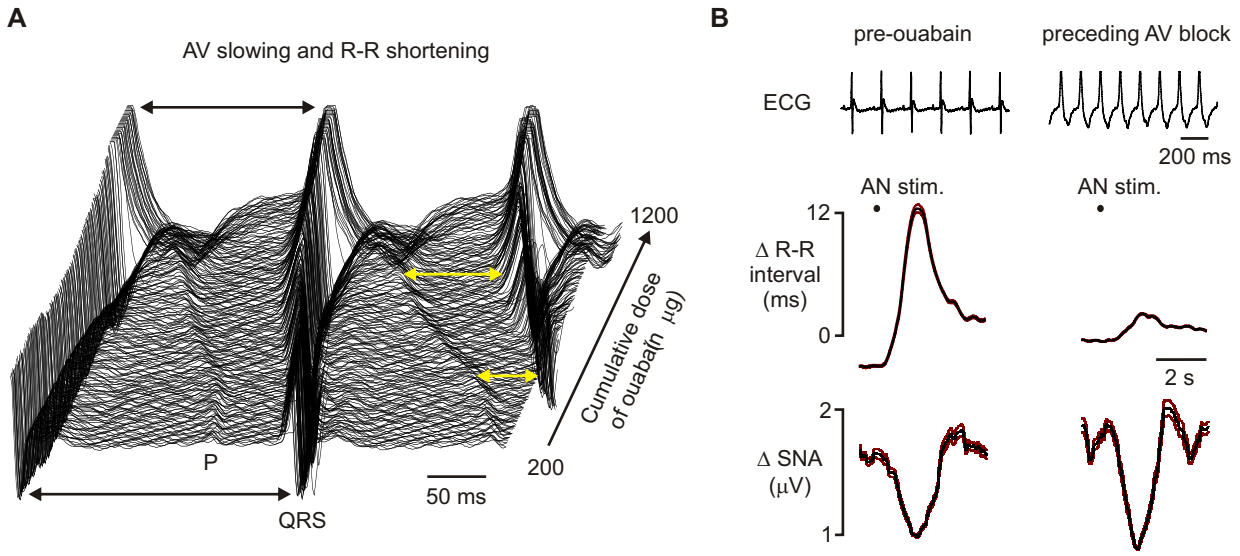

Figure 6.5 *Effect of ouabain on the ECG and baroreflex-evoked slowing of HR and inhibition of SNA*.**A:** Waterfall plot of ECG showing effects of continuous infusion of ouabain (200 µg/kg/min) in a urethane-anaesthetised SD rat. Ouabain causes lengthening of the PR interval (yellow arrows) and shortening of the RR interval (black arrows). **B:** ECG patterns illustrating control and late stages of ouabain intoxication and the corresponding average waveform responses of R-R interval and splanchnic SNA to tetanic stimulation of the aortic nerve (AN). During the control period AN stimulation evokes a profound bradycardia and sympathoinhibition; whereas ouabain infusion leads to almost complete inhibition of the baroreflex heart rate response but leaves the sympathetic response intact.

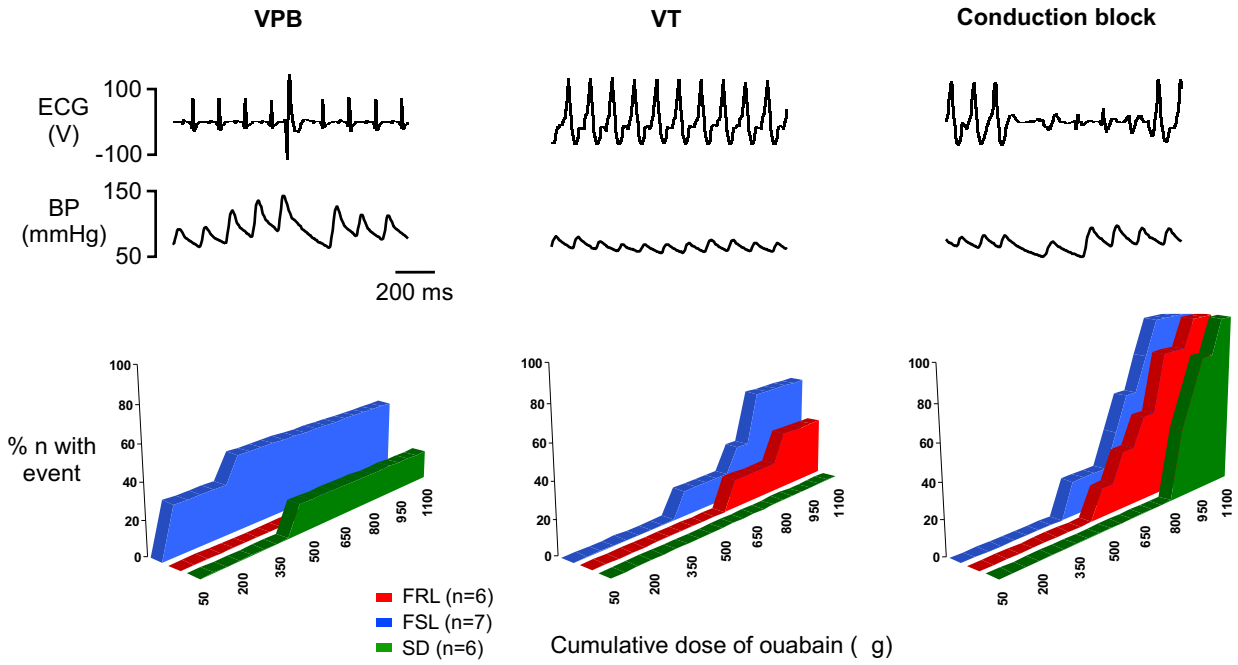

Figure 6.6 *Types and incidence of arrhythmia during continuous infusion of ouabain (200 mg/kg/min) in urethane-anaesthetised SD, FRL and FSL rats.* The top panels show characteristic patterns of ECG and BP used to identify different arrhythmias that occurred sporadically during ouabain infusion (see Methods). The bottom panels show the cumulative incidence of ventricular arrhythmias and / or conduction block in FRL, FSL and SD rat strains.

V. Discussion

The major findings of this study are that conscious FSL rats exhibited reduced HRV and BRS during the day and night and increased LF/HF ratio at night compared to FRL and SD rats. FSL and FRL rats were slightly more susceptible to conduction block elicited by ouabain compared to SD rats, although this result is limited by the small sample number. This effect may be related to the initial high resting HR seen in FRL and FSL rats under urethane anaesthesia due to a reduced vagal tone (see Chapter 4). FSL rats were most susceptible to ventricular tachyarrhythmias, which may be because in anaesthetised conditions there is a combination of impaired reflex vagal activation and sympathetic overactivity in this strain as seen in conscious FSL rats. These findings support the conclusion that FSL rats may have value in understanding neurobiological mechanisms linked to arrhythmia vulnerability in depressive disorders.

Conscious FSL rats had reduced HRV during the day and night compared to controls indicating an underlying reduction in vagal modulation of the sinoatrial node independent of sleep/wake influences. In contrast, LF/HF ratio was increased in FSL rats only at night indicating a relative predominance of sympathetic activity during wakefulness. Depressive symptoms in humans are associated with a reduction in HRV that is thought to be linked to altered sympathovagal control of the heart and increased risk of cardiac complications, including arrhythmias *(Carney et al., 2005b)*. Moreover, some studies have shown an increase in levels of plasma noradrenaline in depressed subjects *(Esler et al., 1982)*.

Genetic vulnerability is an important contributing factor in depression *(Fava and Kendler, 2000)*, although the extent to which reduced HRV in depressive disorders is dependent upon genes or environment is unknown. The present findings demonstrate for the first time that FSL rats, a well validated genetic animal model of depression, exhibits reduced HRV consistent with clinical observations in depression. Other rodent models of depression including olfactory bulbectomy (Ob) and chronic mild stress (CMS) also exhibit higher HR and reduced HRV *(Moffitt et al., 2002; Grippo et al., 2005)*. It is uncertain to what degree changes in cardiovascular status are influenced by the stressful procedures involved in inducing depressed-like behaviour in Ob and CMS models. Hence, one advantage of the behavioural phenotype in FSL rats is that it does not require any external intervention. Furthermore, we compared cardiovascular data obtained in conscious FSL rats to that in

obtained in two established control lines, neither of which shows depressed-like behaviour *(Overstreet et al., 2005)*. These data indicate that an underlying biological abnormality in FSL rats may be linked to the reduction in HRV seen in the conscious state. Whether or not external or early life influences contribute to changes in cardiovascular status in FSL rats is not known.

Conscious FSL rats had significantly reduced BRS during the day and night compared to both FRL and FSL rats. Recent studies demonstrated a reduction in spontaneous BRS in depressed patients *(Watkins and Grossman, 1999; Broadley et al., 2005)*. Indices of spontaneous BRS are inversely related to resting HR due to the influence of sinus cycle length on vagal inputs to the sinoatrial node *(Zaza and Lombardi, 2001)*. We found that FRL rats also exhibit a reduction in BRS that could be almost entirely accounted for by the fact that their heart rates are higher at rest. In contrast, correcting for HR had no effect on the low values of BRS obtained in conscious FSL rats. This may reflect an alteration in reflex regulation of HR independent of resting levels of autonomic tone to the sinoatrial node in FSL rats *(Pagani et al., 1988; Persson et al., 2001)*. There were some similarities between FRL and FSL rats including increased HF power of SAPV compared to SD rats. These characteristics may arise from separate mechanisms. In FRL rats they are likely due to resting tachycardia; whereas, in FSL rats they are likely due to reduced baroreflex buffering of respiratory-related AP oscillations.

Susceptibility to ouabain-induced arrhythmias was examined in FSL and FRL rats compared to SD rats under urethane anaesthesia. Under this anaesthetic, FSL and FRL rats both exhibit a marked lack of vagal tone leading to tachycardia and reduced spontaneous BRS (Chapter 4). These findings indicate that urethane has an exaggerated influence on HR in FSL rats, since under conscious conditions HR was normal in this strain. In FRL rats HR is elevated under urethane as well as in conscious conditions. Ouabain primarily had potent negative dromotropic effects on the heart and led to conduction block in all strains. In contrast, incidence of VPB and VT was higher in FSL rats compared to both SD and FRL rats. The cardiotoxic effects of ouabain are due to a combination of direct effects on the myocardium and increases in autonomic activity *(Yamazaki et al., 1996; Yamazaki et al., 1999)*. The dose of ouabain required to elicit conduction block in FRL and FSL rats was slightly less than in SD rats. One could speculate that, because negative dromotropic effects of ouabain result primarily from exocytotic release of ACh, this difference is because the initial level of vagal tone is lower in FRL and FSL rats compared to SD rats. In

contrast, ventricular tachyarrhythmias are caused primarily via arrhythmogenic actions of intracellular Ca2+ and exocytotic release of noradrenaline. It is possible that the higher incidence of ventricular tachyarrhythmias seen in FSL rats compared to both FRL and SD rats is because there is, additionally, a higher basal level of sympathetic activity in FSL rats. Although limited by a relatively small sample size, our findings indicate that FSL rats are more vulnerable to arrhythmogenic effects of ouabain compared to FRL and SD rats.

Although relatively specific for the cardiac Na+/K+-ATPase, ouabain is known to have other effects centrally and putative direct effects on baroreceptor fibres. A single bolus dose of ouabain (30 μg) was reported to increase discharge of vagal superior laryngeal fibres in rat, which the authors suggest reflects an excitatory effect on afferent baroreceptor activity *(Abreu et al., 1998)*. Our results do not support this finding, since ouabain did not alter the magnitude of SNA inhibition evoked by AN stimulation. In contrast, a decline in reflex bradycardia evoked by AN stimulation was noted during infusion of ouabain, until it was ineffective in producing reflex bradycardia just prior to conduction block. Presumably, this is due to a selective reduction in responsiveness of the sinoatrial node rather than changes in sensitivity of afferent or neural components of the baroreflex, since reflex effects on splanchnic SNA were intact throughout the experiments. We speculate that reduced responsiveness of the sinoatrial node or atrioventricular conduction system to baroreflex input is related to the arrhythmogenic effects of ouabain. This is supported by our observation that the greater the magnitude of resting bradycardia evoked by AN stimulation prior to ouabain infusion, the larger the dose of ouabain required to elicit complete conduction block.

The neurobiological basis of reduced HRV and BRS in depression is unknown. FSL rats exhibit several neurochemical abnormalities that may account for abnormal autonomic regulation of HR seen in this strain. This may include the cholinergic hypersensitivity for which they were originally bred, although several behavioural characteristics in FSL rats have now been shown to be independent of cholinergic responses *(Overstreet, 2002)*. Serotonergic abnormalities have also been observed in several brain regions although cardiovascular brain regions have not been explored *(Yadid et al., 2000; Overstreet et al., 2005)*. Neurotransmitters, such as acetylcholine *(Greco et al., 1999)* or serotonin *(Depres-Brummer et al., 1998)*, modulated by the sleep-wake cycle may also be relevant since indices of cardiac sympathetic activity were increased only at night. Similarly, neuroendocrine factors altered in FSL rats may play a role. For example, corticotrophin-

releasing hormone is diurnally regulated by pre-autonomic hypothalamic nuclei *(Buijs et al., 2003)* and modulates HRV *(Arlt et al., 2003)*. Alternatively these differences in HRV at night may be secondary to autonomic effects of activity, feeding or stress-reactivity known to differ in FSL rats compared to controls *(Yadid et al., 2000; Overstreet et al., 2005)*.

Summary

In conclusion, we demonstrate for the first time reduced HRV and BRS in a genetic animal model of depression, closely resembling the cardiac autonomic abnormalities seen in human depression. Reduced reflex vagal modulation and predominance of sympathetic activity at the sinoatrial node seen in FSL rats may predispose to development of cardiac complications, including arrhythmias. Urethane anaesthesia may exacerbate autonomic abnormalities in FSL rats leading to increased susceptibility to ouabain-induced arrhythmias. Future investigation of biological causes of reduced HRV and BRS in FSL rats may shed light on neurochemical abnormalities underlying increased cardiovascular risk in depression.

Chapter 7 Concluding Remarks and Future Directions

The critical neural circuitry underlying circulation and breathing movements is located within the hypothalamus and lower brainstem. This circuitry is wired from birth to respond to homeostatic challenges that permit survival in the face of raised CO2, injury or blood loss. This circuitry must also adapt to changes in oxygen requirements during exercise, such as when catching prey or fleeing predators, or changes in arousal state. In addition, there must be adaptive solutions to long term physical changes including aging, pregnancy and disease. Hence, identifying and understanding the synaptic and genetic mechanisms that regulate activity of cardiorespiratory circuits are of immense importance. Figure 7.1 shows a simplified schema of the organisation of peripheral afferent and higher order inputs to the lower brainstem that modulate autonomic function and respiration, as a result of this thesis and extensive previous work. Neurotransmitters implicated in different pathways are shown.

The findings of Chapter 3 provide new information about the neuronal targets and function of cholinergic inputs to the RVLM. Cholinergic agonists increase sympathetic activity via activation of pre- and postsynaptic mAChR in the RVLM *(Giuliano et al., 1989; Huangfu et al., 1997)*. This response was presumed to involve the M2 receptor and was thought to excite RVLM neurons mainly via disinhibition *(Giuliano et al., 1989; Milner et al., 1989; Arneric et al., 1990)*. We showed for the first time that some non-TH spinally projecting neurons express mRNA for the M2 or M3 receptor; however, both TH and PPE+ spinally projecting neurons receive inputs from cholinergic terminals. Endogenous cholinergic inputs hence presumably modulate activity of a subpopulation of C1 and non-C1 RVLM neurons via activation of pre and post-synaptic mAChR, respectively.

The specific functional roles of RVLM neurons that receive cholinergic inputs are not known. Presumably many of them are barosensitive vasomotor neurons, as local mAChR activation increased splanchnic SNA, HR, AP and barosensitivity. RVLM neurons that supply cutaneous beds probably do not receive cholinergic inputs, since increases in TBF evoked by central mAChR activation were not mediated via the RVLM. Others may be

non-vasomotor in function; eg RVLM neurons that are low glucose-sensitive and supply the adrenal gland *(Madden et al., 2006)*, although we did not test the effect of local mAChR activation on this subgroup. Future studies could record from multiple sympathetic outflows following direct injection of muscarinic agonists into the RVLM to elucidate precisely which populations of RVLM neurons are affected.

In this thesis it was demonstrated that RVLM mAChR activation differentially affects cardiovascular reflexes, producing a resetting of the sympathetic baroreflex to higher AP and higher gain but attenuating sympathoexcitatory reflexes. This is unlike other amine or peptide receptors in the RVLM that when activated selectively gate effectiveness of one reflex but do not tend to alter others. For example, activation of 5-HT1A *(Miyawaki et al., 2001)* or δ-opiate receptors *(Miyawaki et al., 2002b)* in the RVLM selectively inhibits the somatosympathetic reflex; whereas activation of μ-opiate receptors selectively inhibits the sympathetic baroreflex *(Miyawaki et al., 2002b)*. These data support the notion that different neurotransmitter inputs to the RVLM encode functional specificity in control of sympathetic outflow and reflex function.

The modulation of cardiovascular reflexes by different inputs is presumably critical to certain patterns of behaviour. During exercise, for example, the increase in visceral resistance and buffering capacity of the baroreflex acts to maintain high systemic AP and offset fluctuations of muscle blood flow *(Rowell and O'Leary, 1990; Williamson et al., 2006)*. Other stimuli that reset the baroreflex to higher SNA and AP include air jet stress *(Kanbar et al., 2007)* or activation of the dorsomedial hypothalamus (DMH) *(McDowall et al., 2006)*. Baroreflex adjustments during 'fight or flight' responses or stress may also serve to anticipate cardiovascular challenges accompanying potential sudden movement. Conversely, there is a suppression of baroreflex control during REM sleep, which is accompanied by muscle atonia *(Nagura et al., 2004)*. Similarly, opiates may be released in the RVLM to inhibit the baroreflex during pain or blood loss to promote sympathoinhibition and inactivity. Hence, the set-point and sensitivity of the baroreflex are determined by the CNS depending on behaviour or arousal state.

Our data indicate that the cholinergic pathway from the PPT to the RVLM is one important subcortical pathway involved in resetting of the baroreflex (Figure 7.1). Recent work in humans also indicates the importance of subcortical structures in cardiovascular changes associated with anticipated exercise *(Green et al., 2007)*. Input from cortical regions

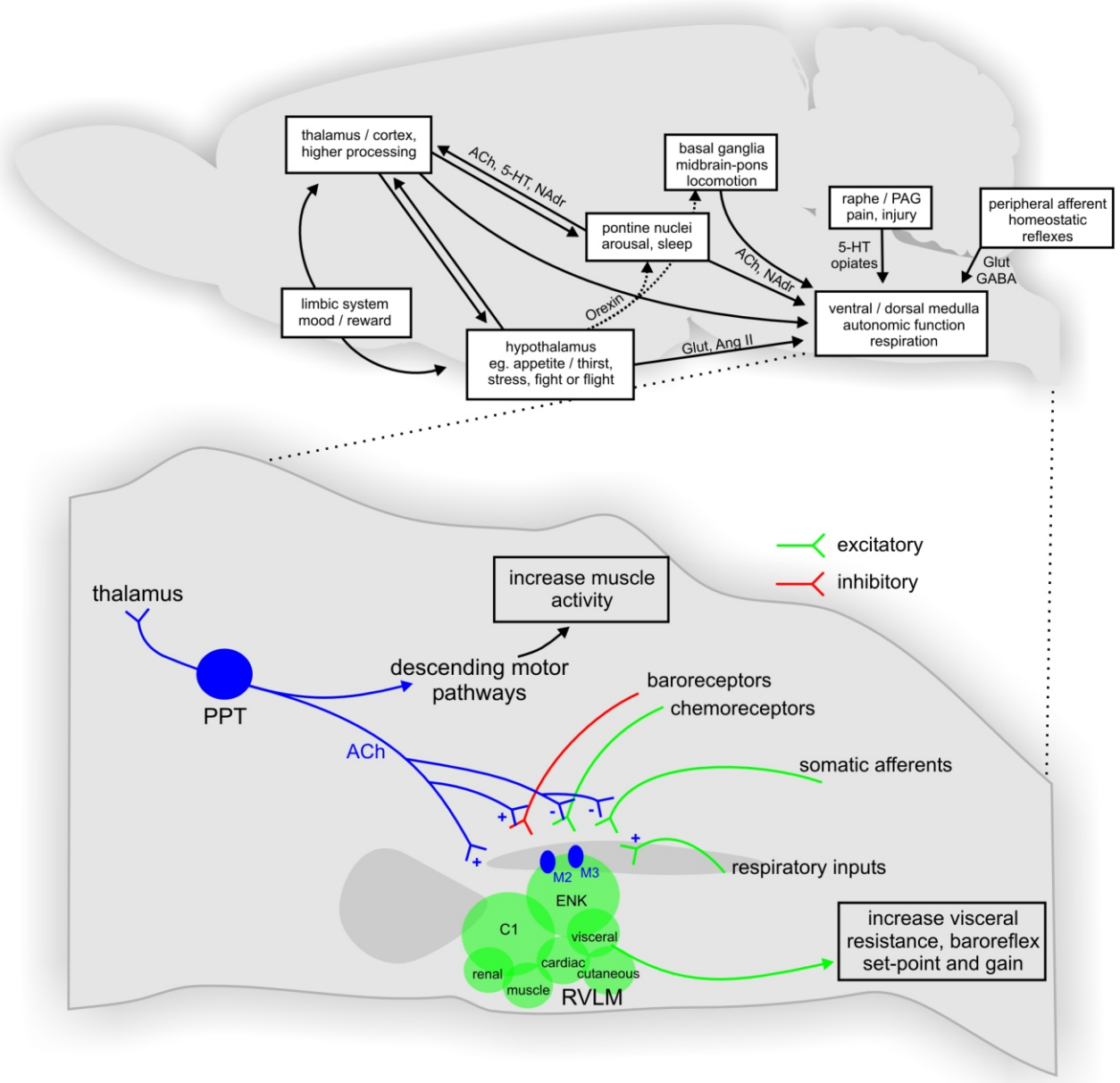

Figure 7.1 *Simplified schema of organisation of peripheral afferent and higher order inputs to the lower brainstem.* Inputs arriving in the dorsal and ventral medulla from higher brain centres are concerned with regulating autonomic function and respiration appropriate to changes in *inter alia* mood, appetite, thirst, sleep and movement. These inputs contain a diverse range of neurotransmitters, some of which are released only under certain conditions. Hence, presumably, their release in the medulla may encode functional specificity in control of vagal or sympathetic outflow and /or respiration. This thesis demonstrates that cholinergic inputs to the RVLM originate from the PPT, which appears capable of parallel adjustments of motor and cardiovascular function. Activation of the PPT modulates presynaptic inputs to the RVLM, leading to an increase in sympathetic baroreflex set-point and gain and attenuation of excitatory reflexes, and also directly excites some RVLM neurons leading to increases in visceral resistance and systemic arterial pressure. This circuit may be crucial to cardiovascular adjustments evoked at the onset of exercise or changes in arousal state.

probably relays via brainstem circuits capable of parallel adjustments of muscle and cardiorespiratory activity, such as the PPT. These circuits can also operate independent of higher input, eg during 'fight or flight' responses *(McDowall et al., 2006; Kanbar et al., 2007)* or in decerebrate animals *(Chong and Bedford, 1997; Koba et al., 2006)* and hence have probably been crucial to survival.

Future studies may examine effects of central mAChR blockade on cardiovascular adjustments, including modulation of the baroreflex, during exercise or sleep in animals. Are the same brain regions involved in baroreflex resetting during 'fight or flight' responses as well as exercise? Moreover, are the same neurochemicals involved, eg are mAChR in the RVLM involved in cardiovascular responses to air jet stress? Recent work has shown that diurnal activation of orexinergic projections from the lateral hypothalamus to the PPT mediates muscle activation during wake and muscle atonia during sleep *(Takakusaki et al., 2005)*. Future studies may determine whether or not orexinergic inputs to the PPT contribute to diurnal variations of AP or baroreflex function.

As described in Chapters 1 and 3, nAChR and mAChR have widespread effects in autonomic and respiratory nuclei within the ventral medulla. As shown in Chapters 4 – 6, rats selectively bred for differences in sensitivity to cholinergic agonists show specific autonomic and respiratory disturbances. These data suggest that genetic differences in central mAChR sensitivity have long term consequences for regulation of cardiorespiratory function. Previously, only gene knockout models have been used to illustrate cardiorespiratory abnormalities following deletion of specific mAChR or nAChR subtypes *(Bymaster et al., 2001; Bymaster et al., 2003b; Fisher et al., 2004)*. These models are useful but the interpretation of central changes is limited because loss of nAChR or M2 or M3 receptors also disrupts peripheral autonomic transmission and studies have examined only knockout rather than knock-in or overexpression models. Future studies might utilise alternative knockout models that target kinases involved in regulation of receptor-G protein phosphorylation (GPRKs). For example, mice lacking GPRK-5 are supersensitive to behavioural and hypothermic effects of OXO and lack mAChR desensitisation *(Gainetdinov et al., 1999)*. Moreover, peripheral mAChR involved in airway and cardiac responses appear to be regulated by a different isoform, GPRK-3 *(Walker et al., 1999)*.

Changes in central mAChR function in FSL rats may be complex and hence interpretation of data is not straightforward. We showed that in some brain regions there are increases in

mRNA indicating increased receptor levels. However, as we and others *(Greco et al., 1998; Daws and Overstreet, 1999)* have shown, this is not the case in all brain regions, which could indicate regional differences in mAChR regulation. Our data also show that mAChR supersensitivity in FSL rats is limited to thermoregulatory responses; whereas sympathetic effects appear unaffected and respiratory depressant effects are attenuated. Hence, mAChR involved in different CNS functions must be regulated independently at the genetic or post-transcriptional level and clearly the breeding protocol used in FSL rats does not result in upregulation of all mAChR systems. Moreover, it is clear that there are several neurotransmitter abnormalities in FSL rats, including changes in serotonin, dopamine and peptide signaling *(Yadid et al., 2000; Overstreet et al., 2005)* that could account for the autonomic and respiratory disturbances. Presumably, these arise due to functional interactions between mAChR and other G-protein coupled receptor pathways, or changes in common intracellular regulatory mechanisms.

The reduction in HRV and BRS seen in FSL rats has several implications. Because we found a reduction in reflex control of vagal input to the heart as well as peripheral sympathetic activity, autonomic disturbances in FSL rats presumably have a central component. The precise areas involved are unclear but the activity of neurons in several key regions of the medulla, including the NTS, RVLM or NA, may be disrupted by variations in nAChR or mAChR function. Future studies may address the involvement of other neurotransmitters such as endogenous opioids, angiotensin or serotonin in central baroreflex pathways in FSL rats, or the functional interaction between cholinergic and other neurotransmitter receptors.

We observed a heightened susceptibility to ouabain-induced arrhythmia in FSL rats under anaesthesia. It remains to be seen whether or not this reflects altered basal levels of autonomic input to the sinus node. The reduction in HRV seen in FSL rats, and increased LF/HF ratio at night reflects a reduction in reflex vagal activity and elevated sympathetic activity. This altered autonomic imbalance has been considered pro-arrhythmic *(Hull et al., 1990; Barron and Lesh, 1996; Zipes and Wellens, 1998; Lombardi, 2002)*. However, issues surrounding interpretation of spectral indices, particularly as a marker of sympathetic activity in rat, are still controversial. The best evidence to data has come from studies using autonomic blockade. For example, in conscious rats LF/HF ratio is reduced by beta-adrenergic receptor blockade with atenolol following pre-treatment with atropine to block vagal inputs *(Waki et al., 2006)*. Ongoing work in our laboratory has also shown

that in conscious FSL rats LF/HF ratio is normalised by atenolol (C. Hildreth, personal communication). Hence, the simplest interpretation and one supported by our data is that the LF/HF ratio does reflect the level of sympathetic activity, particularly against a low background level of vagal activity, as presumably is the case in FSL rats.

FSL rats had an exaggerated increase in HR under urethane anaesthesia compared to the conscious state compared to other strains. This effect was intriguing because non-volatile as well as volatile anaesthetic agents exert their effects by binding specific neurotransmitter gated ion channels (eg. GABA, muscarinic, nicotinic, NMDA, AMPA) *(Hara and Harris, 2002)*. Hence, the exaggerated effect of urethane on HR may reflect underlying changes in nicotinic or GABA receptors, for example, that control HR in FSL rats. Moreover, because urethane altered autonomic activity, it could have contributed to the increased susceptibility to arrhythmia seen in FSL rats.

In humans, perioperative complications associated with anaesthesia including arrhythmias are a major problem *(Newland et al., 2002)*. Many anaesthetic agents bind nAChR and mAChR (for review see *(Cohen et al., 2006)*. Volatile and non-volatile anaesthetics also cause reductions in HRV and BRS *(Constant et al., 2000)*; although to our knowledge there have been no studies that have examined the relative autonomic effects of anaesthetics with actions at cholinergic versus other neurotransmitter receptors. Variations in central cholinergic receptor sensitivity could directly modulate autonomic effects of anaesthetics and hence predispose to, or protect from, anaesthesia-related arrhythmia and possibly death.

The FSL rat is considered to model many of the symptoms seen in depressive disorders *(Yadid et al., 2000; Overstreet et al., 2005)*. Alterations in behaviour, sleep and psychomotor function in FSL rats reflect in part the widespread involvement of mAChR in cortical and subcortical functions *(Yadid et al., 2000; Overstreet et al., 2005)*. Other neurotransmitter disturbances besides ACh, in particular serotonin, are also implicated in behavioural alterations seen in FSL rats *(Overstreet et al., 1998)*. Moreover, two week administration of conventional (eg SSRI) or novel antidepressants can alleviate these symptoms in FSL rats *(Zangen et al., 1997; Yadid et al., 2000)*.

The findings of this thesis are the first to show that FSL rats exhibit cardiovascular disturbances similar to those reported in depressed humans, ie reduced HRV and BRS

(Agelink et al., 2001; Agelink et al., 2002). Increased risk of fatal arrhythmia in patients with depression and cardiovascular disease has been attributed to abnormal autonomic nervous system activity as well as other pro-arrhythmic factors *(Carney et al., 2005a)*. The finding that FSL rats are also more susceptible to ouabain-induced ventricular arrhythmia further supports this possibility. Despite the adverse relationship between depression and cardiac mortality, there is doubt as to the precise aetiology of autonomic disturbances in depressive disorders and whether or not they involve psychosocial or biological factors or a combination of both *(Carney et al., 2005a; Freedland et al., 2005; Gehi et al., 2005a).* The present findings in FSL rats demonstrate that cardiovascular disturbances associated with a depressed phenotype could have a biological foundation in changes in central neurotransmitter sensitivity. Figure 7.2 presents a hypothetical model of how genes that influence muscarinic or related neurotransmitter receptors involved in control of central autonomic outflow could lead to increased cardiovascular risk in depression.

Evidence for hypersensitive mAChR in depression comes from pharmacological challenge studies, which have shown increased cortisol, endorphin and induction of REM sleep in response to mAChR agonists in depressed patients *(Risch et al., 1983; Gillin et al., 1991)*. Also, chronic stress, which may contribute to the pathogenesis of depression, has been shown to increase the sensitivity of mAChR in rat *(Gonzalez and Pazos, 1992; Roman et al., 2006)*. At present, few studies have directly examined the sensitivity of muscarinic or other receptors in control of autonomic outflow in human depression. Intriguingly, the same polymorphisms in the gene encoding the M2 receptor are associated with alcohol dependence and depressive disorders *(Wang et al., 2004)* as well as indices predictive of increased cardiovascular risk (increased LF/HF ratio and delayed heart rate recovery after maximal exercise) *(Hautala et al., 2006).*

Clearly there is a spectrum of neurotransmitter disturbances in FSL rats that could contribute to altered autonomic outflow in this strain. It is also possible that inappropriate regulation of autonomic function by arousal or motor systems contributes to cardiovascular abnormalities seen in FSL rats and depressed humans (see Fig. 7.1). Future studies may determine whether or not conventional or novel antidepressants can alleviate autonomic dysfunction seen in FSL rats. Moreover, the use of agents that target serotonin or noradrenaline uptake selectively, or other agents that target peptide systems or neurotrophins, may help elucidate the underlying causes of autonomic dysfunction seen in FSL rats.

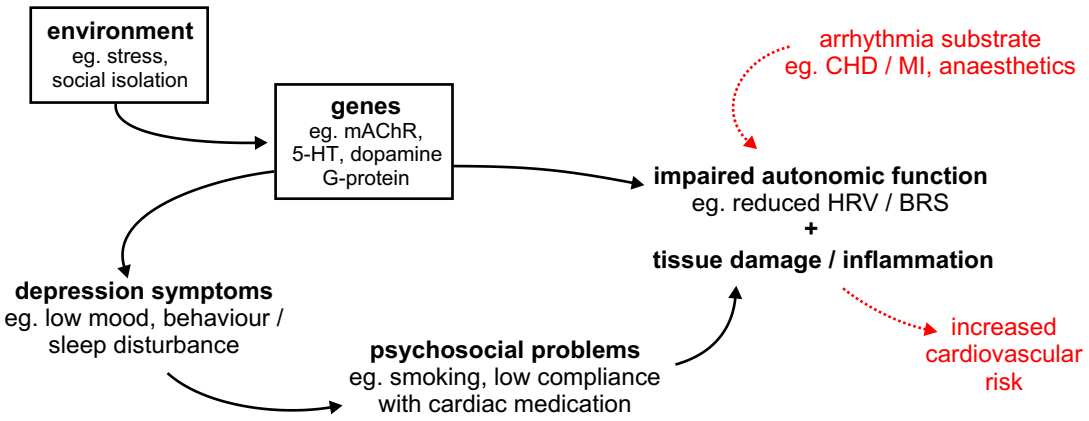

Figure 7.2 *Hypothetical flow diagram of factors predisposing to increased cardiac risk in depression.* A combination of genetic and environmental factors is thought to underlie the onset and recurrence of depression symptoms, mainly as a result of neurotransmitter perturbations in brain regions concerned with mood, behaviour and sleep. Autonomic inputs to the heart are also altered in depression, although the underlying cause is unknown. This thesis shows that a genetic animal model of depression bred for muscarinic receptor hyper-sensitivity, the FSL rat, exhibits similar autonomic disturbances to those reported in human depression (ie. reduced HRV and BRS). This suggests for the first time that a depressed behavioural as well as cardiovascular phenotype in rat may be due to disturbances in similar neurotransmitter systems. It is likely that other factors, including prevalence of smoking, also contribute to increased cardiovascular risk in human depression.

Chapter 8 Appendices

I. Appendix 1

A Guide to R-R Interval Sequence Analysis in Spike 2

A script for use in Spike2 (Cambridge Electronic Design Ltd, UK) to calculate spontaneous heart rate baroreflex sensitivity using the sequence method is transcribed in full at the end of this guide. The algorithm and initial version of the script were written by David Crick and Greg Smith (CED Ltd, UK). The version transcribed below was adapted by the candidate to allow heart rate to be derived from an AP wave (not just ECG) and to increase user-friendliness and enable settings to be altered without going back into the programming.

The version below has default settings of three consecutively lengthening or shortening sequences and a corresponding rise or fall in MAP of 0.5 mmHg, respectively, with no time lag. The first dialogue box will let you change the number of consecutive sequences and or the size of the corresponding change in MAP (Fig 8.1A, Dlg 1). The mode of import of ECG or AP events is alternative (corresponding integers in the dialogue box are 0 peaks, 1 troughs, 2 data rising through level, 3 data falling through level) (Fig. 8.1A, Dlg 2). The script will also let you find sequences corresponding to changes in systolic or diastolic pressure or in fact any waveform in the data file. All you have to do is first create the channel of interest in the data file (eg systolic pressure) (if not already a separate channel) and then choose this channel as the waveform channel containing BP data when the first dialogue box opens up.

Once the script is running, an XY view (X: R-R interval in sec; Y: MAP in mmHg) will pop up containing all lengthening sequences and the slope is displayed (MAP(mmHg)/R-R interval(s)) (Average slope (1)) (Fig. 8.1B). It is inconvenient but naturally the baroreflex sensitivity is the inverse of this value in s/mmHg (x 1000 to obtain ms/mmHg). You have to record this value; it will not remain once you next click OK. Similarly, the next click plots the additional shortening sequences on the XY view and displays the slope (Average slope (0)) – record this too. On the next click you will return to the data file and the XY

view remains open. In the data file, you will find that a heart rate event channel has been created and each sequence is captured in a separate event channel (Fig 8.1B). If you do not save these new memory channels then they will be deleted once you close the file. There are numerous additional things one might do with these channels – for example, the total number of sequences with respect to total number of changes in MAP has been used in cats as an index of "baroreflex effectiveness" *(Di Rienzo et al., 2001)*.

The only catch if you have long recordings is that you have to export the bit of the data file you want to analyse before running the script (2 – 5 mins of data, or longer). Another PhD student in the lab (Cara Hildreth) has overcome this potential frustration by creating a script to export short segments of data for sequence analysis from the main data file before she starts the analysis itself.

The minimum requirement for application of this script is an AP waveform recording. ECG is optional but recommended if there is to be no doubt about the R wave fiducial point or if you suspect vascular remodeling in an animal or if there is doubt over the integrity of the AP wave recording. Changes in arterial stiffness / aortic wave propagation may affect measures of heart rate variability measured using pulse interval. In our experience there is little difference between heart rate variability calculated from R-R interval from the ECG or pulse interval from intra-arterial pressure recordings in rat. There are certainly data in humans to indicate differences between R-R interval variability taken from the ECG and pulse interval variability when AP was recorded non-invasively from a finger cuff *(Constant et al., 1999)*. Recommended minimum sampling rate for AP or ECG is 200 Hz.

Sequence Analysis 2005©

```
'in this version events are extracted from ECG to the MEMchannel as they rise through a level. At present this is set to
'7.8, but obviously can be changed to suit.
'need to have output data stored somewhere.

'18th Jan changes (JP). 1) HR channel changed to event positive MemChan(3,0,0,0)
'2) Added MemImport variables for ECG event channel
'3) Added Dlg for creating heart rate channel and changed to var in MemImport
'4) Changed Interact to all possible interactions 8191
'5) Undelete memory channels

'$BaroRef|Locate areas with baro reflex and mark them
var RWave%;             'the memchan that holds the events from the ECG peaks
var BP% := 1;           'the waveform channel with the BP data
var ec% := 2;           'the waveform channel with ECG data
```

```
var numint% :=3;        'the number of intervals used as a default
var bpchng  :=0.5;      'the minimum fall in BP to seek if consecutive rise or fall in RR periods
var mcl%, mcs%;             'The memory channels to hold our "interesting" places
var mode% :=2;                              'the mode of the ECG event channel for MemImport
var time :=0.08;                    'the minimum interval for detecting ECG events for MemImport
var level :=10;                     'the level for detecting ECG events depending on mode for
MemImport

'make sure we have a time view first
var tv%, xy%;         'the original time view and an xy view
tv% := FileOpen ("", 0, 3, "Browse to find a data file"); 'find a file to open
Interact("find a file to work on",1023); 'find a file
'if ViewKind()<>0 then message("Select a time view first"); halt endif;

DlgCreate("Values to use in baroRef program");  'Start new dialog
DlgChan(1,"Where is the ECG - Channel ?",16384+1);
DlgChan(2,"Where is the BP channel",16384+1);
DlgInteger(3,"How many R-R intervals?",2,6,0,0,1);
DlgReal(4,"What change in BP do you want to seek?",0.000000,20.000000,0,0,0.100000);
DlgButton(0,"Cancel");
DlgButton(1,"OK");
if DlgShow(ec%,bp%,numint%,bpchng) = 0 then    'ok is 0 if user cancels,  variables updated if not
  halt;
endif;

xy% := FileNew(12,1); 'make an xy view
if xy%<=0 then halt endif;
View(tv%);            'back to the time view

DlgCreate("Values for creating memory channel holding ECG events"); 'Start new dialogue
DlgInteger(1,"Detect peak or level?",0,3,0,0,1);
DlgReal(2,"Minimum interval for detecting events?",0.000000,1.000000,0,0,0.100000);
DlgReal(3,"Level?",0.000000,100.000000,0,0,0.100000);
DlgButton(0,"Cancel");
DlgButton(1,"OK");
if DlgShow(mode%,time,level) = 0 then    'ok is 0 if user cancels,  variables updated if not
  halt;
endif;

' Now create a memory channel holding events for ECG peaks
rwave% := MemChan(3,0,0,0);
ChanShow(rwave%);
MemImport(rwave%,ec%,0.0,MaxTime(),mode%,time,level);

mcl% := MemChan(2);    'create a memory channel
if mcl%<=0 then halt endif;
ChanShow(mcl%);        'make it visible
ChanTitle$(mcl%, "Lengthen");
FindIncInc(numint%, bpchng, 0, maxtime(), RWave%, BP%, mcl%, xy%, 1);

mcs% := MemChan(2);    'create a memory channel
if mcs%<=0 then halt endif;
ChanShow(mcs%);        'make it visible
ChanTitle$(mcs%, "Shorten");
FindIncInc(numint%, bpchng, 0, maxtime(), RWave%, BP%, mcs%, xy%, 0);

Interact("Admire data", 1023);
```

```
'n%     The number of periods of consecutive changes we want
'minInc The minimum increment over the n beats that we will accept
'st           Start time of the range to search
'et     End time of the range to search
'ec%    The event channel that marks the peaks
'bp%    Channel holding blood pressure data
'mc%    memory channel to hold marks of the first interesting beat
'xy%    an XY view to fill with the data points
'up%    Selects lengthening rr interval if 1, shortening if zero
'Return the number of marks we inserted
Func FindIncInc(n%, minInc, sT, eT, ec%, bp%, mc%, xy%, up%)
if n% < 2 then return -1 endif;   'stupid count of periods
if (ChanKind(ec%)<2) or (ChanKind(ec%)>8) then return -2 endif;
if (ChanKind(bp%)<>1) and (chankind(bp%)<>9) then return -3 endif;
var ne%, ok%;
ne% := Count(ec%, sT, eT);   'count events in the time range
if ne% <= n% then return 0 endif;
var t[ne%], p[ne%], b[ne%], i%, j%;
if ChanData(ec%, t[], sT, et)<>ne% then return -4 endif;
arrconst(p, t);              'copy all array t into p
arrdiff(p);                  'convert to periods
for i% := 0 to ne%-2 do
  b[i%+1] := Chanmeasure(bp%, 2, t[i%], t[i%+1]);
  next;

var s, slopesum := 0, found% := 0;

'Now search for n% consecutive increasing periods.
for i% := 1 to ne%-2-n% do
  j% := 0;
  if (up% > 0) then
    while (j%<n%-1) and
        (p[i%+j%] < p[i%+j%+1]) and
        (b[i%+j%] < b[i%+j%+1]) do
      j% += 1;
    wEnd;
  else
    while (j%<n%-1) and
        (p[i%+j%] > p[i%+j%+1]) and
        (b[i%+j%] > b[i%+j%+1]) do
      j% += 1;
    wEnd;
  endif;
  if (j% = n%-1) then
    if (up% > 0) then
      ok% := (b[i%+n%-1] - b[i%]) >= minInc;
    else
      ok% := (b[i%+n%-1] - b[i%]) <= minInc;
    endif;
    if ok% then
      MemSetItem(mc%, 0, t[i%-1]);
      View(xy%).XYAddData(1, p[i%:n%], b[i%:n%]);
      s := Slope(p[i%:n%], b[i%:n%]);
      slopesum += s;
      found% += 1;
    endif;
```

```
   endif;
   next;

if found% > 0 then
   Message(Print$("Average slope (%d) is %g", up%, slopesum/found%));
else
   Message("No places meet the criterion %d", up%);
endif;
return found%;
end;


Func Slope(x[], y[])
var coef[2];
FitPoly(coef, y[], x[]);
return coef[1];
end;
```

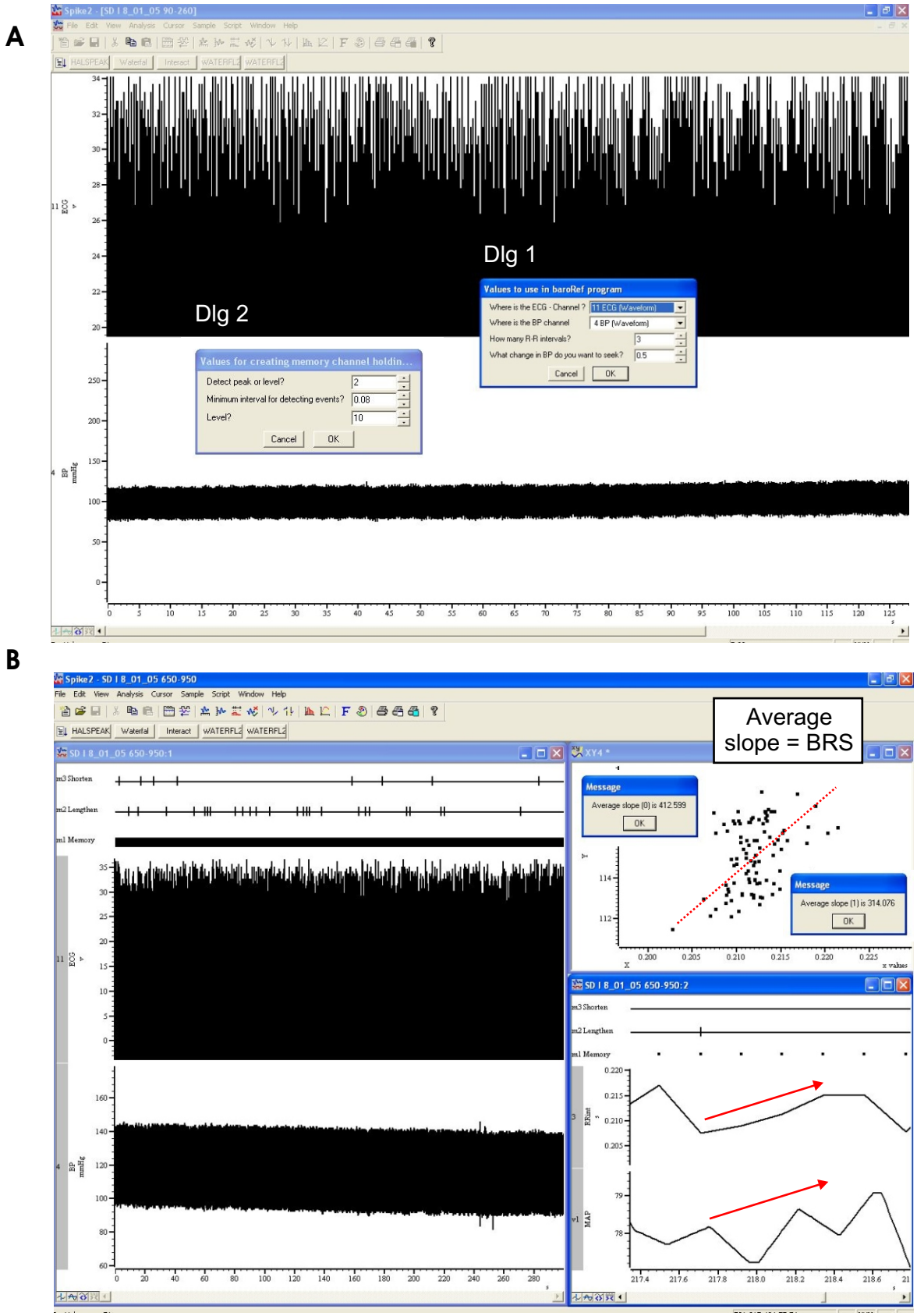

Figure 8.1. *Sequence Analysis in Spike2 software (CED Ltd, UK) using user-defined parameters for detecting R-R or pulse interval baroreflex sequences*

A Guide to Spectral Analysis in Spike 2

Spectral analysis was performed using Spike2 software (Cambridge Electronic Design Ltd, UK) and an Excel® spreadsheet was created to capture data.

Spike2 has an in-built power spectrum analysis tool that converts time series into the frequency domain using a fast-Fourier transform (FFT). The major pitfall when using this tool to create power spectra of AP, R-R interval and nerve activity is inappropriate processing of the raw signals. The critical factor is that all waveforms for spectral analysis must be uniformly re-sampled at a frequency not less than double the highest frequency you are interested in (Nyquist frequency). For example, Mayer wave and respiratory frequencies occur below ~ 3 Hz in rat; hence a resampling rate of 10 Hz is appropriate. If interested in cardiac rhythmicity (~ 6 Hz under anaesthesia) then a resampling rate of 20 Hz is appropriate, and so on… It is OK to resample at higher frequencies, eg. 100 Hz, but bear in mind that the size of the FFT will need to be increased to improve frequency resolution in the power spectra. The frequency resolution = sampling frequency / size of FFT (eg. a size 256 FFT on 10 Hz data will give a spectral resolution of ~0.04 Hz).

Signal processing

Systolic Pressure and R-R Interval

When deriving R-R (or pulse) interval and systolic pressure (or mean or diastolic) from ECG / AP, bear in mind that these will need to be converted into a waveform. I found the easiest method is to create these channels as RealMark data (using Analysis/Measurements/Data Channel). Then using the Create Virtual Channel analysis tool this can be converted into a waveform by linear interpolation (Expression is Rm({ChanNum})) and the sampling interval can be specified (eg. 0.1 sec for a 10 Hz sampling rate). Also make sure that all channels are aligned to the same time origin when resampling (Fig. 8.2A).

SNA (or other waveforms acquired online eg PNA)

Full wave rectify and smooth SNA with a modest time constant (~ 40 ms). Under Channel Process choose Interpolate, and here you can select the sampling interval (0.1 sec for 10

Hz sampling rate) and align the resampling to begin at the same time as all other channels (Fig. 8.2A).

Removal of DC Component

Prior to spectral analysis make sure that the DC component of all channels is removed using Channel Process; this will avoid a very large very low frequency band in the power spectra, which will also influence broadband power. One consideration is the time constant for DC removal; Spike calculates the mean of data in this time period (as a moving average) and subtracts this value from each data point as it moves along the channel. This means that fairly stationary data will be unaffected no matter what the time constant, as long as it is not too small or large (10 – 30 seconds seems appropriate). Also bear in mind the data around the edges of the region selected for spectral analysis; artifacts or dramatic changes from baseline here will dramatically affect the data inside the region of interest if the time constant for DC removal is too large.

Quantifying Spectral Power

Spike 2 result files (Fig. 8.2B, 8.4A) can be copied as text and pasted directly into an Excel® spreadsheet (Fig. 8.3, 8.4B). Power in specific frequency ranges can be summed and the raw values used for calculation of normalised power, LF/HF ratio and other indices such as the α-coefficients (Fig. 8.3, 8.4B). In order to obtain meaningful values for SNA variability, which can then also be compared between treatment regimens and between strains etc, data must be normalised. Absolute deviations of SNA from zero after DC removal (μV) (ie power) can be expressed as a percent of absolute mean SNA of the data segment (μV). Hence, summed power in frequency ranges is expressed as $\%^2$. The advantage of Excel is that data can be linked to embedded graphs that automatically update, and data can be easily transferred to other programs for presentation etc. Moreover, there is also potential for programming using Macros in Excel in order to generate autospectra and calculate the transfer function between SAP and RRI or SNA throughout a range of frequencies.

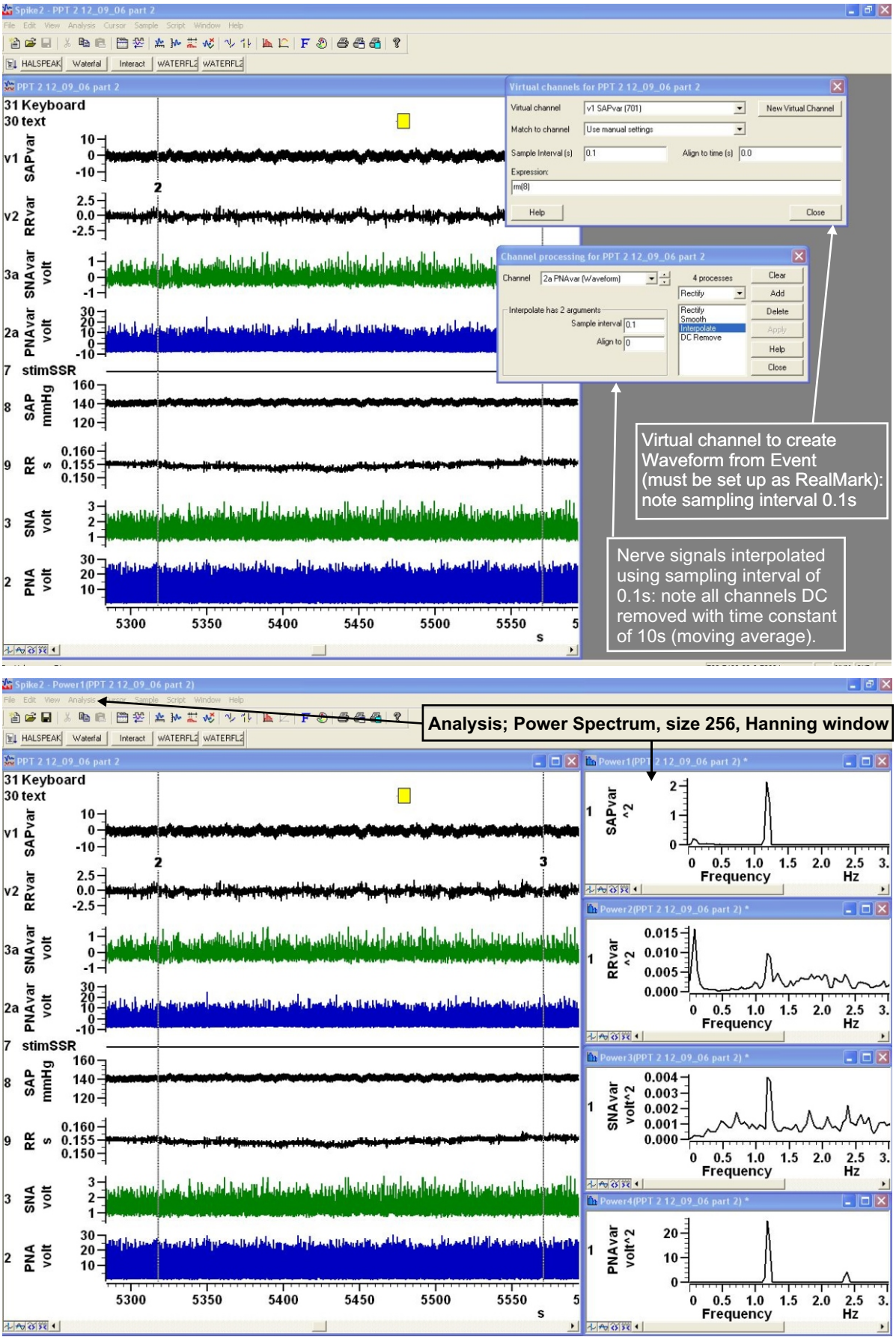

Figure 8.2 *Signal Processing for Spectral Analysis using Spike2 software (CED Ltd, UK)*

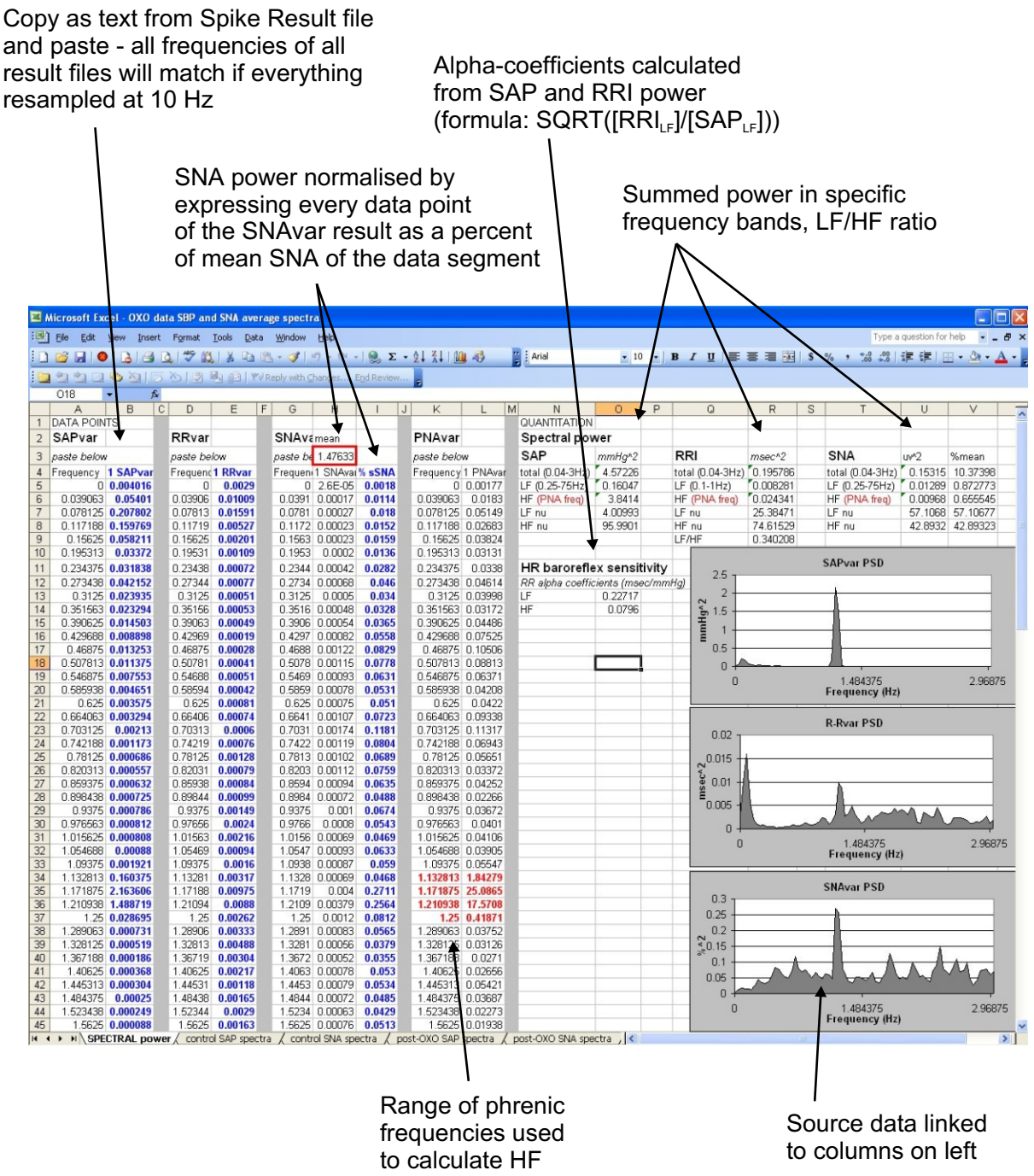

Figure 8.3. *Excel spreadsheet for calculating spectral parameters of SAP, RR interval and sympathetic nerve activity*

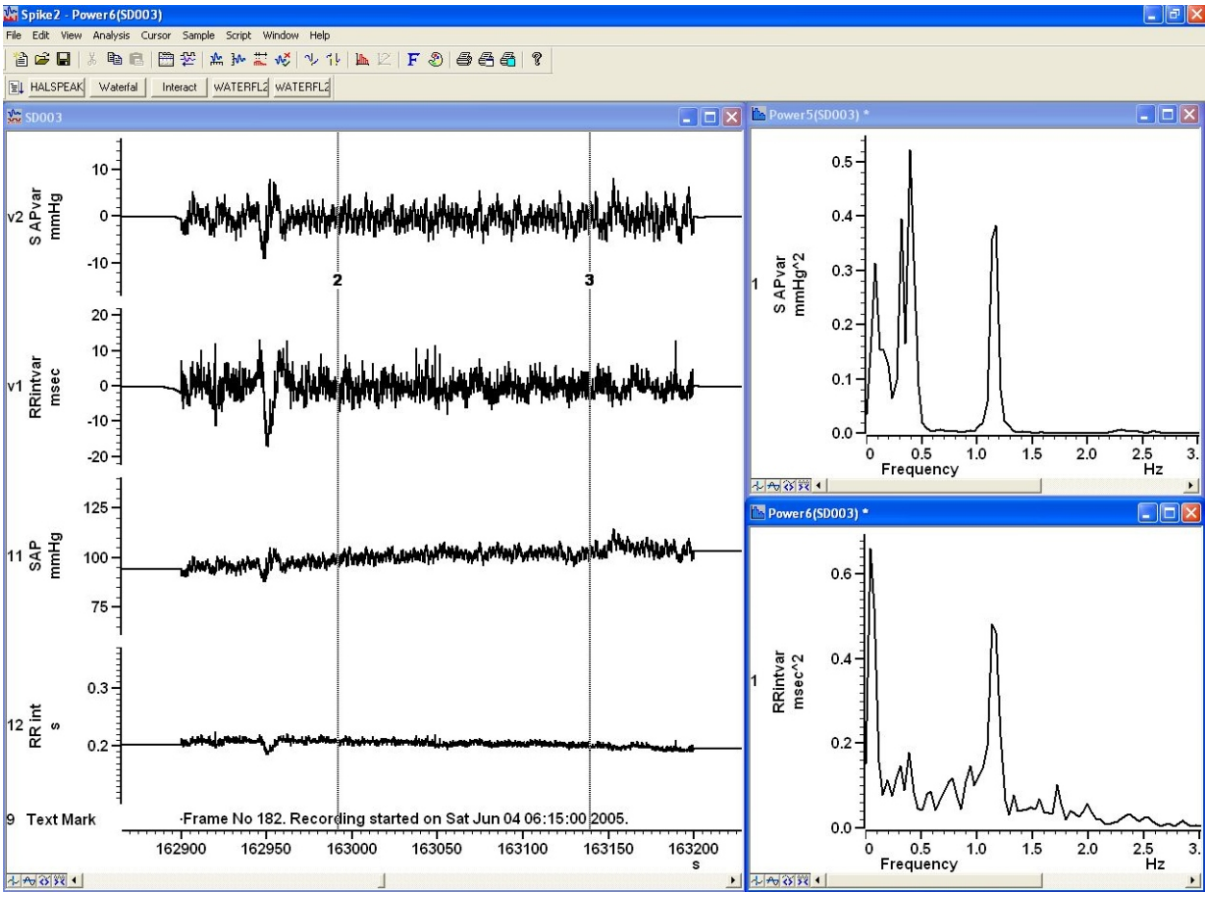

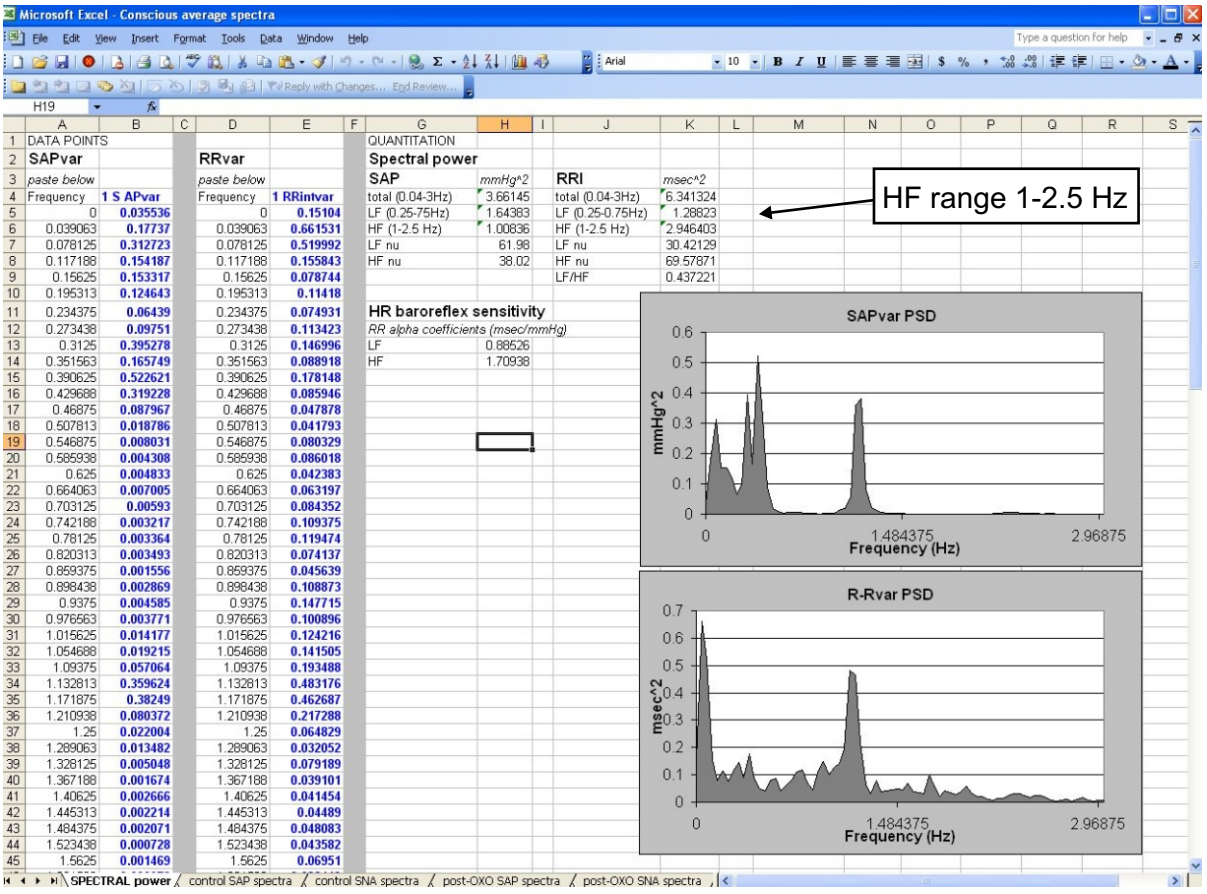

Figure 8.4. *Spectral Analysis of SAP and R-R interval in conscious telemetered rats*

Chapter 9 References

Abrahamsson C, Ahlund C, Nordlander M, Lind L (2003) A method for heart rate-corrected estimation of baroreflex sensitivity. J Hypertens 21:2133-2140.

Abreu GR, Futuro Neto HA, Cabral AM, Vasquez EC (1998) Ouabain produces diverse excitatory effects on afferent baroreceptor nerve activity in SHR and WKY animals. Clin Exp Hypertens 20:85-94.

Adrian ED, Bronk DW, Phillips G (1932) Discharges in mammalian sympathetic nerves. J Physiol 74:115-153.

Agelink MW, Boz C, Ullrich H, Andrich J (2002) Relationship between major depression and heart rate variability. Clinical consequences and implications for antidepressive treatment. Psychiatry Res 113:139-149.

Agelink MW, Majewski T, Wurthmann C, Postert T, Linka T, Rotterdam S, Klieser E (2001) Autonomic neurocardiac function in patients with major depression and effects of antidepressive treatment with nefazodone. J Affect Disord 62:187-198.

Ahern DK, Gorkin L, Anderson JL, Tierney C, Hallstrom A, Ewart C, Capone RJ, Schron E, Kornfeld D, Herd JA, et al. (1990) Biobehavioral variables and mortality or cardiac arrest in the Cardiac Arrhythmia Pilot Study (CAPS). Am J Cardiol 66:59-62.

Aicher SA, Saravay RH, Cravo S, Jeske I, Morrison SF, Reis DJ, Milner TA (1996) Monosynaptic projections from the nucleus tractus solitarii to C1 adrenergic neurons in the rostral ventrolateral medulla: comparison with input from the caudal ventrolateral medulla. J Comp Neurol 373:62-75.

Akselrod S, Gordon D, Ubel FA, Shannon DC, Berger AC, Cohen RJ (1981) Power spectrum analysis of heart rate fluctuation: a quantitative probe of beat-to-beat cardiovascular control. Science 213:220-222.

Alexander R (1946) Tonic and reflex functions of medullary sympathetic cardiovascular centers. J Neurophysiol 9:205-217.

Allen AM (2002) Inhibition of the hypothalamic paraventricular nucleus in spontaneously hypertensive rats dramatically reduces sympathetic vasomotor tone. Hypertension 39:275-280.

Ally A, Meintjes AF, Mitchell JH, Wilson LB (1994) Effects of clonidine on the reflex cardiovascular responses and release of substance P during muscle contraction. Circ Res 75:567-575.

Amendt K, Czachurski J, Dembowsky K, Seller H (1979) Bulbospinal projections to the intermediolateral cell column: a neuroanatomical study. J Auton Nerv Syst 1:103-107.

Anderson CR, McLachlan EM, Srb-Christie O (1989) Distribution of sympathetic preganglionic neurons and monoaminergic nerve terminals in the spinal cord of the rat. J Comp Neurol 283:269-284.

Arai Y, Saul JP, Albrecht P, Hartley LH, Lilly LS, Cohen RJ, Colucci WS (1989) Modulation of cardiac autonomic activity during and immediately after exercise. Am J Physiol 256:H132-141.

Araujo GC, Lopes OU, Campos RR (1999) Importance of glycinergic and glutamatergic synapses within the rostral ventrolateral medulla for blood pressure regulation in conscious rats. Hypertension 34:752-755.

Ardell JL, Randall WC (1986) Selective vagal innervation of sinoatrial and atrioventricular nodes in canine heart. Am J Physiol 251:H764-773.

Arlt J, Jahn H, Kellner M, Strohle A, Yassouridis A, Wiedemann K (2003) Modulation of sympathetic activity by corticotropin-releasing hormone and atrial natriuretic peptide. Neuropeptides 37:362-368.

Armitage AK, Hall GH (1967) Further evidence relating to the mode of action of nicotine in the central nervous system. Nature 214:977-979.

Arneric SP, Giuliano R, Ernsberger P, Underwood MD, Reis DJ (1990) Synthesis, release and receptor binding of acetylcholine in the C1 area of the rostral ventrolateral medulla: contributions in regulating arterial pressure. Brain Res 511:98-112.

Arvidsson U, Riedl M, Elde R, Meister B (1997) Vesicular acetylcholine transporter (VAChT) protein: a novel and unique marker for cholinergic neurons in the central and peripheral nervous systems. J Comp Neurol 378:454-467.

Ashworth-Preece M, Jarrott B, Lawrence AJ (1998a) Nicotinic acetylcholine receptors in the rat and primate nucleus tractus solitarius and on rat and human inferior vagal (nodose) ganglia: evidence from in vivo microdialysis and [125I]alpha-bungarotoxin autoradiography. Neuroscience 83:1113-1122.

Ashworth-Preece MA, Jarrott B, Lawrence AJ (1998b) Nicotinic acetylcholine receptor mediated modulation of evoked excitatory amino acid release in the nucleus tractus solitarius of the rat: evidence from in vivo microdialysis. Brain Res 806:287-291.

Ayensu WK, Pucilowski O, Mason GA, Overstreet DH, Rezvani AH, Janowsky DS (1995) Effects of chronic mild stress on serum complement activity, saccharin preference, and corticosterone levels in Flinders lines of rats. Physiol Behav 57:165-169.

Bacon SJ, Zagon A, Smith AD (1990) Electron microscopic evidence of a monosynaptic pathway between cells in the caudal raphe nuclei and sympathetic preganglionic neurons in the rat spinal cord. Exp Brain Res 79:589-602.
Badoer E, McKinley MJ, Oldfield BJ, McAllen RM (1993) A comparison of hypotensive and non-hypotensive hemorrhage on Fos expression in spinally projecting neurons of the paraventricular nucleus and rostral ventrolateral medulla. Brain Res 610:216-223.
Bago M, Sprtel BM, Dean C (1999) Modulation of sympathetic nerve activity by microinjection of the 5-HT1A receptor agonist 8-OH-DPAT into the rostroventrolateral medulla. J Auton Nerv Syst 76:127-134.
Bailey TW, Hermes SM, Andresen MC, Aicher SA (2006) Cranial visceral afferent pathways through the nucleus of the solitary tract to caudal ventrolateral medulla or paraventricular hypothalamus: target-specific synaptic reliability and convergence patterns. J Neurosci 26:11893-11902.
Bainbridge FA (1915) The influence of venous filling upon the rate of the heart. J Physiol 50:65-84.
Ballanyi K, Onimaru H, Homma I (1999) Respiratory network function in the isolated brainstem-spinal cord of newborn rats. Prog Neurobiol 59:583-634.
Barman SM, Gebber GL (1992) Rostral ventrolateral medullary and caudal medullary raphe neurons with activity correlated to the 10-Hz rhythm in sympathetic nerve discharge. J Neurophysiol 68:1535-1547.
Barman SM, Orer HS, Gebber GL (2002) Differential effects of an NMDA and a non-NMDA receptor antagonist on medullary lateral tegmental field neurons. Am J Physiol Regul Integr Comp Physiol 282:R100-113.
Barman SM, Orer HS, Gebber GL (2005) Role of medullary excitatory amino acid receptors in mediating the 10-Hz rhythm in sympathetic nerve discharge of cats. Brain Res 1049:249-253.
Barres C, Cheng Y, Julien C (2004) Steady-state and dynamic responses of renal sympathetic nerve activity to air-jet stress in sinoaortic denervated rats. Hypertension 43:629-635.
Barron HV, Lesh MD (1996) Autonomic nervous system and sudden cardiac death. J Am Coll Cardiol 27:1053-1060.
Bartsch T, Habler HJ, Janig W (1999) Hypoventilation recruits preganglionic sympathetic fibers with inspiration-related activity in the superior cervical trunk of the rat. J Auton Nerv Syst 77:31-38.
Baudrie V, Laude D, Elghozi JL (2006) Optimal frequency ranges for extracting information on cardiovascular autonomic control from the blood pressure and pulse interval spectrograms in mice. Am J Physiol Regul Integr Comp Physiol.
Baudrie V, Laude D, Elghozi JL (2007) Optimal frequency ranges for extracting information on cardiovascular autonomic control from the blood pressure and pulse interval spectrograms in mice. Am J Physiol Regul Integr Comp Physiol 292:R904-R912.
Baum T, Shropshire AT (1978) Influence of a cholinergic agent, oxotremorine, on sympathetic reflexes. Eur J Pharmacol 52:243-249.
Bedford TG, Loi PK, Crandall CC (1992) A model of dynamic exercise: the decerebrate rat locomotor preparation. J Appl Physiol 72:121-127.
Bellingham MC, Ireland MF (2002) Contribution of cholinergic systems to state-dependent modulation of respiratory control. Respir Physiol Neurobiol 131:135-144.
Benca RM, Overstreet DE, Gilliland MA, Russell D, Bergmann BM, Obermeyer WH (1996) Increased basal REM sleep but no difference in dark induction or light suppression of REM sleep in flinders rats with cholinergic supersensitivity. Neuropsychopharmacology 15:45-51.
Bernardi L, Salvucci F, Suardi R, Solda PL, Calciati A, Perlini S, Falcone C, Ricciardi L (1990) Evidence for an intrinsic mechanism regulating heart rate variability in the transplanted and the intact heart during submaximal dynamic exercise? Cardiovasc Res 24:969-981.
Berrard S, Varoqui H, Cervini R, Israel M, Mallet J, Diebler MF (1995) Coregulation of two embedded gene products, choline acetyltransferase and the vesicular acetylcholine transporter. J Neurochem 65:939-942.
Bertinieri G, di Rienzo M, Cavallazzi A, Ferrari AU, Pedotti A, Mancia G (1985) A new approach to analysis of the arterial baroreflex. J Hypertens Suppl 3:S79-81.
Bertram D, Barres C, Cuisinaud G, Julien C (1998) The arterial baroreceptor reflex of the rat exhibits positive feedback properties at the frequency of mayer waves. J Physiol 513 (Pt 1):251-261.
Bianchi AL, Denavit-Saubie M, Champagnat J (1995) Central control of breathing in mammals: neuronal circuitry, membrane properties, and neurotransmitters. Physiol Rev 75:1-45.
Bianchi AM, Mainardi L, Petrucci E, Signorini MG, Mainardi M, Cerutti S (1993) Time-variant power spectrum analysis for the detection of transient episodes in HRV signal. IEEE Trans Biomed Eng 40:136-144.
Bigger JT, Jr., Fleiss JL, Rolnitzky LM, Steinman RC (1993) Frequency domain measures of heart period variability to assess risk late after myocardial infarction. J Am Coll Cardiol 21:729-736.

Bigger JT, Jr., Fleiss JL, Steinman RC, Rolnitzky LM, Kleiger RE, Rottman JN (1992a) Frequency domain measures of heart period variability and mortality after myocardial infarction. Circulation 85:164-171.
Bigger JT, Jr., Fleiss JL, Steinman RC, Rolnitzky LM, Kleiger RE, Rottman JN (1992b) Correlations among time and frequency domain measures of heart period variability two weeks after acute myocardial infarction. Am J Cardiol 69:891-898.
Blessing WW, Willoughby JO (1985) Inhibiting the rabbit caudal ventrolateral medulla prevents baroreceptor-initiated secretion of vasopressin. J Physiol 367:253-265.
Blessing WW, Willoughby JO (1987) Depressor neurons in rabbit caudal medulla do not transmit the baroreceptor-vasomotor reflex. Am J Physiol 253:H777-786.
Blessing WW, Goodchild AK, Dampney RA, Chalmers JP (1981) Cell groups in the lower brain stem of the rabbit projecting to the spinal cord, with special reference to catecholamine-containing neurons. Brain Res 221:35-55.
Blessing WW, Howe PR, Joh TH, Oliver JR, Willoughby JO (1986) Distribution of tyrosine hydroxylase and neuropeptide Y-like immunoreactive neurons in rabbit medulla oblongata, with attention to colocalization studies, presumptive adrenaline-synthesizing perikarya, and vagal preganglionic cells. J Comp Neurol 248:285-300.
Blinder KJ, Johnson TA, John Massari V (1998a) Negative inotropic vagal preganglionic neurons in the nucleus ambiguus of the cat: neuroanatomical comparison with negative chronotropic neurons utilizing dual retrograde tracers. Brain Res 804:325-330.
Blinder KJ, Gatti PJ, Johnson TA, Lauenstein JM, Coleman WP, Gray AL, Massari VJ (1998b) Ultrastructural circuitry of cardiorespiratory reflexes: there is a monosynaptic path between the nucleus of the solitary tract and vagal preganglionic motoneurons controlling atrioventricular conduction in the cat. Brain Res 785:143-157.
Blinder KJ, Dickerson LW, Gray AL, Lauenstein JM, Newsome JT, Bingaman MT, Gatti PJ, Gillis RA, Massari VJ (1998c) Control of negative inotropic vagal preganglionic neurons in the dog: synaptic interactions with substance P afferent terminals in the nucleus ambiguus? Brain Res 810:251-256.
Boczek-Funcke A, Habler HJ, Janig W, Michaelis M (1992a) Respiratory modulation of the activity in sympathetic neurones supplying muscle, skin and pelvic organs in the cat. J Physiol 449:333-361.
Boczek-Funcke A, Dembowsky K, Habler HJ, Janig W, Michaelis M (1992b) Respiratory-related activity patterns in preganglionic neurones projecting into the cat cervical sympathetic trunk. J Physiol 457:277-296.
Bohmer G, Schmid K, Schmidt P, Stehle J (1987) Cholinergic effects on spike-density and burst-duration of medullary respiration-related neurones in the rabbit: an iontophoretic study. Neuropharmacology 26:1561-1572.
Bonner TI, Buckley NJ, Young AC, Brann MR (1987) Identification of a family of muscarinic acetylcholine receptor genes. Science 237:527-532.
Bonner TI, Young AC, Brann MR, Buckley NJ (1988) Cloning and expression of the human and rat m5 muscarinic acetylcholine receptor genes. Neuron 1:403-410.
Bouairi E, Neff R, Evans C, Gold A, Andresen MC, Mendelowitz D (2004) Respiratory sinus arrhythmia in freely moving and anesthetized rats. J Appl Physiol 97:1431-1436.
Boudinot E, Yamada M, Wess J, Champagnat J, Foutz AS (2004) Ventilatory pattern and chemosensitivity in M1 and M3 muscarinic receptor knockout mice. Respir Physiol Neurobiol 139:237-245.
Bradley SR, Pieribone VA, Wang W, Severson CA, Jacobs RA, Richerson GB (2002) Chemosensitive serotonergic neurons are closely associated with large medullary arteries. Nat Neurosci 5:401-402.
Braun C, Kowallik P, Freking A, Hadeler D, Kniffki KD, Meesmann M (1998) Demonstration of nonlinear components in heart rate variability of healthy persons. Am J Physiol 275:H1577-1584.
Braw Y, Malkesman O, Dagan M, Bercovich A, Lavi-Avnon Y, Schroeder M, Overstreet DH, Weller A (2006) Anxiety-like behaviors in pre-pubertal rats of the Flinders Sensitive Line (FSL) and Wistar-Kyoto (WKY) animal models of depression. Behav Brain Res 167:261-269.
Brezenoff HE (1972) Cardiovascular responses to intrahypothalamic injections of carbachol and certain cholinesterase inhibitors. Neuropharmacology 11:637-644.
Brezenoff HE, Rusin J (1974) Brain acetylcholine mediates the hypertensive response to physostigmine in the rat. Eur J Pharmacol 29:262-266.
Brezenoff HE, Caputi AP (1980) Intracerebroventricular injection of hemicholinium-3 lowers blood pressure in conscious spontaneously hypertensive rats but not in normotensive rats. Life Sci 26:1037-1045.
Brezenoff HE, Giuliano R (1982) Cardiovascular control by cholinergic mechanisms in the central nervous system. Annu Rev Pharmacol Toxicol 22:341-381.
Brezenoff HE, Carney K, Buccafusco JJ (1982) Potentiation of the carotid artery occlusion reflex by a cholinergic system in the posterior hypothalamic nucleus. Life Sci 30:391-400.
Broadley AJ, Korszun A, Jones CJ, Frenneaux MP (2002) Arterial endothelial function is impaired in treated depression. Heart 88:521-523.

Broadley AJ, Frenneaux MP, Moskvina V, Jones CJ, Korszun A (2005) Baroreflex sensitivity is reduced in depression. Psychosom Med 67:648-651.
Brockhaus J, Ballanyi K (1998) Synaptic inhibition in the isolated respiratory network of neonatal rats. Eur J Neurosci 10:3823-3839.
Brown DL, Guyenet PG (1985) Electrophysiological study of cardiovascular neurons in the rostral ventrolateral medulla in rats. Circ Res 56:359-369.
Buccafusco JJ (1996) The role of central cholinergic neurons in the regulation of blood pressure and in experimental hypertension. Pharmacol Rev 48:179-211.
Buccafusco JJ, Brezenoff HE (1978) The hypertensive response to injection of physostigmine into the hypothalamus of the unanesthetized rat. Clin Exp Hypertens 1:219-227.
Buccafusco JJ, Brezenoff HE (1979) Pharmacological study of a cholinergic mechanism within the rat posterior hypothalamic nucleus which mediates a hypertensive response. Brain Res 165:295-310.
Buccafusco JJ, Spector S (1980) Role of central cholinergic neurons in experimental hypertension. J Cardiovasc Pharmacol 2:347-355.
Buijs RM, van Eden CG, Goncharuk VD, Kalsbeek A (2003) The biological clock tunes the organs of the body: timing by hormones and the autonomic nervous system. J Endocrinol 177:17-26.
Bunker SJ, Colquhoun DM, Esler MD, Hickie IB, Hunt D, Jelinek VM, Oldenburg BF, Peach HG, Ruth D, Tennant CC, Tonkin AM (2003) "Stress" and coronary heart disease: psychosocial risk factors. Med J Aust 178:272-276.
Burman KJ, Sartor DM, Verberne AJ, Llewellyn-Smith IJ (2004) Cocaine- and amphetamine-regulated transcript in catecholamine and noncatecholamine presympathetic vasomotor neurons of rat rostral ventrolateral medulla. J Comp Neurol 476:19-31.
Bushnell PJ, Levin ED, Overstreet DH (1995) Spatial working and reference memory in rats bred for autonomic sensitivity to cholinergic stimulation: acquisition, accuracy, speed, and effects of cholinergic drugs. Neurobiol Learn Mem 63:116-132.
Bymaster FP, McKinzie DL, Felder CC, Wess J (2003a) Use of M1-M5 muscarinic receptor knockout mice as novel tools to delineate the physiological roles of the muscarinic cholinergic system. Neurochem Res 28:437-442.
Bymaster FP, Carter PA, Yamada M, Gomeza J, Wess J, Hamilton SE, Nathanson NM, McKinzie DL, Felder CC (2003b) Role of specific muscarinic receptor subtypes in cholinergic parasympathomimetic responses, in vivo phosphoinositide hydrolysis, and pilocarpine-induced seizure activity. Eur J Neurosci 17:1403-1410.
Bymaster FP, Carter PA, Zhang L, Falcone JF, Stengel PW, Cohen ML, Shannon HE, Gomeza J, Wess J, Felder CC (2001) Investigations into the physiological role of muscarinic M2 and M4 muscarinic and M4 receptor subtypes using receptor knockout mice. Life Sci 68:2473-2479.
Byrum CE, Guyenet PG (1987) Afferent and efferent connections of the A5 noradrenergic cell group in the rat. J Comp Neurol 261:529-542.
Byrum CE, Stornetta R, Guyenet PG (1984) Electrophysiological properties of spinally-projecting A5 noradrenergic neurons. Brain Res 303:15-29.
Caberlotto L, Jimenez P, Overstreet DH, Hurd YL, Mathe AA, Fuxe K (1999) Alterations in neuropeptide Y levels and Y1 binding sites in the Flinders Sensitive Line rats, a genetic animal model of depression. Neurosci Lett 265:191-194.
Campos RR, McAllen RM (1999a) Cardiac inotropic, chronotropic, and dromotropic actions of subretrofacial neurons of cat RVLM. Am J Physiol 276:R1102-1111.
Campos RR, McAllen RM (1999b) Tonic drive to sympathetic premotor neurons of rostral ventrolateral medulla from caudal pressor area neurons. Am J Physiol 276:R1209-1213.
Caputi AP, Rossi F, Carney K, Brezenoff HE (1980) Modulatory effect of brain acetylcholine on reflex-induced bradycardia and tachycardia in conscious rats. J Pharmacol Exp Ther 215:309-316.
Carney RM, Freedland KE (2003) Depression, mortality, and medical morbidity in patients with coronary heart disease. Biol Psychiatry 54:241-247.
Carney RM, Freedland KE, Veith RC (2005a) Depression, the autonomic nervous system, and coronary heart disease. Psychosom Med 67 Suppl 1:S29-33.
Carney RM, Freedland KE, Rich MW, Smith LJ, Jaffe AS (1993) Ventricular tachycardia and psychiatric depression in patients with coronary artery disease. Am J Med 95:23-28.
Carney RM, Saunders RD, Freedland KE, Stein P, Rich MW, Jaffe AS (1995) Association of depression with reduced heart rate variability in coronary artery disease. Am J Cardiol 76:562-564.
Carney RM, Freedland KE, Veith RC, Cryer PE, Skala JA, Lynch T, Jaffe AS (1999) Major depression, heart rate, and plasma norepinephrine in patients with coronary heart disease. Biol Psychiatry 45:458-463.
Carney RM, Freedland KE, Stein PK, Watkins LL, Catellier D, Jaffe AS, Yeragani VK (2003) Effects of depression on QT interval variability after myocardial infarction. Psychosom Med 65:177-180.
Carney RM, Blumenthal JA, Stein PK, Watkins L, Catellier D, Berkman LF, Czajkowski SM, O'Connor C, Stone PH, Freedland KE (2001) Depression, heart rate variability, and acute myocardial infarction. Circulation 104:2024-2028.

Carney RM, Blumenthal JA, Freedland KE, Stein PK, Howells WB, Berkman LF, Watkins LL, Czajkowski SM, Hayano J, Domitrovich PP, Jaffe AS (2005b) Low heart rate variability and the effect of depression on post-myocardial infarction mortality. Arch Intern Med 165:1486-1491.
Caulfield MP, Birdsall NJ (1998) International Union of Pharmacology. XVII. Classification of muscarinic acetylcholine receptors. Pharmacol Rev 50:279-290.
Caverson MM, Ciriello J, Calaresu FR (1983) Direct pathway from cardiovascular neurons in the ventrolateral medulla to the region of the intermediolateral nucleus of the upper thoracic cord: an anatomical and electrophysiological investigation in the cat. J Auton Nerv Syst 9:451-475.
Cechetto DF, Saper CB (1988) Neurochemical organization of the hypothalamic projection to the spinal cord in the rat. J Comp Neurol 272:579-604.
Cerutti C, Gustin MP, Paultre CZ, Lo M, Julien C, Vincent M, Sassard J (1991) Autonomic nervous system and cardiovascular variability in rats: a spectral analysis approach. Am J Physiol 261:H1292-1299.
Chalmers J, Pilowsky P (1991) Brainstem and bulbospinal neurotransmitter systems in the control of blood pressure. J Hypertens 9:675-694.
Chalmers JP, Blessing WW, West MJ, Howe PR, Costa M, Furness JB (1981) Importance of new catecholamine pathways in control of blood pressure. Clin Exp Hypertens 3:393-416.
Chemin J, Monteil A, Perez-Reyes E, Bourinet E, Nargeot J, Lory P (2002) Specific contribution of human T-type calcium channel isotypes (alpha(1G), alpha(1H) and alpha(1I)) to neuronal excitability. J Physiol 540:3-14.
Chen QH, Toney GM (2003) Identification and characterization of two functionally distinct groups of spinal cord-projecting paraventricular nucleus neurons with sympathetic-related activity. Neuroscience 118:797-807.
Cheng Z, Powley TL (2000) Nucleus ambiguus projections to cardiac ganglia of rat atria: an anterograde tracing study. J Comp Neurol 424:588-606.
Cheng Z, Powley TL, Schwaber JS, Doyle FJ, 3rd (1999) Projections of the dorsal motor nucleus of the vagus to cardiac ganglia of rat atria: an anterograde tracing study. J Comp Neurol 410:320-341.
Chiou CW, Zipes DP (1998) Selective vagal denervation of the atria eliminates heart rate variability and baroreflex sensitivity while preserving ventricular innervation. Circulation 98:360-368.
Chong RK, Bedford TG (1997) Heart rate, blood pressure, and running speed responses to mesencephalic locomotor region stimulation in anesthetized rats. Pflugers Arch 434:280-284.
Ciriello J (1983) Brainstem projections of aortic baroreceptor afferent fibers in the rat. Neurosci Lett 36:37-42.
Cochrane KL, Nathan MA (1989) Normotension in conscious rats after placement of bilateral electrolytic lesions in the rostral ventrolateral medulla. J Auton Nerv Syst 26:199-211.
Cochrane KL, Nathan MA (1994) Pressor systems involved in the maintenance of arterial pressure after lesions of the rostral ventrolateral medulla. J Auton Nerv Syst 46:9-18.
Cochrane KL, Buchholz RA, Hubbard JW, Keeton TK, Nathan MA (1988) Hypotensive effects of lesions of the rostral ventrolateral medulla in rats are anesthetic-dependent. J Auton Nerv Syst 22:181-187.
Cohen MI, Piercey MF, Gootman PM, Wolotsky P (1974) Synaptic connections between medullary inspiratory neurons and phrenic motoneurons as revealed by cross-correlation. Brain Res 81:319-324.
Cohen S, Hunter CW, Yanni B, Striker P, Hijazi RH (2006) Central anticholinergic syndrome strikes again. J Clin Anesth 18:399-400.
Coleman MJ, Dampney RA (1995) Powerful depressor and sympathoinhibitory effects evoked from neurons in the caudal raphe pallidus and obscurus. Am J Physiol 268:R1295-1302.
Coleridge HM, Coleridge JC (1980) Cardiovascular afferents involved in regulation of peripheral vessels. Annu Rev Physiol 42:413-427.
Coleridge HM, Coleridge JC, Poore ER, Roberts AM, Schultz HD (1984) Aortic wall properties and baroreceptor behaviour at normal arterial pressure and in acute hypertensive resetting in dogs. J Physiol 350:309-326.
Comroe JH, Jr., Mortimer L (1964) The Respiratory And Cardiovascular Responses Of Temporally Separated Aortic And Carotid Bodies To Cyanide, Nicotine, Phenyldiguanide And Serotonin. J Pharmacol Exp Ther 146:33-41.
Connelly CA, Dobbins EG, Feldman JL (1992) Pre-Botzinger complex in cats: respiratory neuronal discharge patterns. Brain Res 590:337-340.
Connerney I, Shapiro PA, McLaughlin JS, Bagiella E, Sloan RP (2001) Relation between depression after coronary artery bypass surgery and 12-month outcome: a prospective study. Lancet 358:1766-1771.
Constant I, Laude D, Murat I, Elghozi JL (1999) Pulse rate variability is not a surrogate for heart rate variability. Clin Sci (Lond) 97:391-397.
Constant I, Laude D, Elghozi JL, Murat I (2000) Assessment of autonomic cardiovascular changes associated with recovery from anaesthesia in children: a study using spectral analysis of blood pressure and heart rate variability. Paediatr Anaesth 10:653-660.

Cooper HE, Parkes MJ, Clutton-Brock TH (2003) CO2-dependent components of sinus arrhythmia from the start of breath holding in humans. Am J Physiol Heart Circ Physiol 285:H841-848.
Cooper HE, Clutton-Brock TH, Parkes MJ (2004) Contribution of the respiratory rhythm to sinus arrhythmia in normal unanesthetized subjects during positive-pressure mechanical hyperventilation. Am J Physiol Heart Circ Physiol 286:H402-411.
Coote JH, Perez-Gonzalez JF (1970) The response of some sympathetic neurones to volleys in various afferent nerves. J Physiol 208:261-278.
Coote JH, Westbury DR (1979) Intracellular recordings from sympathetic preganglionic neurones. Neurosci Lett 15:171-175.
Cowley AW, Jr., Liard JF, Guyton AC (1973) Role of baroreceptor reflex in daily control of arterial blood pressure and other variables in dogs. Circ Res 32:564-576.
Criscione L, Reis DJ, Talman WT (1983) Cholinergic mechanisms in the nucleus tractus solitarii and cardiovascular regulation in the rat. Eur J Pharmacol 88:47-55.
Dahlstrom A, Fuxe K (1964) Localization of monoamines in the lower brain stem. Experientia 20:398-399.
Dahlström A, Fuxe K (1965) Evidence for the existence of monoamine neurons in the central nervous system II. Experimentally induced changes in intraneuronal amine levels of bulbospinal neuron systems. Acta Physiol Scand Suppl 247:1-36.
Dale HH (1962) Otto Loewi. 1873-1961. Biographical Memoirs of Fellows of the Royal Society 8:67-89.
Daly MB, Cook MN (1994) Carotid chemoreceptor control of vascular resistance in resting and contracting skeletal muscle. Adv Exp Med Biol 360:273-275.
Daly MD (1993) Carotid chemoreceptor reflex cardioinhibitory responses: comparison of their modulation by central inspiratory neuronal activity and activity of pulmonary stretch afferents. Adv Exp Med Biol 337:333-343.
Dampney RA (1994a) The subretrofacial vasomotor nucleus: anatomical, chemical and pharmacological properties and role in cardiovascular regulation. Prog Neurobiol 42:197-227.
Dampney RA (1994b) Functional organization of central pathways regulating the cardiovascular system. Physiol Rev 74:323-364.
Dampney RA, Moon EA (1980) Role of ventrolateral medulla in vasomotor response to cerebral ischemia. Am J Physiol 239:H349-358.
Dampney RA, Blessing WW, Tan E (1988) Origin of tonic GABAergic inputs to vasopressor neurons in the subretrofacial nucleus of the rabbit. J Auton Nerv Syst 24:227-239.
Dampney RA, Hirooka Y, Potts PD, Head GA (1996) Functions of angiotensin peptides in the rostral ventrolateral medulla. Clin Exp Pharmacol Physiol Suppl 3:S105-111.
Dampney RA, Polson JW, Potts PD, Hirooka Y, Horiuchi J (2003a) Functional organization of brain pathways subserving the baroreceptor reflex: studies in conscious animals using immediate early gene expression. Cell Mol Neurobiol 23:597-616.
Dampney RA, Tagawa T, Horiuchi J, Potts PD, Fontes M, Polson JW (2000) What drives the tonic activity of presympathetic neurons in the rostral ventrolateral medulla? Clin Exp Pharmacol Physiol 27:1049-1053.
Dampney RA, Horiuchi J, Tagawa T, Fontes MA, Potts PD, Polson JW (2003b) Medullary and supramedullary mechanisms regulating sympathetic vasomotor tone. Acta Physiol Scand 177:209-218.
Dampney RA, Horiuchi J, Killinger S, Sheriff MJ, Tan PS, McDowall LM (2005) Long-term regulation of arterial blood pressure by hypothalamic nuclei: some critical questions. Clin Exp Pharmacol Physiol 32:419-425.
Dani JA, Bertrand D (2006) Nicotinic Acetylcholine Receptors and Nicotinic Cholinergic Mechanisms of the Central Nervous System. Annu Rev Pharmacol Toxicol.
Davidson NS, Goldner S, McCloskey DI (1976) Respiratory modulation of barareceptor and chemoreceptor reflexes affecting heart rate and cardiac vagal efferent nerve activity. J Physiol 259:523-530.
Daws LC, Overstreet DH (1999) Ontogeny of muscarinic cholinergic supersensitivity in the Flinders Sensitive Line rat. Pharmacol Biochem Behav 62:367-380.
Daws LC, Schiller GD, Overstreet DH, Orbach J (1991) Early development of muscarinic supersensitivity in a genetic animal model of depression. Neuropsychopharmacology 4:207-217.
Day MD, Roach AG (1977) Cardiovascular effects of carbachol and other cholinomimetics administered into the cerebral ventricles of conscious cats. Clin Exp Pharmacol Physiol 4:431-442.
de Castro D, Lipski J, Kanjhan R (1994) Electrophysiological study of dorsal respiratory neurons in the medulla oblongata of the rat. Brain Res 639:49-56.
De Ferrari GM, Vanoli E, Curcuruto P, Tommasini G, Schwartz PJ (1992) Prevention of life-threatening arrhythmias by pharmacologic stimulation of the muscarinic receptors with oxotremorine. Am Heart J 124:883-890.
De Ferrari GM, Vanoli E, Stramba-Badiale M, Hull SS, Jr., Foreman RD, Schwartz PJ (1991) Vagal reflexes and survival during acute myocardial ischemia in conscious dogs with healed myocardial infarction. Am J Physiol 261:H63-69.

De Ferrari GM, Salvati P, Grossoni M, Ukmar G, Vaga L, Patrono C, Schwartz PJ (1993) Pharmacologic modulation of the autonomic nervous system in the prevention of sudden cardiac death. A study with propranolol, methacholine and oxotremorine in conscious dogs with a healed myocardial infarction. J Am Coll Cardiol 22:283-290.
Deering J, Coote JH (2000) Paraventricular neurones elicit a volume expansion-like change of activity in sympathetic nerves to the heart and kidney in the rabbit. Exp Physiol 85:177-186.
Dembowsky K, Czachurski J, Seller H (1985) An intracellular study of the synaptic input to sympathetic preganglionic neurones of the third thoracic segment of the cat. J Auton Nerv Syst 13:201-244.
Demiryurek AT, Demiryurek S (2005) Cardiotoxicity of digitalis glycosides: roles of autonomic pathways, autacoids and ion channels. Auton Autacoid Pharmacol 25:35-52.
Depres-Brummer P, Metzger G, Levi F (1998) Pharmacologic restoration of suppressed temperature rhythms in rats by melatonin, melatonin receptor agonist, S20242, or 8-OH-DPAT. Eur J Pharmacol 347:57-66.
Deuchars SA, Milligan CJ, Stornetta RL, Deuchars J (2005) GABAergic neurons in the central region of the spinal cord: a novel substrate for sympathetic inhibition. J Neurosci 25:1063-1070.
Dev NB, Loeschcke HH (1979) A cholinergic mechanism involved in the respiratory chemosensitivity of the medulla oblongata in the cat. Pflugers Arch 379:29-36.
Di Rienzo M, Parati G, Castiglioni P, Tordi R, Mancia G, Pedotti A (2001) Baroreflex effectiveness index: an additional measure of baroreflex control of heart rate in daily life. Am J Physiol Regul Integr Comp Physiol 280:R744-751.
Di Rienzo M, Parati G, Castiglioni P, Omboni S, Ferrari AU, Ramirez AJ, Pedotti A, Mancia G (1991) Role of sinoaortic afferents in modulating BP and pulse-interval spectral characteristics in unanesthetized cats. Am J Physiol 261:H1811-1818.
Dilsaver SC, Peck JA, Overstreet DH (1992) The Flinders Sensitive Line exhibits enhanced thermic responsiveness to nicotine relative to the Sprague-Dawley rat. Pharmacol Biochem Behav 41:23-27.
Dittmar C (1873) Über die Lage des sogenannten Gefäßcentrums in der Medulla oblongata. Arbeiten aus der Physiologischen Anstalt zu Leipzig:103-123.
Djuric VJ, Overstreet DH, Bienenstock J, Perdue MH (1995) Immediate hypersensitivity in the Flinders rat: further evidence for a possible link between susceptibility to allergies and depression. Brain Behav Immun 9:196-206.
Djuric VJ, Cox G, Overstreet DH, Smith L, Dragomir A, Steiner M (1998) Genetically transmitted cholinergic hyperresponsiveness predisposes to experimental asthma. Brain Behav Immun 12:272-284.
Dornhorst AC, Howard P, Leathart GL (1952) Respiratory variations in blood pressure. Circulation 6:553-558.
Dremencov E, Newman ME, Kinor N, Blatman-Jan G, Schindler CJ, Overstreet DH, Yadid G (2005) Hyperfunctionality of serotonin-2C receptor-mediated inhibition of accumbal dopamine release in an animal model of depression is reversed by antidepressant treatment. Neuropharmacology 48:34-42.
Drye RG, Baisden RH, Whittington DL, Woodruff ML (1990) The effects of stimulation of the A5 region on blood pressure and heart rate in rabbits. Brain Res Bull 24:33-39.
DSM-IV (1994) Diagnostic and Statistical Manual of Mental Disorders 4th Edition.
Duffin J (2004) Functional organization of respiratory neurones: a brief review of current questions and speculations. Exp Physiol 89:517-529.
Duffin J, Douse MA (1993) Botzinger expiratory neurones inhibit propriobulbar decrementing inspiratory neurones. Neuroreport 4:1215-1218.
Duffin J, van Alphen J (1995) Cross-correlation of augmenting expiratory neurons of the Botzinger complex in the cat. Exp Brain Res 103:251-255.
Duffin J, Tian GF, Peever JH (2000) Functional synaptic connections among respiratory neurons. Respir Physiol 122:237-246.
Dun NJ, Wu SY, Shen E, Miyazaki T, Dun SL, Ren C (1992) Synaptic mechanisms in sympathetic preganglionic neurons. Can J Physiol Pharmacol 70 Suppl:S86-91.
Eglen RM, Reddy H, Watson N, Challiss RA (1994) Muscarinic acetylcholine receptor subtypes in smooth muscle. Trends Pharmacol Sci 15:114-119.
Ehlert FJ (2003) Pharmacological analysis of the contractile role of M2 and M3 muscarinic receptors in smooth muscle. Receptors Channels 9:261-277.
El Khoury A, Gruber SH, Mork A, Mathe AA (2006) Adult life behavioral consequences of early maternal separation are alleviated by escitalopram treatment in a rat model of depression. Prog Neuropsychopharmacol Biol Psychiatry 30:535-540.
Elghozi JL, Girard A, Laude D (2001) Effects of drugs on the autonomic control of short-term heart rate variability. Auton Neurosci 90:116-121.
Ellenberger HH, Feldman JL (1990) Brainstem connections of the rostral ventral respiratory group of the rat. Brain Res 513:35-42.

Ernsberger P, Arango V, Reis DJ (1988a) A high density of muscarinic receptors in the rostral ventrolateral medulla of the rat is revealed by correction for autoradiographic efficiency. Neurosci Lett 85:179-186.
Ernsberger P, Arneric SP, Arango V, Reis DJ (1988b) Quantitative distribution of muscarinic receptors and choline acetyltransferase in rat medulla: examination of transmitter-receptor mismatch. Brain Res 452:336-344.
Esler M, Turbott J, Schwarz R, Leonard P, Bobik A, Skews H, Jackman G (1982) The peripheral kinetics of norepinephrine in depressive illness. Arch Gen Psychiatry 39:295-300.
Eto M, Toba K, Akishita M, Kozaki K, Watanabe T, Kim S, Hashimoto M, Sudoh N, Yoshizumi M, Ouchi Y (2003) Reduced endothelial vasomotor function and enhanced neointimal formation after vascular injury in a rat model of blood pressure lability. Hypertens Res 26:991-998.
Ezure K (1990) Synaptic connections between medullary respiratory neurons and considerations on the genesis of respiratory rhythm. Prog Neurobiol 35:429-450.
Ezure K, Tanaka I (2000) Identification of deflation-sensitive inspiratory neurons in the dorsal respiratory group of the rat. Brain Res 883:22-30.
Ezure K, Manabe M, Yamada H (1988) Distribution of medullary respiratory neurons in the rat. Brain Res 455:262-270.
Ezure K, Tanaka I, Kondo M (2003) Glycine is used as a transmitter by decrementing expiratory neurons of the ventrolateral medulla in the rat. J Neurosci 23:8941-8948.
Fadel PJ, Ogoh S, Watenpaugh DE, Wasmund W, Olivencia-Yurvati A, Smith ML, Raven PB (2001) Carotid baroreflex regulation of sympathetic nerve activity during dynamic exercise in humans. Am J Physiol Heart Circ Physiol 280:H1383-1390.
Fava M, Kendler KS (2000) Major depressive disorder. Neuron 28:335-341.
Feldberg W, Guertzenstein PG (1972) A vasodepressor effect of pentobarbitone sodium. J Physiol 224:83-103.
Feldberg W, Guertzenstein PG (1976) Vasodepressor effects obtained by drugs acting on the ventral surface of the brain stem. J Physiol 258:337-355.
Feldman JL, Smith JC (1989) Cellular mechanisms underlying modulation of breathing pattern in mammals. Ann N Y Acad Sci 563:114-130.
Feldman JL, Mitchell GS, Nattie EE (2003) Breathing: rhythmicity, plasticity, chemosensitivity. Annu Rev Neurosci 26:239-266.
Feldman JL, Smith JC, Ellenberger HH, Connelly CA, Liu GS, Greer JJ, Lindsay AD, Otto MR (1990) Neurogenesis of respiratory rhythm and pattern: emerging concepts. Am J Physiol 259:R879-886.
Fisher JP, White MJ (2004) Muscle afferent contributions to the cardiovascular response to isometric exercise. Exp Physiol 89:639-646.
Fisher JT, Vincent SG, Gomeza J, Yamada M, Wess J (2004) Loss of vagally mediated bradycardia and bronchoconstriction in mice lacking M2 or M3 muscarinic acetylcholine receptors. Faseb J 18:711-713.
Fouad FM (1994) Cardiac function and dysfunction in hypertension. Cleve Clin J Med 61:351-355.
Franchini KG, Krieger EM (1992) Carotid chemoreceptors influence arterial pressure in intact and aortic-denervated rats. Am J Physiol 262:R677-683.
Frasure-Smith N (1991) In-hospital symptoms of psychological stress as predictors of long-term outcome after acute myocardial infarction in men. Am J Cardiol 67:121-127.
Frasure-Smith N, Lesperance F, Talajic M (1993) Depression following myocardial infarction. Impact on 6-month survival. Jama 270:1819-1825.
Frasure-Smith N, Lesperance F, Talajic M (1995) Depression and 18-month prognosis after myocardial infarction. Circulation 91:999-1005.
Freedland KE, Carney RM, Skala JA (2005) Depression and smoking in coronary heart disease. Psychosom Med 67 Suppl 1:S42-46.
Friedman EM, Irwin MR, Overstreet DH (1996) Natural and cellular immune responses in Flinders sensitive and resistant line rats. Neuropsychopharmacology 15:314-322.
Friedman EM, Becker KA, Overstreet DH, Lawrence DA (2002) Reduced primary antibody responses in a genetic animal model of depression. Psychosom Med 64:267-273.
Funk GD, Smith JC, Feldman JL (1993) Generation and transmission of respiratory oscillations in medullary slices: role of excitatory amino acids. J Neurophysiol 70:1497-1515.
Gainetdinov RR, Bohn LM, Walker JK, Laporte SA, Macrae AD, Caron MG, Lefkowitz RJ, Premont RT (1999) Muscarinic supersensitivity and impaired receptor desensitization in G protein-coupled receptor kinase 5-deficient mice. Neuron 24:1029-1036.
Gao K, Mason P (2001) The discharge of a subset of serotonergic raphe magnus cells is influenced by baroreceptor input. Brain Res 900:306-313.
Garcia-Rill E, Homma Y, Skinner RD (2004) Arousal mechanisms related to posture and locomotion: 1. Descending modulation. Prog Brain Res 143:283-290.

Garcia Perez M, Jordan D (2001) Effect of stimulating non-myelinated vagal axons on atrio-ventricular conduction and left ventricular function in anaesthetized rabbits. Auton Neurosci 86:183-191.
Gatti PJ, Johnson TA, Phan P, Jordan IK, 3rd, Coleman W, Massari VJ (1995) The physiological and anatomical demonstration of functionally selective parasympathetic ganglia located in discrete fat pads on the feline myocardium. J Auton Nerv Syst 51:255-259.
Gatti PJ, Johnson TA, McKenzie J, Lauenstein JM, Gray A, Massari VJ (1997) Vagal control of left ventricular contractility is selectively mediated by a cranioventricular intracardiac ganglion in the cat. J Auton Nerv Syst 66:138-144.
Gattu M, Pauly JR, Urbanawiz S, Buccafusco JJ (1997a) Autoradiographic comparison of muscarinic M1 and M2 binding sites in the CNS of spontaneously hypertensive and normotensive rats. Brain Res 771:173-183.
Gattu M, Wei J, Pauly JR, Urbanawiz S, Buccafusco JJ (1997b) Increased expression of M2 muscarinic receptor mRNA and binding sites in the rostral ventrolateral medulla of spontaneously hypertensive rats. Brain Res 756:125-132.
Gehi A, Haas D, Pipkin S, Whooley MA (2005a) Depression and medication adherence in outpatients with coronary heart disease: findings from the Heart and Soul Study. Arch Intern Med 165:2508-2513.
Gehi A, Mangano D, Pipkin S, Browner WS, Whooley MA (2005b) Depression and heart rate variability in patients with stable coronary heart disease: findings from the Heart and Soul Study. Arch Gen Psychiatry 62:661-666.
Gilbey MP, Jordan D, Richter DW, Spyer KM (1984) Synaptic mechanisms involved in the inspiratory modulation of vagal cardio-inhibitory neurones in the cat. J Physiol 356:65-78.
Gillin JC, Sutton L, Ruiz C, Kelsoe J, Dupont RM, Darko D, Risch SC, Golshan S, Janowsky D (1991) The cholinergic rapid eye movement induction test with arecoline in depression. Arch Gen Psychiatry 48:264-270.
Giuliano R, Ruggiero DA, Morrison S, Ernsberger P, Reis DJ (1989) Cholinergic regulation of arterial pressure by the C1 area of the rostral ventrolateral medulla. J Neurosci 9:923-942.
Gonzalez AM, Pazos A (1992) Modification of muscarinic acetylcholine receptors in the rat brain following chronic immobilization stress: an autoradiographic study. Eur J Pharmacol 223:25-31.
Goodchild AK, Dampney RA, Bandler R (1982) A method for evoking physiological responses by stimulation of cell bodies, but not axons of passage, within localized regions of the central nervous system. J Neurosci Methods 6:351-363.
Goodchild AK, Phillips JK, Lipski J, Pilowsky PM (2001) Differential expression of catecholamine synthetic enzymes in the caudal ventral pons. J Comp Neurol 438:457-467.
Goodchild AK, Llewellyn-Smith IJ, Sun QJ, Chalmers J, Cunningham AM, Pilowsky PM (2000) Calbindin-immunoreactive neurons in the reticular formation of the rat brainstem: catecholamine content and spinal projections. J Comp Neurol 424:547-562.
Gordon CJ (1994) Thermoregulation in laboratory mammals and humans exposed to anticholinesterase agents. Neurotoxicol Teratol 16:427-453.
Gordon FJ, McCann LA (1988) Pressor responses evoked by microinjections of L-glutamate into the caudal ventrolateral medulla of the rat. Brain Res 457:251-258.
Grassi G, Seravalle G, Cattaneo BM, Lanfranchi A, Vailati S, Giannattasio C, Del Bo A, Sala C, Bolla GB, Pozzi M (1995) Sympathetic activation and loss of reflex sympathetic control in mild congestive heart failure. Circulation 92:3206-3211.
Gray PA, Rekling JC, Bocchiaro CM, Feldman JL (1999) Modulation of respiratory frequency by peptidergic input to rhythmogenic neurons in the preBotzinger complex. Science 286:1566-1568.
Gray PA, Janczewski WA, Mellen N, McCrimmon DR, Feldman JL (2001) Normal breathing requires preBotzinger complex neurokinin-1 receptor-expressing neurons. Nat Neurosci 4:927-930.
Greco MA, McCarley RW, Shiromani PJ (1999) Choline acetyltransferase expression during periods of behavioral activity and across natural sleep-wake states in the basal forebrain. Neuroscience 93:1369-1374.
Greco MA, Magner M, Overstreet D, Shiromani PJ (1998) Expression of cholinergic markers in the pons of Flinders rats. Brain Res Mol Brain Res 55:232-236.
Green AL, Wang S, Purvis S, Owen SL, Bain PG, Stein JF, Guz A, Aziz TZ, Paterson DJ (2007) Identifying cardiorespiratory neurocircuitry involved in central command during exercise in humans. J Physiol 578:605-612.
Greene HL, Richardson DW, Barker AH, Roden DM, Capone RJ, Echt DS, Friedman LM, Gillespie MJ, Hallstrom AP, Verter J (1989) Classification of deaths after myocardial infarction as arrhythmic or nonarrhythmic (the Cardiac Arrhythmia Pilot Study). Am J Cardiol 63:1-6.
Grippo AJ, Beltz TG, Weiss RM, Johnson AK (2005) The Effects of Chronic Fluoxetine Treatment on Chronic Mild Stress-Induced Cardiovascular Changes and Anhedonia. Biol Psychiatry 59:309-316.
Guertzenstein PG (1973) Blood pressure effects obtained by drugs applied to the ventral surface of the brain stem. J Physiol 229:395-408.

Guertzenstein PG, Silver A (1973) Further studies on the role of a bilateral chemosensitive zone on the ventral surface of the brain stem in the maintenance of arterial blood pressure. J Physiol 233:27P-28P.
Guinjoan SM, de Guevara MS, Correa C, Schauffele SI, Nicola-Siri L, Fahrer RD, Ortiz-Fragola E, Martinez-Martinez JA, Cardinali DP (2004) Cardiac parasympathetic dysfunction related to depression in older adults with acute coronary syndromes. J Psychosom Res 56:83-88.
Guyenet PG (1984) Baroreceptor-mediated inhibition of A5 noradrenergic neurons. Brain Res 303:31-40.
Guyenet PG (2000) Neural structures that mediate sympathoexcitation during hypoxia. Respir Physiol 121:147-162.
Guyenet PG (2006) The sympathetic control of blood pressure. Nat Rev Neurosci 7:335-346.
Guyenet PG, Wang H (2001) Pre-Botzinger neurons with preinspiratory discharges "in vivo" express NK1 receptors in the rat. J Neurophysiol 86:438-446.
Guyenet PG, Darnall RA, Riley TA (1990) Rostral ventrolateral medulla and sympathorespiratory integration in rats. Am J Physiol 259:R1063-1074.
Guyenet PG, Schreihofer AM, Stornetta RL (2001) Regulation of sympathetic tone and arterial pressure by the rostral ventrolateral medulla after depletion of C1 cells in rats. Ann N Y Acad Sci 940:259-269.
Guyenet PG, Sevigny CP, Weston MC, Stornetta RL (2002) Neurokinin-1 receptor-expressing cells of the ventral respiratory group are functionally heterogeneous and predominantly glutamatergic. J Neurosci 22:3806-3816.
Guyenet PG, Mulkey DK, Stornetta RL, Bayliss DA (2005a) Regulation of ventral surface chemoreceptors by the central respiratory pattern generator. J Neurosci 25:8938-8947.
Guyenet PG, Stornetta RL, Bayliss DA, Mulkey DK (2005b) Retrotrapezoid nucleus: a litmus test for the identification of central chemoreceptors. Exp Physiol 90:247-253; discussion 253-247.
Guyenet PG, Koshiya N, Huangfu D, Verberne AJ, Riley TA (1993) Central respiratory control of A5 and A6 pontine noradrenergic neurons. Am J Physiol 264:R1035-1044.
Guzzetti S, Signorini MG, Cogliati C, Mezzetti S, Porta A, Cerutti S, Malliani A (1996) Non-linear dynamics and chaotic indices in heart rate variability of normal subjects and heart-transplanted patients. Cardiovasc Res 31:441-446.
Habler HJ, Bartsch T, Janig W (1996) Two distinct mechanisms generate the respiratory modulation in fibre activity of the rat cervical sympathetic trunk. J Auton Nerv Syst 61:116-122.
Haji A, Furuichi S, Takeda R (1996) Effects on iontophoretically applied acetylcholine on membrane potential and synaptic activity of bulbar respiratory neurones in decerebrate cats. Neuropharmacology 35:195-203.
Halliday GM, McLachlan EM (1991a) Four groups of tyrosine hydroxylase-immunoreactive neurons in the ventrolateral medulla of rats, guinea-pigs and cats identified on the basis of chemistry, topography and morphology. Neuroscience 43:551-568.
Halliday GM, McLachlan EM (1991b) A comparative analysis of neurons containing catecholamine-synthesizing enzymes and neuropeptide Y in the ventrolateral medulla of rats, guinea-pigs and cats. Neuroscience 43:531-550.
Hallstrom AP, Bigger JT, Jr., Roden D, Friedman L, Akiyama T, Richardson DW, Rogers WJ, Waldo AL, Pratt CM, Capone RJ, et al. (1992) Prognostic significance of ventricular premature depolarizations measured 1 year after myocardial infarction in patients with early postinfarction asymptomatic ventricular arrhythmia. J Am Coll Cardiol 20:259-264.
Hamlin RL (2006) Animal models of ventricular arrhythmias. Pharmacol Ther 113:276-295.
Hara K, Harris RA (2002) The anesthetic mechanism of urethane: the effects on neurotransmitter-gated ion channels. Anesth Analg 94:313-318.
Hara K, Miyawaki T, Minson J, Arnolda L, Llewellyn-Smith I, Chalmers J, Pilowsky P (1997) Role of spinal GABA receptors in depressor responses to chemical stimulation of the A5 area in normal and hypertensive rats. J Auton Nerv Syst 66:53-61.
Hasegawa S, Nishi K, Watanabe A, Overstreet DH, Diksic M (2006) Brain 5-HT synthesis in the Flinders Sensitive Line rat model of depression: an autoradiographic study. Neurochem Int 48:358-366.
Haselton JR, Guyenet PG (1989a) Central respiratory modulation of medullary sympathoexcitatory neurons in rat. Am J Physiol 256:R739-750.
Haselton JR, Guyenet PG (1989b) Electrophysiological characterization of putative C1 adrenergic neurons in the rat. Neuroscience 30:199-214.
Haselton JR, Guyenet PG (1990) Ascending collaterals of medullary barosensitive neurons and C1 cells in rats. Am J Physiol 258:R1051-1063.
Hauptman PJ, Kelly RA (1999) Digitalis. Circulation 99:1265-1270.
Hautala AJ, Rankinen T, Kiviniemi AM, Makikallio TH, Huikuri HV, Bouchard C, Tulppo MP (2006) Heart rate recovery after maximal exercise is associated with acetylcholine receptor M2 (CHRM2) gene polymorphism. Am J Physiol Heart Circ Physiol 291:H459-466.

Haxhiu MA, Jansen AS, Cherniack NS, Loewy AD (1993) CNS innervation of airway-related parasympathetic preganglionic neurons: a transneuronal labeling study using pseudorabies virus. Brain Res 618:115-134.
Haxhiu MA, Mitra J, van Lunteren E, Bruce EN, Cherniack NS (1984) Hypoglossal and phrenic responses to cholinergic agents applied to ventral medullary surface. Am J Physiol 247:R939-944.
Hayashi F, Lipski J (1992) The role of inhibitory amino acids in control of respiratory motor output in an arterially perfused rat. Respir Physiol 89:47-63.
Hayashi F, Fukuda Y (2000) Neuronal mechanisms mediating the integration of respiratory responses to hypoxia. Jpn J Physiol 50:15-24.
Haymet BT, McCloskey DI (1975) Baroreceptor and chemoreceptor influences on heart rate during the respiratory cycle in the dog. J Physiol 245:699-712.
Head GA, McCarty R (1987) Vagal and sympathetic components of the heart rate range and gain of the baroreceptor-heart rate reflex in conscious rats. J Auton Nerv Syst 21:203-213.
Head GA, Mayorov DN (2001) Central angiotensin and baroreceptor control of circulation. Ann N Y Acad Sci 940:361-379.
Head GA, Lukoshkova EV, Mayorov DN, van den Buuse M (2004) Non-symmetrical double-logistic analysis of 24-h blood pressure recordings in normotensive and hypertensive rats. J Hypertens 22:2075-2085.
Head GA, Lukoshkova EV, Burke SL, Malpas SC, Lambert EA, Janssen BJ (2001) Comparing spectral and invasive estimates of baroreflex gain. IEEE Eng Med Biol Mag 20:43-52.
Henderson LA, Keay KA, Bandler R (1998) The ventrolateral periaqueductal gray projects to caudal brainstem depressor regions: a functional-anatomical and physiological study. Neuroscience 82:201-221.
Hernandez CM, Hoifodt H, Terry AV, Jr. (2003) Spontaneously hypertensive rats: further evaluation of age-related memory performance and cholinergic marker expression. J Psychiatry Neurosci 28:197-209.
Hersch SM, Gutekunst CA, Rees HD, Heilman CJ, Levey AI (1994) Distribution of m1-m4 muscarinic receptor proteins in the rat striatum: light and electron microscopic immunocytochemistry using subtype-specific antibodies. J Neurosci 14:3351-3363.
Heslop DJ, Keay KA, Bandler R (2002) Haemorrhage-evoked compensation and decompensation are mediated by distinct caudal midline medullary regions in the urethane-anaesthetised rat. Neuroscience 113:555-567.
Hickie I (2004) Can we reduce the burden of depression? The Australian experience with beyondblue: the national depression initiative. Australas Psychiatry 12 Suppl:S38-46.
Hirooka Y, Polson JW, Potts PD, Dampney RA (1997) Hypoxia-induced Fos expression in neurons projecting to the pressor region in the rostral ventrolateral medulla. Neuroscience 80:1209-1224.
Hirst GD, McLachlan EM (1980) Intracellular recordings from sympathetic preganglionic neurones of the cat [proceedings]. J Physiol 298:37P-38P.
Hökfelt T, Fuxe K, Goldstein M, Johansson O (1974) Immunohistochemical evidence for the existence of adrenaline neurons in the rat brain. Brain Res 66:235-251.
Holtman JR, Jr., Speck DF (1994) Substance P immunoreactive projections to the ventral respiratory group in the rat. Peptides 15:803-808.
Hon EH, Lee ST (1963a) The Fetal Electrocardiogram. I. The Electrocardiogram Of The Dying Fetus. Am J Obstet Gynecol 87:804-813.
Hon EH, Lee ST (1963b) Electronic Evaluation Of The Fetal Heart Rate. Viii. Patterns Preceding Fetal Death, Further Observations. Am J Obstet Gynecol 87:814-826.
Hopkins DA, Armour JA (1984) Localization of sympathetic postganglionic and parasympathetic preganglionic neurons which innervate different regions of the dog heart. J Comp Neurol 229:186-198.
Hopkins DA, Gootman PM, Gootman N, Di Russo SM, Zeballos ME (1984) Brainstem cells of origin of the cervical vagus and cardiopulmonary nerves in the neonatal pig (Sus scrofa). Brain Res 306:63-72.
Horiuchi J, Dampney RA (1998) Dependence of sympathetic vasomotor tone on bilateral inputs from the rostral ventrolateral medulla in the rabbit: role of baroreceptor reflexes. Neurosci Lett 248:113-116.
Horiuchi J, Dampney RA (2002) Evidence for tonic disinhibition of RVLM sympathoexcitatory neurons from the caudal pressor area. Auton Neurosci 99:102-110.
Horiuchi J, Killinger S, Dampney RA (2004) Contribution to sympathetic vasomotor tone of tonic glutamatergic inputs to neurons in the RVLM. Am J Physiol Regul Integr Comp Physiol 287:R1335-1343.
Horiuchi J, Potts PD, Polson JW, Dampney RA (1999) Distribution of neurons projecting to the rostral ventrolateral medullary pressor region that are activated by sustained hypotension. Neuroscience 89:1319-1329.
Hornykiewicz O, Kobinger W (1956) [Effects of physostigmine, tetraethylpyrophosphate, and neostigmine on the blood pressure and pressor reflexes of the carotid sinus in rats.]. Naunyn Schmiedebergs Arch Exp Pathol Pharmakol 228:493-500.

Hosoya Y, Sugiura Y, Okado N, Loewy AD, Kohno K (1991) Descending input from the hypothalamic paraventricular nucleus to sympathetic preganglionic neurons in the rat. Exp Brain Res 85:10-20.
Hu L, Zhu DN, Yu Z, Wang JQ, Sun ZJ, Yao T (2002) Expression of angiotensin II type 1 (AT(1)) receptor in the rostral ventrolateral medulla in rats. J Appl Physiol 92:2153-2161.
Huangfu D, Schreihofer M, Guyenet PG (1997) Effect of cholinergic agonists on bulbospinal C1 neurons in rats. Am J Physiol 272:R249-258.
Huangfu D, Hwang LJ, Riley TA, Guyenet PG (1992) Splanchnic nerve response to A5 area stimulation in rats. Am J Physiol 263:R437-446.
Huangfu DH, Koshiya N, Guyenet PG (1991) A5 noradrenergic unit activity and sympathetic nerve discharge in rats. Am J Physiol 261:R393-402.
Hull SS, Jr., Evans AR, Vanoli E, Adamson PB, Stramba-Badiale M, Albert DE, Foreman RD, Schwartz PJ (1990) Heart rate variability before and after myocardial infarction in conscious dogs at high and low risk of sudden death. J Am Coll Cardiol 16:978-985.
Izzo PN, Deuchars J, Spyer KM (1993) Localization of cardiac vagal preganglionic motoneurones in the rat: immunocytochemical evidence of synaptic inputs containing 5-hydroxytryptamine. J Comp Neurol 327:572-583.
Janczewski WA, Feldman JL (2006) Distinct rhythm generators for inspiration and expiration in the juvenile rat. J Physiol 570:407-420.
Janig W, Habler HJ (2003) Neurophysiological analysis of target-related sympathetic pathways--from animal to human: similarities and differences. Acta Physiol Scand 177:255-274.
Jansen AS, Loewy AD (1997) Neurons lying in the white matter of the upper cervical spinal cord project to the intermediolateral cell column. Neuroscience 77:889-898.
Jansen AS, Wessendorf MW, Loewy AD (1995) Transneuronal labeling of CNS neuropeptide and monoamine neurons after pseudorabies virus injections into the stellate ganglion. Brain Res 683:1-24.
Janssen BJ, Malpas SC, Burke SL, Head GA (1997) Frequency-dependent modulation of renal blood flow by renal nerve activity in conscious rabbits. Am J Physiol 273:R597-608.
Jensen I, Llewellyn-Smith IJ, Pilowsky P, Minson JB, Chalmers J (1995) Serotonin inputs to rabbit sympathetic preganglionic neurons projecting to the superior cervical ganglion or adrenal medulla. J Comp Neurol 353:427-438.
Jeske I, McKenna KE (1992) Quantitative analysis of bulbospinal projections from the rostral ventrolateral medulla: contribution of C1-adrenergic and nonadrenergic neurons. J Comp Neurol 324:1-13.
Jonas BS, Franks P, Ingram DD (1997) Are symptoms of anxiety and depression risk factors for hypertension? Longitudinal evidence from the National Health and Nutrition Examination Survey I Epidemiologic Follow-up Study. Arch Fam Med 6:43-49.
Jones BE (1990) Immunohistochemical study of choline acetyltransferase-immunoreactive processes and cells innervating the pontomedullary reticular formation in the rat. J Comp Neurol 295:485-514.
Jones BE, Beaudet A (1987) Distribution of acetylcholine and catecholamine neurons in the cat brainstem: a choline acetyltransferase and tyrosine hydroxylase immunohistochemical study. J Comp Neurol 261:15-32.
Jones BE, Webster HH (1988) Neurotoxic lesions of the dorsolateral pontomesencephalic tegmentum-cholinergic cell area in the cat. I. Effects upon the cholinergic innervation of the brain. Brain Res 451:13-32.
Jones JF (2001) Vagal control of the rat heart. Exp Physiol 86:797-801.
Jones JF, Wang Y, Jordan D (1995) Heart rate responses to selective stimulation of cardiac vagal C fibres in anaesthetized cats, rats and rabbits. J Physiol 489 (Pt 1):203-214.
Jones JF, Wang Y, Jordan D (1998) Activity of C fibre cardiac vagal efferents in anaesthetized cats and rats. J Physiol 507 (Pt 3):869-880.
Jordan D (2005) Vagal control of the heart: central serotonergic (5-HT) mechanisms. Exp Physiol 90:175-181.
Jordan D, Spyer KM (1981) Effects of acetylcholine on respiratory neurones in the nucleus ambiguus-retroambigualis complex of the cat. J Physiol 320:103-111.
Julien C, Zhang ZQ, Cerutti C, Barres C (1995) Hemodynamic analysis of arterial pressure oscillations in conscious rats. J Auton Nerv Syst 50:239-252.
Julien C, Chapuis B, Cheng Y, Barres C (2003) Dynamic interactions between arterial pressure and sympathetic nerve activity: role of arterial baroreceptors. Am J Physiol Regul Integr Comp Physiol 285:R834-841.
Kachidian P, Poulat P, Marlier L, Privat A (1991) Immunohistochemical evidence for the coexistence of substance P, thyrotropin-releasing hormone, GABA, methionine-enkephalin, and leucin-enkephalin in the serotonergic neurons of the caudal raphe nuclei: a dual labeling in the rat. J Neurosci Res 30:521-530.
Kalia M, Feldman JL, Cohen MI (1979) Afferent projections to the inspiratory neuronal region of the ventrolateral nucleus of the tractus solitarius in the cat. Brain Res 171:135-141.

Kamiya A, Michikami D, Fu Q, Niimi Y, Iwase S, Mano T, Suzumura A (2001) Static handgrip exercise modifies arterial baroreflex control of vascular sympathetic outflow in humans. Am J Physiol Regul Integr Comp Physiol 281:R1134-1139.
Kanbar R, Orea V, Barres C, Julien C (2007) Baroreflex control of renal sympathetic nerve activity during air-jet stress in rats. Am J Physiol Regul Integr Comp Physiol 292:R362-367.
Kangrga IM, Loewy AD (1995) Whole-cell recordings from visualized C1 adrenergic bulbospinal neurons: ionic mechanisms underlying vasomotor tone. Brain Res 670:215-232.
Kanjhan R, Lipski J, Kruszewska B, Rong W (1995) A comparative study of pre-sympathetic and Botzinger neurons in the rostral ventrolateral medulla (RVLM) of the rat. Brain Res 699:19-32.
Kawada T, Uemura K, Kashihara K, Kamiya A, Sugimachi M, Sunagawa K (2004) A derivative-sigmoidal model reproduces operating point-dependent baroreflex neural arc transfer characteristics. Am J Physiol Heart Circ Physiol 286:H2272-2279.
Kawada T, Yamazaki T, Akiyama T, Shishido T, Inagaki M, Uemura K, Miyamoto T, Sugimachi M, Takaki H, Sunagawa K (2001) In vivo assessment of acetylcholine-releasing function at cardiac vagal nerve terminals. Am J Physiol Heart Circ Physiol 281:H139-145.
Kayembe KN, Sasahara M, Hazama F (1984) Cerebral aneurysms and variations in the circle of Willis. Stroke 15:846-850.
Keyl C, Schneider A, Dambacher M, Bernardi L (2001) Time delay of vagally mediated cardiac baroreflex response varies with autonomic cardiovascular control. J Appl Physiol 91:283-289.
Kiely JM, Gordon FJ (1993) Non-NMDA receptors in the rostral ventrolateral medulla mediate somatosympathetic pressor responses. J Auton Nerv Syst 43:231-239.
Kienzle MG, Ferguson DW, Birkett CL, Myers GA, Berg WJ, Mariano DJ (1992) Clinical, hemodynamic and sympathetic neural correlates of heart rate variability in congestive heart failure. Am J Cardiol 69:761-767.
Kirstein SL, Insel PA (2004) Autonomic nervous system pharmacogenomics: a progress report. Pharmacol Rev 56:31-52.
Kleiger RE, Miller JP, Bigger JT, Jr., Moss AJ (1987) Decreased heart rate variability and its association with increased mortality after acute myocardial infarction. Am J Cardiol 59:256-262.
Koba S, Yoshida T, Hayashi N (2006) Differential sympathetic outflow and vasoconstriction responses at kidney and skeletal muscles during fictive locomotion. Am J Physiol Heart Circ Physiol 290:H861-868.
Kobayashi M, Cheng ZB, Tanaka K, Nosaka S (1999) Is the aortic depressor nerve involved in arterial chemoreflexes in rats? J Auton Nerv Syst 78:38-48.
Koshiya N, Guyenet PG (1994a) Role of the pons in the carotid sympathetic chemoreflex. Am J Physiol 267:R508-518.
Koshiya N, Guyenet PG (1994b) A5 noradrenergic neurons and the carotid sympathetic chemoreflex. Am J Physiol 267:R519-526.
Koshiya N, Guyenet PG (1996a) NTS neurons with carotid chemoreceptor inputs arborize in the rostral ventrolateral medulla. Am J Physiol 270:R1273-1278.
Koshiya N, Guyenet PG (1996b) Tonic sympathetic chemoreflex after blockade of respiratory rhythmogenesis in the rat. J Physiol 491 (Pt 3):859-869.
Koshiya N, Smith JC (1999) Neuronal pacemaker for breathing visualized in vitro. Nature 400:360-363.
Koshiya N, Huangfu D, Guyenet PG (1993) Ventrolateral medulla and sympathetic chemoreflex in the rat. Brain Res 609:174-184.
Krieger EM (1989) Arterial baroreceptor resetting in hypertension (the J. W. McCubbin memorial lecture). Clin Exp Pharmacol Physiol Suppl 15:3-17.
Krout KE, Mettenleiter TC, Loewy AD (2003) Single CNS neurons link both central motor and cardiosympathetic systems: a double-virus tracing study. Neuroscience 118:853-866.
Kubo T (1998) Cholinergic mechanism and blood pressure regulation in the central nervous system. Brain Res Bull 46:475-481.
Kubo T, Tatsumi M (1979) Increased pressor responses to physostigmine in spontaneously hypertensive rats. Naunyn Schmiedebergs Arch Pharmacol 306:81-83.
Kubo T, Ishizuka T, Asari T, Fukumori R (1995a) Acetylcholine release in the rostral ventrolateral medulla of spontaneously hypertensive rats. Clin Exp Pharmacol Physiol Suppl 22:S40-42.
Kubo T, Fukumori R, Kobayashi M, Yamaguchi H (1996) Enhanced cholinergic activity in the medulla oblongata of DOCA-salt hypertensive and renal hypertensive rats. Hypertens Res 19:213-219.
Kubo T, Hagiwara Y, Sekiya D, Fukumori R (1998a) Evidence for involvement of the lateral parabrachial nucleus in mediation of cholinergic inputs to neurons in the rostral ventrolateral medulla of the rat. Brain Res 789:23-31.
Kubo T, Fukumori R, Kobayashi M, Yamaguchi H (1998b) Evidence suggesting that lateral parabrachial nucleus is responsible for enhanced medullary cholinergic activity in hypertension. Hypertens Res 21:201-207.

Kubo T, Fukumori R, Kobayashi M, Yamaguchi H (1998c) Altered cholinergic mechanisms and blood pressure regulation in the rostral ventrolateral medulla of DOCA-salt hypertensive rats. Brain Res Bull 45:327-332.
Kubo T, Asari T, Yamaguchi H, Fukumori R (1998d) Baroreceptor activation causes release of acetylcholine in the rostral ventrolateral medulla of the rat. Clin Exp Hypertens 20:245-257.
Kubo T, Hagiwara Y, Sekiya D, Fukumori R (1999) Midbrain central gray is involved in mediation of cholinergic inputs to the rostral ventrolateral medulla of the rat. Brain Res Bull 50:41-46.
Kubo T, Ishizuka T, Fukumori R, Asari T, Hagiwara Y (1995b) Enhanced release of acetylcholine in the rostral ventrolateral medulla of spontaneously hypertensive rats. Brain Res 686:1-9.
Kubo T, Taguchi K, Sawai N, Ozaki S, Hagiwara Y (1997) Cholinergic mechanisms responsible for blood pressure regulation on sympathoexcitatory neurons in the rostral ventrolateral medulla of the rat. Brain Res Bull 42:199-204.
Kubo T, Hagiwara Y, Sekiya D, Chiba S, Fukumori R (2000) Cholinergic inputs to rostral ventrolateral medulla pressor neurons from hypothalamus. Brain Res Bull 53:275-282.
Kubo T, Fukuda K, Mikami A, Maeda A, Takahashi H, Mishina M, Haga T, Haga K, Ichiyama A, Kangawa K, et al. (1986) Cloning, sequencing and expression of complementary DNA encoding the muscarinic acetylcholine receptor. Nature 323:411-416.
Kumada M, Terui N, Kuwaki T (1990) Arterial baroreceptor reflex: its central and peripheral neural mechanisms. Prog Neurobiol 35:331-361.
Kumar NN, Goodchild AK, Li Q, Pilowsky PM (2006) An aldosterone-related system in the ventrolateral medulla oblongata of spontaneously hypertensive and Wistar-Kyoto rats. Clin Exp Pharmacol Physiol 33:71-75.
Kunitake T, Kannan H (2000) Discharge pattern of renal sympathetic nerve activity in the conscious rat: spectral analysis of integrated activity. J Neurophysiol 84:2859-2867.
Kus L, Borys E, Ping Chu Y, Ferguson SM, Blakely RD, Emborg ME, Kordower JH, Levey AI, Mufson EJ (2003) Distribution of high affinity choline transporter immunoreactivity in the primate central nervous system. J Comp Neurol 463:341-357.
La Rovere MT, Bigger JT, Jr., Marcus FI, Mortara A, Schwartz PJ (1998) Baroreflex sensitivity and heart-rate variability in prediction of total cardiac mortality after myocardial infarction. ATRAMI (Autonomic Tone and Reflexes After Myocardial Infarction) Investigators. Lancet 351:478-484.
La Rovere MT, Pinna GD, Hohnloser SH, Marcus FI, Mortara A, Nohara R, Bigger JT, Jr., Camm AJ, Schwartz PJ (2001) Baroreflex sensitivity and heart rate variability in the identification of patients at risk for life-threatening arrhythmias: implications for clinical trials. Circulation 103:2072-2077.
Lang WJ, Rush ML (1973) Cardiovascular responses to injections of cholinomimetic drugs into the cerebral ventricles of unanaesthetized dogs. Br J Pharmacol 47:196-205.
Laude D, Elghozi JL, Girard A, Bellard E, Bouhaddi M, Castiglioni P, Cerutti C, Cividjian A, Di Rienzo M, Fortrat JO, Janssen B, Karemaker JM, Leftheriotis G, Parati G, Persson PB, Porta A, Quintin L, Regnard J, Rudiger H, Stauss HM (2004) Comparison of various techniques used to estimate spontaneous baroreflex sensitivity (the EuroBaVar study). Am J Physiol Regul Integr Comp Physiol 286:R226-231.
Lee SB, Kim SY, Sung KW (1991) Cardiovascular regulation by cholinergic mechanisms in rostral ventrolateral medulla of spontaneously hypertensive rats. Eur J Pharmacol 205:117-123.
Leon LR, Walker LD, DuBose DA, Stephenson LA (2004) Biotelemetry transmitter implantation in rodents: impact on growth and circadian rhythms. Am J Physiol Regul Integr Comp Physiol 286:R967-974.
Leone C, Gordon FJ (1989) Is L-glutamate a neurotransmitter of baroreceptor information in the nucleus of the tractus solitarius? J Pharmacol Exp Ther 250:953-962.
Lesperance F, Frasure-Smith N, Juneau M, Theroux P (2000) Depression and 1-year prognosis in unstable angina. Arch Intern Med 160:1354-1360.
Lesperance F, Frasure-Smith N, Talajic M, Bourassa MG (2002) Five-year risk of cardiac mortality in relation to initial severity and one-year changes in depression symptoms after myocardial infarction. Circulation 105:1049-1053.
Lett HS, Blumenthal JA, Babyak MA, Strauman TJ, Robins C, Sherwood A (2005) Social support and coronary heart disease: epidemiologic evidence and implications for treatment. Psychosom Med 67:869-878.
Levey AI (1993) Immunological localization of m1-m5 muscarinic acetylcholine receptors in peripheral tissues and brain. Life Sci 52:441-448.
Levey AI, Kitt CA, Simonds WF, Price DL, Brann MR (1991) Identification and localization of muscarinic acetylcholine receptor proteins in brain with subtype-specific antibodies. J Neurosci 11:3218-3226.
Levy MN, Yang T, Wallick DW (1993) Assessment of beat-by-beat control of heart rate by the autonomic nervous system: molecular biology technique are necessary, but not sufficient. J Cardiovasc Electrophysiol 4:183-193.
Lewis DI, Coote JH (1990) Excitation and inhibition of rat sympathetic preganglionic neurones by catecholamines. Brain Res 530:229-234.

Li J, Brezenoff HE, Tkacs NC (1997) Identification of pressor regions activated by central cholinergic stimulation in rat brain. Eur J Pharmacol 337:227-233.
Li Q, Goodchild AK, Pilowsky PM (2003) Effect of haemorrhage on the expression of neurotransmitter-related genes in rat ventrolateral medulla: a quantitative real-time RT-PCR study. Brain Res Mol Brain Res 114:46-54.
Li Q, Goodchild AK, Seyedabadi M, Pilowsky PM (2005) Preprotachykinin A mRNA is colocalized with tyrosine hydroxylase-immunoreactivity in bulbospinal neurons. Neuroscience.
Li YH, Ku YH (2002) Involvement of rat lateral septum-acetylcholine pressor system in central amygdaloid nucleus-emotional pressor circuit. Neurosci Lett 323:60-64.
Li YW, Guyenet PG (1995) Neuronal excitation by angiotensin II in the rostral ventrolateral medulla of the rat in vitro. Am J Physiol 268:R272-277.
Li YW, Gieroba ZJ, McAllen RM, Blessing WW (1991) Neurons in rabbit caudal ventrolateral medulla inhibit bulbospinal barosensitive neurons in rostral medulla. Am J Physiol 261:R44-51.
Lieske SP, Thoby-Brisson M, Ramirez JM (2001) Reconfiguration of the central respiratory network under normoxic and hypoxic conditions. Adv Exp Med Biol 499:171-178.
Lieske SP, Thoby-Brisson M, Telgkamp P, Ramirez JM (2000) Reconfiguration of the neural network controlling multiple breathing patterns: eupnea, sighs and gasps [see comment]. Nat Neurosci 3:600-607.
Lipski J, Merrill EG (1980) Electrophysiological demonstration of the projection from expiratory neurones in rostral medulla to contralateral dorsal respiratory group. Brain Res 197:521-524.
Lipski J, McAllen RM, Spyer KM (1975) The sinus nerve and baroreceptor input to the medulla of the cat. J Physiol 251:61-78.
Lipski J, Bellingham MC, West MJ, Pilowsky P (1988) Limitations of the technique of pressure microinjection of excitatory amino acids for evoking responses from localized regions of the CNS. J Neurosci Methods 26:169-179.
Lipski J, Kanjhan R, Kruszewska B, Smith M (1995) Barosensitive neurons in the rostral ventrolateral medulla of the rat in vivo: morphological properties and relationship to C1 adrenergic neurons. Neuroscience 69:601-618.
Lipski J, Kanjhan R, Kruszewska B, Rong W (1996) Properties of presympathetic neurones in the rostral ventrolateral medulla in the rat: an intracellular study "in vivo'. J Physiol 490 (Pt 3):729-744.
Llewellyn-Smith IJ, Dicarlo SE, Collins HL, Keast JR (2005) Enkephalin-immunoreactive interneurons extensively innervate sympathetic preganglionic neurons regulating the pelvic viscera. J Comp Neurol 488:278-289.
Loewy AD (1981) Raphe pallidus and raphe obscurus projections to the intermediolateral cell column in the rat. Brain Res 222:129-133.
Loewy AD, McKellar S, Saper CB (1979) Direct projections from the A5 catecholamine cell group to the intermediolateral cell column. Brain Res 174:309-314.
Loewy AD, Wallach JH, McKellar S (1981) Efferent connections of the ventral medulla oblongata in the rat. Brain Res 228:63-80.
Loewy AD, Marson L, Parkinson D, Perry MA, Sawyer WB (1986) Descending noradrenergic pathways involved in the A5 depressor response. Brain Res 386:313-324.
Lombardi F (2002) Clinical implications of present physiological understanding of HRV components. Card Electrophysiol Rev 6:245-249.
Lombardi F, Malliani A, Pagani M, Cerutti S (1996) Heart rate variability and its sympatho-vagal modulation. Cardiovasc Res 32:208-216.
Lombardi F, Sandrone G, Pernpruner S, Sala R, Garimoldi M, Cerutti S, Baselli G, Pagani M, Malliani A (1987) Heart rate variability as an index of sympathovagal interaction after acute myocardial infarction. Am J Cardiol 60:1239-1245.
Lovick TA, Coote JH (1988) Electrophysiological properties of paraventriculo-spinal neurones in the rat. Brain Res 454:123-130.
Lovick TA, Malpas S, Mahony MT (1993) Renal vasodilatation in response to acute volume load is attenuated following lesions of parvocellular neurones in the paraventricular nucleus in rats. J Auton Nerv Syst 43:247-255.
Luiten PG, ter Horst GJ, Karst H, Steffens AB (1985) The course of paraventricular hypothalamic efferents to autonomic structures in medulla and spinal cord. Brain Res 329:374-378.
Machado BH, Bonagamba LG, Dun SL, Kwok EH, Dun NJ (2002) Pressor response to microinjection of orexin/hypocretin into rostral ventrolateral medulla of awake rats. Regul Pept 104:75-81.
Madden CJ, Sved AF (2003) Cardiovascular regulation after destruction of the C1 cell group of the rostral ventrolateral medulla in rats. Am J Physiol Heart Circ Physiol 285:H2734-2748.
Madden CJ, Stocker SD, Sved AF (2006) Attenuation of homeostatic responses to hypotension and glucoprivation after destruction of catecholaminergic rostral ventrolateral medulla neurons. Am J Physiol Regul Integr Comp Physiol 291:R751-759.

Madden CJ, Ito S, Rinaman L, Wiley RG, Sved AF (1999) Lesions of the C1 catecholaminergic neurons of the ventrolateral medulla in rats using anti-DbetaH-saporin. Am J Physiol 277:R1063-1075.
Mahamed S, Ali AF, Ho D, Wang B, Duffin J (2001) The contribution of chemoreflex drives to resting breathing in man. Exp Physiol 86:109-116.
Mainardi LT, Bianchi AM, Cerutti S (2002) Time-frequency and time-varying analysis for assessing the dynamic responses of cardiovascular control. Crit Rev Biomed Eng 30:175-217.
Maiorov DN, Malpas SC, Head GA (2000) Influence of pontine A5 region on renal sympathetic nerve activity in conscious rabbits. Am J Physiol Regul Integr Comp Physiol 278:R311-319.
Maiorov DN, Wilton ER, Badoer E, Petrie D, Head GA, Malpas SC (1999) Sympathetic response to stimulation of the pontine A5 region in conscious rabbits. Brain Res 815:227-236.
Makeham JM, Goodchild AK, Pilowsky PM (2001) NK1 receptor and the ventral medulla of the rat: bulbospinal and catecholaminergic neurons. Neuroreport 12:3663-3667.
Makeham JM, Goodchild AK, Pilowsky PM (2005) NK1 receptor activation in rat rostral ventrolateral medulla selectively attenuates somato-sympathetic reflex while antagonism attenuates sympathetic chemoreflex. Am J Physiol Regul Integr Comp Physiol 288:R1707-1715.
Malik M (1998) Sympathovagal balance: a critical appraisal. Circulation 98:2643-2644.
Malkesman O, Braw Y, Maayan R, Weizman A, Overstreet DH, Shabat-Simon M, Kesner Y, Touati-Werner D, Yadid G, Weller A (2006) Two different putative genetic animal models of childhood depression. Biol Psychiatry 59:17-23.
Mallard C, Tolcos M, Leditschke J, Campbell P, Rees S (1999) Reduction in choline acetyltransferase immunoreactivity but not muscarinic-m2 receptor immunoreactivity in the brainstem of SIDS infants. J Neuropathol Exp Neurol 58:255-264.
Malpas SC, Head GA, Anderson WP (1996) Renal responses to increases in renal sympathetic nerve activity induced by brainstem stimulation in rabbits. J Auton Nerv Syst 61:70-78.
Mancia G, Grassi G (2000) Mechanisms and clinical implications of blood pressure variability. J Cardiovasc Pharmacol 35:S15-19.
Mandel DA, Schreihofer AM (2006) Central respiratory modulation of barosensitive neurones in rat caudal ventrolateral medulla. J Physiol 572:881-896.
Mann JJ (2005) The medical management of depression. N Engl J Med 353:1819-1834.
Mansier P, Clairambault J, Charlotte N, Medigue C, Vermeiren C, LePape G, Carre F, Gounaropoulou A, Swynghedauw B (1996) Linear and non-linear analyses of heart rate variability: a minireview. Cardiovasc Res 31:371-379.
Marshall JM (1987) Analysis of cardiovascular responses evoked following changes in peripheral chemoreceptor activity in the rat. J Physiol 394:393-414.
Marshall JM (1994) Peripheral chemoreceptors and cardiovascular regulation. Physiol Rev 74:543-594.
Martinka P, Fielitz J, Patzak A, Regitz-Zagrosek V, Persson PB, Stauss HM (2005) Mechanisms of blood pressure variability-induced cardiac hypertrophy and dysfunction in mice with impaired baroreflex. Am J Physiol Regul Integr Comp Physiol 288:R767-776.
Mason P (2001) Contributions of the medullary raphe and ventromedial reticular region to pain modulation and other homeostatic functions. Annu Rev Neurosci 24:737-777.
Massari VJ, Johnson TA, Gillis RA, Gatti PJ (1996) What are the roles of substance P and neurokinin-1 receptors in the control of negative chronotropic or negative dromotropic vagal motoneurons? A physiological and ultrastructural analysis. Brain Res 715:197-207.
Masuda N, Terui N, Koshiya N, Kumada M (1991) Neurons in the caudal ventrolateral medulla mediate the arterial baroreceptor reflex by inhibiting barosensitive reticulospinal neurons in the rostral ventrolateral medulla in rabbits. J Auton Nerv Syst 34:103-117.
Mathers C, Vos T, Stevenson C (1999) The burden of disease and injury in Australia. AIHW Cat. no. PHE 17.
Matsui M, Motomura D, Fujikawa T, Jiang J, Takahashi S, Manabe T, Taketo MM (2002) Mice lacking M2 and M3 muscarinic acetylcholine receptors are devoid of cholinergic smooth muscle contractions but still viable. J Neurosci 22:10627-10632.
Matsukawa K, Komine H, Nakamoto T, Murata J (2006) Central command blunts sensitivity of arterial baroreceptor-heart rate reflex at onset of voluntary static exercise. Am J Physiol Heart Circ Physiol 290:H200-208.
Mattsson H, Arani Z, Astin M, Bayati A, Overstreet DH, Lehmann A (2005) Altered neuroendocrine response and gastric dysmotility in the Flinders Sensitive Line rat. Neurogastroenterol Motil 17:166-174.
Mayer S (1876) Studien zur Physiologie des Herxens und Blutgefasse: V. Uber spontane Blutdruck schwankungen. S-B Akad Wiss Wien, Math-Nat 74:281-307.
McAllen RM (1987) Central respiratory modulation of subretrofacial bulbospinal neurones in the cat. J Physiol 388:533-545.
McAllen RM (2004) Preoptic thermoregulatory mechanisms in detail. Am J Physiol Regul Integr Comp Physiol 287:R272-273.

McAllen RM, Spyer KM (1976) The location of cardiac vagal preganglionic motoneurones in the medulla of the cat. J Physiol 258:187-204.
McAllen RM, Spyer KM (1978a) Two types of vagal preganglionic motoneurones projecting to the heart and lungs. J Physiol 282:353-364.
McAllen RM, Spyer KM (1978b) The baroreceptor input to cardiac vagal motoneurones. J Physiol 282:365-374.
McAllen RM, Blessing WW (1987) Neurons (presumably A1-cells) projecting from the caudal ventrolateral medulla to the region of the supraoptic nucleus respond to baroreceptor inputs in the rabbit. Neurosci Lett 73:247-252.
McAllen RM, Dampney RA (1990) Vasomotor neurons in the rostral ventrolateral medulla are organized topographically with respect to type of vascular bed but not body region. Neurosci Lett 110:91-96.
McAllen RM, May CN (1994) Differential drives from rostral ventrolateral medullary neurons to three identified sympathetic outflows. Am J Physiol 267:R935-944.
McAllen RM, Neil JJ, Loewy AD (1982) Effects of kainic acid applied to the ventral surface of the medulla oblongata on vasomotor tone, the baroreceptor reflex and hypothalamic autonomic responses. Brain Res 238:65-76.
McAllen RM, May CN, Shafton AD (1995) Functional anatomy of sympathetic premotor cell groups in the medulla. Clin Exp Hypertens 17:209-221.
McAllen RM, Trevaks D, Allen AM (2001) Analysis of firing correlations between sympathetic premotor neuron pairs in anesthetized cats. J Neurophysiol 85:1697-1708.
McAllen RM, Habler HJ, Michaelis M, Peters O, Janig W (1994) Monosynaptic excitation of preganglionic vasomotor neurons by subretrofacial neurons of the rostral ventrolateral medulla. Brain Res 634:227-234.
McCaffery JM, Frasure-Smith N, Dube MP, Theroux P, Rouleau GA, Duan Q, Lesperance F (2006) Common genetic vulnerability to depressive symptoms and coronary artery disease: a review and development of candidate genes related to inflammation and serotonin. Psychosom Med 68:187-200.
McCall RB (1988) GABA-mediated inhibition of sympathoexcitatory neurons by midline medullary stimulation. Am J Physiol 255:R605-615.
McCaughran JA, Jr., Murphy D, Schechter N, Friedman R (1983) Participation of the central cholinergic system in blood pressure regulation in the Dahl rat model of essential hypertension. J Cardiovasc Pharmacol 5:1005-1009.
McCrimmon DR, Monnier A, Hayashi F, Zuperku EJ (2000) Pattern formation and rhythm generation in the ventral respiratory group. Clin Exp Pharmacol Physiol 27:126-131.
McCubbin JW, Green JH, Page IH (1956) Baroceptor function in chronic renal hypertension. Circ Res 4:205-210.
McDowall LM, Dampney RA (2006) Calculation of threshold and saturation points of sigmoidal baroreflex function curves. Am J Physiol Heart Circ Physiol 291:H2003-2007.
McDowall LM, Horiuchi J, Killinger S, Dampney RA (2006) Modulation of the baroreceptor reflex by the dorsomedial hypothalamic nucleus and perifornical area. Am J Physiol Regul Integr Comp Physiol 290:R1020-1026.
McGehee DS, Heath MJ, Gelber S, Devay P, Role LW (1995) Nicotine enhancement of fast excitatory synaptic transmission in CNS by presynaptic receptors. Science 269:1692-1696.
Medigue C, Girard A, Laude D, Monti A, Wargon M, Elghozi JL (2001) Relationship between pulse interval and respiratory sinus arrhythmia: a time- and frequency-domain analysis of the effects of atropine. Pflugers Arch 441:650-655.
Mellen NM, Janczewski WA, Bocchiaro CM, Feldman JL (2003) Opioid-induced quantal slowing reveals dual networks for respiratory rhythm generation. Neuron 37:821-826.
Mendelowitz D (1998) Nicotine excites cardiac vagal neurons via three sites of action. Clin Exp Pharmacol Physiol 25:453-456.
Mendelowitz D (1999) Advances in Parasympathetic Control of Heart Rate and Cardiac Function. News Physiol Sci 14:155-161.
Mendelowitz D (2000) Superior laryngeal neurons directly excite cardiac vagal neurons within the nucleus ambiguus. Brain Res Bull 51:135-138.
Merrill EG, Fedorko L (1984) Monosynaptic inhibition of phrenic motoneurons: a long descending projection from Botzinger neurons. J Neurosci 4:2350-2353.
Mesulam MM, Geula C (1992) Overlap between acetylcholinesterase-rich and choline acetyltransferase-positive (cholinergic) axons in human cerebral cortex. Brain Res 577:112-120.
Mesulam MM, Mufson EJ, Levey AI, Wainer BH (1983a) Cholinergic innervation of cortex by the basal forebrain: cytochemistry and cortical connections of the septal area, diagonal band nuclei, nucleus basalis (substantia innominata), and hypothalamus in the rhesus monkey. J Comp Neurol 214:170-197.
Mesulam MM, Mufson EJ, Wainer BH, Levey AI (1983b) Central cholinergic pathways in the rat: an overview based on an alternative nomenclature (Ch1-Ch6). Neuroscience 10:1185-1201.

Miki K, Yoshimoto M, Tanimizu M (2003) Acute shifts of baroreflex control of renal sympathetic nerve activity induced by treadmill exercise in rats. J Physiol 548:313-322.
Milner TA, Pickel VM, Giuliano R, Reis DJ (1989) Ultrastructural localization of choline acetyltransferase in the rat rostral ventrolateral medulla: evidence for major synaptic relations with non-catecholaminergic neurons. Brain Res 500:67-89.
Minson J, Llewellyn-Smith I, Neville A, Somogyi P, Chalmers J (1990a) Quantitative analysis of spinally projecting adrenaline-synthesising neurons of C1, C2 and C3 groups in rat medulla oblongata. J Auton Nerv Syst 30:209-220.
Minson J, Chalmers J, Drolet G, Kapoor V, Llewellyn-Smith I, Mills E, Morris M, Pilowsky P (1990b) Central serotonergic mechanisms in cardiovascular regulation. Cardiovasc Drugs Ther 4 Suppl 1:27-32.
Minson JB, Chalmers JP, Caon AC, Renaud B (1987) Separate areas of rat medulla oblongata with populations of serotonin- and adrenaline-containing neurons alter blood pressure after L-glutamate stimulation. J Auton Nerv Syst 19:39-50.
Miyawaki T, Goodchild AK, Pilowsky PM (2001) Rostral ventral medulla 5-HT1A receptors selectively inhibit the somatosympathetic reflex. Am J Physiol Regul Integr Comp Physiol 280:R1261-1268.
Miyawaki T, Goodchild AK, Pilowsky PM (2002a) Evidence for a tonic GABA-ergic inhibition of excitatory respiratory-related afferents to presympathetic neurons in the rostral ventrolateral medulla. Brain Res 924:56-62.
Miyawaki T, Goodchild AK, Pilowsky PM (2002b) Activation of mu-opioid receptors in rat ventrolateral medulla selectively blocks baroreceptor reflexes while activation of delta opioid receptors blocks somato-sympathetic reflexes. Neuroscience 109:133-144.
Miyawaki T, Goodchild AK, Pilowsky PM (2003) Maintenance of sympathetic tone by a nickel chloride-sensitive mechanism in the rostral ventrolateral medulla of the adult rat. Neuroscience 116:455-464.
Miyawaki T, Minson J, Arnolda L, Chalmers J, Llewellyn-Smith I, Pilowsky P (1996a) Role of excitatory amino acid receptors in cardiorespiratory coupling in ventrolateral medulla. Am J Physiol 271:R1221-1230.
Miyawaki T, Minson J, Arnolda L, Llewellyn-Smith I, Chalmers J, Pilowsky P (1996b) AMPA/kainate receptors mediate sympathetic chemoreceptor reflex in the rostral ventrolateral medulla. Brain Res 726:64-68.
Miyawaki T, Pilowsky P, Sun QJ, Minson J, Suzuki S, Arnolda L, Llewellyn-Smith I, Chalmers J (1995) Central inspiration increases barosensitivity of neurons in rat rostral ventrolateral medulla. Am J Physiol 268:R909-918.
Miyazaki T, Coote JH, Dun NJ (1989) Excitatory and inhibitory effects of epinephrine on neonatal rat sympathetic preganglionic neurons in vitro. Brain Res 497:108-116.
Moffitt JA, Grippo AJ, Holmes PV, Johnson AK (2002) Olfactory bulbectomy attenuates cardiovascular sympathoexcitatory reflexes in rats. Am J Physiol Heart Circ Physiol 283:H2575-2583.
Monnier A, Alheid GF, McCrimmon DR (2003) Defining ventral medullary respiratory compartments with a glutamate receptor agonist in the rat. J Physiol 548:859-874.
Moon EA, Goodchild AK, Pilowsky PM (2002) Lateralisation of projections from the rostral ventrolateral medulla to sympathetic preganglionic neurons in the rat. Brain Res 929:181-190.
Morrison SF, Reis DJ (1989) Reticulospinal vasomotor neurons in the RVL mediate the somatosympathetic reflex. Am J Physiol 256:R1084-1097.
Morrison SF, Milner TA, Reis DJ (1988) Reticulospinal vasomotor neurons of the rat rostral ventrolateral medulla: relationship to sympathetic nerve activity and the C1 adrenergic cell group. J Neurosci 8:1286-1301.
Moss AJ, Hall WJ, Cannom DS, Daubert JP, Higgins SL, Klein H, Levine JH, Saksena S, Waldo AL, Wilber D, Brown MW, Heo M (1996) Improved survival with an implanted defibrillator in patients with coronary disease at high risk for ventricular arrhythmia. Multicenter Automatic Defibrillator Implantation Trial Investigators. N Engl J Med 335:1933-1940.
Motawei K, Pyner S, Ranson RN, Kamel M, Coote JH (1999) Terminals of paraventricular spinal neurones are closely associated with adrenal medullary sympathetic preganglionic neurones: immunocytochemical evidence for vasopressin as a possible neurotransmitter in this pathway. Exp Brain Res 126:68-76.
Mulkey DK, Stornetta RL, Weston MC, Simmons JR, Parker A, Bayliss DA, Guyenet PG (2004) Respiratory control by ventral surface chemoreceptor neurons in rats. Nat Neurosci 7:1360-1369.
Nagura S, Sakagami T, Kakiichi A, Yoshimoto M, Miki K (2004) Acute shifts in baroreflex control of renal sympathetic nerve activity induced by REM sleep and grooming in rats. J Physiol 558:975-983.
Nakamura K, Matsumura K, Hubschle T, Nakamura Y, Hioki H, Fujiyama F, Boldogkoi Z, Konig M, Thiel HJ, Gerstberger R, Kobayashi S, Kaneko T (2004) Identification of sympathetic premotor neurons in medullary raphe regions mediating fever and other thermoregulatory functions. J Neurosci 24:5370-5380.

Nalivaiko E, Blessing WW (2002) Potential role of medullary raphe-spinal neurons in cutaneous vasoconstriction: an in vivo electrophysiological study. J Neurophysiol 87:901-911.
Natarajan M, Morrison SF (2000) Sympathoexcitatory CVLM neurons mediate responses to caudal pressor area stimulation. Am J Physiol Regul Integr Comp Physiol 279:R364-374.
Nattie EE, Li AH (1990) Ventral medulla sites of muscarinic receptor subtypes involved in cardiorespiratory control. J Appl Physiol 69:33-41.
Nattie EE, Li A, Richerson G, Lappi DA (2004) Medullary serotonergic neurones and adjacent neurones that express neurokinin-1 receptors are both involved in chemoreception in vivo. J Physiol 556:235-253.
Neff RA, Mihalevich M, Mendelowitz D (1998a) Stimulation of NTS activates NMDA and non-NMDA receptors in rat cardiac vagal neurons in the nucleus ambiguus. Brain Res 792:277-282.
Neff RA, Humphrey J, Mihalevich M, Mendelowitz D (1998b) Nicotine enhances presynaptic and postsynaptic glutamatergic neurotransmission to activate cardiac parasympathetic neurons. Circ Res 83:1241-1247.
Neff RA, Wang J, Baxi S, Evans C, Mendelowitz D (2003) Respiratory sinus arrhythmia: endogenous activation of nicotinic receptors mediates respiratory modulation of brainstem cardioinhibitory parasympathetic neurons. Circ Res 93:565-572.
Nestler EJ, Barrot M, DiLeone RJ, Eisch AJ, Gold SJ, Monteggia LM (2002) Neurobiology of depression. Neuron 34:13-25.
Newland MC, Ellis SJ, Lydiatt CA, Peters KR, Tinker JH, Romberger DJ, Ullrich FA, Anderson JR (2002) Anesthetic-related cardiac arrest and its mortality: a report covering 72,959 anesthetics over 10 years from a US teaching hospital. Anesthesiology 97:108-115.
Nicholas AP, Hancock MB (1990) Evidence for projections from the rostral medullary raphe onto medullary catecholamine neurons in the rat. Neurosci Lett 108:22-28.
Nicholson C (1985) Diffusion from an injected volume of a substance in brain tissue with arbitrary volume fraction and tortuosity. Brain Res 333:325-329.
Ninomiya I, Nisimaru N, Irisawa H (1971) Sympathetic nerve activity to the spleen, kidney, and heart in response to baroceptor input. Am J Physiol 221:1346-1351.
Nogueira MI, de Rezende BD, do Vale LE, Bittencourt JC (2000) Afferent connections of the caudal raphe pallidus nucleus in rats: a study using the fluorescent retrograde tracers fluorogold and true-blue. Ann Anat 182:35-45.
Norman RA, Jr., Coleman TG, Dent AC (1981) Continuous monitoring of arterial pressure indicates sinoaortic denervated rats are not hypertensive. Hypertension 3:119-125.
Numao Y, Koshiya N, Gilbey MP, Spyer KM (1987) Central respiratory drive-related activity in sympathetic nerves of the rat: the regional differences. Neurosci Lett 81:279-284.
Nuyts S, Van Mellaert L, Lambin P, Anne J (2001) Efficient isolation of total RNA from Clostridium without DNA contamination. J Microbiol Methods 44:235-238.
Odagaki Y, Fuxe K (1995) 5-HT1A, GABAB, and pirenzepine-insensitive muscarinic receptors are functionally coupled to distinct pools of the same kind of G proteins in rat hippocampus. Brain Res 689:129-135.
Oldfield BJ, McLachlan EM (1981) An analysis of the sympathetic preganglionic neurons projecting from the upper thoracic spinal roots of the cat. J Comp Neurol 196:329-345.
Onali P, Olianas MC (1995) Bimodal regulation of cyclic AMP by muscarinic receptors. Involvement of multiple G proteins and different forms of adenylyl cyclase. Life Sci 56:973-980.
Onimaru H, Homma I (2003) A novel functional neuron group for respiratory rhythm generation in the ventral medulla. J Neurosci 23:1478-1486.
Onimaru H, Arata A, Homma I (1989) Firing properties of respiratory rhythm generating neurons in the absence of synaptic transmission in rat medulla in vitro. Exp Brain Res 76:530-536.
Onimaru H, Arata A, Homma I (1997) Neuronal mechanisms of respiratory rhythm generation: an approach using in vitro preparation. Jpn J Physiol 47:385-403.
Onimaru H, Ballanyi K, Homma I (2003) Contribution of Ca2+-dependent conductances to membrane potential fluctuations of medullary respiratory neurons of newborn rats in vitro. J Physiol 552:727-741.
Ootsuka Y, Terui N (1997) Functionally different neurons are organized topographically in the rostral ventrolateral medulla of rabbits. J Auton Nerv Syst 67:67-78.
Ootsuka Y, McAllen RM (2005) Interactive drives from two brain stem premotor nuclei are essential to support rat tail sympathetic activity. Am J Physiol Regul Integr Comp Physiol 289:R1107-1115.
Ootsuka Y, Blessing WW (2006) Activation of 5-HT1A receptors in rostral medullary raphe inhibits cutaneous vasoconstriction elicited by cold exposure in rabbits. Brain Res 1073-1074:252-261.
Ootsuka Y, Blessing WW, McAllen RM (2004) Inhibition of rostral medullary raphe neurons prevents cold-induced activity in sympathetic nerves to rat tail and rabbit ear arteries. Neurosci Lett 357:58-62.
Oshima N, McMullan S, Goodchild AK, Pilowsky PM (2006) A monosynaptic connection between baroinhibited neurons in the RVLM and IML in Sprague-Dawley rats. Brain Res 1089:153-161.

Osterlund MK, Overstreet DH, Hurd YL (1999) The flinders sensitive line rats, a genetic model of depression, show abnormal serotonin receptor mRNA expression in the brain that is reversed by 17beta-estradiol. Brain Res Mol Brain Res 74:158-166.
Overstreet DH (1986) Selective breeding for increased cholinergic function: development of a new animal model of depression. Biol Psychiatry 21:49-58.
Overstreet DH (1993) The Flinders sensitive line rats: a genetic animal model of depression. Neurosci Biobehav Rev 17:51-68.
Overstreet DH (2002) Behavioral characteristics of rat lines selected for differential hypothermic responses to cholinergic or serotonergic agonists. Behav Genet 32:335-348.
Overstreet DH, Russell RW (1982) Selective breeding for diisopropyl fluorophosphate-sensitivity: behavioural effects of cholinergic agonists and antagonists. Psychopharmacology (Berl) 78:150-155.
Overstreet DH, Griebel G (2005) Antidepressant-like effects of the vasopressin V1b receptor antagonist SSR149415 in the Flinders Sensitive Line rat. Pharmacol Biochem Behav 82:223-227.
Overstreet DH, Rezvani AH, Janowsky DS (1990) Impaired active avoidance responding in rats selectively bred for increased cholinergic function. Physiol Behav 47:787-788.
Overstreet DH, Rezvani AH, Janowsky DS (1992a) Genetic animal models of depression and ethanol preference provide support for cholinergic and serotonergic involvement in depression and alcoholism. Biol Psychiatry 31:919-936.
Overstreet DH, Russell RW, Helps SC, Messenger M (1979) Selective breeding for sensitivity to the anticholinesterase DFP. Psychopharmacology (Berl) 65:15-20.
Overstreet DH, Russell RW, Crocker AD, Schiller GD (1984) Selective breeding for differences in cholinergic function: pre- and postsynaptic mechanisms involved in sensitivity to the anticholinesterase, DFP. Brain Res 294:327-332.
Overstreet DH, Russell RW, Hay DA, Crocker AD (1992b) Selective breeding for increased cholinergic function: biometrical genetic analysis of muscarinic responses. Neuropsychopharmacology 7:197-204.
Overstreet DH, Janowsky DS, Pucilowski O, Rezvani AH (1994) Swim test immobility co-segregates with serotonergic but not cholinergic sensitivity in cross-breeds of Flinders Line rats. Psychiatr Genet 4:101-107.
Overstreet DH, Pucilowski O, Rezvani AH, Janowsky DS (1995) Administration of antidepressants, diazepam and psychomotor stimulants further confirms the utility of Flinders Sensitive Line rats as an animal model of depression. Psychopharmacology (Berl) 121:27-37.
Overstreet DH, Friedman E, Mathe AA, Yadid G (2005) The Flinders Sensitive Line rat: A selectively bred putative animal model of depression. Neurosci Biobehav Rev 29:739-759.
Overstreet DH, Janowsky DS, Gillin JC, Shiromani PJ, Sutin EL (1986) Stress-induced immobility in rats with cholinergic supersensitivity. Biol Psychiatry 21:657-664.
Overstreet DH, Daws LC, Schiller GD, Orbach J, Janowsky DS (1998) Cholinergic/serotonergic interactions in hypothermia: implications for rat models of depression. Pharmacol Biochem Behav 59:777-785.
Owens MJ, Overstreet DH, Knight DL, Rezvani AH, Ritchie JC, Bissette G, Janowsky DS, Nemeroff CB (1991) Alterations in the hypothalamic-pituitary-adrenal axis in a proposed animal model of depression with genetic muscarinic supersensitivity. Neuropsychopharmacology 4:87-93.
Ozawa H, Uematsu T (1976) Centrally mediated cardiovascular effects of intracisternal application of carbachol in anesthetized rats. Jpn J Pharmacol 26:339-346.
Padley JR, Li Q, Pilowsky PM, Goodchild AK (2003) Cannabinoid receptor activation in the rostral ventrolateral medulla oblongata evokes cardiorespiratory effects in anaesthetised rats. Br J Pharmacol 140:384-394.
Pagani M, Lombardi F, Guzzetti S, Sandrone G, Rimoldi O, Malfatto G, Cerutti S, Malliani A (1984) Power spectral density of heart rate variability as an index of sympatho-vagal interaction in normal and hypertensive subjects. J Hypertens Suppl 2:S383-385.
Pagani M, Mazzuero G, Ferrari A, Liberati D, Cerutti S, Vaitl D, Tavazzi L, Malliani A (1991) Sympathovagal interaction during mental stress. A study using spectral analysis of heart rate variability in healthy control subjects and patients with a prior myocardial infarction. Circulation 83:II43-51.
Pagani M, Somers V, Furlan R, Dell'Orto S, Conway J, Baselli G, Cerutti S, Sleight P, Malliani A (1988) Changes in autonomic regulation induced by physical training in mild hypertension. Hypertension 12:600-610.
Pagani M, Lombardi F, Guzzetti S, Rimoldi O, Furlan R, Pizzinelli P, Sandrone G, Malfatto G, Dell'Orto S, Piccaluga E, et al. (1986) Power spectral analysis of heart rate and arterial pressure variabilities as a marker of sympatho-vagal interaction in man and conscious dog. Circ Res 59:178-193.
Pahapill PA, Lozano AM (2000) The pedunculopontine nucleus and Parkinson's disease. Brain 123 (Pt 9):1767-1783.
Parer JT, Livingston EG (1990) What is fetal distress? Am J Obstet Gynecol 162:1421-1425; discussion 1425-1427.

Park KH, Long JP (1991) Modulation by physostigmine of head-up tilt- and bilateral carotid occlusion-induced baroreflexes in rats. J Pharmacol Exp Ther 257:50-55.
Parsons SM (2000) Transport mechanisms in acetylcholine and monoamine storage. Faseb J 14:2423-2434.
Passino C, Sleight P, Valle F, Spadacini G, Leuzzi S, Bernardi L (1997) Lack of peripheral modulation of cardiovascular central oscillatory autonomic activity during apnea in humans. Am J Physiol 272:H123-129.
Paton JF, Richter DW (1995) Role of fast inhibitory synaptic mechanisms in respiratory rhythm generation in the maturing mouse. J Physiol 484 (Pt 2):505-521.
Paton JF, Nolan PJ (2000) Similarities in reflex control of laryngeal and cardiac vagal motor neurones. Respir Physiol 119:101-111.
Paton JF, Boscan P, Pickering AE, Nalivaiko E (2005) The yin and yang of cardiac autonomic control: vago-sympathetic interactions revisited. Brain Res Brain Res Rev 49:555-565.
Paton JF, Abdala AP, Koizumi H, Smith JC, St-John WM (2006) Respiratory rhythm generation during gasping depends on persistent sodium current. Nat Neurosci 9:311-313.
Paxinos G, Watson C (1996) The rat brain in stereotaxic coordinates, 3rd Edition. San Diego: Academic Press, Inc.
Pedretti RF, Prete G, Foreman RD, Adamson PB, Vanoli E (2003) Autonomic modulation during acute myocardial ischemia by low-dose pirenzepine in conscious dogs with a healed myocardial infarction: a comparison with beta-adrenergic blockade. J Cardiovasc Pharmacol 41:671-677.
Peever JH, Mateika JH, Duffin J (2001) Respiratory control of hypoglossal motoneurones in the rat. Pflugers Arch 442:78-86.
Pena F, Parkis MA, Tryba AK, Ramirez JM (2004) Differential contribution of pacemaker properties to the generation of respiratory rhythms during normoxia and hypoxia. Neuron 43:105-117.
Pepe S, Overstreet DH, Crocker AD (1988) Enhanced benzodiazepine responsiveness in rats with increased cholinergic function. Pharmacol Biochem Behav 31:15-19.
Persson PB, DiRienzo M, Castiglioni P, Cerutti C, Pagani M, Honzikova N, Akselrod S, Parati G (2001) Time versus frequency domain techniques for assessing baroreflex sensitivity. J Hypertens 19:1699-1705.
Petiot E, Barres C, Chapuis B, Julien C (2001) Frequency response of renal sympathetic nervous activity to aortic depressor nerve stimulation in the anaesthetized rat. J Physiol 537:949-959.
Petrie EC, Peskind ER, Dobie DJ, Veith RC, Raskind MA (2001) Plasma catecholamine and cardiovascular responses to physostigmine in Alzheimer's disease and aging. Psychoneuroendocrinology 26:147-164.
Phillips JK, Goodchild AK, Dubey R, Sesiashvili E, Takeda M, Chalmers J, Pilowsky PM, Lipski J (2001) Differential expression of catecholamine biosynthetic enzymes in the rat ventrolateral medulla. J Comp Neurol 432:20-34.
Piepoli M, Sleight P, Leuzzi S, Valle F, Spadacini G, Passino C, Johnston J, Bernardi L (1997) Origin of respiratory sinus arrhythmia in conscious humans. An important role for arterial carotid baroreceptors. Circulation 95:1813-1821.
Pilowsky P (1995) Good vibrations? Respiratory rhythms in the central control of blood pressure. Clin Exp Pharmacol Physiol 22:594-604.
Pilowsky P, Llewellyn-Smith IJ, Minson J, Chalmers J (1992) Sympathetic preganglionic neurons in rabbit spinal cord that project to the stellate or the superior cervical ganglion. Brain Res 577:181-188.
Pilowsky P, Llewellyn-Smith IJ, Arnolda L, Minson J, Chalmers J (1994a) Intracellular recording from sympathetic preganglionic neurons in cat lumbar spinal cord. Brain Res 656:319-328.
Pilowsky P, Llewellyn-Smith IJ, Lipski J, Minson J, Arnolda L, Chalmers J (1994b) Projections from inspiratory neurons of the ventral respiratory group to the subretrofacial nucleus of the cat. Brain Res 633:63-71.
Pilowsky P, Arnolda L, Chalmers J, Llewellyn-Smith I, Minson J, Miyawaki T, Sun QJ (1996) Respiratory inputs to central cardiovascular neurons. Ann N Y Acad Sci 783:64-70.
Pilowsky PM, Goodchild AK (2002) Baroreceptor reflex pathways and neurotransmitters: 10 years on. J Hypertens 20:1675-1688.
Pilowsky PM, Jiang C, Lipski J (1990) An intracellular study of respiratory neurons in the rostral ventrolateral medulla of the rat and their relationship to catecholamine-containing neurons. J Comp Neurol 301:604-617.
Pilowsky PM, Kapoor V, Minson JB, West MJ, Chalmers JP (1986) Spinal cord serotonin release and raised blood pressure after brainstem kainic acid injection. Brain Res 366:354-357.
Pilowsky PM, Llewellyn-Smith IJ, Minson JB, Arnolda LF, Chalmers JP (1995a) Substance P and serotonergic inputs to sympathetic preganglionic neurons. Clin Exp Hypertens 17:335-344.
Pilowsky PM, Morris MJ, Minson JB, West MJ, Chalmers JP, Willoughby JO, Blessing WW (1987) Inhibition of vasodepressor neurons in the caudal ventrolateral medulla of the rabbit increases both arterial pressure and the release of neuropeptide Y-like immunoreactivity from the spinal cord. Brain Res 420:380-384.

Pilowsky PM, Miyawaki T, Minson JB, Sun QJ, Arnolda LF, Llewellyn-Smith IJ, Chalmers JP (1995b) Bulbospinal sympatho-excitatory neurons in the rat caudal raphe. J Hypertens 13:1618-1623.
Polson JW, Potts PD, Li YW, Dampney RA (1995) Fos expression in neurons projecting to the pressor region in the rostral ventrolateral medulla after sustained hypertension in conscious rabbits. Neuroscience 67:107-123.
Pomeranz B, Macaulay RJ, Caudill MA, Kutz I, Adam D, Gordon D, Kilborn KM, Barger AC, Shannon DC, Cohen RJ, et al. (1985) Assessment of autonomic function in humans by heart rate spectral analysis. Am J Physiol 248:H151-153.
Possas OS, Campos RR, Jr., Cravo SL, Lopes OU, Guertzenstein PG (1994) A fall in arterial blood pressure produced by inhibition of the caudalmost ventrolateral medulla: the caudal pressor area. J Auton Nerv Syst 49:235-245.
Pruvot E, Thonet G, Vesin JM, van-Melle G, Seidl K, Schmidinger H, Brachmann J, Jung W, Hoffmann E, Tavernier R, Block M, Podczeck A, Fromer M (2000) Heart rate dynamics at the onset of ventricular tachyarrhythmias as retrieved from implantable cardioverter-defibrillators in patients with coronary artery disease. Circulation 101:2398-2404.
Pucilowski O, Overstreet DH (1993) Effect of chronic antidepressant treatment on responses to apomorphine in selectively bred rat strains. Brain Res Bull 32:471-475.
Pucilowski O, Overstreet DH, Rezvani AH, Janowsky DS (1993) Chronic mild stress-induced anhedonia: greater effect in a genetic rat model of depression. Physiol Behav 54:1215-1220.
Punnen S, Willette RN, Krieger AJ, Sapru HN (1986) Medullary pressor area: site of action of intravenous physostigmine. Brain Res 382:178-184.
Pyner S, Coote JH (1998) Rostroventrolateral medulla neurons preferentially project to target-specified sympathetic preganglionic neurons. Neuroscience 83:617-631.
Pyner S, Coote JH (2000) Identification of branching paraventricular neurons of the hypothalamus that project to the rostroventrolateral medulla and spinal cord. Neuroscience 100:549-556.
Pyner S, Deering J, Coote JH (2002) Right atrial stretch induces renal nerve inhibition and c-fos expression in parvocellular neurones of the paraventricular nucleus in rats. Exp Physiol 87:25-32.
Quirion R, Wilson A, Rowe W, Aubert I, Richard J, Doods H, Parent A, White N, Meaney MJ (1995) Facilitation of acetylcholine release and cognitive performance by an M(2)-muscarinic receptor antagonist in aged memory-impaired. J Neurosci 15:1455-1462.
Radaelli A, Valle F, Falcone C, Calciati A, Leuzzi S, Martinelli L, Goggi C, Vigano M, Finardi G, Bernardi L (1996) Determinants of heart rate variability in heart transplanted subjects during physical exercise. Eur Heart J 17:462-471.
Rajagopalan S, Brook R, Rubenfire M, Pitt E, Young E, Pitt B (2001) Abnormal brachial artery flow-mediated vasodilation in young adults with major depression. Am J Cardiol 88:196-198, A197.
Ramirez JM, Viemari JC (2005) Determinants of inspiratory activity. Respir Physiol Neurobiol 147:145-157.
Randall WC, Ardell JL (1985) Selective parasympathectomy of automatic and conductile tissues of the canine heart. Am J Physiol 248:H61-68.
Ranson RN, Motawei K, Pyner S, Coote JH (1998) The paraventricular nucleus of the hypothalamus sends efferents to the spinal cord of the rat that closely appose sympathetic preganglionic neurones projecting to the stellate ganglion. Exp Brain Res 120:164-172.
Raven PB, Fadel PJ, Smith SA (2002) The influence of central command on baroreflex resetting during exercise. Exerc Sport Sci Rev 30:39-44.
Rechlin T, Weis M, Spitzer A, Kaschka WP (1994) Are affective disorders associated with alterations of heart rate variability? J Affect Disord 32:271-275.
Reis DJ, Ross CA, Ruggiero DA, Granata AR, Joh TH (1984) Role of adrenaline neurons of ventrolateral medulla (the C1 group) in the tonic and phasic control of arterial pressure. Clin Exp Hypertens A 6:221-241.
Richerson GB (2004) Serotonergic neurons as carbon dioxide sensors that maintain pH homeostasis. Nat Rev Neurosci 5:449-461.
Ricketts JH, Head GA (1999) A five-parameter logistic equation for investigating asymmetry of curvature in baroreflex studies. Am J Physiol 277:R441-454.
Ringwood JV, Malpas SC (2001) Slow oscillations in blood pressure via a nonlinear feedback model. Am J Physiol Regul Integr Comp Physiol 280:R1105-1115.
Risch SC, Janowsky DS, Gillin JC (1983) Muscarinic supersensitivity of anterior pituitary ACTH and B-endorphin release in major depressive illness. Peptides 4:789-792.
Roman V, Hagewoud R, Luiten PG, Meerlo P (2006) Differential effects of chronic partial sleep deprivation and stress on serotonin-1A and muscarinic acetylcholine receptor sensitivity. J Sleep Res 15:386-394.
Rosin DL, Chang DA, Guyenet PG (2006) Afferent and efferent connections of the rat retrotrapezoid nucleus. J Comp Neurol 499:64-89.
Ross CA, Ruggiero DA, Reis DJ (1981) Projections to the spinal cord from neurons close to the ventral surface of the hindbrain in the rat. Neurosci Lett 21:143-148.

Ross CA, Ruggiero DA, Joh TH, Park DH, Reis DJ (1984a) Rostral ventrolateral medulla: selective projections to the thoracic autonomic cell column from the region containing C1 adrenaline neurons. J Comp Neurol 228:168-185.
Ross CA, Ruggiero DA, Park DH, Joh TH, Sved AF, Fernandez-Pardal J, Saavedra JM, Reis DJ (1984b) Tonic vasomotor control by the rostral ventrolateral medulla: effect of electrical or chemical stimulation of the area containing C1 adrenaline neurons on arterial pressure, heart rate, and plasma catecholamines and vasopressin. J Neurosci 4:474-494.
Rowell LB, O'Leary DS (1990) Reflex control of the circulation during exercise: chemoreflexes and mechanoreflexes. J Appl Physiol 69:407-418.
Rudisch B, Nemeroff CB (2003) Epidemiology of comorbid coronary artery disease and depression. Biol Psychiatry 54:227-240.
Ruggiero DA, Giuliano R, Anwar M, Stornetta R, Reis DJ (1990) Anatomical substrates of cholinergic-autonomic regulation in the rat. J Comp Neurol 292:1-53.
Russell RW, Overstreet DH, Messenger M, Helps SC (1982) Selective breeding for sensitivity to DFP: generalization of effects beyond criterion variables. Pharmacol Biochem Behav 17:885-891.
Rye DB, Lee HJ, Saper CB, Wainer BH (1988) Medullary and spinal efferents of the pedunculopontine tegmental nucleus and adjacent mesopontine tegmentum in the rat. J Comp Neurol 269:315-341.
Saigusa T, Granger NS, Godwin SJ, Head GA (2003) The rostral ventrolateral medulla mediates sympathetic baroreflex responses to intraventricular angiotensin II in rabbits. Auton Neurosci 107:20-31.
Saito M, Terui N, Numao Y, Kumada M (1986) Absence of sustained hypertension in sinoaortic-denervated rabbits. Am J Physiol 251:H742-747.
Sakima A, Yamazato M, Sesoko S, Muratani H, Fukiyama K (2000) Cardiovascular and sympathetic effects of L-glutamate and glycine injected into the rostral ventrolateral medulla of conscious rats. Hypertens Res 23:633-641.
Salmoiraghi GC, Burns BD (1960) Localization and patterns of discharge of respiratory neurones in brain-stem of cat. J Neurophysiol 23:2-13.
Salmoiraghi GC, vonBaumgarten (1961) Intracellular potentials from respiratory neurones in brain-stem of cat and mechanism of rhythmic respiration. J Neurophysiol 24:203-218.
Saper CB, Scammell TE, Lu J (2005) Hypothalamic regulation of sleep and circadian rhythms. Nature 437:1257-1263.
Sartor DM, Verberne AJ (2002) Cholecystokinin selectively affects presympathetic vasomotor neurons and sympathetic vasomotor outflow. Am J Physiol Regul Integr Comp Physiol 282:R1174-1184.
Sartor DM, Verberne AJ (2003) Phenotypic identification of rat rostroventrolateral medullary presympathetic vasomotor neurons inhibited by exogenous cholecystokinin. J Comp Neurol 465:467-479.
Sartor DM, Shulkes A, Verberne AJ (2006) An enteric signal regulates putative gastrointestinal presympathetic vasomotor neurons in rats. Am J Physiol Regul Integr Comp Physiol 290:R625-633.
Sartori C, Lepori M, Scherrer U (2005) Interaction between nitric oxide and the cholinergic and sympathetic nervous system in cardiovascular control in humans. Pharmacol Ther 106:209-220.
Sato A, Schmidt RF (1973) Somatosympathetic reflexes: afferent fibers, central pathways, discharge characteristics. Physiol Rev 53:916-947.
Sato T, Kawada T, Inagaki M, Shishido T, Takaki H, Sugimachi M, Sunagawa K (1999) New analytic framework for understanding sympathetic baroreflex control of arterial pressure. Am J Physiol 276:H2251-2261.
Satoh K, Armstrong DM, Fibiger HC (1983) A comparison of the distribution of central cholinergic neurons as demonstrated by acetylcholinesterase pharmacohistochemistry and choline acetyltransferase immunohistochemistry. Brain Res Bull 11:693-720.
Sawchenko PE, Swanson LW (1982) Immunohistochemical identification of neurons in the paraventricular nucleus of the hypothalamus that project to the medulla or to the spinal cord in the rat. J Comp Neurol 205:260-272.
Schafer MK, Eiden LE, Weihe E (1998) Cholinergic neurons and terminal fields revealed by immunohistochemistry for the vesicular acetylcholine transporter. I. Central nervous system. Neuroscience 84:331-359.
Schiller GD, Daws LC, Overstreet DH, Orbach J (1991) Lack of anxiety in an animal model of depression with cholinergic supersensitivity. Brain Res Bull 26:433-435.
Schreihofer AM, Guyenet PG (1997) Identification of C1 presympathetic neurons in rat rostral ventrolateral medulla by juxtacellular labeling in vivo. J Comp Neurol 387:524-536.
Schreihofer AM, Guyenet PG (2000) Sympathetic reflexes after depletion of bulbospinal catecholaminergic neurons with anti-DbetaH-saporin. Am J Physiol Regul Integr Comp Physiol 279:R729-742.
Schreihofer AM, Guyenet PG (2002) The baroreflex and beyond: control of sympathetic vasomotor tone by GABAergic neurons in the ventrolateral medulla. Clin Exp Pharmacol Physiol 29:514-521.
Schreihofer AM, Guyenet PG (2003) Baro-activated neurons with pulse-modulated activity in the rat caudal ventrolateral medulla express GAD67 mRNA. J Neurophysiol 89:1265-1277.

Schreihofer AM, Stornetta RL, Guyenet PG (1999) Evidence for glycinergic respiratory neurons: Botzinger neurons express mRNA for glycinergic transporter 2. J Comp Neurol 407:583-597.
Schreihofer AM, Stornetta RL, Guyenet PG (2000) Regulation of sympathetic tone and arterial pressure by rostral ventrolateral medulla after depletion of C1 cells in rat. J Physiol 529 Pt 1:221-236.
Schreihofer AM, Ito S, Sved AF (2005) Brain stem control of arterial pressure in chronic arterial baroreceptor-denervated rats. Am J Physiol Regul Integr Comp Physiol 289:R1746-1755.
Schwartz PJ, Stone HL (1980) Left stellectomy in the prevention of ventricular fibrillation caused by acute myocardial ischemia in conscious dogs with anterior myocardial infarction. Circulation 62:1256-1265.
Schwartz PJ, Billman GE, Stone HL (1984) Autonomic mechanisms in ventricular fibrillation induced by myocardial ischemia during exercise in dogs with healed myocardial infarction. An experimental preparation for sudden cardiac death. Circulation 69:790-800.
Schwartz PJ, La Rovere MT, Vanoli E (1992) Autonomic nervous system and sudden cardiac death. Experimental basis and clinical observations for post-myocardial infarction risk stratification. Circulation 85:I77-91.
Schwartz PJ, Vanoli E, Stramba-Badiale M, De Ferrari GM, Billman GE, Foreman RD (1988) Autonomic mechanisms and sudden death. New insights from analysis of baroreceptor reflexes in conscious dogs with and without a myocardial infarction. Circulation 78:969-979.
Serova L, Sabban EL, Zangen A, Overstreet DH, Yadid G (1998) Altered gene expression for catecholamine biosynthetic enzymes and stress response in rat genetic model of depression. Brain Res Mol Brain Res 63:133-138.
Seyedabadi M, Goodchild AK, Pilowsky PM (2001) Differential role of kinases in brain stem of hypertensive and normotensive rats. Hypertension 38:1087-1092.
Seyedabadi M, Li Q, Padley JR, Pilowsky PM, Goodchild AK (2006) A novel pressor area at the medullo-cervical junction that is not dependent on the RVLM: efferent pathways and chemical mediators. J Neurosci 26:5420-5427.
Shao XM, Feldman JL (1997) Respiratory rhythm generation and synaptic inhibition of expiratory neurons in pre-Botzinger complex: differential roles of glycinergic and GABAergic neural transmission. J Neurophysiol 77:1853-1860.
Shao XM, Feldman JL (2000) Acetylcholine modulates respiratory pattern: effects mediated by M3-like receptors in preBotzinger complex inspiratory neurons. J Neurophysiol 83:1243-1252.
Shao XM, Feldman JL (2001) Mechanisms underlying regulation of respiratory pattern by nicotine in preBotzinger complex. J Neurophysiol 85:2461-2467.
Shao XM, Feldman JL (2005) Cholinergic neurotransmission in the preBotzinger Complex modulates excitability of inspiratory neurons and regulates respiratory rhythm. Neuroscience 130:1069-1081.
Shayit M, Yadid G, Overstreet DH, Weller A (2003) 5-HT(1A) receptor subsensitivity in infancy and supersensitivity in adulthood in an animal model of depression. Brain Res 980:100-108.
Shi H, Lewis DI, Coote JH (1988) Effects of activating spinal alpha-adrenoreceptors on sympathetic nerve activity in the rat. J Auton Nerv Syst 23:69-78.
Shimojo M, Wu D, Hersh LB (1998) The cholinergic gene locus is coordinately regulated by protein kinase A II in PC12 cells. J Neurochem 71:1118-1126.
Shiromani PJ, Overstreet D (1994) Free-running period of circadian rhythms is shorter in rats with a genetically upregulated central cholinergic system. Biol Psychiatry 36:622-626.
Shiromani PJ, Klemfuss H, Lucero S, Overstreet DH (1991a) Diurnal rhythm of core body temperature is phase advanced in a rodent model of depression. Biol Psychiatry 29:923-930.
Shiromani PJ, Overstreet D, Levy D, Goodrich CA, Campbell SS, Gillin JC (1988) Increased REM sleep in rats selectively bred for cholinergic hyperactivity. Neuropsychopharmacology 1:127-133.
Shiromani PJ, Velazquez-Moctezuma J, Overstreet D, Shalauta M, Lucero S, Floyd C (1991b) Effects of sleep deprivation on sleepiness and increased REM sleep in rats selectively bred for cholinergic hyperactivity. Sleep 14:116-120.
Skinner MR, Ramage AG, Jordan D (2002) Modulation of reflexly evoked vagal bradycardias by central 5-HT1A receptors in anaesthetized rabbits. Br J Pharmacol 137:861-873.
Sleight P, La Rovere MT, Mortara A, Pinna G, Maestri R, Leuzzi S, Bianchini B, Tavazzi L, Bernardi L (1995) Physiology and pathophysiology of heart rate and blood pressure variability in humans: is power spectral analysis largely an index of baroreflex gain? Clin Sci (Lond) 88:103-109.
Smith JC, Ellenberger HH, Ballanyi K, Richter DW, Feldman JL (1991) Pre-Botzinger complex: a brainstem region that may generate respiratory rhythm in mammals. Science 254:726-729.
Smith JC, Butera RJ, Koshiya N, Del Negro C, Wilson CG, Johnson SM (2000) Respiratory rhythm generation in neonatal and adult mammals: the hybrid pacemaker-network model. Respir Physiol 122:131-147.
Smith JE, Jansen AS, Gilbey MP, Loewy AD (1998) CNS cell groups projecting to sympathetic outflow of tail artery: neural circuits involved in heat loss in the rat. Brain Res 786:153-164.

Snowball RK, Dampney RA, Lumb BM (1997) Responses of neurones in the medullary raphe nuclei to inputs from visceral nociceptors and the ventrolateral periaqueductal grey in the rat. Exp Physiol 82:485-500.
Springell DA, Costin NS, Pilowsky PM, Goodchild AK (2005) Hypotension and short-term anaesthesia induce ERK1/2 phosphorylation in autonomic nuclei of the brainstem. Eur J Neurosci 22:2257-2270.
St-John WM, Waki H, Dutschmann M, Paton JF (2006) Maintenance of eupnea of in situ and in vivo rats following riluzole: A blocker of persistent sodium channels. Respir Physiol Neurobiol.
Stanek KA, Neil JJ, Sawyer WB, Loewy AD (1984) Changes in regional blood flow and cardiac output after L-glutamate stimulation of A5 cell group. Am J Physiol 246:H44-51.
Stasinopoulos T, Goodchild AK, Christie MJ, Chalmers J, Pilowsky PM (2000) Delta opioid receptor immunoreactive boutons appose bulbospinal CI neurons in the rat. Neuroreport 11:887-891.
Stein PK, Carney RM, Freedland KE, Skala JA, Jaffe AS, Kleiger RE, Rottman JN (2000) Severe depression is associated with markedly reduced heart rate variability in patients with stable coronary heart disease. J Psychosom Res 48:493-500.
Steinbusch HW (1981) Distribution of serotonin-immunoreactivity in the central nervous system of the rat-cell bodies and terminals. Neuroscience 6:557-618.
Stewart RA, North FM, West TM, Sharples KJ, Simes RJ, Colquhoun DM, White HD, Tonkin AM (2003) Depression and cardiovascular morbidity and mortality: cause or consequence? Eur Heart J 24:2027-2037.
Stocker SD, Keith KJ, Toney GM (2004) Acute inhibition of the hypothalamic paraventricular nucleus decreases renal sympathetic nerve activity and arterial blood pressure in water-deprived rats. Am J Physiol Regul Integr Comp Physiol 286:R719-725.
Stocker SD, Hunwick KJ, Toney GM (2005) Hypothalamic paraventricular nucleus differentially supports lumbar and renal sympathetic outflow in water-deprived rats. J Physiol 563:249-263.
Stocker SD, Simmons JR, Stornetta RL, Toney GM, Guyenet PG (2006) Water deprivation activates a glutamatergic projection from the hypothalamic paraventricular nucleus to the rostral ventrolateral medulla. J Comp Neurol 494:673-685.
Stornetta RL, Akey PJ, Guyenet PG (1999) Location and electrophysiological characterization of rostral medullary adrenergic neurons that contain neuropeptide Y mRNA in rat medulla. J Comp Neurol 415:482-500.
Stornetta RL, Schreihofer AM, Pelaez NM, Sevigny CP, Guyenet PG (2001) Preproenkephalin mRNA is expressed by C1 and non-C1 barosensitive bulbospinal neurons in the rostral ventrolateral medulla of the rat. J Comp Neurol 435:111-126.
Stornetta RL, Sevigny CP, Schreihofer AM, Rosin DL, Guyenet PG (2002) Vesicular glutamate transporter DNPI/VGLUT2 is expressed by both C1 adrenergic and nonaminergic presympathetic vasomotor neurons of the rat medulla. J Comp Neurol 444:207-220.
Strack AM, Sawyer WB, Marubio LM, Loewy AD (1988) Spinal origin of sympathetic preganglionic neurons in the rat. Brain Res 455:187-191.
Strack AM, Sawyer WB, Hughes JH, Platt KB, Loewy AD (1989) A general pattern of CNS innervation of the sympathetic outflow demonstrated by transneuronal pseudorabies viral infections. Brain Res 491:156-162.
Sun MK, Guyenet PG (1985) GABA-mediated baroreceptor inhibition of reticulospinal neurons. Am J Physiol 249:R672-680.
Sun MK, Spyer KM (1991a) Responses of rostroventrolateral medulla spinal vasomotor neurones to chemoreceptor stimulation in rats. J Auton Nerv Syst 33:79-84.
Sun MK, Spyer KM (1991b) Nociceptive inputs into rostral ventrolateral medulla-spinal vasomotor neurones in rats. J Physiol 436:685-700.
Sun MK, Reis DJ (1993) Differential responses of barosensitive neurons of rostral ventrolateral medulla to hypoxia in rats. Brain Res 609:333-337.
Sun MK, Reis DJ (1994) Hypoxia selectively excites vasomotor neurons of rostral ventrolateral medulla in rats. Am J Physiol 266:R245-256.
Sun MK, Hackett JT, Guyenet PG (1988a) Sympathoexcitatory neurons of rostral ventrolateral medulla exhibit pacemaker properties in the presence of a glutamate-receptor antagonist. Brain Res 438:23-40.
Sun MK, Young BS, Hackett JT, Guyenet PG (1988b) Reticulospinal pacemaker neurons of the rat rostral ventrolateral medulla with putative sympathoexcitatory function: an intracellular study in vitro. Brain Res 442:229-239.
Sun QJ, Goodchild AK, Chalmers JP, Pilowsky PM (1998) The pre-Botzinger complex and phase-spanning neurons in the adult rat. Brain Res 809:204-213.
Sun QJ, Minson J, Llewellyn-Smith IJ, Arnolda L, Chalmers J, Pilowsky P (1997) Botzinger neurons project towards bulbospinal neurons in the rostral ventrolateral medulla of the rat. J Comp Neurol 388:23-31.

Sun W, Panneton WM (2002) The caudal pressor area of the rat: its precise location and projections to the ventrolateral medulla. Am J Physiol Regul Integr Comp Physiol 283:R768-778.
Sundaram K, Sapru H (1988) Cholinergic nerve terminals in the ventrolateral medullary pressor area: pharmacological evidence. J Auton Nerv Syst 22:221-228.
Sundaram K, Krieger AJ, Sapru H (1988) M2 muscarinic receptors mediate pressor responses to cholinergic agonists in the ventrolateral medullary pressor area. Brain Res 449:141-149.
Sved AF, Ito S, Madden CJ (2000) Baroreflex dependent and independent roles of the caudal ventrolateral medulla in cardiovascular regulation. Brain Res Bull 51:129-133.
Swanson LW, Kuypers HG (1980) The paraventricular nucleus of the hypothalamus: cytoarchitectonic subdivisions and organization of projections to the pituitary, dorsal vagal complex, and spinal cord as demonstrated by retrograde fluorescence double-labeling methods. J Comp Neurol 194:555-570.
Swanson LW, Sawchenko PE, Wiegand SJ, Price JL (1980) Separate neurons in the paraventricular nucleus project to the median eminence and to the medulla or spinal cord. Brain Res 198:190-195.
Taguchi K, Kato M, Kikuta J, Abe K, Chikuma T, Utsunomiya I, Miyatake T (1999) The effects of morphine-induced increases in extracellular acetylcholine levels in the rostral ventrolateral medulla of rat. J Pharmacol Exp Ther 289:1539-1544.
Takakusaki K, Takahashi K, Saitoh K, Harada H, Okumura T, Kayama Y, Koyama Y (2005) Orexinergic projections to the cat midbrain mediate alternation of emotional behavioural states from locomotion to cataplexy. J Physiol 568:1003-1020.
Takeda S, Eriksson LI, Yamamoto Y, Joensen H, Onimaru H, Lindahl SG (2001) Opioid action on respiratory neuron activity of the isolated respiratory network in newborn rats. Anesthesiology 95:740-749.
Tanaka H, Shimojo M, Wu D, Hersh LB (1998) Regulation of the cholinergic gene locus. J Physiol Paris 92:149-152.
Tanaka M, Nagashima K, McAllen RM, Kanosue K (2002) Role of the medullary raphe in thermoregulatory vasomotor control in rats. J Physiol 540:657-664.
Tao L, Nicholson C (1996) Diffusion of albumins in rat cortical slices and relevance to volume transmission. Neuroscience 75:839-847.
TaskForce (1996) Heart rate variability: standards of measurement, physiological interpretation and clinical use. Task Force of the European Society of Cardiology and the North American Society of Pacing and Electrophysiology. Circulation 93:1043-1065.
Taylor EW, Jordan D, Coote JH (1999) Central control of the cardiovascular and respiratory systems and their interactions in vertebrates. Physiol Rev 79:855-916.
Taylor JA, Carr DL, Myers CW, Eckberg DL (1998) Mechanisms underlying very-low-frequency RR-interval oscillations in humans. Circulation 98:547-555.
Thoby-Brisson M, Ramirez JM (2001) Identification of two types of inspiratory pacemaker neurons in the isolated respiratory neural network of mice. J Neurophysiol 86:104-112.
Thrasher TN (2002) Unloading arterial baroreceptors causes neurogenic hypertension. Am J Physiol Regul Integr Comp Physiol 282:R1044-1053.
Tian GF, Peever JH, Duffin J (1999) Botzinger-complex, bulbospinal expiratory neurones monosynaptically inhibit ventral-group respiratory neurones in the decerebrate rat. Exp Brain Res 124:173-180.
Tillet Y (1988) Adrenergic neurons in sheep brain demonstrated by immunohistochemistry with antibodies to phenylethanolamine N-methyltransferase (PNMT) and dopamine-beta-hydroxylase (DBH): absence of the C1 cell group in the sheep brain. Neurosci Lett 95:107-112.
Tizabi Y, Rezvani AH, Russell LT, Tyler KY, Overstreet DH (2000) Depressive characteristics of FSL rats: involvement of central nicotinic receptors. Pharmacol Biochem Behav 66:73-77.
Tizabi Y, Overstreet DH, Rezvani AH, Louis VA, Clark E, Jr., Janowsky DS, Kling MA (1999) Antidepressant effects of nicotine in an animal model of depression. Psychopharmacology (Berl) 142:193-199.
Toth ZE, Gallatz K, Fodor M, Palkovits M (1999) Decussations of the descending paraventricular pathways to the brainstem and spinal cord autonomic centers. J Comp Neurol 414:255-266.
Trimarchi GR, Buccafusco JJ (1987) Changes in regional brain synaptosomal high affinity choline uptake during the development of hypertension in spontaneously hypertensive rats. Neurochem Res 12:247-254.
Tseng CJ, Ger LP, Lin HC, Tung CS (1994) The pressor effect of nicotine in the rostral ventrolateral medulla of rats. Chin J Physiol 37:83-87.
Tsukamoto K, Yin M, Sved AF (1994) Effect of atropine injected into the nucleus tractus solitarius on the regulation of blood pressure. Brain Res 648:9-15.
Tucker DC, Saper CB, Ruggiero DA, Reis DJ (1987) Organization of central adrenergic pathways: I. Relationships of ventrolateral medullary projections to the hypothalamus and spinal cord. J Comp Neurol 259:591-603.
van den Buuse M (1994) Circadian rhythms of blood pressure, heart rate, and locomotor activity in spontaneously hypertensive rats as measured with radio-telemetry. Physiol Behav 55:783-787.

van Melle JP, de Jonge P, Ormel J, Crijns HJ, van Veldhuisen DJ, Honig A, Schene AH, van den Berg MP (2005) Relationship between left ventricular dysfunction and depression following myocardial infarction: data from the MIND-IT. Eur Heart J 26:2650-2656.
Vanoli E, De Ferrari GM, Stramba-Badiale M, Hull SS, Jr., Foreman RD, Schwartz PJ (1991) Vagal stimulation and prevention of sudden death in conscious dogs with a healed myocardial infarction. Circ Res 68:1471-1481.
Varagic V (1955) The action of eserine on the blood pressure of the rat. Br J Pharmacol Chemother 10:349-353.
Veith RC, Lewis N, Linares OA, Barnes RF, Raskind MA, Villacres EC, Murburg MM, Ashleigh EA, Castillo S, Peskind ER, et al. (1994) Sympathetic nervous system activity in major depression. Basal and desipramine-induced alterations in plasma norepinephrine kinetics. Arch Gen Psychiatry 51:411-422.
Verberne AJ (1995) Cuneiform nucleus stimulation produces activation of medullary sympathoexcitatory neurons in rats. Am J Physiol 268:R752-758.
Verberne AJ, Owens NC (1998) Cortical modulation of the cardiovascular system. Prog Neurobiol 54:149-168.
Verberne AJ, Sartor DM (2004) CCK-induced inhibition of presympathetic vasomotor neurons: dependence on subdiaphragmatic vagal afferents and central NMDA receptors in the rat. Am J Physiol Regul Integr Comp Physiol 287:R809-816.
Verberne AJ, Stornetta RL, Guyenet PG (1999a) Properties of C1 and other ventrolateral medullary neurones with hypothalamic projections in the rat. J Physiol 517 (Pt 2):477-494.
Verberne AJ, Sartor DM, Berke A (1999b) Midline medullary depressor responses are mediated by inhibition of RVLM sympathoexcitatory neurons in rats. Am J Physiol 276:R1054-1062.
Verner TA, Goodchild AK, Pilowsky PM (2004) A mapping study of cardiorespiratory responses to chemical stimulation of the midline medulla oblongata in ventilated and freely breathing rats. Am J Physiol Regul Integr Comp Physiol 287:R411-421.
von Kanel R (2004) Platelet hyperactivity in clinical depression and the beneficial effect of antidepressant drug treatment: how strong is the evidence? Acta Psychiatr Scand 110:163-177.
Waki H, Katahira K, Polson JW, Kasparov S, Murphy D, Paton JF (2006) Automation of analysis of cardiovascular autonomic function from chronic measurements of arterial pressure in conscious rats. Exp Physiol 91:201-213.
Walker JK, Peppel K, Lefkowitz RJ, Caron MG, Fisher JT (1999) Altered airway and cardiac responses in mice lacking G protein-coupled receptor kinase 3. Am J Physiol 276:R1214-1221.
Walker JL, Weetman DF (1970) Oxotremorine-induced hypertension in the anaesthetized rat. Br J Pharmacol 39:490-500.
Walker MJ, Curtis MJ, Hearse DJ, Campbell RW, Janse MJ, Yellon DM, Cobbe SM, Coker SJ, Harness JB, Harron DW, et al. (1988) The Lambeth Conventions: guidelines for the study of arrhythmias in ischaemia infarction, and reperfusion. Cardiovasc Res 22:447-455.
Wallis E, Overstreet DH, Crocker AD (1988) Selective breeding for increased cholinergic function: increased serotonergic sensitivity. Pharmacol Biochem Behav 31:345-350.
Wang H, Wessendorf MW (2002) Mu- and delta-opioid receptor mRNAs are expressed in periaqueductal gray neurons projecting to the rostral ventromedial medulla. Neuroscience 109:619-634.
Wang J, Wang X, Irnaten M, Venkatesan P, Evans C, Baxi S, Mendelowitz D (2003) Endogenous acetylcholine and nicotine activation enhances GABAergic and glycinergic inputs to cardiac vagal neurons. J Neurophysiol 89:2473-2481.
Wang J, Irnaten M, Neff RA, Venkatesan P, Evans C, Loewy AD, Mettenleiter TC, Mendelowitz D (2001) Synaptic and neurotransmitter activation of cardiac vagal neurons in the nucleus ambiguus. Ann N Y Acad Sci 940:237-246.
Wang JC, Hinrichs AL, Stock H, Budde J, Allen R, Bertelsen S, Kwon JM, Wu W, Dick DM, Rice J, Jones K, Nurnberger JI, Jr., Tischfield J, Porjesz B, Edenberg HJ, Hesselbrock V, Crowe R, Schuckit M, Begleiter H, Reich T, Goate AM, Bierut LJ (2004) Evidence of common and specific genetic effects: association of the muscarinic acetylcholine receptor M2 (CHRM2) gene with alcohol dependence and major depressive syndrome. Hum Mol Genet 13:1903-1911.
Wang JJ, Chen YH, Li KY, Sun FY (2005) Differential sensitivity of GABAergic and glycinergic inputs to orexin-A in preganglionic cardiac vagal neurons of newborn rats. Acta Pharmacol Sin 26:1442-1447.
Wang SC, Ranson SW (1939) Autonomic responses to electrical stimulation of the lower brainstem. J Comp Neurol 71:437-455.
Wang WZ, Wang XM, Rong WF, Wang JJ, Yuan WJ (2000) [Effect of acetylcholine on the discharge of presympathetic neurons of the rostral ventrolateral medulla of rats]. Sheng Li Xue Bao 52:468-472.
Watkins LL, Grossman P (1999) Association of depressive symptoms with reduced baroreflex cardiac control in coronary artery disease. Am Heart J 137:453-457.

Watkins LL, Blumenthal JA, Davidson JR, Babyak MA, McCants CB, Jr., Sketch MH, Jr. (2006) Phobic anxiety, depression, and risk of ventricular arrhythmias in patients with coronary heart disease. Psychosom Med 68:651-656.
Whang W, Albert CM, Sears SF, Jr., Lampert R, Conti JB, Wang PJ, Singh JP, Ruskin JN, Muller JE, Mittleman MA (2005) Depression as a predictor for appropriate shocks among patients with implantable cardioverter-defibrillators: results from the Triggers of Ventricular Arrhythmias (TOVA) study. J Am Coll Cardiol 45:1090-1095.
White SW, Pitsillides KF, Parsons GH, Hayes SG, Gunther RA, Cottee DB (2001) Coronary-bronchial blood flow and airway dimensions in exercise-induced syndromes. Clin Exp Pharmacol Physiol 28:472-478.
Wickman K, Clapham DE (1995) Ion channel regulation by G proteins. Physiol Rev 75:865-885.
Willette RN, Punnen S, Krieger AJ, Sapru HN (1984) Cardiovascular control by cholinergic mechanisms in the rostral ventrolateral medulla. J Pharmacol Exp Ther 231:457-463.
Williamson JW, Fadel PJ, Mitchell JH (2006) New insights into central cardiovascular control during exercise in humans: a central command update. Exp Physiol 91:51-58.
Woodruff ML, Baisden RH, Whittington DL (1986) Effects of electrical stimulation of the pontine A5 cell group on blood pressure and heart rate in the rabbit. Brain Res 379:10-23.
Woolf NJ, Butcher LL (1989) Cholinergic systems in the rat brain: IV. Descending projections of the pontomesencephalic tegmentum. Brain Res Bull 23:519-540.
Wulsin LR (2004) Is depression a major risk factor for coronary disease? A systematic review of the epidemiologic evidence. Harv Rev Psychiatry 12:79-93.
Xiong Y, Okada J, Tomizawa S, Takayama K, Miura M (1998) Difference in topology and numbers of barosensitive catecholaminergic and cholinergic neurons in the medulla between SHR and WKY rats. J Auton Nerv Syst 70:200-208.
Yadid G, Nakash R, Deri I, Tamar G, Kinor N, Gispan I, Zangen A (2000) Elucidation of the neurobiology of depression: insights from a novel genetic animal model. Prog Neurobiol 62:353-378.
Yamashita H (1977) Effect of baro- and chemoreceptor activation on supraoptic nuclei neurons in the hypothalamus. Brain Res 126:551-556.
Yamazaki T, Akiyama T, Kawada T (1999) Effects of ouabain on in situ cardiac sympathetic nerve endings. Neurochem Int 35:439-445.
Yamazaki T, Akiyama T, Kitagawa H, Takauchi Y, Kawada T (1996) Elevation of either axoplasmic norepinephrine or sodium level induced release of norepinephrine from cardiac sympathetic nerve terminals. Brain Res 737:343-346.
Yasui Y, Cechetto DF, Saper CB (1990) Evidence for a cholinergic projection from the pedunculopontine tegmental nucleus to the rostral ventrolateral medulla in the rat. Brain Res 517:19-24.
Zagon A, Smith AD (1993) Monosynaptic projections from the rostral ventrolateral medulla oblongata to identified sympathetic preganglionic neurons. Neuroscience 54:729-743.
Zangen A, Overstreet DH, Yadid G (1997) High serotonin and 5-hydroxyindoleacetic acid levels in limbic brain regions in a rat model of depression: normalization by chronic antidepressant treatment. J Neurochem 69:2477-2483.
Zangen A, Overstreet DH, Yadid G (1999) Increased catecholamine levels in specific brain regions of a rat model of depression: normalization by chronic antidepressant treatment. Brain Res 824:243-250.
Zangen A, Nakash R, Overstreet DH, Yadid G (2001) Association between depressive behavior and absence of serotonin-dopamine interaction in the nucleus accumbens. Psychopharmacology (Berl) 155:434-439.
Zangen A, Nakash R, Roth-Deri I, Overstreet DH, Yadid G (2002) Impaired release of beta-endorphin in response to serotonin in a rat model of depression. Neuroscience 110:389-393.
Zaza A, Lombardi F (2001) Autonomic indexes based on the analysis of heart rate variability: a view from the sinus node. Cardiovasc Res 50:434-442.
Zheng Y, Barillot JC, Bianchi AL (1991) Patterns of membrane potentials and distributions of the medullary respiratory neurons in the decerebrate rat. Brain Res 546:261-270.
Zhou SY, Gilbey MP (1992) Respiratory-related activity of lower thoracic and upper lumbar sympathetic preganglionic neurones in the rat. J Physiol 451:631-642.
Zipes DP, Wellens HJ (1998) Sudden cardiac death. Circulation 98:2334-2351.